UNIVERSITÀ DEGLI STUDI DI MILANO

Ph.D. Programme in Food Systems

Department of Food, Environmental and Nutritional Sciences (DeFENS)

Chemistry and Biochemistry

XXXIV Cycle

Natural and Nature-inspired Compounds as Antimicrobial Agents: Extraction, Synthesis and Biological Investigation

[CHIM/06]

Giorgia Catinella

R12444

Tutor: Prof. Sabrina Dallavalle

Ph.D. Dean: Prof. Ella Pagliarini

2020/2021

INDEX

ABBREVIATIONS

Å	Ångström
Ac_2O	acetic anhydride
ACN	acetonitrile
ACT	acetone
AIBN	2,2-azobisisobutyronitrile
AMR	antimicrobial resistance
AZX	azoxystrobin
BBr_3	boron tribromide
BCl_3	boron trichloride
BHI	Brain Hearth Infusion
$Bi(OTf)_3$	bismuth(III) trifluoromethanesulfonate
Boc	*tert*-butyloxycarbonyl
BSL	biosafety level
CBr_4	carbon tetrabromide
CCl_4	carbon tetrachloride
CD_3OD	deuteromethanol
$CDCl_3$	deuterochloroform
CH_3I	methyl iodide
$CHCl_3$	chloroform
CHX	cyclohexane
CPE	cytopathic effect
Cs_2CO_3	caesium carbonate
$CuBr_2$	copper(II) bromide
CuI	copper Iodide
$CuSO_4 \cdot 5H_2O$	copper(II) sulfate pentahydrate
DAI	days after inoculation
DBH_2	decylubiquinol
DCM	dichloromethane
DCPIP	2,6-dichlorophenolindophenol

DIPEA	*N*,*N*-diisopropylethylamine
DMA	*N*, *N'*-dimethylacetamide
DMAP	4-dimethylaminopyridine
DME	dimethoxyethane
DMF	*N*,*N*-dimethylformamide
DMP	Dess-Martin periodinane
DMSO	dimethyl sulfoxide
DPPA	diphenylphosphorylazide
dppp	1,3-Bis(diphenylphosphino)propane
EDC·HCl	*N*-(3-dimethylaminopropyl)-*N*′-ethylcarbodiimide hydrochloride
eq	equivalent
Et_2O	diethylether
EtOAc	ethyl acetate
EtOH	ethanol
ETP	petroleum ether
FBS	fetal bovine serum
FC	flash chromatography
FCS	fetal calf serum
FXP	fluxapyroxad
FRAC	Fungicide resistance action committee
GABA	γ-aminobutyric acid
GSE	grapefruit seeds extract
Hex	hexane
HGT	horizontal gene transfer
HIO_4	periodic acid
HOBt	1-hydroxybenzotriazole
IC_{50}	half maximal inhibitory concentration
ISP	iron-sulfur protein
K_2CO_3	potassium carbonate

KF	potassium fluoride
KOH	potassium hydroxide
K_3PO_4	tripotassium phosphate
LDA	lithium diisopropylamide
$LiAlH_4$	lithium aluminium hydride
$LiOH \cdot H_2O$	lithium hydroxide monohydrate
m.p.	melting point
MBC	minimal bactericidal concentration
MEM	Minimum Essential Medium
MeOH	methanol
MIC	minimal inhibitory concentration
min	minute
β-MOA	β-methoxyacrilate
MW	microwave
$NaBH_4$	sodium borohydride
NaH	sodium hydride
$NaIO_4$	sodium periodate
NaN_3	sodium azide
NaOH	sodium hydroxide
$NaSO_4$	Sodium sulphate
NBS	*N*-bromosuccinimide
n-BuLi	butyllithium
NIS	*N*-iodosuccinimide
$P(Cy) \cdot HBF_4$	tricyclohexylphosphine tetrafluoroborate
$P(OEt)_3$	triethylphosphite
PBr_3	phosphorus tribromide
PBS	phosphate-buffered saline
PDB	protein data bank
$Pd(OAc)_2$	palladium acetate
$Pd(PPh_3)_4$	tetrakis(triphenylphosphine)palladium

$PdCl_2(PPh_3)_2$	bis(triphenylphosphine)palladium (II) dichloride
PFU	Plaque Forming Units
PMA	phosphomolybdic acid
PPh_3	triphenylphosphine
PRNT	Plaque Reduction Neutralization Test
QoI	quinone outside inhibitor
p-TsOH	*para*-toluensulfonic acid
RES	resistant
ROS	Reactive Oxygen Species
rt	room temperature
SAR	structure-activity relationship
SD	standard deviation
SDGs	austainable Development Goals
SDHI	succinate-deidrogenase inhibitor
TBAI	tetrabutylammonium iodide
t-BuOH	*tert*-butyl alcohol
TEA	triethylamine
TES	triethylsylane
TFA	trifluoroacetic acid
TG	triglycerides
THF	tetrahydrofuran
WHO	World Health Organization
WT	Wild-type

ABSTRACT

Nowadays the presence of agents and pathogens in food supply chain that developed antimicrobial resistance (AMR) is an increasing problem for human health. World Health Organization (WHO) defined the antimicrobial resistance as one of the top five public health threats. Antimicrobial resistance can be transmitted from microorganisms to microorganisms in different ways (phages, trasposoms and plasmins), resulting in horizontal gene transfer (HGT). It is important to highlight that antimicrobials are used in all sectors of food supply chain: as antifungal and pesticides to maximise the crops; as antibiotics in animal production and in aquaculture; as preservatives for the shelves food life; as antiviral agents in functional foods. The escalating emergence of AMR in food supply chain make it necessary the search for new antimicrobial compounds. In this context, nature can be a potent source of inspiration for the development of new and innovative antimicrobials.

The focus of this PhD thesis was to contribute to the expansion of the arsenal of antifungal, antibacterial and antiviral compounds by paying particular attention to natural and nature-inspired compounds. Two different strategies were followed.

The first strategy was based on the development of a synthetic approach to build novel antifungal and antibacterial agents. In the field of antifungals, we concentrated on the design and synthesis of a collection of strobilurin derivatives. Strobilurins, or more correctly quinone outside inhibitors (QoI), originate from a natural compound discovered in 1977 and cover almost 20% of the fungicide's world sales. In particular, this class of compounds is used against *Pyricularia oryzae*, a rice blast responsible of the biggest part of losses of global production. In the last decades, several resistance mechanisms, based on the mutation in the target site gene of strobilurins, have been developed. Mutation G143A is by far the most important mechanism of resistance and has a strong effect on the activity of QoIs. For this reason, our strategy was based on the development of multi-target compounds, which can

improve the efficacy and overcame the resistance, acting simultaneously on multiple, well-known and validated targets. In fact, starting from strobilurins' pharmacophore, we created new analogues connecting in different position the pharmacophore of another class of antifungal agents, e.g. succinate-dehydrogenase inhibitors. The novel compounds were tested against wild-type and resistant-strobilurin strains of *P. oryzae. In silico* modeling studies gave important information about the structural requirement of the new antifungal compounds.

About antibacterial and preservatives agents, we focused on stilbenoids. Stilbenoids belong to the class of polyphenols, in which resveratrol is the most studied compound. They are produced by plants as means of defence against pathogens invasion and stress factors. Several studies showed their surprising biological activities, such as anticancer, antioxidant, neuroprotective and antimicrobial. In particular, we investigated dimers of resveratrol such as dehydro-δ-viniferin and dehydro-ε-viniferin, carrying out structure-activity-relationship (SAR) studies. Moreover, we modified the scaffold of monomeric stilbenoids with the aim of obtaining compounds able to overcome the outer membrane of Gram-negative bacteria.

The second approach was directed to extraction and isolation of bioactive natural products from vegetal matrices. In order to give our contribution on the research against COVID-19, we focused on grapefruit seeds, inspired by the known antiviral activities of grapefruit seeds extract (GSE). A small collection of extracts and five pure isolated secondary metabolites, belonging to the class of limonoids and flavonoid glycosides, were isolated and investigated for the ability to counteract SARS-CoV-2 infection, by studying both the potential antiviral effect as well as the ability to reduce uncontrolled oxidative stress response.

1 INTRODUCTION

Climate change and environmental degradation are a crucial threat for all the world population and the reduction of the effects of these problems is a challenge for all countries. Recently, the European Commission has among its 2019-2024 priorities the European Green Deal, a set of proposals to make the European Union the first climate-neutral continent in the world by 2050.

To improve the well-being, the health of citizens and future generations, the European Green Deal aims to act in several sectors: climate, environment and oceans, energy, agriculture, industry, finance development, transports, research and innovation. In this context, the Farm to Fork strategy is the heart of the European Green Deal and it is central also to achieve the United Nations' Sustainable Development Goals (SDGs) (EU, 2020). Sustainable food systems are designed to boost the economy, improve the quality of life and care for nature. In the last decades, consumers have become more conscious about health and food safety and quality. They are empowered to choose sustainable food, fresher, less processed, and derived from eco-sustainable sources.

Moreover, the COVID-19 pandemic, which still worries the world nowadays, has considerably influenced the agri-food supply chain and food products' choices. In the first year of the pandemic, the large food supply chain adapted very well to the short-run disruptions caused by continuous lockdown. For example, only the meat processing and fruit-vegetable production showed vulnerability in Canada and United States (Hobbs, 2021). The current food system has been remarkably adapted; nevertheless, the COVID-19 highlighted the necessity of a more robust and resilient food system in all sectors.

The food supply chain refers to the processes that describe how food ends up from a farm to our tables, including procedures such as production, processing, distribution, consumption, and arrangement. The food that arrives inside our homes, through the food supply chain, irreversibly moves from

producers to consumers; on the other hand, money goes to people who work in the various stages of the food chain. Each step of the supply chain requires workers (farmers, food technologists, industrialists, transporters, etc.) and natural (fruits, vegetables, meat and fish) resources. Since a food supply chain is like a domino, when part of the food supply chain is affected, the entire food supply chain is affected as well, often leading to price changes. In addition, both movements of food and money are facilitated by "pulls" and "pushes". In a food supply chain, producers and processors push (supply food) and consumers pull (demand food), thereby facilitating the dominos (food) to fall towards the consumers. Similarly, producers and processors pull money and consumers push money to facilitate money movement from consumers to producers (Figure 1.1).

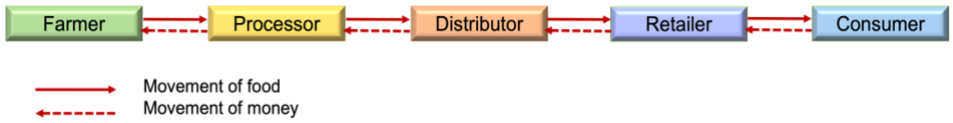

Figure 1.1 *Movement of food and money in a simple food supply chain*

One of the factors that influences the price variation within the food supply chain and the fluctuation on the market is the risk linked to pathogenic factors (Kuo and Chen, 2010). In fact, one of the critical factors is microbiological food safety, due to the possibility that harmful microorganisms grow and multiply in food products. This can result in food poisoning, increased foodborne outbreaks, such as the recent Sars-CoV-2 pandemic, and the consequent reduction of availability of healthy food (Havelaar *et al.*, 2010). Drought can also significantly affect the availability of irrigation water used in agricultural production and cause crop failure (Magan *et al.*, 2011).

The difference between "food safety" and "food security" is commonly misunderstood, even if strongly related issues are described. Food safety is precisely the inverse of food risk and is the probability that a given food will not cause health problems for living beings after consumption (Henson and Traill, 1993).

Food security, on the other hand, is defined as guaranteeing, daily, that all people have both physical and economic access to nutrition (Carvalho, 2006). The factors that influence food security are several and well known: possible microbial contamination of food, government laws, drought, global and national market fluctuations, globalization and population growth. In particular, food globalization is the most critical factor responsible for the increase in foodborne illnesses due to microbes (Aung and Chang, 2014).

Pathogenic bacteria are the most common contaminants in food, followed by viruses, synthetic pesticides and mycotoxins (Van Boxstael *et al.*, 2013).

Harmful microorganisms on food carry a greater risk of cross-contamination, causing inevitable poisoning and loss of healthy food. Therefore, food safety is the aspect to be safeguarded in food production to protect the consumer from potential health risks and to reduce food losses significantly (Bryden, 2012). The focus is mainly on the microbiological quality throughout the food chain, to minimize the risk of foodborne diseases and, consequently, to improve food safety. According to the directives of Food and Agriculture Organization (FAO), more rigorous policies are introduced to reduce the risk of food contamination and guarantee public health (Elkhishin *et al.*, 2017). In addition to ensuring food supply, food security also faces up to fundamental issues such as food contamination and foodborne outbreaks. An outbreak of this type is defined as an episode in which multiple people become ill due to the consumption/nourishment of a typical food (Greig and Ravel, 2009).

Food poisoning, and associated symptoms vary, depend on the nature of the hazard (biological, chemical or physical) and depend on the ability to cause toxic effects on human health.

1.1 ANTIMICROBIALS

To avoid contamination of food resources and to make every process in the food supply chain safe, from farm to fork, antimicrobials have been widely used since about 1950. Antimicrobials are a large category of molecules used to prevent and treat infections caused by microorganisms in humans, animals, and plants. Antifungals, which control and treat infections caused by fungi, antibacterials, which act on bacteria, antivirals, which fight viruses and finally antiparasitics, which block the action of parasites are considered antimicrobials. Therefore, they occupy an ample space in the food supply chain (Figure 1.2). For example, fungicides are used both pre-harvest and post-harvest in crops to maximize production or to protect post-harvest fruit and vegetables (Leyva Salas et al., 2017). The use of antibacterial agents in animal husbandry is widespread and has not only a therapeutic basis, but it is also linked to prevention. For example, in the case of infectious diseases on a sheep, the entire flock is usually treated to prevent the spread of the disease (Economou and Gousia, 2015). In addition, antimicrobial agents are introduced into long-term foods as preservatives or food additives. Food additives are substances added to foods to preserve their flavor, taste, and appearance. These have been used since ancient times: salting, the use of vinegar for pickles or the use of sulfur dioxide in certain wines. Since the second half of the XX century, with the growing demand for food, and the consequent increase in interest from the consumers, both natural and artificial additives have been used. This has led to the advent of labeling, inserted to make the content present in foods processed by industry and used for sustenance visible to all. In recent years, several studies have been reported on active packaging, i.e. innovative packaging with antimicrobial activity to maintain the quality and integrity of food shelves (Mahato *et al.*, 2021). Another important risk inside the entire food supply chain is the contamination of food by viruses. Typically, foodborne viral diseases are due to raw foods, such as shellfish, fruit, and vegetables. Viruses can replicate in food and reach

humans. An excellent method to increase human antiviral immunological defense is the development of functional and nutraceutical foods, enriched with antiviral compounds (Alkhatib, 2020).

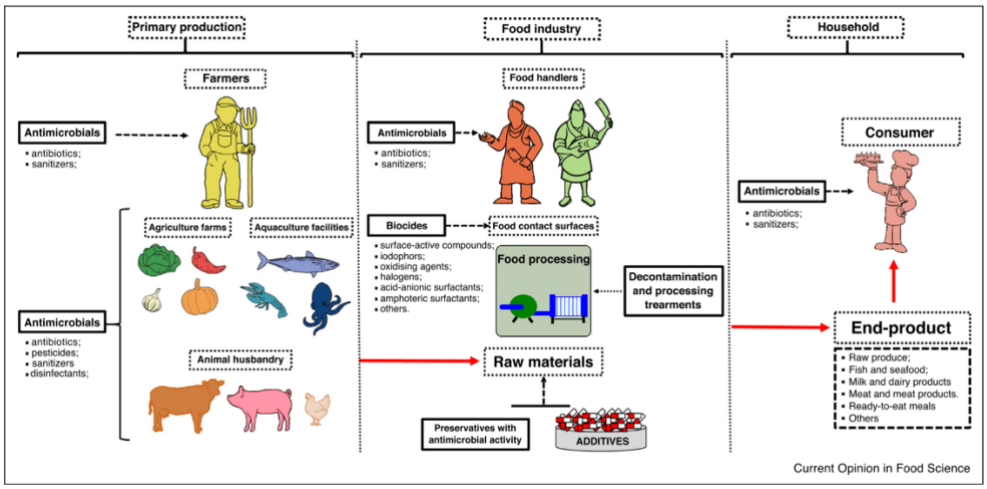

Figure 1.2 *Schematic overview of the main sources of antimicrobials and routes of trasmission of antimicrobial resistance along the food chain (red arrows) (Oniciuc et al., 2019)*

1.1.1 Antifungals

With the increasing growth of world population, a major concern is related to the loss of food. The United Nations Food and Agriculture Organization estimates that around 1.3 billion tons of food is lost or wasted every year (Leyva Salas *et al.*, 2017). Historical writings report that already in the Middle Ages wheat crops were destroyed by a dark and dusty dust, now attributable to the spores of *Tilletia* spp., called bunt mushroom or smelly smut. In 1876, the Phytophthora genus was defined by Anton de Bary as "plant destroyer", having led to the death of more than a million people. Fungi cause huge problems in food supply chain, as they are able to live in harsh environments (Pitt and Hocking, 2009) and, together with fungus-like organisms (FLOs), they cause more plant disease than any other group of plant pests. Furthermore, some fungal genera such as *Aspergillus*, *Penicillium*, *Alternaria* and *Fusarium* can produce secondary metabolites, called mycotoxins, which can have a toxic effect on humans and animals. Fungi, in the form of spores, can deposit and grow at different stages of the product's life: in the field, after

harvesting, during processing, storage and handling. Most plant diseases are caused by fungi, which kill plant cells and/or stress plant. Sources of fungal infections include crop debris, infected seeds, soil, neighboring crops and weeds; in fact, through the wind, the splashes of water or the movements of a contaminated soil, the fungi spread to the plant where they enter through natural openings (such as stomata) or through wounds caused by other factors such as pruning, crops or insects, and other diseases (Sanzani *et al.*, 2016).

Fungi such as Downy mildews and Powdery mildews are responsible for the most common leaf diseases, while other fungi such as *Pythium*, *Fusarium* and *Rhizoctonia* species are soilborne diseases. However, the fungus considered most dangerous because it threatens rice crops is the *Magnaporthe oryzae* (or *Pyricularia oryzae*). In fact, rice is the main source of nourishment for more than half of the world population and the loss of rice crops is a serious economic hardship (Khush, 2005). The disease caused by *Magnaporthe oryzae*, a filamentous ascomycete fungus, on rice is the most destructive in the world. The infection can involve all the leaf tissues, but the infection of the cob can lead to the complete loss of the grain. Generally, crop losses of 10-30% are estimated. Furthermore, *Magnaporthe oryzae* can also affect various grasses and related species, including barley, wheat and millet crops (Couch *et al.*, 2005).

Another particularly infesting fungus is *Botrytis cinerea*, known as gray mold. Due to the availability of the genome sequence and its economic relevance, *B. cinerea* is the most studied necrotrophic fungal pathogen. It can remain latent for long periods before rotting the host tissues (Williamson *et al.*, 2007). It is more destructive on mature or senescent tissues of dicotyledonous hosts. Its ability to attack different species at different stages of the production chain greatly increases management costs. Although applications of biocontrol on crops are recognized (Moser *et al.*, 2008), fungicides remain the most common method of controlling *Botrytis*. Fungicides specifically targeted against *Botrytis* ("botryticides") account for 10% of the world fungicide market.

Wheat diseases are instead caused by *Puccinia* spp., a serious threat also due to the emergence of the Ug99 breed. Among the most harmful pathogenic fungi, there are two species of *Fusarium*. *F. graminearum* primarily affects cereals and some non-cereal species, while *F. oxysporum* has a wide range of hosts, including tomato, cotton, and banana crops (Dean *et al.*, 2012).

To avoid contamination by fungi on the post-harvest products, various disinfection treatments with ozone, chlorine, acidified hydrogen peroxide, etc. or waxes with active coatings containing fungicidal agents and preservatives are used. On the other hand, for field crops, fungal contamination is controlled using fungicides (Davies *et al.*, 2021). Antifungal agents, called fungicides when they kill fungi or fungistatic if they inhibit the growth of fungi, can affect either only certain phases of the fungus life cycle, or they can induce host resistance. In addition to synthetic fungicides, there is also a large range of products identified as biopesticides (microbials, non-viable microbes, biochemicals, genetically modified microbes and transgenic plants). All pesticides that are used in the food chain are regulated by specific institutions, for example in the United States the institution is the Environmental Protection Agency (EPA) (McGrath, 2009). Fungicides can be classified in several ways. The Fungicide Resistance Action Committee (FRAC) has published a list of 43 groups of fungicides based on their mode of action (FRAC, 2021). A summary classification is to separate contact fungicides with multitarget action and fungicides with single-site mode of action. The latter are usually less toxic to non-target organisms and most of the new single mode of action fungicides are considered by the US EPA to be low risk. The disadvantage of fungicides of this type is the greater likelihood of development of resistance.

At first the most used fungicides in agriculture were inorganic type fungicides, starting from 1950 organic compounds have been synthesized and then commercialized, most of which having a specific biological action. Fungicides are essentially classified according to their mechanism of action. Numerous benzimidazoles, for example carbendazim and benomyl inhibit the biosynthesis of microtubules. They act by forming complexes with β-tubulin

and thus leading to an increase in acid production and tubulin polymerization. Several dicarboximides target the glutathione system. For example, iprodione is a contact fungicide with a preventive and eradicating action and acts against *Botrytis* spp. and *Sclerotonia* spp, as well as vinclozolin.

Other fungicides act on the decoupling of oxidative phosphorylation: fluazinam induces mitochondrial membrane disorder. Strobilurins, compounds of natural origin deriving from forest mushrooms, are used to inhibit mitochondrial respiratory chain. These compounds specifically inhibit the cytochrome bc1 complex (complex III). An example of this group of fungicides is given by azoxystrobin, with protective, eradicating, translaminar and systemic properties (Smart, 2003) (Figure 1.3).

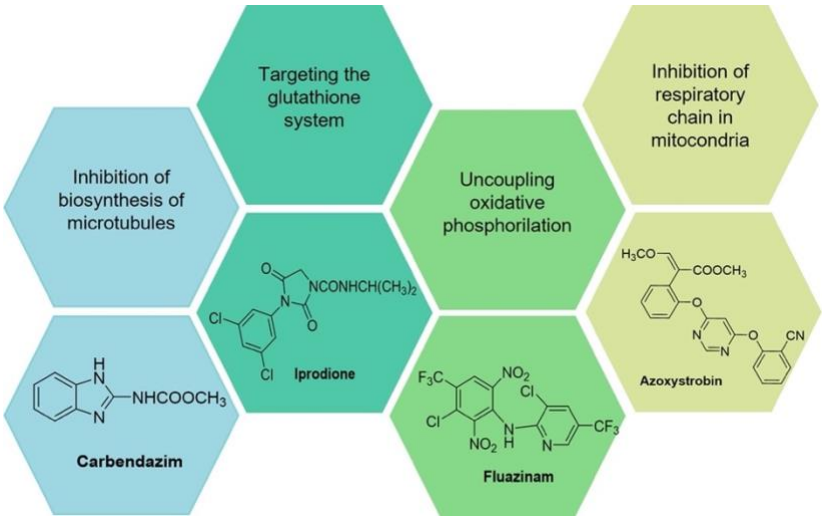

Figure 1.3 *Examples of fungicides classified according to their mechanism of action*

The antifungal sector is affected by the development of antimicrobial resistance (AMR). Once the pathogenic fungus develops a single mutation, (qualitative resistance) in its genetic sequence there is a deleterious loss of disease control which cannot be limited by using higher rates of fungicide or more frequent applications. On the other hand, quantitative resistance marks from the modification of several interacting genes. In this case, the resistance can be recovered either by using greater quantities of fungicide or by applying it more frequently, or by choosing another compound of the same class but

with greater activity. Methylbenzimidazole carbamate (MBC) acting β-tubulins assembly in mitosis, and strobilurins, quinone outside inhibitor (QoI) fungicides, have developed qualitative resistance, while demethylation inhibitory (DMI) fungicides have shown quantitative resistance. The most studied strategies for the development of new antifungals, in order to overcome resistance, concern in particular the research for compounds with potential antifungal activity obtained from natural sources (bacteria, plants and fungi) (Srinivasan *et al.*, 2014). For several decades, natural products have been exploited as fungicides; their structural diversity makes them particularly attractive. Furthermore, these compounds are often less hazardous to the environment, less toxic to non-target organisms and show a high potential for finding new mechanisms of action. A natural product can be used as it is or sometimes it is necessary to make chemical changes to make it either more effective as a fungicide or more stable. Creating synthetic compounds based on the structure and physical properties of the natural product is an adequate method for obtaining new compounds with antifungal activity.

1.1.2 Antibacterials

Several studies have shown that pathogenic bacteria are the leading cause of food epidemics; more than 50% of foodborne outbreaks in the United States result from bacterial infections (Newell *et al.*, 2010; Van Doren *et al.*, 2013).
The cost of illness (COI) was evaluated for some potentially foodborne diseases (e.g. campylobacteriosis, salmonellosis, listeriosis). In New Zealand, the cost of foodborne infections has been estimated at $86 million annually, with about 90% due to campylobacteriosis (Lake *et al.*, 2010). A research conducted by the United States Department of Agriculture (USDA) reported that in the USA five foodborne pathogens (*Campylobacter*, *Salmonella*, *L. monocytogenes*, *E. coli* O157:H7 and *E.coli* non-O157:H7 STEC) cost $6.9 billion annually (Hoffmann *et al.*, 2012). Some of the prevalent foodborne pathogens are reported below (Table 1.1).

Table 1.1 *Selected examples of foodborne outbreaks and recalls caused by pathogenic bacteria (Elkhishin et al., 2017)*

Foodborne outbreak	Pathogenic bacteria	Country	Casualties	Estimated economic losses
Bean sprouts	*Salmonella*	USA	115 people infected, 25 % of ill persons were hospitalized	Contaminated bean sprouts and any remaining products were destroyed
Nut mix	*Salmonella*	New Zealand	No illnesses were reported	Contaminated nut mixes batches were recalled
Fresh cream	*E. coli*	New Zealand	No illnesses were reported	8,700 bottles of fresh cream distributed to retail and foodservice outlets were recalled
Cheese	*L. monocytogenes*	Australia and New Zealand	No illnesses were reported	Cheese was recalled from Australian and New Zealand supermarkets
Chicken	*Salmonella*	Puerto Rico and USA	No illnesses were reported	More than 23,000 units (approximately 102,000 pounds) of contaminated chicken were recalled
Cheeses	*L. monocytogenes*	USA	Six ill persons hospitalized. One death in Minnesota	All cheese products made on a specified date or earlier were recalled and destroyed
Sprouts	*E. coli* O104:H4	Europe and North America	More than 4,000 per- sons were infected	Ban by the EU on the importation of fenugreek seeds and various other seeds, beans, and sprouts from Egypt that were the source of the sprouts responsible for the outbreaks in Germany and France
Spinach	*E. coli* O157:H7	USA	Not specified	Spinach was recalled and banned to sell

Among the bacterial species, *Salmonella* spp., are the significant causes of important foodborne epidemics and diseases, involving real threats to humans all over the world. A scientific survey showed that in the United States, the estimated annual economic loss due to *Salmonella* infections was 2.4 billion dollars in 2014 (Dewey-Mattia *et al.*, 2018). In the USA, there was also an increase of the diseases linked to salmonellosis, going from 18% in 2006 to 38% in 2013 (Dewey-Mattia *et al.*, 2013; Painter *et al.*, 2013). The various

Salmonella spp. can be found in various foods of animal origin, such as red and white meat, due to improper handling and storage of food.

Several strains of *E. coli* can thrive in the intestine of many host species. For example, *E. coli* O157:H7 is recognized as a dangerous foodborne pathogen and can be found in foods from beef and minced meet. Along with this, the *E. coli* producing the Shiga toxin (STEC) are listed as responsible for many outbreaks around the world, resulting in a public cost of $280 million annually in the United States (Hoffmann *et al.*, 2012). These bacteria have been detected mainly in fresh products such as fruits and vegetables. These strains were responsible for an outbreak in the UK, in 2007, (Jay *et al.*, 2007) e in Germany, in 2011 (Rasko *et al.*, 2011).

The primary pathogenic bacterium affecting products of the milk supply chain is *L. monocytogenes*, carrier of various food epidemics that quickly affect infants and elderly. Unlike other bacteria, infection by this bacterium has a high mortality rate of 20-30% (Gillespie *et al.*, 2009), with an estimated economic loss of $2.6 billion in the United States per year (Hoffmann *et al.*, 2012). Between 2009 and 2010, Europe was hit by one of the most severe recognized listeriosis, with a total of 26 infected people, including eight victims in three different states (Schoder *et al.*, 2014).

The severity of the disease caused by *L. monocytogenes* and the difficulties to stop this bacterium in the environment have underlined the importance of improving the food safety system against *Listeria*. Lately, outbreaks of listeriosis have been associated with the ability of *L. monocytogenes* to remain viable within a food throughout the production process (Hoelzer *et al.*, 2012) and improper conservation processes.

Pathogenic bacteria correlated with foodborne outbreaks are one of the most important cause of foodborne illness and have a significant influence on future energies to improve food security. In food supply chain, it is essential to be able to manage all food safety problems that can arise at different stages. It is therefore vital to constantly develop new strategies to reduce the probability of delivering an unsafe product. According to international organizations

(FAO/WHO), agri-food products present the most significant concern in terms of microbiological risks affecting public health (Maskey *et al.*, 2020).

Although the pathogenic bacteria contained in foods mainly of animal origin are well known and over the years they have been fought and eliminated using antibacterial agents, this is no longer enough in recent years.

Since the discovery of penicillin by Alexander Fleming (Tan and Tatsumura, 2015) in 1928, there has been an exponential growth in the use of antibiotics, always associated with the research for new antibiotic classes. Even today, penicillin and other antibiotics are produced in huge quantities. From a scientific point of view, the term antibiotic defines a natural or synthetic chemical substance capable of inhibiting both the growth and survival of bacteria. Among antibiotics, methicillin is one of the most effective. However, a recent study showed that sepsis cases increased from 621,000 to 1,141,000 between 2000 and 2008 (Hayden *et al.*, 2016), due to the emergence of methicillin-resistant *S. aureus* (MRSA). MRSA evidenced the beginning of the development of antibiotic resistance due to pathogens defined ESKAPE (acronym of *Enterococcus faecium*, *S. aureus*, *Klebsiella pneumoniae*, *Acinetobacter baumannii*, *Pseudomonas aeruginosa* and *Enterobacteriaceae*) (Boucher *et al.*, 2009). Four of the six ESKAPE pathogens (*K. pneumoniae*/*E. coli*, *A. baumannii*, *P. aeruginosa*, and *Enterobacter* species) are Gram-negative species.

Antibiotic resistance leads to more than 23,000 and 25,000 deaths per year in the United States and in European, respectively. In addition, deaths are projected to increase from around 700,000 per year to 10 million per year by 2050 due to the presence of drug-resistant microbes threatening global health (Kumar *et al.*, 2020).

In food supply chain, the use of antibiotics is mainly aimed at the growth and weight gain of livestock (herds or flocks), which are regularly fed with low doses of antibiotics in food or water to avoid diseases in animals who live in often crowded and unhealthy spaces. This causes an accumulation of antibiotics in the environment and contributes to the achievement of antibiotic

resistance in microorganisms that encounter an antibiotic (Allen, 2014). Antibiotic resistance is transmitted to humans precisely through the consumption of contaminated food and drink or due to direct contact with animals or the exposure to contaminated environments. Both animal and human pathogens act as donors of antibiotic resistance genes (ARG) to pathogens that infect humans. For example, the continued use of fluoroquinolones (e.g., enrofloxacin) in animal husbandry has given to the spread of ciprofloxacin-resistant *Salmonella*, *Campylobacter* and *E. coli*. Thus, also the abuse in Europe of a glycopeptide (avoparcin) as antibiotic and growth promoter in animals has led to the growth of vancomycin-enterococci resistant (VRE), both in livestock and on the meat of these animals that reaches our tables (Marshall and Levy, 2011).

Recently, the World Health Organization (De Freitas, 2017) included nine Gram-negative bacteria in the list of the twelve “priority pathogens”, for which new antibiotics are urgently needed. The difficult to obtain compounds endowed with Gram-negative antibacterial activity is due to presence of a double membrane. The cytoplasmic membrane is surrounded by a thin layer of peptidoglycan chains (inner membrane, IM), further covered by an outer membrane (OM) (Richter and Hergenrother, 2019).

The OM is constituted of an asymmetric bilayer with an inner leaflet consisting of phospholipids and an outer leaflet of chains of lipopolysaccharides (LPS). LPS layer is composed of the hydrophobic lipid A connected to a hydrophilic negatively charged core of oligosaccharides binding the hydrophilic O antigen. The negative charges are stabilized by divalent cations (Ca^{2+} or Mg^{2+}), resulting in a very tight stacking of LPS molecules, which limits membrane permeation. Moreover, a hydration sphere created by the hydrophilic portion of LPS further obstructs the passage of hydrophobic molecules across the membrane. On the contrary, the OM protein channels, called porins, can be exploited by the small hydrophilic charged or uncharged molecules (≤600 g/mol) to go into the periplasmic space. In addition, antibiotics capable of moving divalent cations (Ca^{2+} or Mg^{2+}) between LPS oligosaccharide portions

(e.g., amino glycosides and polymyxins) can also move across the OM. However, to cross the lipophilic IM, the hydrophilic molecules must exploit the energy-dependent transporter proteins specific to the solute or the proton driving force (PMF), which is dependent on the proton gradient, pH and membrane potential. The presence of several efflux pumps is also a difficult obstacle to overcome, in fact these membrane proteins are able to expel drugs, after their passage through the OM and IM (Figure 1.4) (Richter and Hergenrother, 2019).

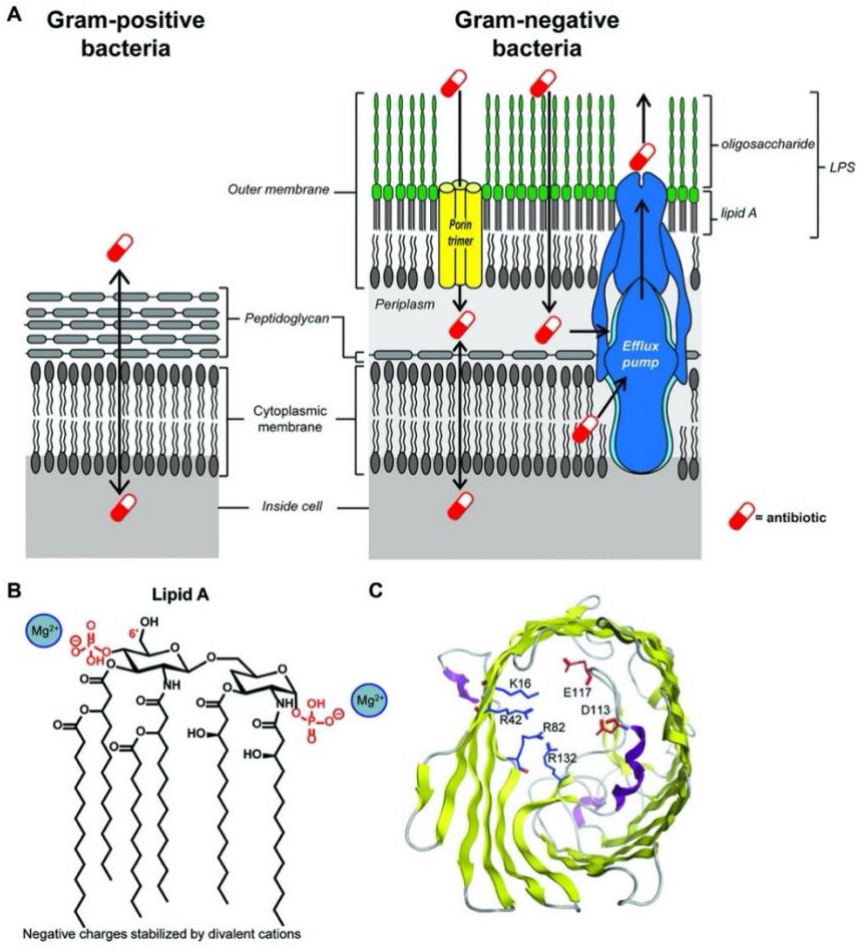

Figure 1.4 *(A) Gram-negative cellular envelope (right) consisting of two lipid membranes, whereas Gram-positive bacteria (left) present only one lipid membrane. (B) The structure of lipid A, the hydrophilic portion of LPS. The core oligosaccharide is linked to the 6' carbon. (C) Top view of OmpF, the prototypical porin from (Richter and Hergenrother, 2019)*

1.1.3 Antiviral agents

Viruses are recognized as one of the most serious risks to human health and economy. Throughout history, various virus epidemics and pandemics have threatened the world's population (Ianevski *et al.*, 2018). In 1997, avian influenza A (H5N1) spread directly from poultry to humans. In 2009, a swine influenza A virus H1N1 caused a pandemic influenza, followed by Middle East Respiratory Syndrome (MERS), caused by a new deadly MERS-CoV (> 30% mortality) in 2012. Nowadays, we have witnessed the loss of thousands of people due to the 2019-nCoV viral pneumonia outbreak, which began in China in December 2019 and officially declared as a pandemic by WHO on 11th March 2020 (Luo and Gao, 2020). Viruses are a group of microorganisms very different from bacterial pathogens of food origin, in fact they are formed by nucleic acids, enclosed within a protein coating called capsid. The viral agent cannot replicate within food, but only within living cells of humans, other animals, plants, or bacteria (Newell *et al.*, 2010). The viral life cycle opens when the virus connects, through electrostatic adsorption, to specific receptors in the host cell. Once penetration into the host cell occurs, the removal of the viral coating and the release of viral nucleic acids happens. In this way, thanks to the resources of the host cell, the virus begins transcription and synthesis of the first viral proteins, followed by nucleic acids replication and, in the case of the retrovirus, the viral integrase (IN) incorporates the viral nucleic acids in the host DNA. Finally, late viral proteins also undergo transcription and translation, and their assembly leads to new viral particles, called "virions", which can be released to infect other cells (Mattio *et al.*, 2020). Some foodborne viruses are extremely stable in the environment and can resist some food processing techniques. In particular, human enteric viruses are mainly transmitted via fecal-oral route and come into contact with humans through various ways, including the consumption of contaminated foods. Among the human enteric viruses, noroviruses (NoV) are the most significant from an epidemiological point of view; they are the leading cause of acute

gastroenteritis worldwide and are recognized as a major cause of foodborne illness (Sabrià *et al.*, 2016). One study has shown that in USA, hNoVs are responsible for approximately 58% of all nationally acquired foodborne illnesses of known etiology (Moore *et al.*, 2015). Besides hNoVs, other groups of viruses can be transmitted via food, such as human enteroviruses (poliovirus, coxsackievirus and echovirus), enteric adenoviruses, hepatitis A and E viruses, rotaviruses, and sapoviruses (Edwards and Dunlop, 2019).

To prevent and control the spread of viruses in long term, the most effective protection is the implementation of specific vaccines for the virus to be combated. Indeed, vaccines represent a significant number (about 47%) of all antiviral agents (185) considering the period between 2015 and 2019 (Newman and Cragg, 2020). Despite this, vaccine development requires a significant amount of time and money (Mahmoud, 2016). Another cure for viruses is treatment with antiviral agents, and many new classes of drugs targeting a wide variety of human viruses have been recently developed. However, antiviral drugs are also subject to continuous challenges in terms of drug dose and phase of selection and intervention (Alkhatib, 2020).

Nutrition plays a particularly interesting role not only in preventing the onset of viral diseases but also in the possibility of strengthening the immune system. Only in recent years, the research has given more attention to the development of functional foods and nutraceuticals. Functional foods and nutraceuticals, therefore enriched with antiviral agents, can be safe and economically advantageous strategies in the fight against viruses. For example, one study found that the optimal intake of specific micronutrients controls the impact of infections from virulent strains, including lower and upper respiratory tract infections, by optimizing a well-functioning immune system (Calder *et al.*, 2020). The introduction of these foods, also linked to an appropriate lifestyle, could help in limiting the contracting of viruses and as an adjuvant therapy to reduce the effects of the disease. Still few studies concern the role of functional foods in communicable diseases (MC), specifically on the defense of the immune system against viral infections, such as COVID-

19. Functional foods, such as fruit, vegetables, oily fish, olive oil, nuts, and legumes, already contain active ingredients or nutraceuticals with important antiviral actions, including polyphenols, terpenoids, flavonoids, alkaloids, sterols, pigments and unsaturated fatty acids (Alkhatib *et al.*, 2018). In addition, most of these foods contain natural vitamins and minerals (e.g. vitamins C, D, B6, B12, A, E and minerals of zinc, copper, iron and selenium) and other phenolic compounds with immunoprotective activity, having antioxidant and anti-inflammatory properties (López-Varela *et al.*, 2002). Recently, studies have shown that fermented food products, such as yogurt, fermented fruit, plants and beverages, containing probiotics, can improve the profile of gut bacteria and respiratory capacity related to the gut-lung axis (García-Burgos *et al.*, 2020).

An interesting example of functional food is olive oil with its constituents (leaves and bark) which appears to act as an immunostimulant; several studies show its ability to act against cardiovascular disease, diabetes and cancer (García-Burgos *et al.*, 2020). Olive oil contains not only unsaturated fatty acids, but also several polyphenols including oleuropein and hydroxytyrosol, which have different antioxidant and anti-inflammatory properties to which a significant antiviral and antibacterial potential is linked. Oleuropein has shown potential antiviral activity against respiratory syncytial virus (RSV), a common upper respiratory virus (URI) (Alkhatib, 2020).

Citrus fruits also contain, in all their parts (peel, pulp, seeds), many compounds, mainly terpenoids and flavonoids, with various biological properties. In a recent study, grapefruit seed extract (GSE) has showed virucidal activity against avian influenza virus (AIV), Newcastle disease virus (NDV) and infectious and bursal disease virus (IBDV) (Komura *et al.*, 2019).

A new being developed strategy involves the production of enriched foods with bioactive compounds. From a circular economy perspective, even the product waste can give a fundamental contribution to making food enriched. In fact, the waste often contains secondary metabolites with interesting biological properties, including antivirals. The natural compounds can be

isolated from waste and inserted into the food that will end up on the market, becoming part of the food supply chain.

1.2 ANTIMICROBIAL RESISTANCE (AMR)

As mentioned in the sections above, nowadays antimicrobial resistance (AMR) is the most urgent problem worldwide. The World Health Organization (WHO) considers antimicrobial resistance as one of the top five public health priorities, noting that: “Antimicrobial resistance is rising to dangerously high levels in all parts of the world. New resistance mechanisms are emerging and spreading globally, threatening our ability to treat common infectious diseases” (WHO, 2017). In fact, multidrug-resistant bacteria (MDR) currently cause about 25,000 deaths in Europe every year (Cassini *et al.*, 2019) and they weigh on the economy about 1.5 billion euros per year. Antimicrobial resistance (AMR) is defined as the ability of a microorganism to evolve and multiply in order to resist the effects of an antimicrobial agent to which it was previously sensitive. Identifying when and where AMR occurs is particularly difficult, in fact the agri-food system is struggling with uncertain pathological geographies and temporalities due to the evolution of microbial ecologies. Some studies have shown that pathogenic microorganisms, including pathogens resistant to treatment with antibiotics or antifungals, can be transmitted from animals to humans through the domesticated food supply chain. Resistance across food supply chain is hard to control as resistance genes because they can move through bacteria of different species (Hughes *et al.*, 2021). As already explained, antimicrobials include any substances with a growth inhibiting or killing effect on microorganisms, either in a clinical setting or on materials and surfaces to reduce bacterial load.

Antimicrobial resistance can be divided into three categories: microbiological resistance (*in vitro* resistance or epidemiological resistance), drug resistance and clinical resistance (*in vivo* resistance) (Verraes *et al.*, 2013). *In vitro* resistance is defined as a lower susceptibility of microorganisms to antimicrobials above a breakpoint defined by the upper limit of normal susceptibility of the species concerned. This type of resistance can be confirmed genotypically by demonstrating the presence of a given

antimicrobial resistance gene or resistance mechanism using molecular techniques. Drug resistance is based on pharmacokinetic parameters and the normal susceptibility of a microbial species. When the minimum inhibitory concentration (MIC) of the antimicrobial for the specific microorganism is in the concentration range that can be achieved by that antimicrobial, then it is sensitive; when the MIC of the antimicrobial for that microorganism is higher than the concentration that can be reached at the site of infection, then the microorganism has developed resistance. At the end, clinical resistance (resistance *in vivo*) means an infection by a specific bacterium that can no longer be treated adequately, and treatment failures are also highlighted (Verraes *et al.*, 2013).

In general, microorganisms can be resistant to antimicrobials through four different mechanisms (Figure 1.5): by degradation of antimicrobial (inactivation of a drug); by modifying a drug target; by limiting the absorption of the antimicrobial; by modifying the permeability of the cell wall (efflux pumps) (Reygaert, 2018).

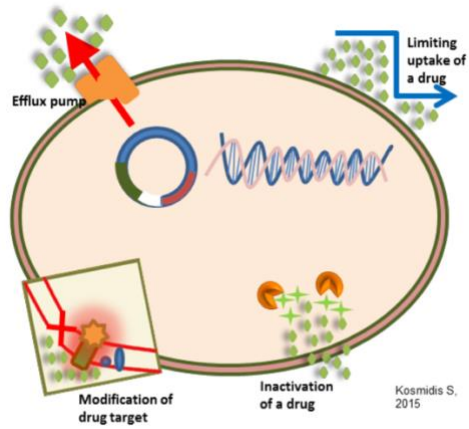

Figure 1.5 *General antimicrobial resistance mechanisms (Reygaert, 2018)*

Among these mechanisms, the most common is enzymatic degradation, for example b-lactamase enzymes hydrolyze the β-lactam ring of β-lactam antibiotics (cephalosporins) (Livermore and Woodford, 2006) or

acyltransferase, nucleotransferase and phosphotransferase inactivate aminoglycosides (Wright, 1999).

The modification of the target generally indicates that the antimicrobial loses its ability to bind a certain target and therefore its activity; examples are mutations in gyrase and topoisomerase genes which are the targets of quinolone and fluoroquinolone antibiotics. In particular, methicillin-resistant *S. aureus* (MRSA) is an example of target modification (Bodhi, 2000). In the case of a change in the permeability of the cell wall, there is an alteration in the entry of the antimicrobial or an increase in efflux. Efflux can be increased specifically with the acquisition of specific genes, as the case for resistance to tetracycline (Annunziato, 2019). Another cause of increased efflux may be the overexpression of physiologically present efflux pumps, resulting in a multidrug-resistant phenotype. Finally, the normal physiological pathway can be changed by the cell by inserting an alternative step, which usually consists of an extra-enzyme. In *E. coli* and *Citrobacter* sp. a further dihydrofolate reductase is produced, with an R-plasmid-determined trimethoprim resistance (Verraes et al., 2013). In the case of fungi, another factor that leads to high levels of resistance consists in the formation of biofilms capable of shielding most of the antifungal agents on the market. In this case, the resistance mechanisms are drastically different from the usual ones and the resistance is multifactorial, with various contributing mechanisms, including the presence of the biofilm matrix, the metabolic and physiological state of the cells, the increase in the number of cells at the internal biofilms, the different composition of sterols and stress responses, etc (Mathé and Van Dijck, 2013).

AMR can be distinguished into intrinsic and acquired. In the first case, resistance is an intrinsic characteristic of a bacterial species or genus towards a given antimicrobial. Thus, the action of the antibiotic does not work and can even worsen the infection (Brachman, 2006). In the second case, resistance is acquired when a susceptible strain develops resistance because of a recent evolution of the strain. Usually, the cause is a spontaneous mutation that

occurs within a bacterial population, or the acquisition of a specific resistance gene by horizontal gene transfer (HGT) (Verraes et al., 2013).

Considering the adaptability and versatility of microorganisms, we can only expect an increasing incidence of antimicrobial resistance to antimicrobials in use throughout the food chain, from agricultural production, through food processing, to the consumer. For this reason, it is necessary to continue the research also relying on new strategies.

1.3 NOVEL STRATEGIES TO OVERCOME AMR

Although each category (antibacterial, antifungal, antiviral) belonging to antimicrobials has its own unique and specific challenges, surprisingly many factors can be brought together. Over the centuries, all foodborne pathogens have developed efficient and effective capabilities to exploit food as a vehicle for pathogen transfer at all levels of the food chain. As we have seen, the involved mechanisms are complex and varied and the pathogens always develop new resistance to antimicrobials. The described approaches by WHO to alleviate the problem of resistance are numerous and concern different fields of action: (1) collaboration between governments, non-governmental organizations, professional groups and international agencies; (2) new networks undertaking surveillance of antimicrobial use and AMR; (3) international approaches for control of counterfeit antimicrobials; (4) incentives for research and development of new antimicrobials and vaccines; (5) new programs and strengthened existing programs to contain AMR (Uchil *et al.*, 2014).

Although a common challenge with most chemical treatments is their effectiveness at dosages and treatment times that do not also adversely affect the products, in agri-food field scientific research is essential to strengthen our current arsenal of antimicrobial agents. From an economic point of view, research for new antimicrobials is not very profitable compared to drugs aimed at chronic diseases. Nevertheless, it is still one of the most effective solutions and a challenge for scientists. Novel compounds can be synthetic, semi-synthetic, or natural products extracted and isolated from different types of matrices (plants, fungi, marine species). Moreover, it is crucial to look for new and more potent anti-infective drugs and to develop antimicrobials with different scaffolds and with new mechanisms of action (Annunziato, 2019). To summarize, the new innovative molecules are part of one or more of these categories:

- multitarget compounds in order to eliminate cross-resistance to known antibiotics,
- new chemical classes, with particular attention to natural compounds,
- compounds acting on new targets,
- molecules with new mechanisms of action.

To protect and protract the use of existing antimicrobial agents, a complementary strategy for discovering new active molecules is the use of antimicrobial adjuvants. Adjuvants are compounds that are not necessarily antimicrobial, but which combined with current antibiotics enhance their activity by minimizing or blocking resistance (Wright, 2016). The concept of antibiotic adjuvant borrows from the success of combinations of antibiotics with even different mechanisms of action can give rise to synergies, covering the microbial spectrum and suppressing resistance (Annunziato, 2019). The result of the sum of the single agents (synergy) is more effective than the single bioactive molecule. One of the most known synergy includes the combination of aminoglycoside with penicillin (e.g. gentamicin+ampicillin) for the treatment of enterococcal infections. A synergistic example in the pre-harvest fungal control habit is the fungicide blends from Bayer and Syngenta which have launched combinations of two fungicides with distinct modes of action and which show additive effects on fungal inhibition (Davies *et al.*, 2021). In general, mixtures of fungicides that act synergistically allow the use of reduced doses of each compound for the desired level of inhibition, potentially reducing costs and environmental impact.

1.4 NATURAL COMPOUNDS AS ANTIMICROBIALS

In recent years, considerable efforts have been made to find natural antimicrobials capable of inhibiting bacterial and fungal growth in food. Common synthetic food preservatives are benzoic acid and benzoates, used in soft-drinks, beer, margarine and acidic foods; nitrites and nitrates presented in processed meats (sausages, hot dogs, bacon, ham and smoked fish) and sulfites consumed in dried fruits, shredded coconut, fruit-based pie fillings. All these synthetic food preservatives are known for their life-threatening side effects (Pisoschi *et al.*, 2018). For these reasons, there is a growing demand for natural products that can serve as fungicides in crops, as alternative food preservatives (Tajkarimi *et al.*, 2010) and as bioactive additives in enriched foods. Nature offers a multitude of structurally interesting compounds from various sources. In fact, natural antimicrobials can be obtained from plants, animals, bacteria, algae and fungi. Since ancient times, natural materials, such as herbs, spices, roots, leaves, barks have been used as traditional medicines, flavorings, or food preservatives. Today, many drugs have been inspired by natural products, which constitute a wide biodiversity of molecules in terms of chemical space and biological properties (Mattio *et al.*, 2020).

In a review by Newman and coworkers it was reported the situation of natural compounds approved in various biological areas between 1981 and 2019. It is interesting to observe that 36 out of the 162 approved antibiotic agents were biologics or vaccines. For the remaining 126 agents, just over 48% of the total consisted of unaltered natural products (N) and derivatives of natural products (ND), while only 22.2% were totally synthetic (mainly based on quinolones). In the same review it is noted that the approved antifungal agents are instead for the most part synthetic, while the antivirals are mostly made up of vaccines. The small molecules used as antivirals are instead synthetic molecules with a portion of natural inspiration (Figure 1.6) (Newman and Cragg, 2020).

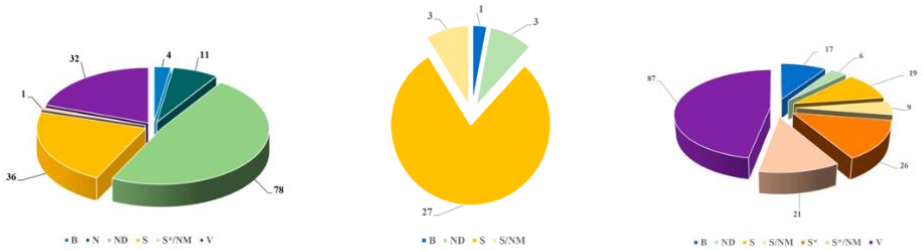

Figure 1.6 *antibiotic, antifungal and antiviral drugs by source. "B": Biological; usually a large (>50 residues) peptide or protein either isolated from an organism/cell line or produced by biotechnological means in a surrogate host; "N": Natural product; "NB": Natural product "Botanical" (in general these have been recently approved); "ND": Derived from a natural product and is usually a semisynthetic modification; "S": Totally synthetic drug, often found by random screening/modification of an existing agent; "S*": Made by total synthesis, but the pharmacophore is/was from a natural product; "V": Vaccine (Newman and Cragg, 2020)*

We can divide the antimicrobial natural compounds considering their origin.

Antimicrobials from plants. To this class of compounds belong mostly secondary metabolites. The main groups of natural compounds responsible for the antimicrobial activity of plants are made up of phenols, phenolic acids, quinones, saponins, flavonoids, tannins, coumarins, terpenoids and alkaloids (Lai and Roy, 2004). Clearly, the variations in the structure and chemical composition of these compounds determine substantial differences in their antimicrobial action. This activity inhibits the generation of reactive oxygen species, eliminating free radicals and reducing the growth redox potential. In this way, the growth of unwanted microorganisms is also reduced (Cueva *et al.*, 2010). The antimicrobial activity of phenolic compounds is influenced not only by the number of hydroxyl groups but also by their location (Dorman and Deans, 2000). Recent studies report the antimicrobial capacity of essential oils (EO) of plants. The low molecular weight compound mixture of EOs has several biochemical properties that often increase the efficacy of antimicrobial activity. The antimicrobial activity is due not only to the chemical composition but also to the lipophilic properties, the potency of the functional groups or the solubility in water and EOs (Dorman and Deans, 2000). Furthermore, an excellent source of precious bioactive compounds is constituted by food processing waste, such as fruit pomace, seeds, peels, unused pulps. In fact, phenolic compounds (polyphenols, tannins and flavonoids) and many other

bioactive components can be extracted and obtained from waste products (Engels et al., 2009). One study has shown that total phenols in lemon, orange and grapefruit peels are 15% higher than the amount found in peeled fruit (Gorinstein et al., 2001).

Antimicrobials from animals. Antimicrobial compounds of animal origin include primary metabolites such as lactoferrin, chitosane and milk-derived peptides. Lactoferrin is an iron-binding glycoprotein found in milk that acts as an antimicrobial against various species of bacteria and as an antiviral. In the United States, the use of lactoferrin on beef and associated products as a preservative has been approved (Gyawali and Ibrahim, 2014). The antimicrobial properties of this protein are reported against foodborne microorganisms including *Carnobacterium*, *L. monocytogenes*, *E. coli* and *Klebsiella* (Al-Nabulsi and Holley, 2005). Recently, the chitosan has gotten considerable interest in the food sector as an antimicrobial. Chitosan is a polysaccharide naturally present in the exoskeletons of shellfish and arthropods (Tikhonov *et al*., 2006). The major limitation for its application as a food preservative has been its insolubility in water at neutral or higher pH. This limitation was overcome by using derivatives of the N-alkylated disaccharide chitosan, which showed good antibacterial activity against *E. coli* and *S. aureus* (Gyawali and Ibrahim, 2014). Among dairy products, casein contain proteins with multifunctional properties, including antimicrobial properties against a wide range of pathogenic microorganisms such as *E. coli*, *Helicobacter*, *Listeria*, *Salmonella*, *Staphylococcus*, yeast and filamentous fungi (Gyawali and Ibrahim, 2014). Casein accounts for 80% of total milk protein and is a rich source of bioactive peptides, for example isracidin has been shown to be effective against *S. aureus*, *L. monocytogenes* and *C. albicans* (Gyawali and Ibrahim, 2014).

Antimicrobials from marine species, fungi and bacteria. In recent years, interest in natural sources such as marine species (algae, sea sponges) and

fungi has been growing. The rich diversity of these species offers bioactive compounds with a wide range of biological activities, such as antibiotic, antiviral, antioxidant, antifouling, anti-inflammatory, cytotoxic, antimitotic, and other activities (Plaza *et al*., 2010). Only recently, the antimicrobial activity of marine species, in particular algae, and fungi is being evaluated in food preservation. For example, phlorotannins, isolated from brown marine algae, inhibit the growth of food-borne pathogenic bacteria and antibiotic-resistant bacteria (Eom *et al.*, 2012). Among the mushrooms, we must distinguish the edible mushrooms on which research is taking the first steps and fungi. Already from the 1970s, from wood rooting basidiomycetes fungi such as *Strobilurus tenacellus* (Pers. Ex Fr.) Singer and *Oudemansiella mucida* (Schrad. Ex Fr.) Hohn, or from the gliding bacterium *Myxococcus fulvus* (Bartlett *et al*., 2002) compounds, called strobilurins, have been isolated. Structurally, their common feature is the presence of a portion of methyl (E)-3-methoxy-2-(5-phenylpenta-2,4-dienyl) acrylate (β-methoxy acrylate) (Fernandez-Ortuno *et al*., 2010). The isolation of this class of compounds provided the starting point for the development of a collection of compounds with antifungal activity. In fact, even today this class of compounds is among the best-selling in the world in the agricultural sector.

1.5 BIBLIOGRAPHY

Al-Nabulsi, A.A. and Holley, R.A., 2005. Effect of bovine lactoferrin against Carnobacterium viridans, Food Microbiol., 22(2–3), 179–187. doi:10.1016/j.fm.2004.06.001.

Alkhatib, A., 2020. Antiviral functional foods and exercise lifestyle prevention of coronavirus, Nutrients, 12(9), 1–17. doi:10.3390/nu12092633.

Alkhatib, A., Tsang, C. and Tuomilehto, J., 2018. Olive oil nutraceuticals in the prevention and management of diabetes: From molecules to lifestyle, Int. J. Mol. Sci., 19(7). doi:10.3390/ijms19072024.

Allen, H.K., 2014. Antibiotic resistance gene discovery in food-producing animals, Curr. Opin. Microbiol., 19(1), 25–29. doi:10.1016/j.mib.2014.06.001.

Annunziato, G., 2019. Strategies to overcome antimicrobial resistance (AMR) making use of non-essential target inhibitors: A review, Int. J. Mol. Sci., 20(23). doi:10.3390/ijms20235844.

Aung, M.M. and Chang, Y.S., 2014. Traceability in a food supply chain: Safety and quality perspectives, Food Control, 39(1), 172–184. doi:10.1016/j.foodcont.2013.11.007.

Bartlett, D.W., Clough, J.M., Godwin, J.R., Hall, A.A., Hamer, M. and Parr-Dobrzanski, B., 2002. The strobilurin fungicides, Pest Manag. Sci., 58(7), 649–662. doi:10.1002/ps.520.

Bodhi, B., 2000. Samyutta Nikaya - The Connected Discourses of the Buddha: a translation of the, 183(22), 6525–6531. doi:10.1128/JB.183.22.6525.

Boucher, H.W., Talbot, G.H., Bradley, J.S., Edwards, J.E., Gilbert, D., Rice, L.B., Scheld, M., Spellberg, B. and Bartlett, J., 2009. Bad bugs, no drugs: No ESKAPE! An update from the Infectious Diseases Society of America, Clin. Infect. Dis., 48(1), 1–12. doi:10.1086/595011.

Van Boxstael, S., Habib, I., Jacxsens, L., De Vocht, M., Baert, L., Van De

Perre, E., Rajkovic, A., Lopez-Galvez, F., Sampers, I., Spanoghe, P., De Meulenaer, B. and Uyttendaele, M., 2013. Food safety issues in fresh produce: Bacterial pathogens, viruses and pesticide residues indicated as major concerns by stakeholders in the fresh produce chain, Food Control, 32(1), 190–197. doi:10.1016/j.foodcont.2012.11.038.

Brachman, P.S., 2006. Gastroenteritis at a University in Texas: An Epidemiologic Case Study, Emerg. Infect. Dis., 12(7), 1180–1180. doi:10.3201/eid1207.060457.

Bryden, W.L., 2012. Mycotoxin contamination of the feed supply chain: Implications for animal productivity and feed security, Anim. Feed Sci. Technol., 173(1–2), 134–158. doi:10.1016/j.anifeedsci.2011.12.014.

Reygaert, W.C., 2018. An overview of the antimicrobial resistance mechanisms of bacteria, AIMS Microbiol., 4(3), 482–501. doi:10.3934/microbiol.2018.3.482.

Calder, P.C., Carr, A.C., Gombart, A.F. and Eggersdorfer, M., 2020. Reply to 'comment on: Optimal nutritional status for a well-functioning immune system is an important factor to protect against viral infections. nutrients 2020, 12, 1181', Nutrients, 12(8), 1–3. doi:10.3390/nu12082326.

Carvalho, F.P., 2006. Agriculture, pesticides, food security and food safety, Environ. Sci. Policy, 9(7–8), 685–692. doi:10.1016/j.envsci.2006.08.002.

Cassini, A., Högberg, L.D., Plachouras, D., Quattrocchi, A., Hoxha, A., Hopkins, S., *et al.*, 2019. Attributable deaths and disability-adjusted life-years caused by infections with antibiotic-resistant bacteria in the EU and the European Economic Area in 2015: a population-level modelling analysis, Lancet Infect. Dis., 19(1), 56–66. doi:10.1016/S1473-3099(18)30605-4.

Couch, B.C., Fudal, I., Lebrun, M.H., Tharreau, D., Valent, B., Van Kim, P., Nottéghem, J.L. and Kohn, L.M., 2005. Origins of host-specific populations of the blast pathogen Magnaporthe oryzae in crop domestication with subsequent expansion of pandemic clones on rice and weeds of rice,

Genetics, 170(2), 613–630. doi:10.1534/genetics.105.041780.

Cueva, C., Moreno-Arribas, M.V., Martín-Álvarez, P.J., Bills, G., Vicente, M.F., Basilio, A., Rivas, C.L., Requena, T., Rodríguez, J.M. and Bartolomé, B., 2010. Antimicrobial activity of phenolic acids against commensal, probiotic and pathogenic bacteria, Res. Microbiol., 161(5), 372–382. doi:10.1016/j.resmic.2010.04.006.

Davies, C.R., Wohlgemuth, F., Young, T., Violet, J., Dickinson, M., Sanders, J.W., Vallieres, C. and Avery, S. V., 2021. Evolving challenges and strategies for fungal control in the food supply chain, Fungal Biol. Rev., 36, 15–26. doi:10.1016/j.fbr.2021.01.003.

Dean, R., Van Kan, J.A.L., Pretorius, Z.A., Hammond-Kosack, K.E., Di Pietro, A., Spanu, P.D., Rudd, J.J., Dickman, M., Kahmann, R., Ellis, J. and Foster, G.D., 2012. The Top 10 fungal pathogens in molecular plant pathology, Mol. Plant Pathol., 13(4), 414–430. doi:10.1111/j.1364-3703.2011.00783.x.

Dewey-Mattia, D., Bennett, S.D., Mungai, E. and Gould, L.H., 2013. Surveillance for Foodborne Disease Outbreaks United States, 2013 Annual Report.

Dewey-Mattia, D., Manikonda, K., Hall, A.J., Wise, M.E. and Crowe, S.J., 2018. Surveillance for Foodborne Disease Outbreaks — United States, 2009–2015, MMWR. Surveill. Summ., 67(10), 1–11. doi:10.15585/mmwr.ss6710a1.

Van Doren, J.M., Neil, K.P., Parish, M., Gieraltowski, L., Gould, L.H. and Gombas, K.L., 2013. Foodborne illness outbreaks from microbial contaminants in spices, 1973-2010, Food Microbiol., 36(2), 456–464. doi:10.1016/j.fm.2013.04.014.

Dorman, H.J.D. and Deans, S.G., 2000. Antimicrobial agents from plants: Antibacterial activity of plant volatile oils, J. Appl. Microbiol., 88(2), 308–316. doi:10.1046/j.1365-2672.2000.00969.x.

Economou, V. and Gousia, P., 2015. Agriculture and food animals as a source

of antimicrobial-resistant bacteria, Infect. Drug Resist., 8, 49–61. doi:10.2147/IDR.S55778.

Edwards, D. and Dunlop, D.J., 2019. *Food Microbiology: fundamentals and frontiers*. Edited by M.P. Doyle, F. Diez-Gonzalez, and C. Hill. Washington, DC, USA: ASM Press. doi:10.1128/9781555819972.

Elkhishin, M.T., Gooneratne, R. and Hussain, M.A., 2017. Microbial Safety of Foods in the Supply Chain and Food Security, Adv. Food Technol. Nutr. Sci. - Open J., 3(1), 22–32. doi:10.17140/aftnsoj-3-141.

Engels, C., Knödler, M., Zhao, Y.Y., Carle, R., Gänzle, M.G. and Schieber, A., 2009. Antimicrobial activity of gallotannins isolated from mango (Mangifera indica L.) kernels, J. Agric. Food Chem., 57(17), 7712–7718. doi:10.1021/jf901621m.

Eom, S.H., Kim, Y.M. and Kim, S.K., 2012. Antimicrobial effect of phlorotannins from marine brown algae, Food Chem. Toxicol., 50(9), 3251–3255. doi:10.1016/j.fct.2012.06.028.

EU, 2020. Farm to Fork Strategy, DG SANTE/Unit 'Food Inf. Compos. food waste"', (DG SANTE/Unit 'Food Inf. Compos. food waste"'), 23.

Fernandez-Ortuno, D., Tores A., J., de Vicente, A. and Perez-garcia, A., 2010. The QoI Fungicides, the Rise and Fall of a Successful Class of Agricultural Fungicides, Fungicides [Preprint]. doi:10.5772/13205.

FRAC, 2021. FRAC Code List FRAC Code List ©* 2021: Fungal control agents sorted by cross resistance pattern and mode of action (including coding for FRAC Groups on product labels), 17.

De Freitas, L.C., 2017. *WHO (2017) Global priority list of antibiotic-resistant bacteria to guide research, discovery, and development of new antibiotics.*, Cad. Pesqui. Available at: http://www.cdc.gov/drugresistance/threat-report-2013/.

García-Burgos, M., Moreno-Fernández, J., Alférez, M.J.M., Díaz-Castro, J.

and López-Aliaga, I., 2020. New perspectives in fermented dairy products and their health relevance, J. Funct. Foods, 72(April), 104059. doi:10.1016/j.jff.2020.104059.

Gillespie, I.A., McLauchlin, J., Little, C.L., Penman, C., Mook, P., Grant, K. and O'Brien, S.J., 2009. Disease presentation in relation to infection foci for non-pregnancy- associated human listeriosis in England and Wales, 2001 to 2007, J. Clin. Microbiol., 47(10), 3301–3307. doi:10.1128/JCM.00969-09.

Gorinstein, S., Martín-Belloso, O., Park, Y.S., Haruenkit, R., Lojek, A., Íž, M., Caspi, A., Libman, I. and Trakhtenberg, S., 2001. Comparison of some biochemical characteristics of different citrus fruits, Food Chem., 74(3), 309–315. doi:10.1016/S0308-8146(01)00157-1.

Greig, J.D. and Ravel, A., 2009. Analysis of foodborne outbreak data reported internationally for source attribution, Int. J. Food Microbiol., 130(2), 77–87. doi:10.1016/j.ijfoodmicro.2008.12.031.

Gyawali, R. and Ibrahim, S.A., 2014. Natural products as antimicrobial agents, Food Control, 46, 412–429. doi:10.1016/j.foodcont.2014.05.047.

Havelaar, A.H., Brul, S., de Jong, A., de Jonge, R., Zwietering, M.H. and ter Kuile, B.H., 2010. Future challenges to microbial food safety, Int. J. Food Microbiol., 139(SUPPL. 1), S79–S94. doi:10.1016/j.ijfoodmicro.2009.10.015.

Hayden, G.E., Tuuri, R.E., Scott, R., Losek, J.D., Blackshaw, A.M., Schoenling, A.J., Nietert, P.J. and Hall, G.A., 2016. Triage sepsis alert and sepsis protocol lower times to fluids and antibiotics in the ED, Am. J. Emerg. Med., 34(1), 1–9. doi:10.1016/j.ajem.2015.08.039.

Henson, S. and Traill, B., 1993. The demand for food safety. Market imperfections and the role of government, Food Policy, 18(2), 152–162. doi:10.1016/0306-9192(93)90023-5.

Hobbs, J.E., 2021. Food supply chain resilience and the COVID-19 pandemic: What have we learned?, Can. J. Agric. Econ., 69(2), 189–196.

doi:10.1111/cjag.12279.

Hoelzer, K., Pouillot, R., Gallagher, D., Silverman, M.B., Kause, J. and Dennis, S., 2012. Estimation of Listeria monocytogenes transfer coefficients and efficacy of bacterial removal through cleaning and sanitation, Int. J. Food Microbiol., 157(2), 267–277. doi:10.1016/j.ijfoodmicro.2012.05.019.

Hoffmann, S., Batz, M.B. and Morris, J.G., 2012. Annual cost of illness and quality-adjusted life year losses in the united states due to 14 foodborne pathogens, J. Food Prot., 75(7), 1292–1302. doi:10.4315/0362-028X.JFP-11-417.

Hughes, A., Roe, E. and Hocknell, S., 2021. Food supply chains and the antimicrobial resistance challenge: On the framing, accomplishments and limitations of corporate responsibility, Environ. Plan. A, 1–18. doi:10.1177/0308518X211015255.

Ianevski, A., Zusinaite, E., Kuivanen, S., Strand, M., Lysvand, H., Teppor, M., Kakkola, L., Paavilainen, H., Laajala, M., Kallio-Kokko, H., Valkonen, M., Kantele, A., Telling, K., Lutsar, I., Letjuka, P., Metelitsa, N., Oksenych, V., Bjørås, M., Nordbø, S.A., Dumpis, U., Vitkauskiene, A., Öhrmalm, C., Bondeson, K., Bergqvist, A., Aittokallio, T., Cox, R.J., Evander, M., Hukkanen, V., Marjomaki, V., Julkunen, I., Vapalahti, O., Tenson, T., Merits, A. and Kainov, D., 2018. Novel activities of safe-in-human broad-spectrum antiviral agents, Antiviral Res., 154, 174–182. doi:10.1016/j.antiviral.2018.04.016.

Jay, M.T., Cooley, M., Carychao, D., Wiscomb, G.W., Sweitzer, R.A., Crawford-Miksza, L., Farrar, J.A., Lau, D.K., O'Connell, J., Millington, A., Asmundson, R. V., Atwill, E.R. and Mandrell, R.E., 2007. Escherichia coli O157:H7 in feral swine near spinach fields and cattle, central California coast, Emerg. Infect. Dis., 13(12), 1908–1911. doi:10.3201/eid1312.070763.

Khush, G.S., 2005. What it will take to Feed 5.0 Billion Rice consumers in 2030, Plant Mol. Biol., 59(1), 1–6. doi:10.1007/s11103-005-2159-5.

Komura, M., Suzuki, M., Sangsriratanakul, N., Ito, M., Takahashi, S., Alam,

M.S., Ono, M., Daio, C., Shoham, D. and Takehara, K., 2019. Inhibitory effect of grapefruit seed extract (Gse) on avian pathogens, J. Vet. Med. Sci., 81(3), 466–472. doi:10.1292/jvms.18-0754.

Kumar, S.B., Arnipalli, S.R. and Ziouzenkova, O., 2020. Antibiotics in food chain: The consequences for antibiotic resistance, Antibiotics, 9(10), 1–26. doi:10.3390/antibiotics9100688.

Kuo, J.C. and Chen, M.C., 2010. Developing an advanced Multi-Temperature Joint Distribution System for the food cold chain, Food Control, 21(4), 559–566. doi:10.1016/j.foodcont.2009.08.007.

Lai, P. and Roy, J., 2004. Antimicrobial and Chemopreventive Properties of Herbs and Spices, Curr. Med. Chem., 11(11), 1451–1460. doi:10.2174/0929867043365107.

Lake, R.J., Cressey, P.J., Campbell, D.M. and Oakley, E., 2010. Risk ranking for foodborne microbial hazards in New Zealand: Burden of disease estimates, Risk Anal., 30(5), 743–752. doi:10.1111/j.1539-6924.2009.01269.x.

Leyva Salas, M., Mounier, J., Valence, F., Coton, M., Thierry, A. and Coton, E., 2017. Antifungal microbial agents for food biopreservation—a review, Microorganisms, 5(3), 1–35. doi:10.3390/microorganisms5030037.

Livermore, D.M. and Woodford, N., 2006. The β-lactamase threat in Enterobacteriaceae, Pseudomonas and Acinetobacter, Trends Microbiol., 14(9), 413–420. doi:10.1016/j.tim.2006.07.008.

López-Varela, S., González-Gross, M. and Marcos, A., 2002. Functional foods and the immune system: A review, Eur. J. Clin. Nutr., 56, S29–S33. doi:10.1038/sj.ejcn.1601481.

Luo, G. and Gao, S.J., 2020. Global health concerns stirred by emerging viral infections, J. Med. Virol., 92(4), 399–400. doi:10.1002/jmv.25683.

Magan, N., Medina, A. and Aldred, D., 2011. Possible climate-change effects

on mycotoxin contamination of food crops pre- and postharvest, Plant Pathol., 60(1), 150–163. doi:10.1111/j.1365-3059.2010.02412.x.

Mahato, D.K., Mishra, A.K. and Kumar, P., 2021. Nanoencapsulation for Agri-Food Applications and Associated Health and Environmental Concerns, Front. Nutr., 8(April), 1–6. doi:10.3389/fnut.2021.663229.

Mahmoud, A., 2016. New vaccines: challenges of discovery, Microb. Biotechnol., 9(5), 549–552. doi:10.1111/1751-7915.12397.

Marshall, B.M. and Levy, S.B., 2011. Food animals and antimicrobials: Impacts on human health, Clin. Microbiol. Rev., 24(4), 718–733. doi:10.1128/CMR.00002-11.

Maskey, R., Fei, J. and Nguyen, H.-O., 2020. Critical factors affecting information sharing in supply chains, Prod. Plan. Control, 31(7), 557–574. doi:10.1080/09537287.2019.1660925.

Mathé, L. and Van Dijck, P., 2013. Recent insights into Candida albicans biofilm resistance mechanisms, Curr. Genet., 59(4), 251–264. doi:10.1007/s00294-013-0400-3.

Mattio, L.M., Catinella, G., Pinto, A. and Dallavalle, S., 2020. Natural and nature-inspired stilbenoids as antiviral agents, Eur. J. Med. Chem., 202. doi:10.1016/j.ejmech.2020.112541.

McGrath, M.T., 2009. Fungicides and other Chemical Approaches for use in Plant Disease Control, Encycl. Microbiol., 412–421. doi:10.1016/B978-012373944-5.00357-6.

Moore, M.D., Goulter, R.M. and Jaykus, L.-A., 2015. Human Norovirus as a Foodborne Pathogen: Challenges and Developments, Annu. Rev. Food Sci. Technol., 6(1), 411–433. doi:10.1146/annurev-food-022814-015643.

Moser, R., Pertot, I., Elad, Y. and Raffaelli, R., 2008. Farmers' attitudes toward the use of biocontrol agents in IPM strawberry production in three countries, Biol. Control, 47(2), 125–132. doi:10.1016/j.biocontrol.2008.07.012.

Newell, D.G., Koopmans, M., Verhoef, L., Duizer, E., Aidara-Kane, A., Sprong, H., Opsteegh, M., Langelaar, M., Threfall, J., Scheutz, F., der Giessen, J. van and Kruse, H., 2010. Food-borne diseases - The challenges of 20years ago still persist while new ones continue to emerge, Int. J. Food Microbiol., 139(SUPPL. 1), S3–S15. doi:10.1016/j.ijfoodmicro.2010.01.021.

Newman, D.J. and Cragg, G.M., 2020. Natural products as sources of new drugs over the nearly four decades from 01/1981 to 09/2019, J. Nat. Prod., 83(3), 770–803. doi:10.1021/acs.jnatprod.9b01285.

Oniciuc, E.-A., Likotrafiti, E., Alvarez-Molina, A., Prieto, M., López, M. and Alvarez-Ordóñez, A., 2019. Food processing as a risk factor for antimicrobial resistance spread along the food chain, Curr. Opin. Food Sci., 30, 21–26. doi:10.1016/j.cofs.2018.09.002.

Painter, J.A., Hoekstra, R.M., Ayers, T., Tauxe, R. V., Braden, C.R., Angulo, F.J. and Griffin, P.M., 2013. Attribution of foodborne illnesses, hospitalizations, and deaths to food commodities by using outbreak data, United States, 1998-2008, Emerg. Infect. Dis., 19(3), 407–415. doi:10.3201/eid1903.111866.

Pisoschi, A.M., Pop, A., Georgescu, C., Turcuş, V., Olah, N.K. and Mathe, E., 2018. An overview of natural antimicrobials role in food, Eur. J. Med. Chem., 143, 922–935. doi:10.1016/j.ejmech.2017.11.095.

Pitt, J. and Hocking, A., 2009. *Fungi and Food Spoilage*, Springer New York. doi:10.1007/978-0-387-92207-2.

Plaza, M., Santoyo, S., Jaime, L., García-Blairsy Reina, G., Herrero, M., Señoráns, F.J. and Ibáñez, E., 2010. Screening for bioactive compounds from algae, J. Pharm. Biomed. Anal., 51(2), 450–455. doi:10.1016/j.jpba.2009.03.016.

Rasko, D.A., Webster, D.R., Sahl, J.W., Bashir, A., Boisen, N., Scheutz, F., Paxinos, E.E., Sebra, R., Chin, C.-S., Iliopoulos, D., Klammer, A., Peluso, P., Lee, L., Kislyuk, A.O., Bullard, J., Kasarskis, A., Wang, S., Frimodt-Møller, J.,

Struve, C., Petersen, A.M., Krogfelt, K.A., Nataro, J.P., Eric E. Schadt and Waldor, M.K., 2011. Origins of the E. coli Strain Causing an Outbreak of Hemolytic–Uremic Syndrome in Germany, N. Engl. J. Med., 365(8), 709–717. doi: 10.1056/NEJMoa1106920

Richter, M.F. and Hergenrother, P.J., 2019. The challenge of converting Gram-positive-only compounds into broad-spectrum antibiotics, Ann. N. Y. Acad. Sci., 1435(1), 18–38. doi:10.1111/nyas.13598.

Sabrià, A., Pintó, R.M., Bosch, A., Bartolomé, R., Cornejo, T., Torner, N., Martínez, A., Simón, M. de, Domínguez, A. and Guix, S., 2016. Norovirus shedding among food and healthcare workers exposed to the virus in outbreak settings, J. Clin. Virol., 82, 119–125. doi:10.1016/j.jcv.2016.07.012.

Sanzani, S.M., Reverberi, M. and Geisen, R., 2016. Mycotoxins in harvested fruits and vegetables: Insights in producing fungi, biological role, conducive conditions, and tools to manage postharvest contamination, Postharvest Biol. Technol., 122, 95–105. doi:10.1016/j.postharvbio.2016.07.003.

Schoder, D., Stessl, B., Szakmary-Brändle, K., Rossmanith, P. and Wagner, M., 2014. Population diversity of Listeria monocytogenes in quargel (acid curd cheese) lots recalled during the multinational listeriosis outbreak 2009/2010, Food Microbiol., 39, 68–73. doi:10.1016/j.fm.2013.11.006.

Smart, N., 2003. FUNGICIDES, in Encycl. Food Sci. Nutr. Elsevier, 2832–2842. doi:10.1016/B0-12-227055-X/00543-5.

Srinivasan, A., Lopez-Ribot, J.L. and Ramasubramanian, A.K., 2014. Overcoming antifungal resistance, Drug Discov. Today Technol., 11(1), 65–71. doi:10.1016/j.ddtec.2014.02.005.

Tajkarimi, M.M., Ibrahim, S.A. and Cliver, D.O., 2010. Antimicrobial herb and spice compounds in food, Food Control, 21(9), 1199–1218. doi:10.1016/j.foodcont.2010.02.003.

Tan, S.Y. and Tatsumura, Y., 2015. Alexander Fleming (1881–1955):

Discoverer of penicillin, Singapore Med. J., 56(7), 366–367. doi:10.11622/smedj.2015105.

Tikhonov, V.E., Stepnova, E.A., Babak, V.G., Yamskov, I.A., Palma-Guerrero, J., Jansson, H.B., Lopez-Llorca, L. V., Salinas, J., Gerasimenko, D. V., Avdienko, I.D. and Varlamov, V.P., 2006. Bactericidal and antifungal activities of a low molecular weight chitosan and its N-/2(3)-(dodec-2-enyl)succinoyl/-derivatives, Carbohydr. Polym., 64(1), 66–72. doi:10.1016/j.carbpol.2005.10.021.

Uchil, R.R., Kohli, G.S., Katekhaye, V.M. and Swami, O.C., 2014. Strategies to combat antimicrobial resistance, J. Clin. Diagnostic Res., 8(7), 8–11. doi:10.7860/JCDR/2014/8925.4529.

Verraes, C., Van Boxstael, S., Van Meervenne, E., Van Coillie, E., Butaye, P., Catry, B., de Schaetzen, M.A., Van Huffel, X., Imberechts, H., Dierick, K., Daube, G., Saegerman, C., De Block, J., Dewulf, J. and Herman, L., 2013. Antimicrobial resistance in the food chain: A review, Int. J. Environ. Res. Public Health, 10(7), 2643–2669. doi:10.3390/ijerph10072643.

WHO, 2017. Global action plan on antimicrobial resistance, World Heal. Organ., 1–28.

Williamson, B., Tudzynski, B., Tudzynski, P. and Van Kan, J.A.L., 2007. Botrytis cinerea: The cause of grey mould disease, Mol. Plant Pathol., 8(5), 561–580. doi:10.1111/j.1364-3703.2007.00417.x.

Wright, G.D., 1999. Aminoglycoside-modifying enzymes, Curr. Opin. Microbiol., 2(5), 499–503. doi:10.1016/S1369-5274(99)00007-7.

Wright, G.D., 2016. Antibiotic Adjuvants: Rescuing Antibiotics from Resistance, Trends Microbiol., 24(11), 862–871. doi:10.1016/j.tim.2016.06.009.

2 AIM OF THE THESIS

Antimicrobials are used in the entire food supply chain, from farm to fork. All sectors from primary production, through the food industry, up to household, are subject to the use of antifungals, antibacterials, antivirals that play different roles at all levels of food production. In agriculture there is a wide application of fungicides, necessary to maximize crops and protect pre- and post-harvest products. Antibacterial agents are also widely used, and they play multiple function. They are administered in livestock farms both to take care of animals, but also to protect them and prevent antimicrobial diseases; additionally, they are introduced during food treatments as additives and preservatives to extend the product shelf-life. Viruses can contaminate food and reach humans, becoming a risk to their health. One possibility to counteract viruses is to create foods enriched with antivirals that increase the human immunological response. The use and sometimes even the abuse of antimicrobials in the food supply chain has led to the development of microorganisms resistant to common antimicrobial agents. Antimicrobial resistance is considered by WHO one of the top five public health priorities and several institutions around the world are working to study new defense strategies. The strategies involve various political, economic, and scientific fields. In the agri-food field, scientific research has concentrated on several perspectives: the study of dosages and treatment times in order to preserve the antimicrobials already in use; the benefit of adjuvants that combined with current antibiotics improve their activity; the improvement of the arsenal of antimicrobial compounds with new innovative molecules. The novel antimicrobial compounds can have one or more of these characteristics: multitarget action, novel scaffolds, ability to hit original targets and to act with new mechanisms of action. As we highlighted in the introduction, the secondary metabolites derived from natural resources are an incredible inspiration to develop novel antimicrobial agents.

Considering the above, the aim of this PhD thesis was to expand the arsenal of antimicrobials following chemical approaches. In particular, we investigated natural and nature-inspired molecules with potential fungicidal, antibacterial, and antiviral activity using synthetic approach and extraction-isolation method from natural waste.

The first part of the thesis was dedicated to rational design and synthesis of new compounds with antifungal potential against *Pyricularia oryzae*, one of the most aggressive fungal diseases of cultivated rice worldwide. Starting from the pharmacophore of strobilurins, natural compounds isolated for the first time from basidiomycetes, new derivatives were prepared to obtain more complex compounds. The idea was to combine the pharmacophore of strobilurins, acting on complex III cytochrome bc1, to the pharmacophore of succinate dehydrogenase inhibitors (SDHI), acting on complex II cytochrome bc1, in order to create multitarget compounds overcoming the resistance developed against most of the marketed fungicides. Additionally, we aimed at creating a new *in silico* model for *P.oryzae* cytochrome bc1 in complex with azoxystrobin, to unlock the way for a further rational design of new highly active compounds, with the possibility to overcome the strobilurin resistance in *P. oryzae*.

A second part of the work was focused on structural-activity relationship (SAR) studies on dehydro-δ-viniferin and dehydro-ε-viniferin, natural polyphenols derived from grapes. In a previously study, conducted in our laboratory, these two dimers of resveratrol resulted to be potential antibacterial agents against Gram-positive bacteria. To identify the structural elements relevant to the antimicrobial potency on the foodborne pathogen *L. monocytogenes* Scott A, a series of simplified analogues of dehydro-δ-viniferin and dehydro-ε-viniferin was designed. In an attempt to extend the spectrum of antimicrobial activity of stilbenoids against Gram-negative bacteria we also designed a series of resveratrol and pterostilbene derivatives containing functional groups able to

increase the interaction with the negatively charged portion of the lipopolysaccharides constituting the outer membrane of Gram-negative bacteria.

A further aim of this thesis was the investigation of natural matrices as new sources of antiviral compounds. In particular, we focused on grapefruit seeds, intrigued by recent studies reporting the virucidal activity against avian influenza virus (AIV) and Newcastle disease virus (NDV) of grapefruit seed extract (GSE). Fascinated by the possibility of having a safe and easily accessible weapon against COVID-19, we planned to obtain a collection of GS extracts and pure single molecules to evaluate their antioxidant activity and virucidal activity.

3 RESULTS AND DISCUSSION

3.1 SYNTHESIS AND MOLECULAR MODELING OF STROBILURIN-BASED FUNGICIDES ACTIVE AGAINST THE RICE BLAST PATHOGEN *PYRICULARIA ORYZAE*

The results of this section are published in (Kunova *et al.*, 2021).

ABSTRACT. In last decades, fungicide-resistant pathogens increased exponentially requiring urgent solutions for crop disease management. In order to generate novel multitarget fungicides and to investigate their structure-activity relationship (SAR), a small collection of compounds containing both strobilurin and succinate-dehydrogenase pharmacophore was synthesized and tested against *Pyricularia oryzae*. Some analogues were endowed very good activity against wild-type strain of *P. oryzae*, with compound **6b** showing promising activity also against strobilurin-resistant strains. The first three-dimensional model of *P. oryzae* cytochrome bc1 complex containing azoxystrobin as a ligand was developed. The model was validated with a set of commercially available strobilurins, and it explained exhaustively both the resistance mechanism to strobilurins caused by the mutation G143A and the activity of metyltetraprole against strobilurin-resistant strains. The obtained results indicate the essential structural requirements of strobilurin-like derivatives in the cytochrome bc1 active site and will lead the further rational design of new fungicides capable of overcoming the resistance caused by the G143A mutation in the rice pathogen.

3.1.1 Introduction

Rice feeds half of worldwide population and for this reason it is considered the most important staple. Moreover, rice is defined a multifunctional crop because it can be used as food, feed, and feedstock for bioenergy production (Phitsuwan and Ratanakhanokchai, 2014). Italy is the main rice producer in Europe with an area of 234,133 ha and the amount of rice production is over

1.5 million tons per year (Graziano *et al.*, 2020). Rice blast, caused by the fungus *Pyricularia oryzae*, is one of the most serious fungal diseases of cultivated rice worldwide, causing each year 10–30% yield losses corresponding to ca. 70 billion USD of economic loss (Scheuermann *et al.*, 2012; Nalley *et al.*, 2016; Asibi *et al.*, 2019). *P. oryzae* is a filamentous ascomycete fungus and the cycle begins with a first infected cell, called appressorium, which breaks the tough cuticle of the rice plant; inside the plant, the fungus produces invasive hyphae that quicky colonize living host cells and secret effector molecules (Asibi *et al.*, 2019). Chemical control is crucial to fight against crop diseases. In the last years, 150 different fungicidal compounds have been placed on the agriculture market (Brent and Hollomon, 2007). In 2019, the total value of sale of fungicides was evaluated in approximately 16.35 billion dollars with the expectation of growth of 4.3% from 2020 to 2027 (Triandafyllidou and McAuliffe, 2014).

Fifty-six different specific fungicide and bactericide modes of action are available and classified in the Fungicide Resistance Action Committee (FRAC) code list, also including fungicides with unknown modes of action. In 2015, a few classes of fungicides dominated the overall market. Among these antifungal agents, there were strobilurins, derived from a natural compound discovered in 1977 by the German group of Anke and Steglich. They reported for first time the antifungal activity of strobilurin A (Figure 3.1), isolated from the fungus *Strobilurus tenacellus* (Feng *et al.*, 2020). Strobilurin A showed a high activity against the fungi *in vitro*, on artificial media, but the results *in vivo* were completely different. The presence of the triene system carried out to rapid photolytic, oxidative or metabolic degradation, leading to the molecule's degradation in greenhouse condition.

With the aim of stabilizing the triene portion, the central double bond was incorporated into a benzene ring. This second-generation, constituted of an enol ether stilbene structure (Figure 3.1), showed a higher activity in greenhouse test and a higher mitochondrial target activity. These results led to a further generation of strobilurins in which the three substructures of the

molecule, side chain, central ring, and pharmacophore were modified to obtain improvement in stability and activity. Starting from the enol ether stilbene, two different strategies of modification were attempted: modification of the side chain and modification of the β-methoxyacrilate (β-MOA) pharmacophore. The central ring, an *ortho* disubstituted benzene, was kept almost unchanged. The first commercial strobilurin, azoxystrobin, is an evolution of the enol ether stilbene, modified only on the side chain. Its systemic activity was due to a good partition coefficient (logPOW < 5.0) and significant metabolic stability (Figure 3.1).

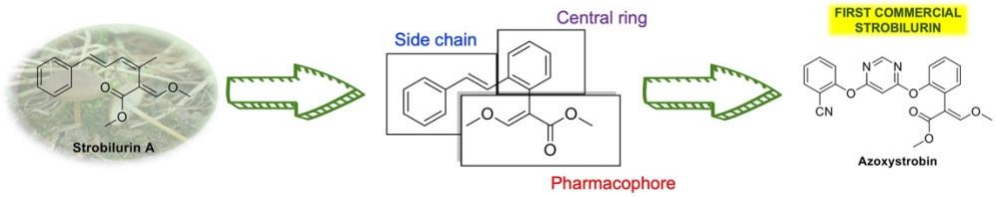

Figure 3.1 *General scheme of strobilurins' history*

As SAR studies confirmed, β-MOA could be replaced with bioisosteric moieties. Derivatives with oxime ether (e.g. kresoxim-methyl) showed a notable increase of binding affinity. In 2019, 20 different quinone outside inhibitors (QoIs, strobilurins) were present on the market. Different types of pharmacophores have been developed, including methoxy-acrylate, but also methoxy-acetamide, oximino-acetamide, methoxy-carbamate, oximino-acetate, dihydrodioxazine, benzyl-carbamate, oxazolidine-diones and imidazolinones (Figure 3.2). Recently methyltetraprole, containing a new optimized pharmacophore with reduced steric hindrance to act against the mutated enzyme, has shown promising results.

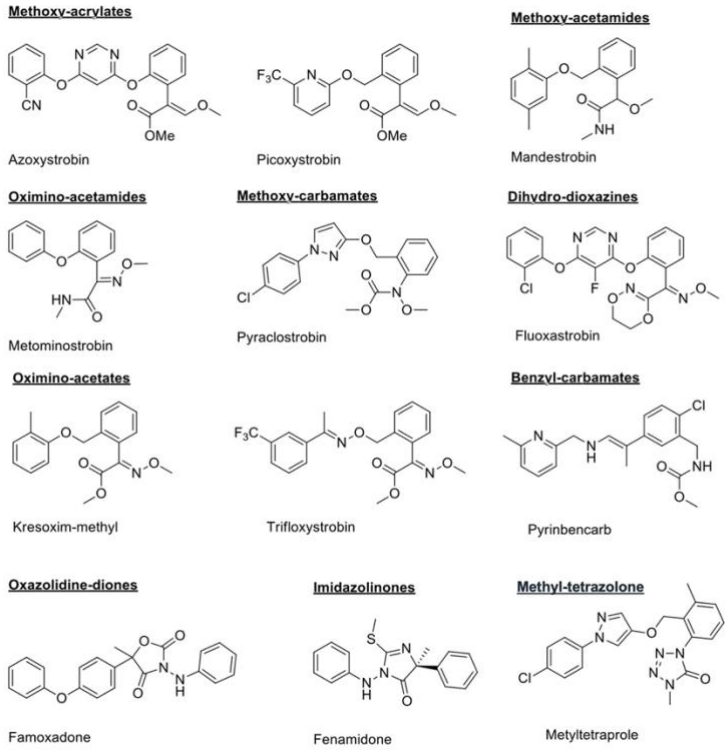

Figure 3.2 *Strobilurins on the market and methytetraprole*

Strobilurins, as suggest the definition “quinone outside inhibitors (QoI)”, act on the oxidative phosphorylation, inhibiting the Complex III.

Complex III (Figure 3.3) is a highly conserved complex, formed by three subunit, cyt b, the Rieske [2Fe2S] iron-sulfur protein (ISP) and cytochrome c_1. The enzyme catalyses the electron transfer from ubiquinol, generated in complex I and II, to cytochrome c. The successive reactions are known as Q-cycle and have as consequence the dislocation of two protons through the membrane for each oxidized ubiquinol. Ubiquinol binds at the Qo site of the cytochrome b where it is oxidized. The two electrons delivered by ubiquinol go to two different redox centers. The first electron goes to the “Rieske” iron sulfur cluster via cytochrome c_1 to the cytochrome c. The second electron goes to trough the heme b_L to heme b_H. Heme b_H is close in the inner site of the inner membrane of mitochondria (Q_i site) and the electron of the heme b_H

is transferred to a ubiquinone which is reduced to ubiquinol (this require 2 electrons). The whole cycle requires the oxidation of 2 molecules of ubiquinol with the four electrons going half to Cyt c and half to ubiquinone. At the same time 4 protons are transferred outside the inner mitochondrial membrane (Link *et al.*, 2003).

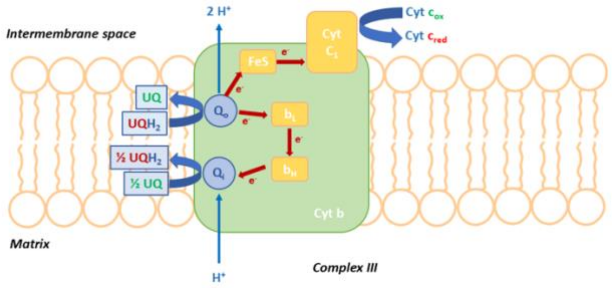

Figure 3.3 *Complex III. The homodimeric bc1 complex presents three catalytic subunits: cytochrome b (cyt b) with two b-type haems (b_H and b_L), the Rieske iron–sulfur HL catalytic subunits: cytochrome b (cyt b) with two b-type haems (b_H and b_L), the Rieske iron–sulfur protein (FeS) and cytochrome c_1 (cyt c_1) with one c-type haem. The two binding sites for inhibitors and protein (FeS) and cytochrome c_1 (cyt c_1) with one c-type haem. The two binding sites for inhibitors ubiquinone (UQ), Qi and Qo, are shown. The bifurcated electron transfer pathway from the Qo site is and ubiquinone (UQ), Qi and Qo, are shown. The bifurcated electron transfer pathway from the Qo shown by red arrows (Musso et al., 2020).*

Qo and Qi sites are both targets of potent and selective inhibitors. In particular, inhibitors binding at the Qo site of cytochrome b can be classified according to the position occupied within the site, as some bind closely to the Rieske protein (e. g. stigmatellin), while other bind close to heme b_L (e. g. strobilurins, famoxadone).

In strobilurins, the intrinsic activity is determined primarily by the binding affinity to the Qo site of the bc_1 complex of the respiratory chain. The binding of strobilurin at the Qo site prevent the binding of ubiquinol and then its oxidation (Musso *et al.*, 2020). This structure is well preserved in all organisms, but despite this, no toxic effects are observed on higher organisms due to metabolic inactivation of the toxicophoric. Some common feature about the SAR of QoIs compounds have been proposed (Ishigami *et al.*, 2015):

- The carbonyl group, or an isostere of it, is essential as hydrogen bond acceptor with the N-H proton of Glu272 (yeast enzyme numbering).
- The carbonyl must have an s-*(E)*-orientation, to better satisfy the first requisite.
- The ester methoxy group can be replaced with no-hydrogen acceptor groups without a considerable loss of activity
- The side chain must be connected to the phenyl ring in *ortho* position

These structure features match with binding pocket's residues. The pocket can be divided into three main regions: pharmacophore, linker region and hydrophobic tail (Figure 3.4 A). This Q_O site within cyt b is composed from components including the C-terminal domain of transmembrane helix C, surface helix cd1 and the region including the "PEWY" (Pro, Glu272, Trp, Tyr) loop to transmembrane helix F1 (Figure 3.4 B). These components form the large, bifurcately and predominantly hydrophobic pocket (Fisher *et al.*, 2020).

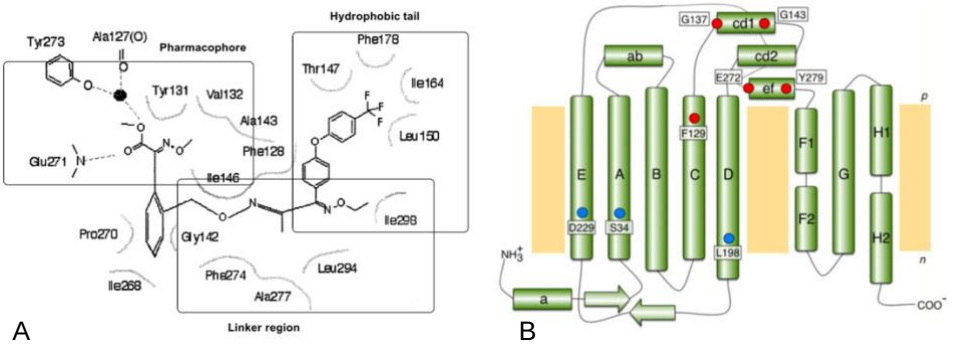

Figure 3.4 *(A) Structure of strobilurin binding pocket 10 (B) Cartoon of the secondary structure and membrane disposition of cyt b, displaying the location of Qo (red) and Qi (blue) sites (Saccharomyces cerevisiae notation). Transmembrane and surface helices are identified in upper and lower cases, respectively. 'n' and 'p' refer to the negative and positive sides of the energized inner mitochondrial membrane.*

Strobilurin fungicides have been a milestone in the fungicide market, and they are still among the best-selling agrochemicals worldwide. Despite their excellent fungicidal abilities, belonging to a class of compounds that act with a single site mode of action, they are predisposed to develop resistance in fungal pathogens. In fact, mutation of many aminoacids have been observed in complex III. Mutations leading to QoI resistance include G143A, F129L and

G137R. Mutation G143A is the most important mechanism of resistance and has a strong effect on the activity of QoIs, leading to a steric interference with the central ring of most of QoI resulting in markedly reduced binding affinity.

In order to expand the knowledge on strobilurin fungicides and find new antifungal agents with the capability to bypass the resistance, we decided to prepare a collection of strobilurin derivatives binding the strobilurin moiety with the pharmacophore β-methoxyacrilate to another pharmacophore acting on complex II of mitochondrial respiratory chain. Succinate-dehydrogenase inhibitors (SDHIs) have as target the ubiquinone-binding sites in the mitochondrial complex II. The "core" of the molecule, which is attached to the carbonyl of an amide group, is used for the chemical classification of SDHI and it is essential for the binding, entering deeply into the active site of SDHI (Xiong *et al.*, 2015).

In our research group, a first-generation of strobilurin derivatives characterized by a three ring-based structure containing the methyl-(E)-β-methoxyacrylate and a carboxamide were synthesized (Zuccolo *et al.*, 2019). The pilot compound showed good *in vitro* mycelium growth inhibition of the rice blast pathogen, *Pyricularia oryzae*, but it almost completely lost its activity on strobilurin-resistant strains (Figure 3.5).

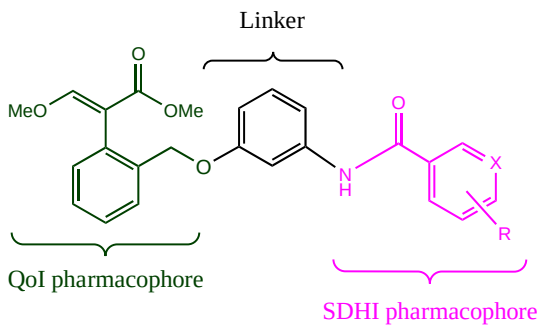

Figure 3.5 *General skeleton of strobilurin derivatives, starting from the first generation of compounds*

3.1.2 Materials and Methods

3.1.2.1 Chemistry

Procedures for the synthesis, isolation, and characterization data for the various strobilurin analogues obtained are described in the experimental part 3.1.4.

All reagents and solvents were reagent grade or were purified by standard methods before use. Melting points were determined in open capillaries on an SMP3 apparatus and are uncorrected.

^{1}H NMR spectra were recorded on 300 and 600 MHz spectrometers; ^{13}C NMR spectra were recorded on 300 and 600 MHz spectrometers. Solvents were routinely distilled prior to use; anhydrous THF and Et_2O were obtained by distillation from sodium benzophenone ketyl; anhydrous CH_2Cl_2 was obtained by distillation from phosphorus pentoxide.

All reactions requiring anhydrous conditions were performed under a positive nitrogen flow, and all glassware was oven-dried. Isolation and purification of the compounds were performed by flash column chromatography on silica gel 60 (230–400 mesh). Analytical TLC was conducted on TLC plates (silica gel 60 F_{254}, aluminum foil). Compounds on TLC plates were detected under UV light at 254 and 365 nm or were revealed by spraying with 10% phosphomolybdic acid (PMA) in EtOH.

3.1.2.2 Antifungal activity

Fungal strains

Four strains of *Pyricularia oryzae* were used; two strains belonging to the Italian population and sensitive to quinone outside inhibitor (QoI) fungicides (WT): A2.5.2 and TA102; and two strains belonging to the Japanese population and resistant to QoI (RES): PO1312 and PO1336. The strains belong to a vast collection of monoconidial isolates maintained at the laboratory of plant pathology, University of Milan (Kunova *et al.*, 2013, 2014).

The strains were maintained as single-spore isolates on malt-agar medium (MA: 20 g/L malt extract, Oxoid, U.K.; 15 g/L agar, Oxoid, U.K.) at 4 °C.

Fungicides

The commercial fungicides azoxystrobin (AZX, Amistar SC—suspension concentrate, 22.9% ai., Syngenta Crop Protection) and fluxapyroxad (FXP, Sercadis EC—emulsifiable concentrate, 30% ai., BASF Italia, S.p.A.) were used as standards to evaluate the activity of QoI (azoxystrobin) and SDHI (fluxapyroxad) fungicides.

Inhibition of Mycelium Growth of P. oryzae by Novel Compounds

The inhibitory activity of the novel dual compounds and commercial fungicides on the mycelium growth of *P. oryzae* was evaluated as described previously (Zuccolo *et al.*, 2019). In short: a mycelium plug (0.5 cm in diameter) obtained from actively growing fungal colonies of *P. oryzae* A2.5.2, TA102, PO1312, and PO1336 was transferred to MA medium plates supplemented or not with commercial fungicides (AZX, FXP) and tested compounds at the concentration of 25 mg/L in three biological replicates. Due to the low solubility of the tested dual molecules in water, they were dissolved in acetone. Therefore, two controls were included: MA medium (C, control) and MA medium supplemented with acetone at the final concentration of 1% v/v (ACT). The plates were incubated at 24 °C in the dark. The mycelium growth was measured at 7 days after inoculation (DAI), and the inhibition of mycelium growth (%) was calculated by comparing the mycelium growth on control and fungicide-supplemented plates. The inhibition percentage was calculated as I% = (C- T)/C*100, where C = mycelium growth in the control medium and T = mycelium growth in the medium added with the tested compound. For AZX and FXP, the control was MA medium. For tested compounds, the control was considered ACT.

Enzyme Inhibition Assay for the Measurement of QoI and SDHI Action

P. oryzae mitochondrial fraction from the A2.5.2 strain was prepared as described previously (Zuccolo *et al.*, 2019).

The SDHI action was evaluated measuring the succinate:quinone oxidoreductase (SQR) activity (i.e., the succinate dehydrogenase activity; EC 1.3.5.1) of the mitochondrial fraction in the presence of **6b** compound using a method based on the use of the redox dye, 2,6-dichlorophenolindophenol (DCPIP) (Ye *et al.*, 2014), with some modifications as described previously (Zuccolo *et al.*, 2019). The enzyme reaction was monitored at 595 nm at fixed times using a fixed wavelength microplate reader (iMarkTM; Bio-Rad Laboratories, Inc., Hercules, CA, USA). To calculate the SQR reaction rate, the absorbance decreases due to the DCPIP reduction during the 2–60 min time interval was considered. Fluxapyroxad (37047, Sigma Aldrich, Milan, Italy) was used as the reference SDHI.

The strobilurin-like (QoI) action was evaluated measuring the decylubiquinol:Cyt *c* reductase activity (i.e., the Cyt *bc1* complex activity; EC 1.10.2.2) of the mitochondrial fraction in the presence of the **6b** compound, using the method described by Zhu et al. (Zhu *et al.*, 2012) with some modifications (Zuccolo *et al.*, 2019). Azoxystrobin (31697, Sigma Aldrich, Milan, Italy) was used as the reference QoI.

In both enzyme assays, the enzyme rate in the presence of the tested molecule ($rate_{molecule}$) was compared to that achieved in the presence of the compound diluent DMSO ($rate_{DMSO}$), in order to calculate the percent of inhibition (I %) as follows:

$$I = \frac{rate_{molecule} - rate_{DMSO}}{rate_{DMSO}} \times 100$$

Statistical Analysis

The mycelium growth data for each treatment were grouped based on the QoI resistance of *P. oryzae* strains (WT or RES) and were submitted to ANOVA followed by a Tukey's HSD post hoc test for multiple comparisons ($P < 0.05$) using the TukeyC package and R software, version R4.0.0 (Faria *et al.*, 2020; R Core Team, 2020).

Similarly, ANOVA followed by posthoc Tukey's HSD test for multiple comparisons was used for enzymatic activity data analysis.

3.1.2.3 In Silico Modeling

Homology Modeling of Cytochrome bc1 Complex

The *Pyricularia oryzae* cytochrome *bc1* complex (complex III) primary structures were downloaded from the UniProt Protein Knowledgebase database (entry: Q85KP9 form *P. grisea* and G4N4E1 from *P. oryzae*, respectively (Zuccolo *et al.*, 2019). After a protein BLAST search of the Protein Data Bank (RCSB PDB) database for homolog templates, the crystallographic structure of bovine cytochrome *bc1* (PDB ID: 1SQB (Esser *et al.*, 2004)), co-crystallized with azoxystrobin, chains E and N, was selected as a template for both subunits. Two alignments produced by the ClustalΩ software and manually optimized for cytochrome b and 1SQB chain N were used. Comparative model building was carried out by Schrödinger BioLuminate (BioLuminate, Schrödinger, 2020). Multiple Sequence Viewer/Editor in the knowledge-based model set- ting, including azoxystrobin, heme groups, and Fe-S clusters. The geometry of the final model was checked by the Ramachandran plot.

Ligand Preparation

Available/commercial ligands were downloaded from PubChem, and original ones were built with the Maestro 3D Builder tool. All ligands were prepared for docking with the LigPrep panel, using the OPLS3e (Harder *et al.*, 2016) force field.

Molecular Docking and Affinity Calculations

The molecular docking procedure was carried out with the Schrödinger Small-Molecule Drug Discovery Suite (Schrödinger, 2020). The QoI binding site of the cytochrome *bc1* complex was identified by the presence of azoxystrobin transferred from the bovine cytochrome *bc1* complex (PDB ID: 1SQB (Esser *et al.*, 2004)). Molecular docking was carried out via Glide in its extra precision

(XP) mode (Friesner *et al.*, 2004, 2006; Halgren *et al.*, 2004). Before the docking procedures, our model of cytochrome *bc1* complex was prepared and energy-minimized via the BioLuminate Protein Preparation Wizard with the OPLS3e (Harder *et al.*, 2016) force field. The same force field was applied in all the molecular docking procedures. The binding free energy of all the complexes produced by our molecular docking pipeline was evaluated via both Glide XP Score and Prime MM-GBSA that combines molecular mechanics with generalized Born and surface area scoring function (Li *et al.*, 2011). The accuracy of the proposed methods is associated with a low level of accuracy. Glide XP Score is an empirical scoring function that approximates the ligand binding free energy, and that is generally good enough to separate ligands putatively from non-ligands. In Eberini *et al.* 2008 (Eberini *et al.*, 2008), we used an empirical scoring function for estimating ligand binding free energy after molecular docking: the comparison between computed and experimental affinities (i.e., dissociation constants, Ki, computed from ΔG values) showed approx. one order of magnitude accuracy for our predictions. An approach associated with a higher level of accuracy than the one based on Glide XP Score is based on MM-GBSA that allows the ligand to relax in the binding site.

Mutant Generation and Evaluation

The evaluation of the impact of G143A mutation on the enzyme stability and on the affinity for compound **6b** was carried out with the Maestro BioLuminate Residue Scanning Tool, which considers the impact of a mutation on the stability of the protein (ΔStability) and on the affinity (ΔAffinity) for the tested ligand(s), expressed in kcal/mol (Beard *et al.*, 2013).

3.1.3 Results and Discussion

Starting from the best compound of the first-generation analogues (**1**), characterized by three aromatic rings, containing the β-MOA connected by a linker to a carboxamide, we synthetized a new generation of strobilurin derivatives (Scheme 3.1). We maintained unaltered the strobilurin

pharmacophore and focused our attention on the spatial orientation of bioactive molecular sites, on the role and nature of the linker and on the nature and substitution pattern of the SDHI pharmacophore. For the first scope, we prepared derivatives **2** and **3** with the two moieties positioned in *ortho* and *para* relative positions on the central ring, respectively (Scheme 3.1). Moreover, we changed the position of the substituent (methyl group) on the benzamide ring (compounds **4** and **5**). Successively, we investigated the effect of the introduction of diverse substituents on the benzamide ring. Thus, we prepared compounds **6a**–**g** bearing substituents with different steric and stereoelectronic properties. After this, we modified the nature of the aromatic ring in the SDHI moiety, replacing the benzamide with a heterocyclic amide (compounds **7** and **8**). Compound **8** is characterized by the pyrazole carboxamide found in the commercial SDHI inhibitor fluxapyroxad.

Finally, we focused our attention on the linker between the two bioactive sites. In compounds **9a**–**c**, we increased the distance between the strobilurin and SDHI moieties, using glycine, β-alanine, and γ-aminobutyric acid (GABA) as linkers. In addition, a further aromatic ring was placed between the two active moieties in compound **10** (Scheme 3.1).

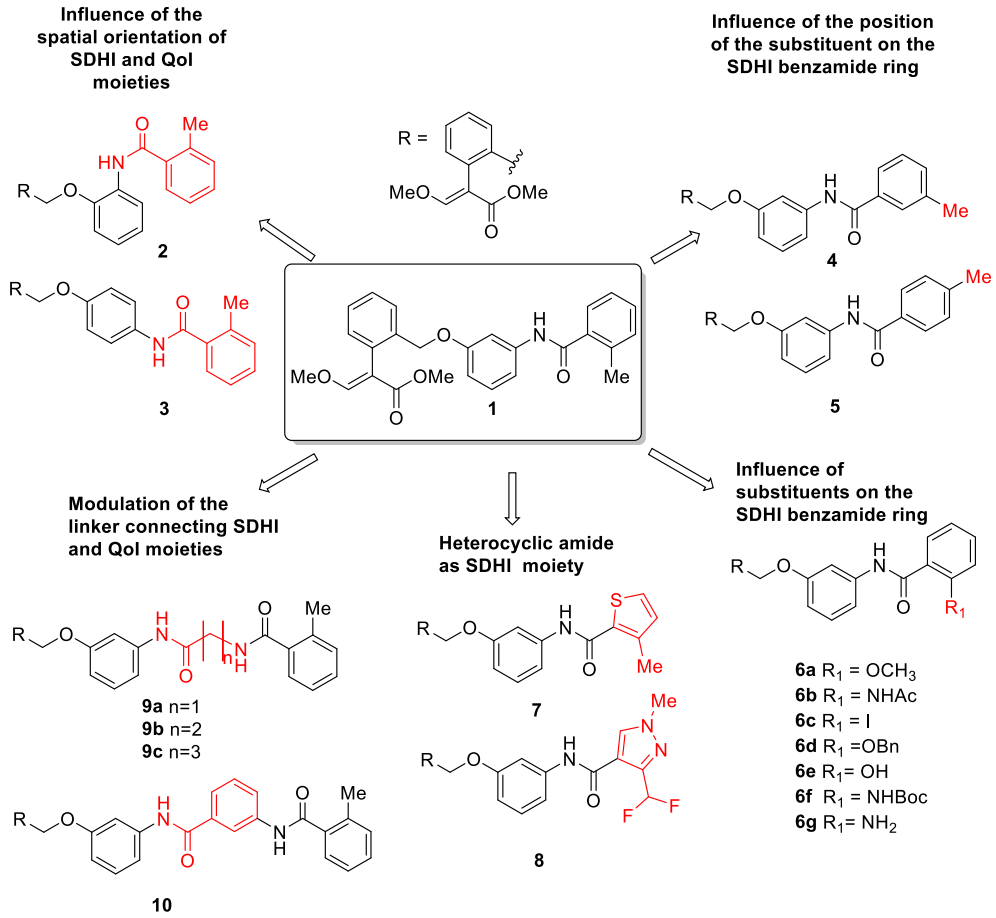

Scheme 3.1 *Design strategy to optimize the structure of new dual SDHI-QoI inhibitors*

3.1.3.1 Chemistry

The strobilurin pharmacophore was prepared following a three-steps reaction pathway (Scheme 3.2). Iodination of β-methoxyacrylate was followed by a cross-coupling Suzuki reaction with 2-methyl-1-phenylboronic acid with the catalyst $Pd(PPh_3)_4$ (Zuccolo *et al.*, 2019).

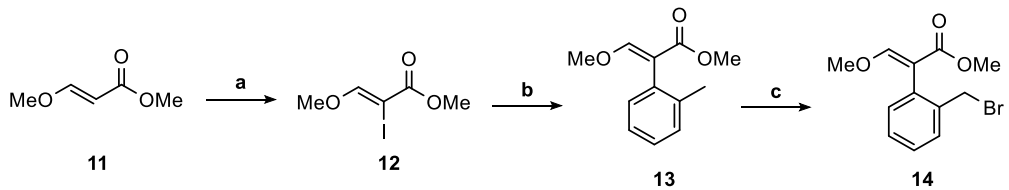

Scheme 3.2 *Synthesis of scaffold* ***14****. (a) I_2, Py, DCM, 0°C to rt: 86%; (b) 2-methyl-1-phenyl boronic acid, $Pd(PPh_3)_4$, K_3PO_4, dioxane/H_2O, 90°C: 95%; (c) NBS, AIBN, CCl_4, reflux: 78%.*

The compound **14** was condensed with the suitable *tert*-butyl-hydroxyphenylcarbamate (**15a, 15b, 15c)**, followed by removal of the Boc protecting group to obtain the scaffolds **17a**, **17b** and **17c**, with the amine group in different position (Scheme 3.3).

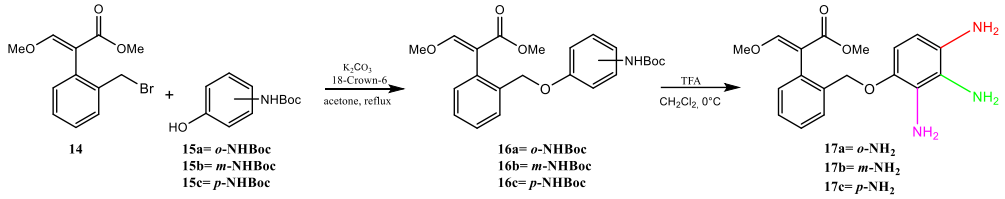

Scheme 3.3 *K_2CO_3, 18crown6, acetone, reflux, 82%; 10% V/V trifluoroacetic acid, CH_2Cl_2, 0 °C, 90%.*

The key reaction to build the final compounds was the coupling reaction between the scaffolds (**17a**, **17b**, **17c**) and the suitable carboxylic acid using EDC·HCl and HOBt as coupling reagents and DIPEA bases at 0 °C (Scheme 3.4). From **17a** and **17c** after amidation with the 2-methylbenzoic acid, we obtained the compounds **2** and **3**, respectively. Following the same procedure from **17b**, all the other analogues (**4**-**10**) were prepared.

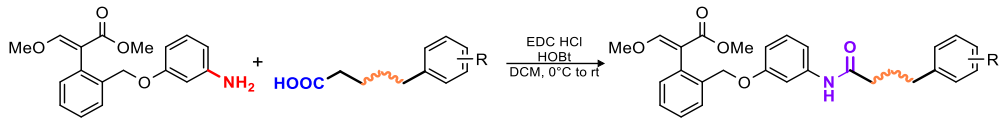

Scheme 3.4 *example of general coupling reaction between **17b** and suitable acid.*

3.1.3.2 Biological Activity

The inhibitory activity of compounds **2-10** on growth of *P. oryzae* was evaluated and compared to the activity of compound **1** (Figure 3.6, Table 3.1). The commercial fungicides azoxystrobin (AZX; QoI) and fluxapyroxad (FXP, SDHI) and all synthesized compounds were tested at concentration 25 mg/L. AZX inhibited > 90% the growth of wild type (WT) strains, while the strobilurin-resistant (RES) strains were inhibited to < 50%. On the contrary, FXP (SDHI) showed low activity on WT strains (65% inhibition), but > 90% inhibition of RES strains. The best antifungal behavior was shown by compound **6b** on both wild-type and strobilurin-resistant strains, with more than 80% inhibition.

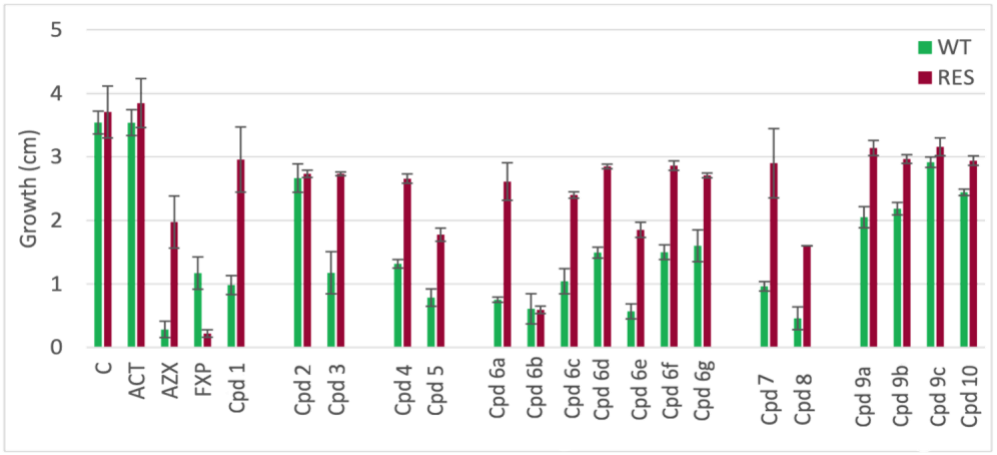

Figure 3.6 *Mycelium growth of wild type (WT) and QoI-resistant (RES) Pyricularia oryzae strains on control malt-extract agar media (C = control, ACT = 1% acetone) and media supplemented with azoxystrobin (AZX), fluxapyroxad (FXP) or dual compounds (Cpds **1a**, **7-15**) at a concentration 25 mg/L. Error bars represent standard deviation of the mean.*

Table 3.1 *Inhibition of mycelium growth of wild type (WT) and QoI-resistant (RES) Pyricularia oryzae strains on control malt-extract agar media (Control, ACT = 1% acetone) and media supplemented with azoxystrobin (AZX), fluxapyroxad (FXP) or dual compounds (Cpds **1a**, **7-15**) at a concentration 25 mg/L.*

	WT		RES	
Compound	**% Inhibition[a]**	**Tukey HSD[b]**	**% Inhibition**	**Tukey HSD**
Control	0	a	0	a
ACT	0	a	-4	a
AZX	92	m	47	c
FXP	67	f h i	94	d
1	72	h i j	20	b
2	25	b c	26	b
3	67	f g h i	26	b
4	63	e f g h	28	b
5	78	j k l	52	c
6a	79	i j k l	30	b
6b	83	k l	84	d
6c	71	h i j	35	b
6d	58	e f g	23	b
6e	84	k l m	50	c
6f	58	e f	23	b
6g	55	e	27	b
7	73	h i j k	22	b
8	87	l m	57	c
9a	42	d	15	b

9b	38	d	20	b
9c	18	b	15	b
10	31	c d	21	b

[a] Inhibition (%) was calculated as I% = (C-T)/C*100, where C = is growth on control medium, and T = is growth on treated medium.
[b] Tukey post hoc test of mycelium growth data. The different letters indicate statistically significant differences between mean growth (*P*>0.05).

Given the promising biological activity of compound **6b**, we assumed that it maintained good Qo and SDH inhibitory activity. The measurement of decylubiquinol:Cyt *c* reductase activity (i.e. the Cyt *bc1* complex activity) was performed to evaluate the QoI action of the selected compound. To this purpose, the reduction rate of Cyt *c* mediated by the mitochondrial fraction of *P. oryzae* was measured, using decylubiquinol (DBH_2) as the electron-donor substrate. The DBH_2:Cyt *c* reductase activity was inhibited by 58 ± 18 % by the compound **6b** (50 µM). A similar inhibition value (61 ± 10 %) was observed for azoxystrobin (50 µM), thus confirming that **6b** retained the QoI action.

SDH enzymatic assay was performed measuring the electron transfer rate mediated by the mitochondrial fraction of *P. oryzae* in the presence of 2,3-dimethoxy-5-methyl-*p*-benzoquinone and succinate by a colorimetric method, using the redox dye 2,6-dichlorophenolindophenol (DCPIP, Figure 3.7).

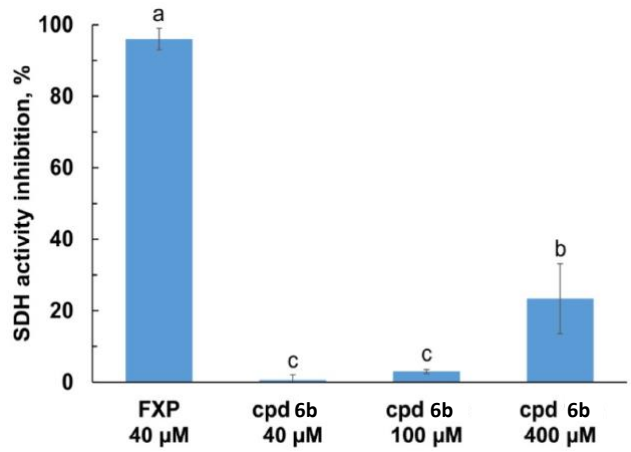

Figure 3.7 *Effect of compound* ***11b*** *on the P. oryzae mitochondrial SDH activity. To evaluate the percent of inhibition due to the SDHI action, the rates of the succinate:2,3-dimethoxy-5-methyl-p-benzoquinone dehydrogenase activity of the mitochondrial fraction were measured at 25 °C (λ = 595 nm) using DCPIP in the presence of* ***11b*** *and the reference compound,*

fluxapyroxad, at the indicated concentrations. Data represent the mean ± standard deviation of at least three independent trials. Different superscript letters indicate statistically significant differences (Tukey HSD, p ≤ 0.01).

Fluxapyroxad showed >90% inhibition of SDH activity at the concentration 40 µM. Surprisingly, at the same concentration, no SDH inhibition was observed for compound **6b**. By increasing the concentration to 400 µM, approximately 23% inhibition of the SDH enzyme activity was observed.

3.1.3.3 In silico modeling and docking

In order to have available a structure for *P. oryzae* cytochrome *bc1* in complex with azoxystrobin, we built a 3D model by homology. The Ramachandran plot (Figure 3.8), the side chain packing, and the stereo chemical quality were carefully checked to confirm that all these parameters were suitable and consistent with typical values found in template crystallographic structures.

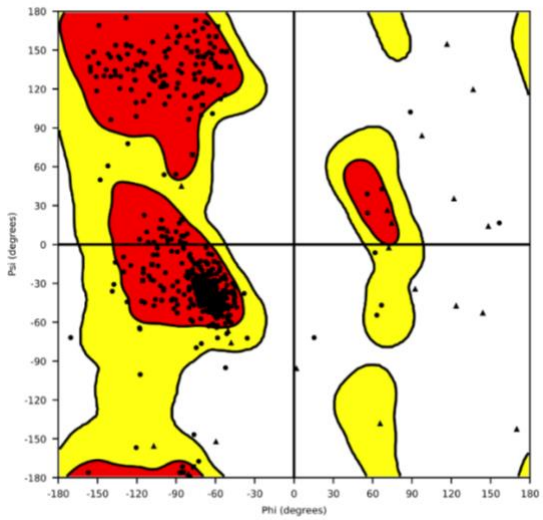

Figure 3.8 *Ramachandran plot of the three-dimensional model for Pyricularia oryzae cytochrome bc1 complex. Red and yellow regions are respectively favored and allowed regions. Triangles refer to G, squares to P and dots to the remaining amino acids.*

The final model, containing azoxystrobin, was transferred by the selected template (PDB ID: 1SQB). The selected docking procedure was validated testing commercial strobilurin QoI (azoxystrobin, trifloxystrobin, kresoxim-methyl and metominostrobin) (Figure 3.9). Moreover, metyltetraprole, active

also against strobilurin-resistant pathogens (Suemoto *et al.*, 2019; Matsuzaki *et al.*, 2020), was included to validate the QoI binding site of the model.

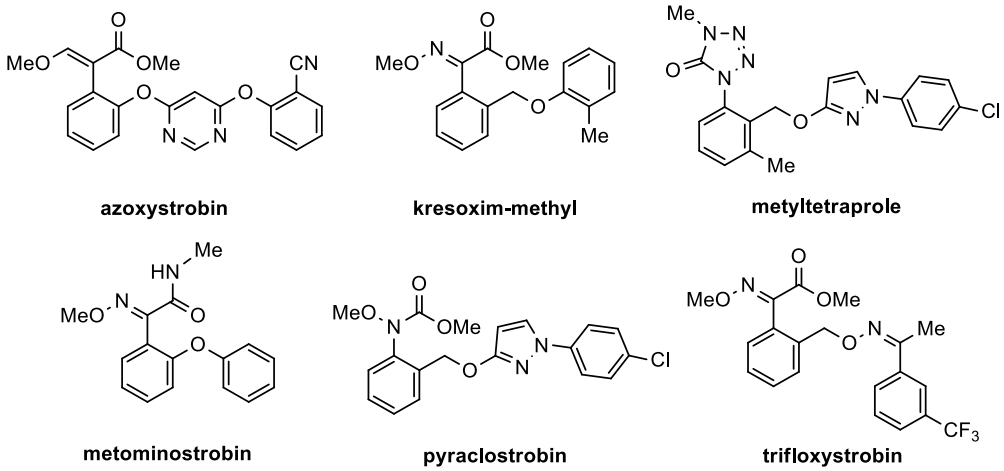

Figure 3.4 *Validation set of marketed strobilurins and metyltetraprole*

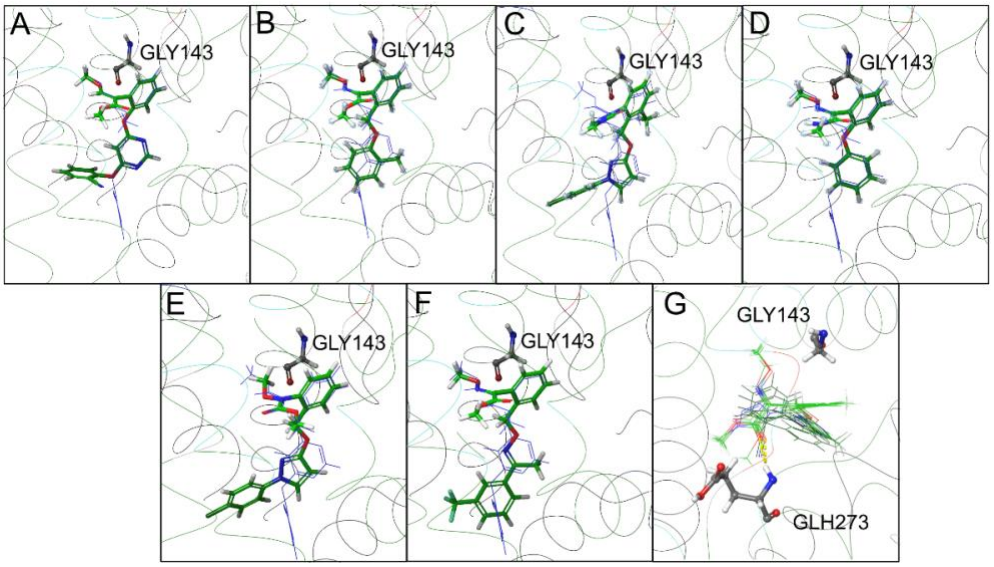

Figure 3.10 *Top-scoring docking poses within the cytochrome b binding pocket of the commercial strobilurin fungicides included in the validation set: A) azoxystrobin, B) kresoxim-methyl, C) metyltetraprole, D) metominostrobin, E) pyraclostrobin (the second top-scoring pose), F) trifloxystrobin. In G) all validation set poses are reported to highlight their binding mode and the interaction with GLU273.*

Table 3.2 *Top-scoring docking solutions for all chemicals in the validation-set. [a]Glide XP score indicates the approx. binding affinity (kcal/mol) of the top-scoring binding pose. [b]MM-GBSA*

indicates a more accurate binding affinity (kcal/mol) of the top-scoring binding pose. [c]Number of poses for each compound obtained by the molecular docking procedure. [d]Range of the binding affinities (kcal/mol) for each tested chemical of the validation set. [e]Number of generated poses with an orientation similar to azoxystrobin (as transferred from the template) for each tested compound of the validation set.

Ligand	Glide XP[a] [kcal/mol]	MM-GBSA[b] [kcal/mol]	Number of poses[c]	Range[d] [kcal/mol]	Orientation of the generated poses[e]
azoxystrobin	-10.6	-76.4	5	(-10.6; -9.4)	5/5
trifloxystrobin	-9.8	-65.6	2	(-9.8; -9.7)	2/2
kresoxym-methyl	-10.4	-68.9	1	(-10.4)	1/1
metominostrobin	-9.9	-79.3	1	(-9.9)	1/1
pyraclostrobin	-8.4	-61.7	5	(-10.0; -5.7)	3/5
metyltetraprole	-10.2	-62.9	2	(-10.2; -9.8)	2/2

The top-scoring docking solution for all the validation-set compounds showed a binding mode highly similar to the azoxystrobin placement in the bovine cytochrome *bc1* (PDB ID: 1SQB) (Esser *et al.*, 2004), in which the pharmacophore was very close to the G143 protein residue (Figure 3.10, Table 3.2). The superposition of the top-scoring poses for the entire validation set confirmed a key role for Glu273 (Figure 3.10 G) as observed in other organisms (Palsdottir *et al.*, 2003).

After validating the method, the five most active synthesized compounds (**5**, **6a**, **6b**, **6e** and **8**) were docked to expand the knowledge about their binding interactions (Table 3.3). All the five selected molecules showed a top-scoring pose with an orientation similar to the co-crystallized azoxystrobin in 1SQB and to the validation set, i.e. with the methoxyacrylate moiety close to G143; some other poses with higher energy values showed an orientation not compatible with the azoxystobin/strobilurin binding mode.

Table 3.3 *Top-scoring docking solutions for the selected five novel compounds showing the highest biological activity against Pyricularia oryzae. [a]Glide XP score indicates the approx. binding affinity (kcal/mol) of the top-scoring binding poses. [b]MM-GBSA indicates a more accurate binding affinity (kcal/mol) of the top-scoring binding pose. [c]Number of poses for each compound obtained by the molecular docking procedure. [d]Range of the binding affinities (kcal/mol) of individual poses for each tested novel compound. [e]Number of generated poses with an orientation similar to azoxystrobin (as transferred from the template) for each tested novel compound.*

Ligand	Glide XP[a] [kcal/mol]	MM-GBSA[b] [kcal/mol]	Number of poses[c]	Range[d] [kcal/mol]	Orientation of the generated poses[e]
5	-11.7	-83.9	3	(-11.7; -9.1)	3/3
6a	-9.1	-60.3	5	(-9.1; -7.4)	1/5
6b	-9.4	-59.6	5	(-9.4; -7.4)	3/5
6e	-12.6	-83.3	5	(-12.6; -11.6)	5/5
8	-12.2	-78.7	2	(-12.2; -10.8)	2/2

The top-scoring poses of all five compounds exhibited an extremely similar binding mode, described by a strong overlap of the common rings and functional groups, as reported in Figure 3.11.

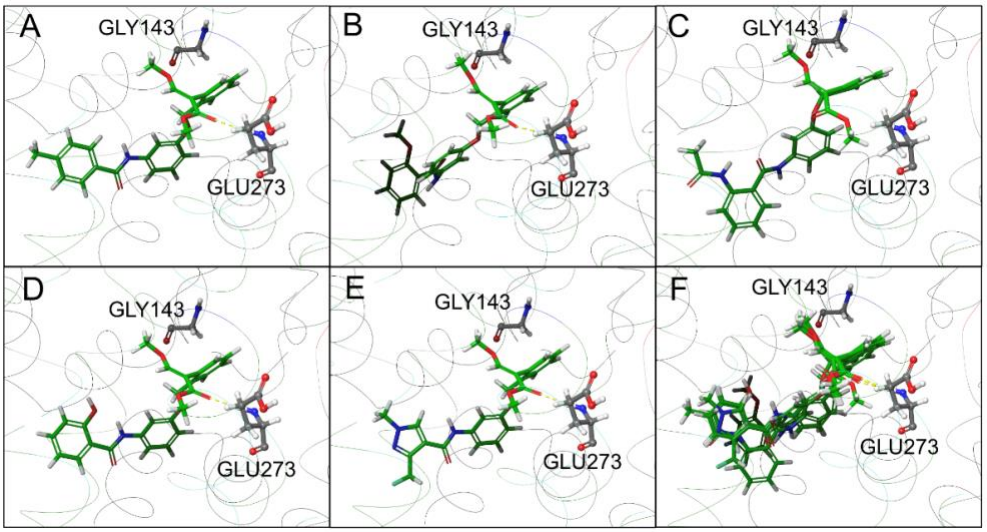

Figure 3.11 *Top-scoring docking poses for compounds A)* ***5****, B)* ***6a****, C)* ***6b****, D)* ***6e****, E)* ***8****. In F) the top-scoring docking poses for all the tested compounds are reported.*

The ligand interaction diagram for azoxystrobin, metyltetraprole and compound **6b** (Figure 3.12) showed the role of Glu273 in the formation of a stable H-bond between the carbonyl function of the ester group and the amide function of the protein backbone. Moreover, in both azoxystrobin and metyltetraprole, Phe129 played a stabilizing role through the formation of a π-π stacking interaction with the aromatic ring distal with respect to the methoxyacrylic function.

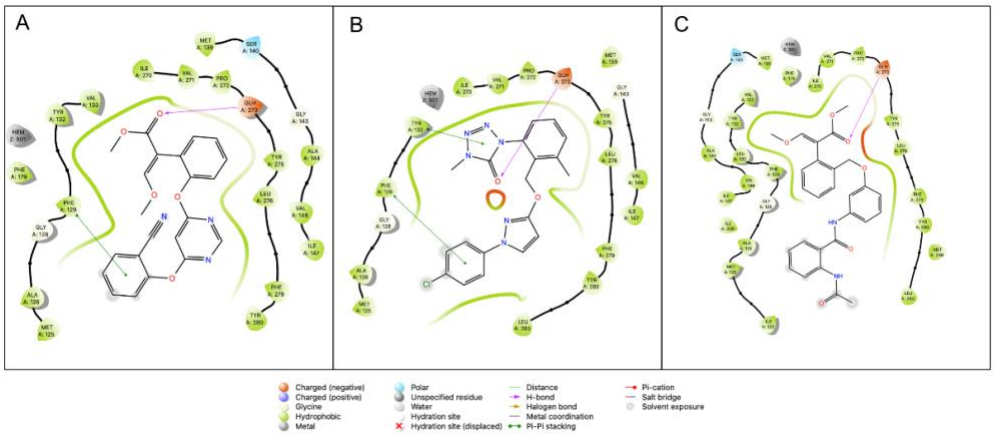

Figure 3.12 *Ligand interaction diagram for (A) azoxystrobin, (B) metyltetraprole and (c) compound* ***6b****. H-bond between the carbonyl function of the ester group and Glu273 is pointed out by the purple arrow, π-π stacking between the distal aromatic ring and Phe129 is pointed out by green line.*

Since compound **6b** maintained its biological activity also against strobilurin-resistant strains containing the G143A mutation (Figure 3.6), we examined the impact of this mutation on cytochrome *bc1* complex using a specific residue scan tool. The mutant protein showed a positive unfavorable ΔAffinity (approx. 5.7 kcal/mol), similar to the ΔAffinity value for azoxystrobin (approx. 4.7 kcal/mol) on the same mutant. On the contrary, the impact of the same mutation on the molecular recognition of metyltetraprole was negligible (approx. -0.7 kcal/mol), suggesting that the correctly oriented and less bulky methyltetrazolone ring did not negatively interact with the methyl group of A143.

3.1.4 Summary

The results evidently show that the spatial orientation of the two pharmacophores (QoI and SDHI), the nature of the linker and the substitution patterns of the bioactive site deeply influence the antifungal activity of the new derivatives. In particular, placing the two pharmacophores in *ortho* position on the central ring (Figure 3.3, compound **2**) led to a significant decrease of the activity against the wild-type strains, while compound **3**, with the two pharmacophores in *para* position, maintained a good activity. Probably, the

introduction of a group in the *ortho* position originates a steric impediment to the binding of the QoI-pharmacophore in the cytochrome *b* binding pocket, while *meta* and *para* orientations do not interfere with the binding.

The arrangement of the methyl group on the benzamide ring also affects the biological activity of the compounds. In fact, the compound **5** with the methyl group in *para* on the carboxamide ring had higher activity on the resistant strains (52% inhibition) than compounds **4** (28%) and **1** (20%).

The worst antifungal performance was showed increasing the length of the spacer. Compounds **9a**-**c**, with glycine, β-alanine and γ-aminobutyric acid as linkers, and **10**, with an additional aromatic ring between the two active moieties showed low activity. In particular, the activity decreased with the increase of the chain length.

Switching the benzamide with a heterocyclic amide (compounds **7** and **8**), maintained a good activity on WT strains (73% and 87%, respectively). Interestingly, compound **8**, which was featured with the pyrazole carboxamide found in the commercial SDHI inhibitor fluxapyroxad, also inhibited the RES strains (57% inhibition).

The group of compounds with different steric and stereoelectronic substituent on benzamide ring showed major effect on the activity of both the strains. Compounds **6a** and **6c** exhibited activity comparable to the reference scaffold **1**, while **6d**, **6g** and **6f** were endowed with lower efficacy. Compounds **6b** and **6e** showed excellent inhibition of wild type strains (> 80% inhibition), with compound **6b** maintaining a strong activity also on resistant strains.

Although 6b had an excellent antifungal activity against WT and RES strains of *P. oryzae*, in the SQR assay it showed low activity against the SDH enzyme. For this reason, we decided to investigate the binding mode of the compound to cytochrome *bc1* by developing a 3D model of *P. oryzae* cytochrome *bc1* supramolecular assembly in complex with azoxystrobin. Testing the putative binding site of our novel compound on the 3D model, we noticed that compound **6b** showed the same molecular recognition mechanism of azoxystrobin for the *P. oryzae* cytochrome *bc1* Qo binding site.

To conclude, the unique biological activity of compound 6b against resistant strains of *P. oryzae* can't be explain by our simulation, as the G143A mutation negatively impacts on the binding of the compound. We considered that additional targets other than cytochrome *bc1* and SDH could be involved in the observed activity. Another interesting hypothesis is that 6b could biotransform in *P. oryzae*, resulting in a compound able to effectively overcome the resistance.

3.1.5 Experimental section

3.1.5.1 General information

See chapter 3.1.2.1 for General information.

3.1.5.2 Experimental procedures

Compounds **15a, 15c** (Kim *et al.*, 2011; Huang *et al.*, 2018), (E)-methyl 2-(2-(bromomethyl)phenyl)-3-methoxyacrylate (Zuccolo *et al.*, 2019), **17b** (Zuccolo et al., 2019) (Zuccolo *et al.*, 2019), **19a** (Zhou *et al.*, 2015), **20** (Crestey *et al.*, 2015), 2-benzyloxybenzoic acid (Baramov *et al.*, 2019) and 2-*tert*-butoxycarbonylaminobenzoic acid (Vilaivan, 2006) were prepared as reported in literature.

(Z)-Methyl 2-iodo-3-methoxyacrylate (12)

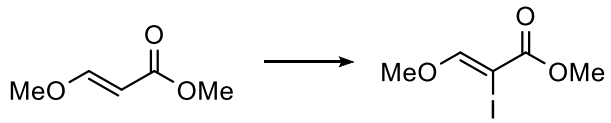

12

To a solution of methyl (*z*)-3-methoxyacrylate (1.30 g, 11.2 mmol) in a 1:1 CH_2Cl_2/pyridine mixture (20 mL) was prepared. A solution of iodine (8.56 g, 33.7 mmol) was added dropwise to the aforementioned mixture (100 mL) at 0°C under a nitrogen atmosphere for 45min. The resulting mixture was stirred in the dark at room temperature for 72 h. The mixture was diluted with diethyl ether (100 mL) and washed, in order, with water (80 mL), HCl 37% (3×20 mL), water (80 mL), $Na_2S_2O_3$ (3x30ml or until discoloration) and brine (50 mL). The organic layer was dried with Na_2SO_4 and the solvent was evaporated at reduced pressure. The oily residue was stripped twice with heptane to remove residual traces of pyridine. The oil was crystallized from ETP to afford **2** (2.38g, 89%) as a light-yellow solid.

Mp: 50-52 °C. Spectroscopic data were in accordance with the literature (Zuccolo *et al.*, 2019)

Methyl 3-methoxy-2-(*o*-tolyl)acrylate (13)

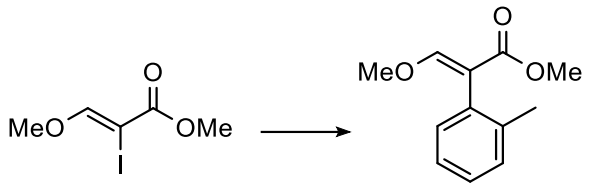

12 **13**

A solution of (E)-methyl 2-iodo-3-methoxyacrylate (12) (880 mg, 3.63 mmol), 2-methyl phenil boronic acid (593 mg, 3.63 mmol) and K_3PO_4 (2.31g, 10.9 mmol) in a solution of dioxane/water 5:1 (20 mL) was degassed by bubbling nitrogen through for 45min. $Pd(PPh_3)_4$ (21 mg, 0.005mmol) was added to the solution. The reaction was stirred at 90 °C for 8h protected from light.

The reaction mixture was diluted with ethyl acetate (20 mL) and the organic phase was washed with water (30mL). The water phase was extracted with ethyl acetate (3x30 mL). The combined organic phases were finally washed with brine (30 mL), dried on Na_2SO_4 and the solvent was evaporated at reduced pressure. A brown-dark oil was obtained. The oil was purified by flash column (SiO_2, 6:4 CH2Cl2/CHX). The purified product 13 was isolated (661 mg, 88%) as a white-transparent oil.

Spectroscopic data were in accordance with the literature (Zuccolo et al., 2019).

(E)-Methyl 2-(2-(bromomethyl)phenyl)-3-methoxyacrylate (14)

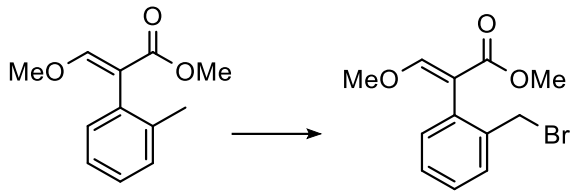

13 **14**

To a solution of 13 (737 mg, 3.47 mmol) in dry carbon tethrachloride (10 mL), N-bromosuccinimide (700 mg, 3.93 mmol) and 2,2'-azo-bisisobutyronitrile (117.24 mg, 0.714 mmol) were added. The resulting mixture was stirred at reflux in the dark for 6h. The reaction was filtered to remove succinimide and the solid residue was washed with dichloromethane (2 mL). The filtrated was concentrated at reduced pressure and the oily residue was purified by flash chromatography (SiO_2, 8:2 ETP/Et2O) to afford 14 (464 mg, 45%) as a white solid.

Mp: 65-65 °C

Spectroscopic data were in accordance with the literature (Zuccolo et al., 2019)

Methyl (E)-2-(2-([2[[tertbutoxycarbonyl]amino]phenoxy]methyl)phenyl)-3methoxyacrylate (16a).

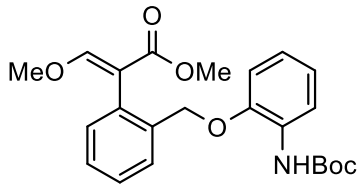

16a

Compound **15a** (200 mg, 0.96 mmol) was added at room temperature to a suspension of anhydrous K_2CO_3 (142 mg, 1.03 mmol) in acetone (4 mL) and the resulting mixture was stirred at reflux for 30 min. After cooling to room temperature, (*E*)-methyl 2-(2- (bromomethyl)phenyl)-3-methoxyacrylate (210 mg, 0.73 mmol) and 18-crown-6 (499 mg, 2.06 mmol) were then added, and the reaction mixture was stirred at reflux for 3 h. Acetone was removed at reduced pressure and the residue was diluted with ethyl acetate (20 mL). The organic layer was washed with water (3×20 mL) and brine (20 mL), then dried with anhydrous Na_2SO_4 and concentrated under reduced pressure. The residue was purified by flash column chromatography in petroleum ether/ethyl acetate 3:1 to obtain compound **16a** (72 mg, 23 %) as a white waxy solid.

Rf:0.34 in hexane/ethylacetate 3:1.

^{1}H NMR (300MHz, CDCl3): δ 8.09(d, *J*= 6.9 Hz, 1H), 7.57 (s, 1H), 7.49–7.44 (m, 1H), 7.39–7.32 (m, 2H), 7.21–7.16 (m, 1H), 7.13 (s, 1H).

^{13}C NMR (75 MHz, CDCl3): δ 163.9, 159.8, 153.9, 146.8, 135.5, 132.3, 131.2, 128.4, 128.1, 127.8 (x 2C), 122.1, 121.2, 118.2, 111.5, 110.2, 80.2, 69.0, 51.3, 28.4 (× 3C).

(*E*)-Methyl 2-(2-([2-aminophenoxy]methyl)phenyl)-3-methoxyacrylate (17a).

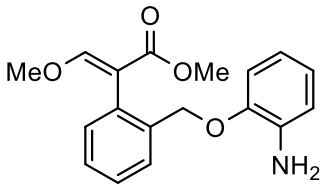

17a

To a solution of compound **16a** (72 mg, 0.17 mmol) in dry CH_2Cl_2 (1 mL), trifluoroacetic acid (100 µL) was added dropwise at 0 °C and the reaction was stirred at 0 °C for 3 h. The solvent was evaporated. Traces of TFA were removed by addition and evaporation of toluene (2 × 1 mL). The residue was dissolved in CH_2Cl_2 and washed with a sat. solution of $NaHCO_3$. The organic phase was dried over anhydrous Na_2SO_4 and the solvent was removed in vacuo. Compound **17a** (54 mg, 98%) was obtained as oil.
Rf: 0.28 in hexane/ethylacetate 2:1.

^{1}H NMR (300 MHz, $CDCl_3$): δ 7.57 (s, 1H), 7.56–7.52 (m, 1H), 7.36–7.26 (m, 2H), 7.21–7.15 (m, 1H), 6.81–6.62 (m, 4H), 4.88 (s, 2H), 3.80 (s, 3H), 3.69 (s, 3H) ppm.

^{13}C NMR (75 MHz, $CDCl_3$): δ 167.9, 160.0, 146.5, 136.5, 136.2, 131.4, 131.0, 128.1, 127.8, 127.8, 121.3, 118.3, 115.1, 112.0, 110.2, 68.5, 62.0, 51.7.

Methyl (*E*)-2-(2-([4-[[tert-butoxycarbonyl]-amino]phenoxy]methyl)phenyl)-3-methoxyacrylate (16c).

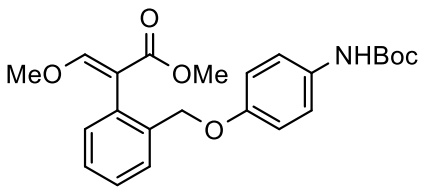

16c

Compound **15c** (209 mg, 1.01 mmol) was added at room temperature to a suspension of anhydrous K_2CO_3 (151 mg, 1.09 mmol) in acetone (4 mL), and the resulting mixture was stirred at reflux for 30 min. After cooling to room temperature, (*E*)-methyl 2-(2-(bromomethyl)phenyl)-3-methoxyacrylate (222 mg, 0.78 mmol) and 18-crown-6 (529 mg, 2.18 mmol) were added and the reaction mixture was stirred at reflux for 3 h. Acetone was removed at reduced pressure and the residue was diluted with ethyl acetate (20 mL). The organic layer was washed with water (3 × 20 mL) and brine (20 mL). The organic layer was dried over anhydrous Na_2SO_4 and concentrated under reduced pressure. The residue was purified by flash chromatography in petroleum ether/ethyl acetate 3:1 to obtain compound **16c** (207 mg, 64%) as a white sticky solid.
Rf: 0.18 in hexane/ethyl acetate 3:1.

^{1}H NMR (300 MHz, $CDCl_3$): δ 7.57 (s, 1H), 7.54–7.49 (m, 1H), 7.36–7.27 (m, 2H), 7.21 (d, J = 8.9 Hz, 2H), 7.18–7.14 (m, 1H), 6.88–6.79 (m, 2H), 6.34 (s, 1H), 4.99 (s, 2H), 3.81 (s, 3H), 3.70 (s, 3H), 1.51 (s, 9H).

^{13}C NMR (75 MHz, $CDCl_3$): δ 167.8, 160.0, 155.0, 153.1, 136.1, 131.5, 131.2, 130.9, 128.4, 128.0, 127.4 (x 2C), 120.6, 115.2 (× 2C), 110.2, 80.2, 68.4, 61.9, 51.6, 28.3 (× 3C).

(*E*)-Methyl 2-(2-([4-aminophenoxy]methyl)phenyl)-3-methoxyacrylate (17c).

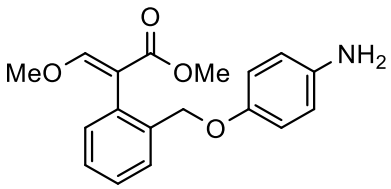

17c

To a solution of compound **16c** (109 mg, 0.26 mmol) in dry CH_2Cl_2 (1.5 mL), trifluoroacetic acid (150 µL) was added dropwise at 0 °C and the reaction was stirred 3 h at 0 °C. The solvent was evaporated and the crude was treated with toluene (2 × 1 mL) to remove TFA. The residue was dissolved in CH_2Cl_2 and washed with a sat. solution of $NaHCO_3$. The organic phase was dried with anhydrous Na_2SO_4 and the solvent was removed *in vacuo*. Compound 21 (78 mg, 95%) was obtained as an oil.
Rf: 0.11 in hexane/ethylacetate 2:1.

^{1}H NMR (300 MHz, $CDCl_3$): *δ* 7.60 (s, 1H), 7.56–7.52 (m, 1H), 7.36–7.26 (m, 2H), 7.18–7.13 (m, 1H), 6.77–6.71 (m, 2H), 6.63–6.57 (m, 2H), 4.99 (s, 2H), 3.84 (s, 3H), 3.72 (s, 3H) ppm.

^{13}C NMR (75 MHz, $CDCl_3$): *δ* 167.9, 160.0, 146.5, 136.5, 136.2, 131.4, 131.0, 128.1, 127.8, 127.6, 121.3, 118.3, 115.1, 112.0, 110.2, 68.5, 61.9, 51.6 ppm.

General procedure for the synthesis of compounds 2 and 3.

To a solution of 2-methylbenzoic acid (0.26 mmol) in CH_2Cl_2 (1.5 mL) at 0 °C under nitrogen atmosphere, EDC•HCl (0.33 mmol) and HOBt (0.33 mmol) were added. The reaction mixture was stirred for 30 min at 0 °C, then a solution of aniline (compound **17a** or **17c**, 0.22 mmol) in CH_2Cl_2 (1 mL) and DIPEA (0.44mmol) were added dropwise at 0 °C. The reaction was stirred for 24 h at room temperature, then the mixture was diluted with ethyl acetate and washed with sat. NH_4Cl, sat. $NaHCO_3$, and brine. The organic phase was dried over anhydrous Na_2SO_4, and the solvent was removed by evaporation. The residue was purified by flash chromatography to give the desired compound.

Methyl (E)-3-methoxy-2-(2-(2-[2-methylbenzamido]-phenoxy)-methyl)-phenyl)-acrylate (2).

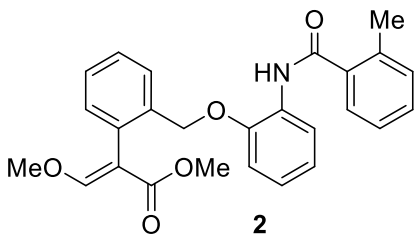

2

Obtained according to the above procedure from 2-methylbenzoic acid and aniline **17a**. Purified by flash chromatography in hexane:ethyl acetate 3:1 (26 mg, 35 %). Yellow sticky solid.
Rf: 0.21 in hex/EtOAc 2:1.

^{1}H NMR (300 MHz, $CDCl_3$): δ 8.56–8.48 (m, 1H), 8.22 (s, 1H), 7.52 (s, 1H), 7.49–7.39 (m, 2H), 7.37–7.27 (m, 3H), 7.25–7.14 (m, 3H), 7.05–6.96 (m, 2H), 6.90–6.83 (m, 1H), 5.04 (s, 2H), 3.70 (s, 3H), 3.61 (s, 3H), 2.49 (s, 3H).

^{13}C NMR (75 MHz, $CDCl_3$): δ 167.8, 167.7, 160.1, 147.5, 136.6, 135.5, 131.4 (x 2C), 131.3, 130.2, 128.2, 127.9, 127.5, 127.2, 125.9, 124.8, 123.9, 121.3, 120.0, 111.9, 109.9, 69.2, 61.9, 51.7, 20.0.

3-Methoxy-2-(2-(4-[2-methyl-benzoylamino]phenoxymethyl)phenyl)acrylic acid methyl ester (3).

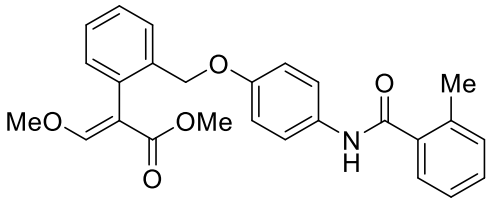

3

Obtained according to general procedure from 2-methylbenzoic acid and amine **17c**. Purified by flash chromatography in hex:EtOAc 55:45 (61 mg, 64 %). White solid.

Rf: 0.60 in hexane/ethyl acetate 1:1.

Mp: 182 °C.

^{1}H NMR (300 MHz, $CDCl_3$): *δ* 7.58 (s, 1H), 7.56–7.42 (m, 4H), 7.40–7.30 (m, 4H), 7.29–1.22 (m, 2H); 7.20–7.15 (m, 2H), 6.95–6.85 (m, 2H), 4.96 (s, 2H), 3.83 (s, 3H), 3.71 (s, 3H), 2.49 (s, 3H).

^{13}C NMR (75 MHz, $CDCl_3$): *δ* 167.8 (x 2C), 159.9, 155.9, 136.6, 136.0, 131.3, 131.2, 131.1, 131.0, 130.1, 128.0, 127.5, 127.4, 126.6, 125.8, 121.7, 115.3, 110.2, 68.4, 61.9, 51.6, 19.7.

General procedure for the synthesis of compounds 4, 5, 6a, 6b, and 7.

To a solution of suitable benzoic acid (0.18 mmol) in CH_2Cl_2 (1 mL) at 0 °C under nitrogen atmosphere, EDC•HCl (0.19 mmol) and HOBt (0.19 mmol) were added. The reaction mixture was stirred at 0 °C for 1 h. After that, a solution of compound **17b** (0.16 mmol) in CH_2Cl_2 (0.7 mL) and DIPEA (0.32 mmol, 56 µL) was added dropwise at 0 °C. The reaction mixture was stirred at room temperature for 8 h. Further amounts of benzoic acid (0.18 mmol), EDC•HCl (0.19 mmol), HOBt (0.19 mmol), and DIPEA (0.32 mmol, 56 µL) were added at 0 °C after 24 and 48 h, and then the reaction was stirred for a further 24 h. The mixture was diluted with ethyl acetate (15 mL) and washed with a sat. NH_4Cl (3×20 mL), sat. $NaHCO_3$ (20 mL) solution, and brine (20 mL). The organic layer was dried over anhydrous Na_2SO_4, and the solvent was removed at reduced pressure. The residue was purified by flash chromatography to give the desired compounds.

Methyl (*E*)-3-methoxy-2-(2-([3-[3-methylbenzamido]phenoxy]methyl)phenyl)acrylate (4).

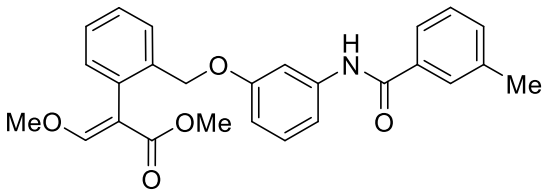

4

Obtained according to the above procedure from compound **17b** and 3-methylbenzoic acid. The crude was purified by flash chromatography in hexane/ethyl acetate 3:1 to give compound **4** (58.3 mg, 84 %) as a white waxy solid.

^{1}H NMR (600 MHz, $CDCl_3$): *δ* 7.92 (s, 1H), 7.70 (s, 1H), 7.67 (d, J = 6.3 Hz, 1H), 7.58 (s, 1H), 7.55 (d, J = 7.3 Hz, 1H), 7.28–7.36 (m, 4H), 7.25 (s, 1H), 7.20 (dd, J = 8.3, 8.3 Hz, 1H), 7.16 (d, J = 7.3 Hz, 1H), 7.11 (s, 1H), 6.68 (dd, J = 1.4, 8.2 Hz, 1H), 4.98 (s, 2H), 3.82 (s, 3H), 3.67 (s, 3H), 2.41 (s, 3H).

^{13}C NMR (150 MHz, $CDCl_3$): δ 168.1, 165.8, 160.4, 159.2, 139.3, 138.6, 136.2, 135.0, 132.5, 131.1, 130.9, 129.7, 128.5, 128.2, 127.9, 127.6, 127.5, 124.0, 112.4, 111.5, 109.9, 106.3, 67.9, 62.1, 51.7, 21.4.

Methyl (*E*)-3-methoxy-2-(2-([3-[4-methylbenzamido]phenoxy]methyl)phenyl)acrylate (5).

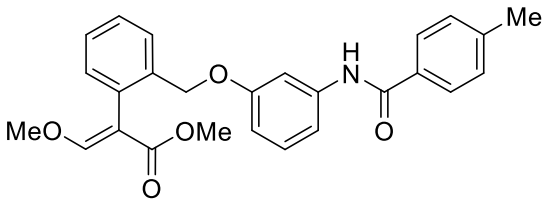

5

Obtained according to general procedure from **17b** and 4-methylbenzoic acid. The crude was purified by flash chromatography in hexane/ethyl acetate 3:1 to give compound **5** (56.5 mg, 82 %) as a white waxy solid.

^{1}H NMR (600 MHz, $CDCl_3$): *δ* 7.93 (s, 1H), 7.81–7.77 (m, 2H), 7.59 (s, 1H), 7.55 (dd, J = 1.3, 7.6 Hz, 1H), 7.36–7.28 (m, 3H), 7.27-7.23 (m, 2H), 7.20 (dd, J = 8.1, 8.2 Hz, 1H), 7.15 (dd, J = 1.3, 7.1, 1H), 7.07–7.09 (m, 1H), 6.68 (ddd, J = 0.8, 2.4, 8.2 Hz, 1H), 4.98 (s, 2H), 3.82 (s, 3H), 3.68 (s, 3H), 2.40 (s, 3H).

^{13}C NMR (150 MHz, $CDCl_3$): *δ* 168.1, 165.5, 160.4, 159.2, 142.2, 139.3, 136.2, 132.1, 131.1, 130.9, 129.7, 129.3, 128.9, 128.2, 127.5 (×2), 127.1, 120.3, 112.4, 111.4, 109.9, 106.2, 67.8, 62.1, 51.8, 21.5.

Methyl (E)-3-methoxy-2-(2-([3-[2-methoxybenzamido]phenoxy]methyl)phenyl)acrylate (6a).

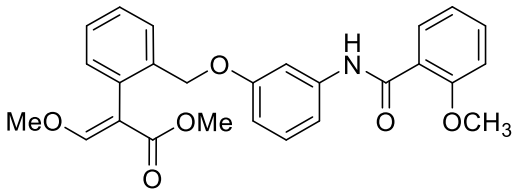

6a

Obtained according to the general procedure from **17b** and 2-metoxybenzoic acid and purified by flash chromatography in hexane:ethyl acetate 3:1 (81.0 mg, 64%). White waxy solid.

^{1}H NMR (600 MHz, $CDCl_3$): δ = 9.77 (s, 1H), 8.27 (dd, J = 7.8, 19 Hz, 1H), 7.59 (s, 1H), 7.58–7.47 (m, 2H), 7.40–7.32 (m, 3H), 7.22–7.11 (m, 4H), 7.03 (d, J = 8.3 Hz, 1H), 6.77–6.59 (m, 1H), 4.99 (s, 2H), 4.04 (s, 3H), 3.83 (s, 3H), 3.70 (s, 3H).

^{13}C NMR (75 MHz, $CDCl_3$): δ 168.9, 163.1, 160.1, 159.4, 157.2, 139.5, 136.0, 133.2, 132.5, 131.3, 131.0, 129.6, 128.1, 127.7, 127.5, 121.9, 121.7, 112.9, 111.5, 110.5, 110.0, 107.3, 68.1, 62.0, 56.2, 51.7.

Methyl (*E*)-3-methoxy-2-(2-([3-[2-acetamidobenzamido]phenoxy]methyl)phenyl)acrylate (6b).

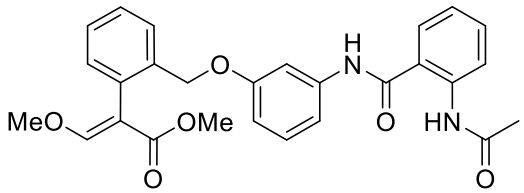

6b

Obtained according to the general procedure from compound **17b** and 2-acetamidobenzoic acid and purified by flash chromatography in hexane:ethyl acetate 1:1 (50 mg, 59%) to give a white waxy solid.

^{1}H NMR (300 MHz, $CDCl_3$): *δ* 8.26 (d, J = 7.9 Hz, 1H), 7.79–7.72 (m, 1H), 7.66 (d, J = 8.0 Hz, 1H), 7.56 (s, 1H), 7.54–7.37 (m, 3H), 7.36–7.27 (m, 2H), 7.18–7.13 (m, 1H), 7.06 (dd, J = 8.4, 1.7 Hz, 1H), 6.81 (d, J = 7.8 Hz, 1H), 6.71 (t, J = 2.1 Hz, 1H), 5.02 (m, 2H), 3.74 (s, 3H), 3.61 (s, 3H), 2.11 (s, 3H).

^{13}C NMR (75 MHz, $CDCl_3$): *δ* 167.8, 162.3, 160.3, 160.0, 154.6, 147.6, 138.7, 135.6 (×2 C), 134.7, 131.3, 130.7, 128.2, 127.7, 127.3, 127.1, 126.9, 126.7, 120.9, 120.2, 116.5, 114.6, 110.0, 68.2, 62.1, 51.8, 24.1.

Methyl (*E*)-3-methoxy-2-(2-([3-[3-methylthiophene-2-carboxamido]-phenoxy]-methyl)- phenyl)-acrylate (7).

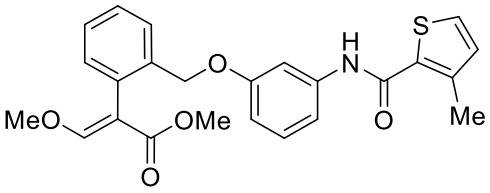

7

Prepared according to the general procedure from **17b** and 2-methylthiophene-3-carboxylic acid. Purified by flash chromatography in hexane:ethyl acetate 3:1 (79 mg, 62%). White waxy solid.

^{1}H NMR (600 MHz, $CDCl_3$): δ 7.59 (s, 1H), 7.57–7.51 (m, 2H), 7.36–7.29 (m, 3H), 7.22–7.14 (m, 4H), 6.93 (d, J = 5.1 Hz, 1H), 6.68 (dd, J = 1.8, 7.8 Hz, 1H), 4.98 (s, 2H), 3.83 (s, 3H), 3.69 (s, 3H), 2.57 (s, 3H).

^{13}C NMR (150 MHz, $CDCl_3$): δ 168.2, 161.4, 160.4, 159.5, 142.4, 139.0, 136.1, 132.4, 131.3, 131.1, 130.8, 129.7, 128.1, 127.6 (×2C), 127.1, 112.8, 111.5, 110.1, 106.9, 68.0, 62.0, 51.7, 15.8.

General procedure for the synthesis of compounds 6c, d, f, 9a-c, 10.

To a solution of a suitable acid (0.26 mmol) in CH_2Cl_2 (1.5 mL) at 0 °C under nitrogen atmosphere, EDC•HCl (0.33 mmol) and HOBt (0.33 mmol) were added. The reaction mixture was stirred at 0 °C for 30 min. After that, a solution of amine **17b** (0.22 mmol) in abs. CH_2Cl_2 (1 mL) was added dropwise at 0 °C. Then, DIPEA (0.44mmol) was added dropwise at 0 °C, and the reaction mixture was stirred at room temperature for 24 h. The reaction mixture was diluted with ethyl acetate and washed with 1M HCl, a saturated solution of $NaHCO_3$, and brine. The organic phase was dried over anhydrous Na_2SO_4, and the solvent was removed in vacuo. The residue was purified by flash chromatography to give the desired compounds.

Methyl (*E*)-3-iodo-2-(2-([3-[2-methoxybenzamido]phenoxy]methyl)phenyl)acrylate (6c).

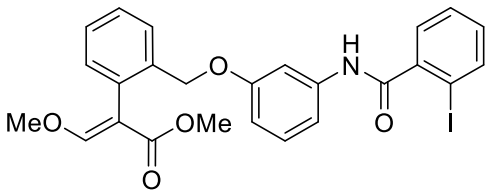

6c

Prepared according to general procedure from **17b** and 2-iodobenzoic acid. Purified by flash chromatography in hexane:ethyl acetate 2:1 (87 mg, 86%). White solid. Rf: 0.46 hexane:ethyl acetate 1:1.

^{1}H NMR (300 MHz, $CDCl_3$): *δ* 7.93-7.87 (m, 1H), 7.59 (s, 1H), 7.58–7.49 (m, 3H), 7.42 (t, J = 7.5 Hz, 1H), 7.35–7.30 (m, 3H), 7.24–7.10 (m, 4H), 6.74–6.69 (m, 1H), 4.98 (s, 2H), 3.83 (s, 3H), 3.66 (s, 3H).

^{13}C NMR (75 MHz, $CDCl_3$): *δ* 167.9, 167.0, 160.1, 159.4, 142.2, 140.0, 138.7, 136.0, 131.4, 131.3, 130.9, 129.8, 128.5, 128.3, 128.1, 127.6, 127.5, 112.4, 111.6, 110.1, 106.7, 92.3, 68.1, 61.9, 51.6.

2-(2-(3-[2-Benzyloxybenzoylamino]phenoxymethyl)phenyl)-3-methoxy-acrylic acid methyl ester (6d).

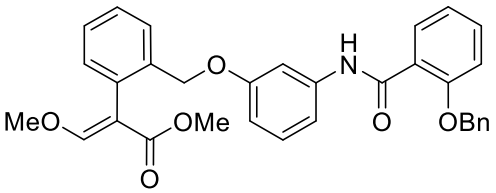

6d

Prepared according to general procedure from **17b** and 2-benzyloxybenzoic acid. Purified by flash chromatography in hex:EtOAc 6:4 (59 mg, 71%). Brown oil. Rf: 0.13 hex:EtOAc 7:3.

^{1}H-NMR (600 MHz, $CDCl_3$): δ 9.95 (1H, s); 8.33 (1H, dd, J = 1.4 Hz, 7.8 H, 1H); 7.58 (s, 1H); 7.57–7.49 (m, 4H); 7.49–7.42 (m, 3H); 7.39–7.30 (m, 2H); 7.18 (d, J = 7.8 Hz, 1H); 7.16–7.12 (m, 1H); 7.06–7.02 (m, 1H); 6.66 (dd, J = 1.6 Hz, 7.8 Hz, 1H); 6.56 (dd, J = 2.5 Hz; 8.3 Hz, 1H); 5.24 (s, 2H); 4.89 (s, 2H); 3.83 (s, 3H); 3.70 (s, 3H).

^{13}C-NMR (150 MHz, $CDCl_3$): δ 167.9, 162.9, 160.1, 159.3, 156.6, 139.6, 136.0, 135.2, 133.2, 132.6, 131.4, 130.9, 129.3, 129.2 (× 4C), 128.6 (× 2C), 128.0, 127.8, 127.5, 121.9, 112.6, 112.2, 110.3, 110.0, 106.7, 71.8, 68.1, 62.0, 51.7.

2-(2-(3-[2-Hydroxy-benzoylamino]-phenoxymethyl)-phenyl)-3-methoxy-acrylic acid methyl ester (6e).

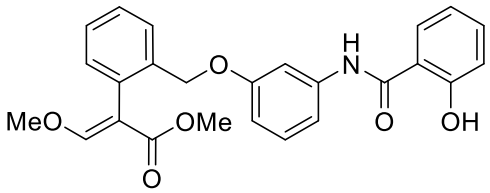

6e

To a solution of compound **6d** (40 mg, 0.076 mmol) in ethyl acetate (0.6 mL), 10% Pd/C (8 mg) was added. The suspension was evaporated under vacuum and flushed with H_2 gas (×3). The reaction mixture was stirred overnight under H_2 at room temperature, then it was filtered through a plug of celite and the residue purified by flash chromatography in hex:EtOAc 6:4 to give compound **6e** in 91% yield. Pale oil. Rf: 0.44 in hex:EtOAc 6:4.

^{1}H-NMR (600 MHz, $CDCl_3$): δ 12.15 (bs, 1H), 8.24 (s, 1H), 7.73 (dd, J = 1.2 Hz, 8.1 Hz, 1H), 7.63 (s, 1H); 7.57 (dd, J = 1.9 Hz, 7.6 Hz, 1H), 7.45–7.41 (m, 1H), 7.40 (dd, J = 1.6 Hz, 7.8 Hz, 1H), 7.38–7.31 (m, 2H), 7.28–7.22 (m, 1H), 7.19 (dd, J = 1.9 Hz, 7.3 Hz, 1H), 7.01 (d, J = 8.1 Hz, 1H), 6.94 (dd, J = 2.2 Hz, 2.2 Hz, 1H), 6.90 (dd, J = 7.8 Hz, 7.8 Hz, 1H), 6.77 (dd, J = 2.4 Hz, 8.2 Hz, 1H), 5.02 (s, 2H); 3.86 (s, 3H); 3.72 (s, 3H).

^{13}C-NMR (150 MHz, $CDCl_3$): δ 168.5, 168.4, 161.9, 160.6, 159.0, 138.1, 136.2, 134.5, 131.1, 130.9, 130.8, 129.8, 128.4, 127.8, 127.6, 127.3, 125.9, 118.7 (× 2C), 114.6, 113.1, 112.5, 109.8, 106.8, 67.7, 62.1, 51.9.

2-(2-(3-[2-tert-Butoxycarbonylamino-benzoylamino]phenoxymethyl)phenyl)-3-methoxyacrylic acid methyl ester (6f).

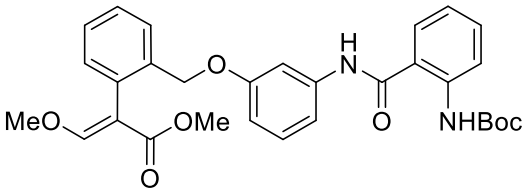

6f

Prepared according to general procedure from **17b** and 2-tert-butoxycarbonylamino-benzoic acid. Purified by flash chromatography in hexane:ethyl acetate 8:2→6:4 (28 mg, 41%). Pale oil. Rf: 0.48 hexane:ethyl acetate 4:6.

^{1}H-NMR (600 MHz, $CDCl_3$): δ 9.88 (s, 1H), 8.34 (d, J = 8.2 Hz, 1H), 8.09 (s, 1H), 7.62 (d, J = 7.9 Hz, 1H); 7.60 (s, 1H), 7.57 (d, J = 7.3 Hz, 1H), 7.46–7.42 (m, 1H), 7.37–7.30 (m, 2H), 7.30–7.22 (m, 2H), 7.17 (d, J = 7.6 Hz, 1H), 7.05–7.00 (m, 2H), 6.37 (d, J = 7.9 Hz, 1H), 4.99 (s, 2H), 3.84 (s, 3H), 3.66 (s, 3H), 1.51 (s, 9H).

^{13}C-NMR (150 MHz, $CDCl_3$): δ 168.2, 167.3, 160.4, 159.2, 153.1, 140.2, 138.6, 136.1, 132.6, 131.0, 130.9, 129.8, 128.3, 127.6, 127.4, 126.9, 121.5, 120.5, 120.1, 112.9, 111.9, 109.9, 106.9, 80.4, 67.8, 62.0, 51.8, 28.3 (× 3C).

2-(2-(3-[2-Aminobenzoylamino]phenoxymethyl)phenyl)-3-methoxy-acrylic acid methyl ester (6g).

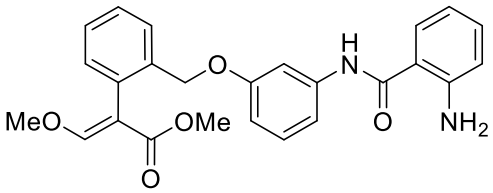

6g

To a stirred solution of compound **6f** (28 mg, 0.05 mmol) in dry CH_2Cl_2 (0.3 mL), TFA (30 µL) was added at 0 °C. The reaction mixture was warmed to room temperature and stirred for 2 h. The reaction mixture was concentrated in vacuo. The residue was diluted with ethyl acetate and washed with a saturated solution of $NaHCO_3$ and brine. The organic phase was dried over anhydrous Na_2SO_4 and the solvent was removed in vacuo. The residue was purified by flash chromatography in hexane:ethyl acetate 6:4 to afford compound **6g** (12 mg, 52% yield). Yellow oil. Rf: 0.24 in hexane:ethyl acetate 1:1.

^{1}H-NMR (600 MHz, $CDCl_3$): δ 8.07 (s, 1H), 7.60 (s, 1H), 7.59–7.54 (m, 2H), 7.37–7.29 (m, 2H), 7.29–7.24 (m, 2H), 7.23–7.15 (m, 2H), 7.07 (m, 1H), 6.84 (d, J = 8.3 Hz, 1H), 7.82–7.77 (m, 1H), 6.69 (dd, J = 1.8 Hz, 8.3 Hz, 1H), 4.98 (s, 2H), 3.83 (s, 3H), 3.68 (s, 3H).

^{13}C-NMR-NMR (150 MHz, $CDCl_3$): δ 168.2, 167.2, 160.4, 159.1, 146.2, 139.0, S11 136.1, 132.7, 131.1 (×2C), 130.9, 129.7, 128.2, 127.6, 127.5, 118.7, 118.6, 117.8, 112.9, 111.5, 109.9, 106.8, 67.8, 62.1, 51.8.

(*E*)-Methyl 2-(2-([3-[3-[difluoromethyl]-1-methyl-1H-pyrazole-4-carboxamido]phenoxy]methyl)phenyl)-3-methoxyacrylate (8).

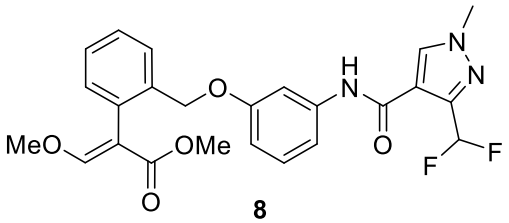

8

Prepared according to the general procedure from **17b** and 3-(difluoromethyl)-1-methyl-1H-pyrazole-4-carboxylic acid. Purified by flash chromatography in hexane:ethyl acetate 45:55 (93 mg, 57%). White solid. MP: 139–141 °C. Rf: 0.07 hexane:ethyl acetate 1:1.

^{1}H NMR (300 MHz, $CDCl_3$): *δ* 8.07 (m, 1H), 8.04 (s, 1H), 7.59 (s, 1H), 7.57–7.53 (m, 1H), 7.38–7.28 (m, 2H), 7.24–7.14 (m, 3H), 713–7.10 (m, 1H); 6.97 (t, J = 54.4 Hz, 1H), 6.72–6.63 (m, 1H), 4.97 (s, 2H), 3.94 (s, 3H), 3.83 (s, 3H), 3.70 (s, 3H).

^{13}C NMR (75 MHz, $CDCl_3$): *δ* 168.2 (x 2C), 160.5, 159.3, 143.5, 138.9, 136.1, 131.2, 130.9, 129.8, 128.2, 127.7, 127.6 (x 2C), 117.2, 114.5, 112.4, 111.2, 109.9, 106.6, 68.0, 62.0, 51.8, 39.6.

3-(2-Methylbenzamido)propanoic acid (19b).

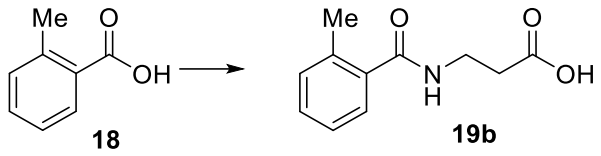

18 19b

To a solution of *β*-alanine (688 mg, 7.72 mmol) in water (8 mL), pH was adjusted to 10 with 2M NaOH, then 2-methylbenzoyl chloride (1.43 g, 9.26 mmol) was added, and the reaction was stirred at rt. The reaction was acidified to pH 2 by adding conc. HCl, and the resulting mixture was extracted with ethyl acetate. The organic phase was dried over anhydrous Na_2SO_4, and the solvent was evaporated. The crude was purified by flash chromatography in hexane:ethyl acetate 1:1 to hexane:ethyl acetate 1:1 + 1% CH_3COOH to give 384 mg (24%) of the title compound. White solid; MP: 103–105 °C. Rf: 0.14 in hexane:ethyl acetate 1:1.

^{1}H NMR (300 MHz, $CDCl_3$): *δ* 7.36–7.27 (m, 2H); 7.23–7.14 (m, 2H); 6.40 (t, J = 5.1 Hz, 1H); 3.74–3.65 (m, 2H); 2.70 (t, J = 6.1 Hz, 2H); 2.41 (s, 3H).

3-(2-Methylbenzamido)-butanoic acid (19c).

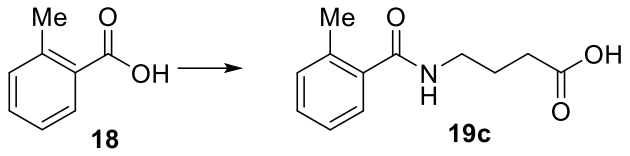

To a solution of GABA (747 mg, 7.24 mmol) in water (3 mL), 2M NaOH was added (10 mL), and the solution was cooled at 0°C. Then, 2- methylbenzoyl chloride (1.34g, 8.69 mmol) was added dropwise, and the reaction was stirred for 2 h at 0 °C and overnight at rt. The reaction was acidified to pH 2 by adding conc. HCl, and the resulting mixture was extracted in ethyl acetate. The organic phase was dried over anhydrous Na_2SO_4, and the solvent was evaporated. The resulting crude was purified by flash chromatography from hexane:ethyl acetate 1:1 to hexane:ethyl acetate 1:1 + 1% CH_3COOH to give 657 mg (41%) of the title compound. White solid; MP: 89 °C. Rf: 0.12 in hexane:ethyl acetate 1:1.

^{1}H NMR (300 MHz, $CDCl_3$): δ 7.37–7.27 (m, 2H), 7.24–7.15 (m, 2H), 6.06 (t, J = 6.4 Hz, 1H), 3.55–3.43 (m, 2H), 2.47 (t, J = 7.1 Hz, 2H), 2.43 (3H, s), 2.00–1.88 (2H, m).

3-Methoxy-2-(2-(3-[2-[2-methylbenzoylamino]-acetylamino]-phenoxymethyl)-phenyl)- acrylic acid methyl ester (9a).

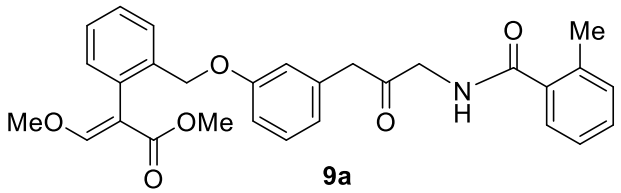

9a

Prepared according to the general procedure from **17b** and **19a**. Purified by flash chromatography in hexane:ethyl acetate 45:55 (18 mg, 18%). Light yellow solid; MP: 170 °C. Rf: 0.21 in hexane:ethyl acetate 45:55.

^{1}H NMR (300 MHz, $CDCl_3$): *δ* 8.50 (s, 1H), 7.60 (s, 1H), 7.57–7.40 (m, 2H), 7.40–7.29 (m, 3H), 7.28–7.07 (m, 6), 6.75 (s, 1H), 6.67 (s, 1H), 4.95 (s, 2H), 4.29 (d, J = 4.7 Hz, 2H), 3.84 (s, 3H), 3.74 (s, 3H), 2.48 (s, 3H).

^{13}C NMR (75 MHz, $CDCl_3$): *δ* 170.8, 168.1, 166.9, 160.4, 159.4, 138.9, 136.5, 136.2, 135.2, 131.2, 131.1, 130.5, 129.8, 128.3, 127.8 (× 2C), 127.2, 126.0, 112.3, 111.1, 110.1, 106.7, 68.1, 62.1, 51.9, 44.8, 29.7, 19.9.

3-Methoxy-2-(2-(3-[3-[2-methylbenzoylamino]-propionylamino]-phenoxymethyl)-phenyl)- acrylic acid methyl ester (9b).

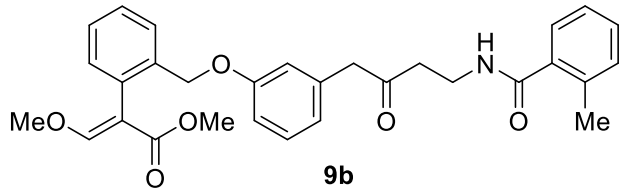

9b

Prepared according to general procedure from **17b** and **19b**. Purified by flash chromatography in hexane:ethyl acetate 1:10 (53 mg, 49%). Green solid; MP: 140 °C. Rf: 0.2 in hexane:ethyl acetate 1:1.

^{1}H NMR (300 MHz, $CDCl_3$): δ 7.88 (s, 1H), 7.59 (s, 1H), 7.56–7.49 (m, 1H), 7.36–7.27 (m, 4H), 7.22–7.11 (m, 5H), 6.98 (s, 1H), 6.69–6.60 (m, 2H), 4.94 (s, 2H), 3.82 (s, 3H), 3.75 (dd, J = 10.3, 4.4 Hz, 2H), 3.72 (s, 3H), 2.70 (t, J =5.8, 2H), 2.41 (s, 3H).

^{13}C NMR (75 MHz, $CDCl_3$): δ 170.5, 169.9, 168.1, 160.3, 159.2, 139.1, 136.1 (x 2C), 135.9, 131.2, 131.0, 130.9, 129.9, 129.6, 128.1, 127.5 (×2C), 126.8, 125.8, 112.1, 110.9, 109.9, 106.4, 67.9, 62.0, 51.7, 36.6, 35.7, 19.8.

3-Methoxy-2-(2-(3-[4-[2-methylbenzoylamino]butyrylamino]phenoxymethyl)phenyl)acrylic acid methyl ester (9c).

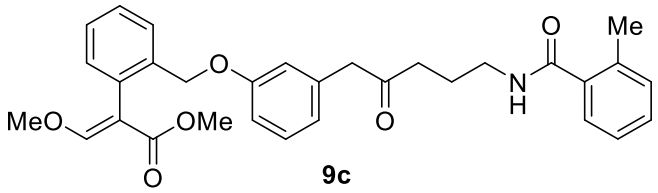

9c

Prepared according to general procedure from **17b** and **19c**. Purified by flash chromatography in hexane:ethyl acetate 1:10 (44 mg, 40%). Light green solid; MP: 136 °C. Rf: 0.2 in hexane:ethyl acetate 1:1.

^{1}H NMR (300 MHz, $CDCl_3$): *δ* 8.79 (s, 1H), 7.58 (s, 1H), 7.57–7.50 (m, 1H), 7.38– 7.27 (4H, m), 7.25–7.11 (6H, m), 6.63 (d, J = 7.6 Hz, 1H), 6.21 (1H, t, J = 5.5 Hz), 4.94 (s, 2H), 3.81 (s, 3H), 3.71 (s, 3H), 3.58–3.49 (m, 2H), 2.50–2.41 (m, 5H), 2.05–1.94 (m, 2H).

^{13}C NMR (75 MHz, $CDCl_3$): *δ* 171.1, 168.1, 160.2, 159.2, 139.5, 136.1, 136.0, 135.9, 131.2, 131.1 (× 2C), 130.9, 130.0, 129.5, 128.1, 127.7, 127.5, 126.7, 125.8, 112.1, 110.6, 109.9, 106.3, 67.9, 61.9, 51.7, 39.1, 34.9, 26.3, 19.8.

3-Methoxy-2-(2-(3-[3-[2-methylbenzoylamino]benzoylamino]phenoxymethyl)phenyl)acrylic acid methyl ester (10).

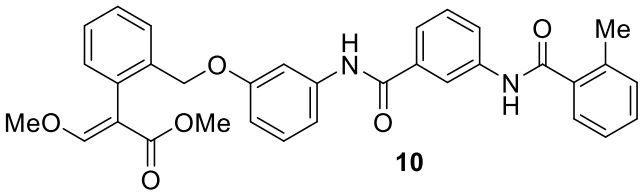

10

Prepared according to the general procedure from **17b** and 3-(2-methylbenzoylamino)benzoic acid (**20**). Purified by flash chromatography in hexane:ethyl acetate 2:1 (40 mg, 33%). Light green solid; MP: 129–131 °C. Rf: 0.36 in hexane:ethyl acetate 1:1.

^{1}H NMR (300 MHz, $CDCl_3$): *δ* 8.13 (s, 1H), 8.05 (s, 1H), 7.93 (d, J = 7.5 Hz, 1H), 7.76–7.65 (m, 2H), S14 7.59 (s, 1H), 7.60–7.08 (m, 12H), 6.70 (dd, J = 8.2, 1.7 Hz, 1H), 4.98 (s, 2H), 3.83 (s, 3H), 3.67 (s, 3H), 2.51 (s, 3H).

^{13}C NMR (75 MHz, $CDCl_3$): *δ* 168.2, 168.1, 165.1, 160.3, 159.1, 139.1, 138.5, 136.5, 136.1, 135.9, 135.6, 131.3, 131.1, 130.8, 130.4, 129.7, 129.4, 128.2, 127.5, 127.4, 126.6, 125.9, 123.1, 122.8, 118.6, 112.6, 111.5, 109.9, 67.9, 62.0, 51.7, 19.8.

3.1.6 Bibliography

Asibi, A.E., Chai, Q. and Coulter, J.A., 2019. Rice Blast: A Disease with Implications for Global Food Security, Agronomy, 9(8), 451. doi:10.3390/agronomy9080451.

Baramov, T., Schmid, B., Ryu, H., Jeong, J., Keijzer, K., von Eckardstein, L., Baik, M. and Süssmuth, R.D., 2019. How Many O-Donor Groups in Enterobactin Does It Take to Bind a Metal Cation?, Chem. – A Eur. J., 25(28), 6955–6962. doi:10.1002/chem.201900453.

Beard, H., Cholleti, A., Pearlman, D., Sherman, W. and Loving, K.A., 2013. Applying Physics-Based Scoring to Calculate Free Energies of Binding for Single Amino Acid Mutations in Protein-Protein Complexes, PLoS One, 8(12), e82849. doi:10.1371/journal.pone.0082849.

Brent, K.J. and Hollomon, D., 2007. In: FRAC Monogr. No.2 (Ed.) FUNGICIDE RESISTANCE : THE ASSESSMENT OF RISK.

Crestey, F., Frederiksen, K., Jensen, H.S., Dekermendjian, K., Larsen, P.H., Bastlund, J.F., Lu, D., Liu, H., Yang, C.R., Grunnet, M. and Svenstrup, N., 2015. Identification and Electrophysiological Evaluation of 2-Methylbenzamide Derivatives as Na v 1.1 Modulators, ACS Chem. Neurosci., 6(8), 1302–1308. doi:10.1021/acschemneuro.5b00147.

Eberini, I., Rocco, A.G., Mantegazza, M., Gianazza, E., Baroni, A., Vilardo, M.C., Donghi, D., Galliano, M. and Beringhelli, T., 2008. Computational and experimental approaches assess the interactions between bovine β-lactoglobulin and synthetic compounds of pharmacological interest, J. Mol. Graph. Model., 26(6), 1004–1013. doi:10.1016/j.jmgm.2007.08.006.

Esser, L., Quinn, B., Li, Y., Zhang, M., Elberry, M., Yu, L., Yu, C. and Xia, D., 2004. Crystallographic Studies of Quinol Oxidation Site Inhibitors: A Modified Classification of Inhibitors for the Cytochrome bc 1 Complex, J. Mol. Biol., 341(1), 281–302. doi:10.1016/j.jmb.2004.05.065.

Faria, J.C., Jelihovschi, E.G. and Allaman, I.B., 2020. Conventional Tukey Yest, UESCILheus, Bras.

Feng, Y., Huang, Y., Zhan, H., Bhatt, P. and Chen, S., 2020. An Overview of Strobilurin Fungicide Degradation:Current Status and Future Perspective, Front. Microbiol., 11, 1–11. doi:10.3389/fmicb.2020.00389.

Fisher, N., Meunier, B. and Biagini, G.A., 2020. The cytochrome bc 1 complex as an antipathogenic target, FEBS Lett., 594(18), 2935–2952. doi:10.1002/1873-3468.13868.

Friesner, R.A., Banks, J.L., Murphy, R.B., Halgren, T.A., Klicic, J.J., Mainz, D.T., Repasky, M.P., Knoll, E.H., Shelley, M., Perry, J.K., Shaw, D.E., Francis, P. and Shenkin, P.S., 2004. Glide: A New Approach for Rapid, Accurate Docking and Scoring. 1. Method and Assessment of Docking Accuracy, J. Med. Chem., 47(7), 1739–1749. doi:10.1021/jm0306430.

Friesner, R.A., Murphy, R.B., Repasky, M.P., Frye, L.L., Greenwood, J.R., Halgren, T.A., Sanschagrin, P.C. and Mainz, D.T., 2006. Extra Precision Glide: Docking and Scoring Incorporating a Model of Hydrophobic Enclosure for Protein−Ligand Complexes, J. Med. Chem., 49(21), 6177–6196. doi:10.1021/jm051256o.

Graziano, S., Marmiroli, N. and Gullì, M., 2020. Proteomic analysis of reserve proteins in commercial rice cultivars, Food Sci. Nutr., 8(4), 1788–1797. doi:10.1002/fsn3.1375.

Halgren, T.A., Murphy, R.B., Friesner, R.A., Beard, H.S., Frye, L.L., Pollard, W.T. and Banks, J.L., 2004. Glide: A New Approach for Rapid, Accurate Docking and Scoring. 2. Enrichment Factors in Database Screening, J. Med. Chem., 47(7), 1750–1759. doi:10.1021/jm030644s.

Harder, E., Damm, W., Maple, J., Wu, C., Reboul, M., Xiang, J.Y., Wang, L., Lupyan, D., Dahlgren, M.K., Knight, J.L., Kaus, J.W., Cerutti, D.S., Krilov, G., Jorgensen, W.L., Abel, R. and Friesner, R.A., 2016. OPLS3: A Force Field Providing Broad Coverage of Drug-like Small Molecules and Proteins, J.

Chem. Theory Comput., 12(1), 281–296. doi:10.1021/acs.jctc.5b00864.

Huang, R., Li, Z., Ren, P., Chen, W., Kuang, Y., Chen, J., Zhan, Y., Chen, H. and Jiang, B., 2018. N -Phenyl- N -aceto-vinylsulfonamides as Efficient and Chemoselective Handles for N-Terminal Modification of Peptides and Proteins, European J. Org. Chem., 2018(6), 829–836. doi:10.1002/ejoc.201701715.

Ishigami, I., Hikita, M., Egawa, T., Yeh, S. and Rousseau, D.L., 2015. Proton translocation in cytochrome c oxidase: Insights from proton exchange kinetics and vibrational spectroscopy, Biochim. Biophys. Acta - Bioenerg., 1847(1), 98–108. doi:10.1016/j.bbabio.2014.09.008.

Kim, E.-M., Jung, C., Choi, E., Gao, C., Kim, S., Lee, S. and Kwon, O., 2011. Highly conductive polyaniline copolymers with dual-functional hydrophilic dioxyethylene side chains, Polymer (Guildf)., 52(20), 4451–4455. doi:10.1016/j.polymer.2011.07.052.

Kunova, A., Palazzolo, L., Forlani, F., Catinella, G., Musso, L., Cortesi, P., Eberini, I., Pinto, A. and Dallavalle, S., 2021. Structural investigation and molecular modeling studies of strobilurin-based fungicides active against the rice blast pathogen pyricularia oryzae, Int. J. Mol. Sci., 22(7). doi:10.3390/ijms22073731.

Kunova, A., Pizzatti, C., Bonaldi, M. and Cortesi, P., 2014. Sensitivity of Nonexposed and Exposed Populations of Magnaporthe oryzae from Rice to Tricyclazole and Azoxystrobin, Plant Dis., 98(4), 512–518. doi:10.1094/PDIS-04-13-0432-RE.

Kunova, A., Pizzatti, C. and Cortesi, P., 2013. Impact of tricyclazole and azoxystrobin on growth, sporulation and secondary infection of the rice blast fungus, *Magnaporthe oryzae*, Pest Manag. Sci., 69(2), 278–284. doi:10.1002/ps.3386.

Li, J., Abel, R., Zhu, K., Cao, Y., Zhao, S. and Friesner, R.A., 2011. The VSGB 2.0 model: A next generation energy model for high resolution protein

structure modeling, Proteins Struct. Funct. Bioinforma., 79(10), 2794–2812. doi:10.1002/prot.23106.

Link, T.A., Iwata, M., Björkman, J., van der Spoel, D., Stocker, A. and Iwata, S., 2003. Molecular Modeling of Inhibitors at Qi and Qo Sites in Cytochromebc1 Complex, in Chem. Crop Prot. Weinheim, FRG: Wiley-VCH Verlag GmbH & Co. KGaA, 110–127. doi:10.1002/3527602038.ch10.

Matsuzaki, Y., Yoshimoto, Y., Arimori, S., Kiguchi, S. and Harada, T., 2020. Bioorganic & Medicinal Chemistry Discovery of metyltetraprole : Identification of tetrazolinone pharmacophore to overcome QoI resistance, Bioorg. Med. Chem., 28(1), 115211. doi:10.1016/j.bmc.2019.115211.

Musso, L., Fabbrini, A. and Dallavalle, S., 2020. Natural Compound-Derived Cytochrome bc1 Complex Inhibitors as Antifungal Agents, Molecules, 25(19), 4582. doi:10.3390/molecules25194582.

Nalley, L., Tsiboe, F., Durand-Morat, A., Shew, A. and Thoma, G., 2016. Economic and Environmental Impact of Rice Blast Pathogen (Magnaporthe oryzae) Alleviation in the United States, PLoS One, 11(12), e0167295. doi:10.1371/journal.pone.0167295.

Palsdottir, H., Lojero, C.G., Trumpower, B.L. and Hunte, C., 2003. Structure of the Yeast Cytochrome bc 1 Complex with a Hydroxyquinone Anion Qo Site Inhibitor Bound, J. Biol. Chem., 278(33), 31303–31311. doi:10.1074/jbc.M302195200.

Phitsuwan, P. and Ratanakhanokchai, K., 2014. Can we create 'Elite Rice'—a multifunctional crop for food, feed, and bioenergy production?, Sustain. Chem. Process., 2(1), 10. doi:10.1186/2043-7129-2-10.

R Core Team, 2020. *R: A language and environment for statistical computing*, R Core Team, R Found. Stat. Comput. Vienna, Austria. Available at: http://www.r-project.org/index.html.

Scheuermann, K.K., Vieira Raimondi, J., Marschalek, R., De Andrade, A. and

Wickert, E., 2012. Magnaporthe oryzae Genetic Diversity and Its Outcomes on the Search for Durable Resistance, in Mol. Basis Plant Genet. Divers. InTech. doi:10.5772/33479.

Schrödinger Release 2020-3; BioLuminate, Schrödinger, LLC: New York, NY, USA, 2020

Schrödinger Release 2020-3; Schrödinger, LLC, New York, NY, USA, 2020

Suemoto, H., Matsuzaki, Y. and Iwahashi, F., 2019. Metyltetraprole, a novel putative complex III inhibitor, targets known QoI-resistant strains of *Zymoseptoria tritici* and *Pyrenophora teres*, Pest Manag. Sci., 75(4), 1181–1189. doi:10.1002/ps.5288.

Triandafyllidou, A. and McAuliffe, M.L., 2014. *Migrant Smuggling Data and Research: A Global Review of the emerging evidence base*.

Vilaivan, T., 2006. A rate enhancement of tert-butoxycarbonylation of aromatic amines with Boc_2O in alcoholic solvents, Tetrahedron Lett., 47(38), 6739–6742. doi:10.1016/j.tetlet.2006.07.097.

Xiong, L., Shen, Y.-Q., Jiang, L.-N., Zhu, X.-L., Yang, W.-C., Huang, W. and Yang, G.-F., 2015. Succinate Dehydrogenase: An Ideal Target for Fungicide Discovery, in ACS Symp. Ser., 175–194. doi:10.1021/bk-2015-1204.ch013.

Ye, Y., Ma, L., Dai, Z., Xiao, Y., Zhang, Y., Li, D., Wang, J. and Zhu, H., 2014. Synthesis and Antifungal Activity of Nicotinamide Derivatives as Succinate Dehydrogenase Inhibitors, J. Agric. Food Chem., 62(18), 4063–4071. doi:10.1021/jf405437k.

Zhou, X., Wang, Q., Zhao, W., Xu, S., Zhang, W. and Chen, J., 2015. Palladium-catalyzed ortho-arylation of benzoic acid derivatives via C–H bond activation using an aminoacetic acid bidentate directing group, Tetrahedron Lett., 56(6), 851–855. doi:10.1016/j.tetlet.2014.12.134.

Zhu, X., Wang, F., Li, H., Yang, W., Chen, Q. and Yang, G., 2012. Design, Synthesis, and Bioevaluation of Novel Strobilurin Derivatives, Chinese J.

Chem., 30(9), 1999–2008. doi:10.1002/cjoc.201200607.

Zuccolo, M., Kunova, A., Musso, L., Forlani, F., Pinto, A., Vistoli, G., Gervasoni, S., Cortesi, P. and Dallavalle, S., 2019. Dual-active antifungal agents containing strobilurin and SDHI-based pharmacophores, Sci. Rep., 9(1), 11377. doi:10.1038/s41598-019-47752-x.

3.2 NATURE-INSPIRED VINIFERIN BENZOFURAN ANALOGUES AS ANTIMICROBIAL AGENTS AGAINST THE FOODBORNE PATHOGEN *L. MONOCYTOGENES*

The results of this section are published in Catinella *et al.* (Catinella *et al.*, 2020).

ABSTRACT. A first study on the antimicrobial activity of resveratrol derivatives against a series of bacteria allowed to identify dehydro-δ-viniferin (**21**) and dehydro-ε-viniferin (**22**), characterized by a versatile benzofuran core, as encouraging antibacterial agents on Gram-positive foodborne bacteria. With the aim of recognise the structural requirements necessary for the antimicrobial activity on the foodborne pathogen *L. monocytogenes* Scott A, a collection of simplified analogues of the two dehydro-viniferin compounds was designed and carried out, systematically removing the aromatic portions of the parent precursors. In this way, we could clarify the most significant structural features implicated in the antibacterial activity. In the case of the simplified dehydro-δ-viniferin derivatives, we found a significant loss of activity, while in the structural simplification of dehydro-ε-viniferin, the analogue **27** showed improved antimicrobial potency (MIC 8 μg/mL, MBC>64 μg/mL). To complete the profile of the compounds, the cytotoxicity of all the synthesized molecules was evaluated.

3.2.1 Introduction

Among promising natural antimicrobial preservatives, polyphenols have received enormous interest in inactivating spoilage and pathogenic microorganisms and in improving microbial safety.

Polyphenols are secondary metabolites mostly found in foods such as fruits, vegetables, whole grains, chocolate, coffee, wine, and tea. This enormous class of molecules, originated by shikimate and polyketide pathways, has several roles in plants: pigment formation, resistance to environmental stresses including defence mechanisms against pathogens or UV radiation,

or activity as chemical messengers. Several studies show that polyphenols are responsible for various beneficial effects on human health, including antioxidant, cardioprotective, neuroprotective, chemopreventive, anti-inflammatory, immunomodulatory, antiallergic properties (Ofosu *et al.*, 2020). Polyphenols can be found in nature as aglycones or linked to carbohydrate moieties or organic acids. For the multitude of chemical structures, they can be classified in two main groups, flavonoid and non-flavonoid derivatives, diverging in the number of rings and in the structural patterns that link the rings together (de La Rosa *et al.*, 2010).

One of the subgroups of non-flavonoid derivatives is constituted by stilbenoids, or polyhydroxystilbenes. Stilbenoid compounds are composed of a common skeleton with two phenolic moieties linked by a central carbon-carbon double bond. The ethylene bridge can be found in the *E* or *Z* configuration, but *trans* isomers are usually the most stable and thus the most frequent in nature. Resveratrol is the most known and studied molecule belonging to stilbenoids. It was isolated for the first time in 1939 from the roots of the white hellebore *Veratrum grandiflorum*. It exhibits a lot of biological properties, but its use is limited in humans due to its low bioavailable (Pecyna *et al.*, 2020). Instead, pterostilbene (*trans*-3,5-dimethoxy-4'-hydroxystilbene), isolated in plant species such as *Pterocarpus marsupium* and *Vitis,* containing two methoxy moieties in place of the hydroxy groups of resveratrol, showed higher bioavailability in comparison to the parent compound.

Monomeric stilbenoids are usually exposed to radical oxidative coupling conducting to the formation of oligomeric stilbenoids (Akinwumi *et al.*, 2018) (Figure 3.13). Consequently, not only classic stilbenoid monomers, but also 2-arylbenzofurans, phenanthrenes, and similar compounds belong to this large class of natural products (Rivière *et al.*, 2012). The structures developed by radical oxidation consist of 2-8 units of resveratrol and are characterised by three-dimensional and chiral polyphenolic compounds. Depending on the regioisomeric way of dimerization, different oligomers are formed. However, in addition to oxidative couplings, the oligomers can undergo further

modifications and rearrangements, as for example occurs in the formation of viniferins, characterized by a 2,3-dihydrobenzofuran core (Ito *et al.*, 1999).

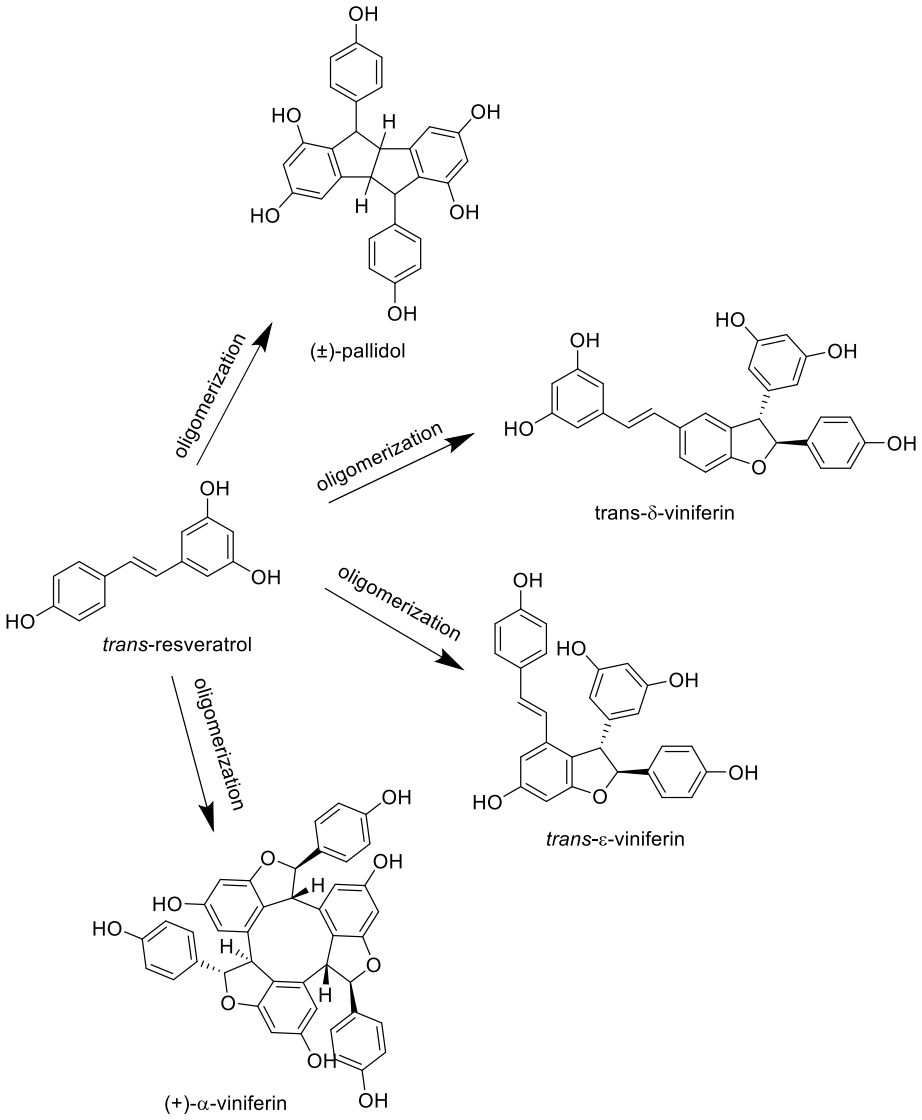

Figure 3.13 *examples of oligomers derived from resveratrol*

Remarkably, 2,3-substituted benzofuran compounds belong to a big number of natural products with several biological activities, such as antioxidant, antiproliferative, antimicrobial, immunomodulatory, and anti-inflammatory properties (Khanam and Shamsuzzaman, 2015; Naik *et al.*, 2015; Chand *et al.*, 2017; Miao *et al.*, 2019)

In the last years, numerous studies showed that the benzofuran scaffold is an attracting choice to design antimicrobial agents. In particular, in a recent study conducted in our laboratory, dehydro-δ-viniferin exhibited a very interesting antibacterial activity against Gram-positive bacterium *L. monocytogenes*. The dimer provoked a net damage of the cytoplasmic membrane with significant membrane depolarization, a loss of membrane integrity, and severe morphological changes. Viniferifuran (or dehydro-ε-viniferin) showed a significant antimicrobial activity as well (Mattio *et al.*, 2019).

3.2.2 Materials and Methods

3.2.2.1 Chemical synthesis

Procedures for the synthesis, isolation, and characterization data for the various compounds obtained are detailed in the experimental section 3.2.3.

3.2.2.2 Evaluation of minimal inhibitory concentration (MIC) and minimal bactericidal concentration (MBC)

All synthesized derivatives were stored in dry form at −20 °C and solubilised in DMSO at a final concentration of 4.096 mg/mL prior to use for MIC and MBC determination. Concisely, *L. monocytogenes* was cultivated in Brain Hearth Infusion BHI (Sigma, Italy) at 37°C for 24 h under shaking condition (200 rpm). After the growth, cells were diluted in BHI to 0.2 OD 600 nm and then used for the 96-well plate inoculum. The concentrations tested ranged from 1 up to 512 µg/mL. The assay was carried out according to Mattio *et al.*, 2019 (Mattio *et al.*, 2019).

3.2.2.3 Citotoxicity on human skin normal WS1 fibroblast cells

The normal human skin WS1 fibroblast cells (ATCC CRL-1502) were cultured in Eagle's Minimum Essential Medium plus 10% fetal bovine serum at 37 ◦C and 5% CO_2. Cytotoxic potency was assessed by a growth inhibition assay (CellTiter 96® AQueous One Solution Cell Proliferation Assay MTS, Promega). The cells were seeded in a 96-well plate, and 24 h later were exposed to the compounds (concentration range 1−200 µM). After 48 h of

exposure, 20 µL of 3-(4,5-dimethylthiazol-2-yl)-5-(3-carboxymethoxyphenyl)-2-(4-sulfophenyl)-2H-tetrazolium salt was added to each well. The absorbance was measured using a FLUOstar OPTIMA plate reader (BMG Labtech GmbH, Offenburg, Germany) at 492 nm after 4 h of incubation at 37 °C in 5% CO_2. The IC_{50} was defined as the drug concentration causing 50% cell growth inhibition, determined by the dose−response curves. Experiments were performed in triplicate.

3.2.3 Results and Discussion

Structure-activity relationship (SAR) studies on the compounds **21** and **22** were conducted to offer a clearer comprehension of the activity of these compounds. Maintaining the benzofuran scaffold, we designed a small collection of simplified compounds of viniferifuran and dehydro-δ-viniferin, which are reported in figure 3.14.

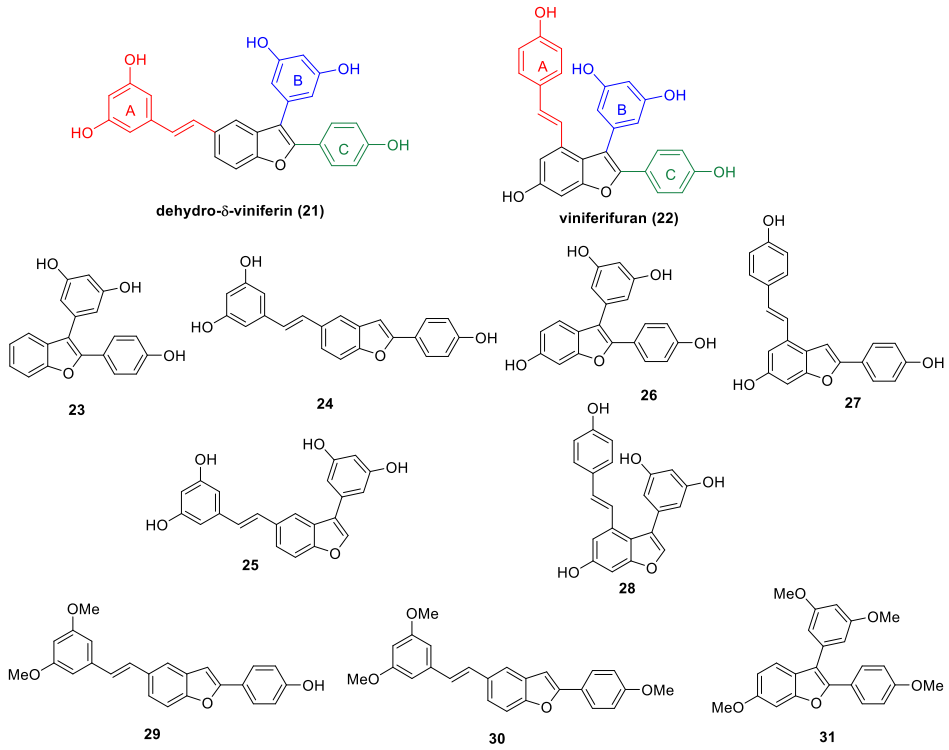

Figure 3.14 *Structures of compounds **21** and **22** and of the simplified analogues **23-31.***

To prepare the various viniferin benzofuran analogues it was essential applying different synthetic approaches considering the nature of the benzofuran substitution pattern.

Firstly, we focused on the synthesis of the simplified analogues of compound **21**. Starting from 2-iodophenol **32** and 1-ethynyl-4-methoxybenzene **33**, following the approach described by Markina *et al.* (Markina *et al.*, 2013), the 2-aryl substituted benzofuran intermediate **34** was prepared by a Cu-catalyzed tandem Sonogashira coupling-cyclization reaction. After the iodination of **34** with NIS to obtain compound **35** in good yield, a Suzuki coupling between **35** and (3,5-dimethoxyphenyl)boronic acid was carried out to give the permethylated intermediate **36**. By deprotection of the phenolic -OH with BBr_3, the 2,3-disubstituted benzofuran **23** was successfully obtained (Scheme 3.5).

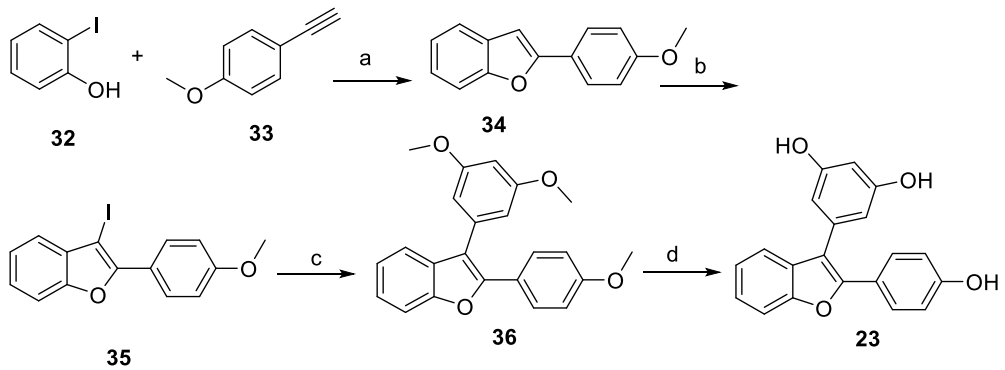

Scheme 3.5 *Reagents and conditions: a) i) $PdCl_2(PPh_3)_2$ (5% mol), CuI (3% mol), TEA/THF 1:1, N_2, 40 °C, 40 min; ii) ACN, 100 °C, 90 min, 50%; b) NIS, p-TsOH, ACN, N_2, overnight, 74%; c) (3,5-dimethoxyphenyl)boronic acid, K_2CO_3, $PdCl_2$(dppf)·DCM, THF/H_2O 1:1, MW, 70 °C, 30 min, 83%; d) BBr_3, DCM, 0 °C to rt, overnight, 61%.*

Based on the key Cu-catalyzed tandem Sonogashira coupling-cyclization, the synthesis of compound **24** was performed (Scheme 3.6). In this case it was required starting from an iodophenol with a suitable moiety in position 4 to link in a second time the styryl functionality. Thus, compound **38** was prepared by the reaction between **37** and **33**, then it was converted into the aldehyde **39** by $LiAlH_4$ reduction, followed by Dess-Martin periodinane oxidation. Following a Wittig-Horner olefination under microwave irradiation with diethyl (3,5-

dimethoxyphenyl)phosphonate compound **30** was obtained in good yield (Vo and Elofsson, 2016). The most critical step of this synthesis was the final deprotection. In several works the demethylation of stilbenoid compounds was realised using BBr_3 in CH_2Cl_2 (Kraus and Gupta, 2009; Miliovsky *et al.*, 2013). Nevertheless, following these conditions compound **30** was only partially demethylated forming the compound **29**. For this reason, we tried an alternative route based on the use of boron trichloride/tetra-*n*-butylammonium iodide (BCl_3/TBAI) (Vo and Elofsson, 2016). This second method resulted more effective and allowed to obtain demethylated compound **24**, purified using semi-preparative HPLC.

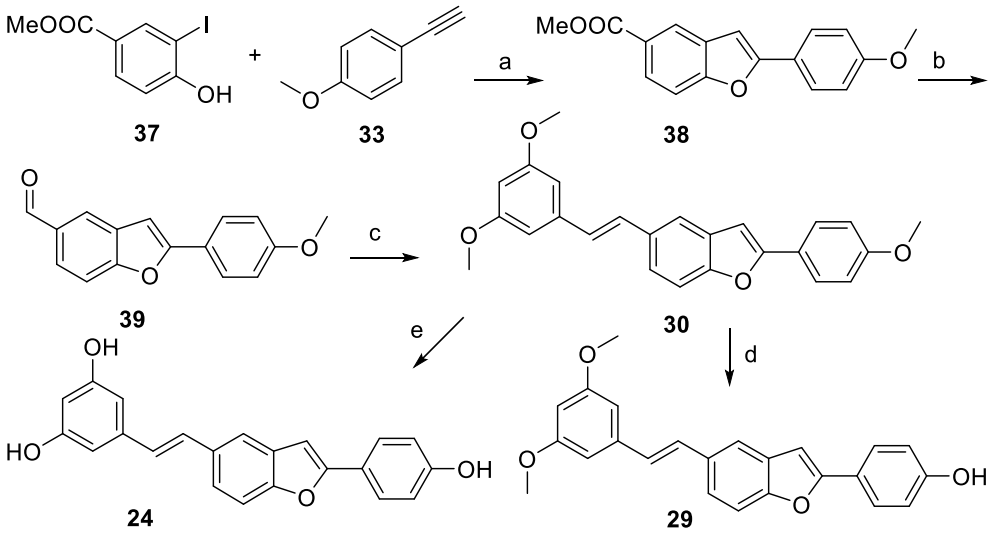

Scheme 3.6 *Reagents and conditions: a) i) $PdCl_2(PPh_3)_2$ (5% mol), CuI (3% mol), TEA/THF 1:1, N_2, 40 °C, 40 min; ii) ACN, 100 °C, 90 min, 62%; b) i) $LiAlH_4$, THF, N_2, 0 °C, 10 min, 77%; ii) DMP, DCM, 0 °C 15 min, rt, 90 min, 85%; c) diethyl (3,5-dimethoxyphenyl)phosphonate, NaH, THF, MW, 120 °C, 30 min, 76%; d) BBr_3, DCM, 0 °C to rt, overnight, 60%; e) BCl_3, TBAI, DCM, N_2, 0 °C to rt, 6h, 35%.*

For the functionalization of positions 3 and 5 of the benzofuran ring it was necessary a diverse synthetic approach (Scheme 3.7). Following the procedure optimized by Liu et al., we prepared the heterocyclic core starting from **40** by a succession of alkylation with bromoacetaldehyde dimethylacetal and cyclodehydration using Amberlyst-15 (Liu *et al.*, 2016). By bromination of **42** and treatment with KOH in MeOH we introduced the bromine in position 3

(Saitoh *et al.*, 2009). Then, compound **45** was obtained by Suzuki coupling of compound **44** with (3,5 dimethoxyphenyl) boronic acid. Again, a reduction with $LiAlH_4$ and oxidation using Dess-Martin periodinane led to aldehyde **46**. By Wittig-Horner olefination between **46** and diethyl(3,5-dimethoxyphenyl)phosphonate under microwave irradiation at 120 °C we synthesized compound **47**. Also in this case, final deprotection was troublesome. After several efforts, we obtain compound **25** in 14% yield by treatment with BBr_3 and difficult purification by flash chromatography.

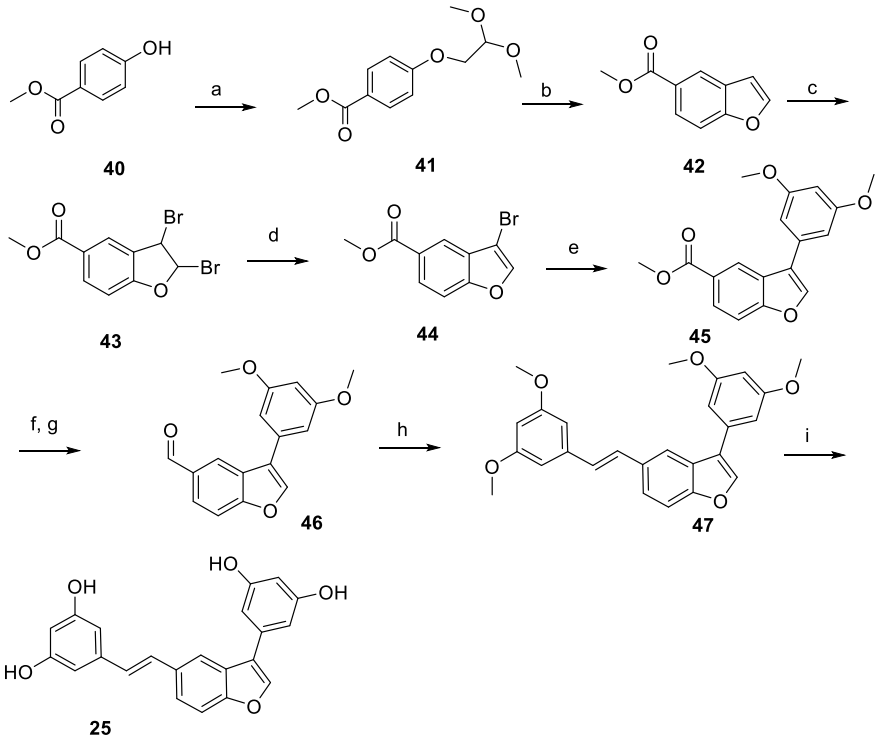

Scheme 3.7 *Reagents and conditions: a) 2-bromo-1,1-dimethoxyethane, Cs_2CO_3, ACN, reflux, 3 days, 61%; b) amberlyst-15, toluene, reflux, 6h, 51%; c) Br_2, DCM, 0 °C to rt, 75 min, 82%; d) KOH, MeOH, THF, 0 °C, 20 min, 82%; e) (3,5-dimethoxyphenyl)boronic acid, $Pd(PPh_3)_4$, Na_2CO_3, DME:H_2O 5:1, 80 °C, overnight, 74%; f) $LiAlH_4$, THF, 0 °C, 10 min, 97%; g) DMP, DCM, 0 °C to rt, 90 min, 78%; h) diethyl (3,5-dimethoxyphenyl)phosphonate, NaH, THF, MW, 120 °C, 30 min, 80%; i) BBr_3, DCM, 0 °C to rt, overnight, 14%.*

Continuously, we concentrated on the synthesis of dehydro-ε-viniferin analogues. The construction of 3-arylbenzofuran was performed employing the procedure of Kim and Choi (Kim and Choi, 2009), a versatile and mild

practice consisting in the cyclization of the corresponding β-aryloxyketone using $Bi(OTf)_3$. Thus, the reaction of *m*-methoxyphenol with α-bromoketone **49**, obtained by treatment of 3,5-dimethoxyacetophenone **48** with $CuBr_2$**,** afforded compound **50**. After a cyclo-dehydratation reaction with $Bi(OTf)_3$, involving an intramolecular Friedel-Craft acylation followed by dehydration, the *β*-aryloxyketone **50** gave the desired benzofuran **51**. To prepare the benzofuran **53**, the same synthetic approach was followed starting from the ketone **52**. In both cases the presence of the electron donating methoxy group gave an indispensable advantage for the intramolecular cyclization.

The connection of an additional aromatic ring on C-2 of compound **51** was achieved by direct arylation by using $Pd(OAc)_2$ and $P(Cy)_3{\cdot}HBF_4$ (Lindgren *et al.*, 2016). At the end, deprotection of permethylated intermediate **31** with BBr_3 provided simplified compound **26** in 52% yield (Scheme 3.8).

In the case of the preparation of compound **28**, the deprotection with BBr_3 was performed directly on compound **54** before introducing the styryl moiety in position 4, to avoid the formation of side products. Final Heck coupling with *p*OH styrene gave the desired scaffold **28**.

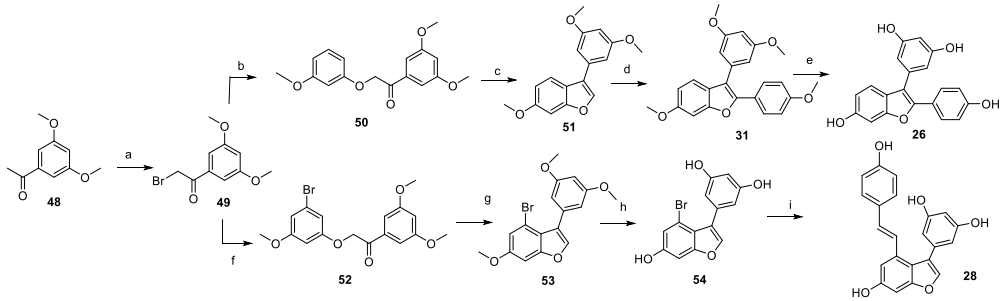

Scheme 3.8 Reagents and conditions: a) $CuBr_2$, EtOAc:$CHCl_3$, reflux, overnight, 67%; b) m-methoxyphenol, K_2CO_3, acetone, N_2, reflux, 2h, 90%; c) $Bi(OTf)_3$, DCM, N_2, reflux, overnight, 43%; d) p-methoxybromobenzene, $Pd(OAc)_2$, PCy_3HBF_4, K_2CO_3, pivalic acid, DMA, N_2, 100 °C, 20h, 80%; e) BBr_3, DCM, 0 °C to rt, overnight, 52%; f) 3-bromo-5-methoxyphenol, K_2CO_3, acetone, N_2, reflux, 2h, 89%; g) $Bi(OTf)_3$, DCM, N_2, reflux, overnight, 83%; h) BBr_3, DCM, 0 °C to rt, overnight, 91%; i) p-hydroxystyrene, $Pd(OAc)_2$, TEA, dppp, DMF, N_2, 120 °C, 20h, 80%.

Finally, the last simplified analogue was prepared starting from compound **55** which was methylated to obtain compound **56** as reported by Iino (Iino *et al.*, 2009). The benzofuran analogue **58** was achieved by a sequence of alkylation

with bromoacetaldehyde dimethylacetal and cyclodehydration using Amberlyst-15, as described above. The successive reaction was the treatment with N-bromosuccinimide (NBS) to get 2-bromobenzofuran **59** which was isolated in high yield as the only isomer using dichloroethane as the solvent and DMF as the catalyst, as illustrated by Liu (Liu *et al.*, 2016). Then, Suzuki coupling with 4-(methoxyphenyl)boronic acid, followed by conversion of the ester group into aldehyde gave compound **61**, which by olefination reaction gave compound **62**. At the end, compound **27** was obtained after deprotection of -OMe groups (Scheme 3.9).

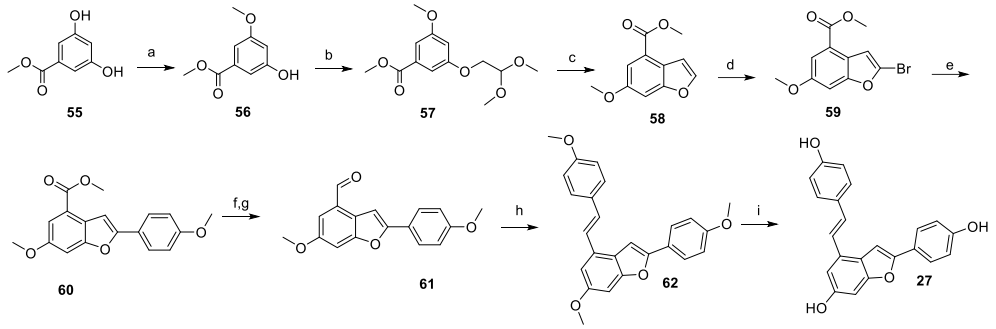

Scheme 3.9 *Reagents and conditions: a) K_2CO_3, CH_3I, DMF, rt, 45h, 35%; b) 2-bromo-1,1-dimethoxyethane, Cs_2CO_3, CH_3CN, reflux, 72h, 67%; c) Amberlyst-15, C_6H_5Cl, 120 °C, 3h, 63%; d) NBS, DMF cat., $ClCH_2CH_2Cl$, 75 °C, 3h, 80%; e) (4-methoxyphenyl)boronic acid, $Pd(PPh_3)_4$, K_2CO_3, DMF, 70 °C, overnight, 91%; f) $LiAlH_4$, DCM, 0 °C, 10 min., 89%; g) DMP, DCM, 0 °C to rt, 90 min, 97%; h) diethyl (4-methoxybenzyl)phosphonate, NaH, dry THF, 120 °C - MW, 30 min, 54%; i) BBr_3, 0 °C to rt, 6h, 24%.*

The two parent compound dehydro-viniferins (**21** and **22**) and all the synthesized simplified compounds **23**–**31** were tested against the foodborne pathogen *L. monocytogenes* Scott A and compared to the natural monomers, resveratrol and pterostilbene.

Firstly, the results showed that dehydro-δ-viniferin **21** (MIC 2 µg/mL) was more active than its regioisomer viniferifuran **22** (MIC 16 µg/mL).

As we can notice in the table 3.4, the selective removal of aromatic rings from the scaffold of molecule **21** significantly decreases antibacterial activity. In fact, the analogues **23**, **24** and **25**, obtained from the removal of the aromatic moieties A, B and C, respectively, exhibited lower activity than their precursor.

In particular, the derivative **24** led to a completely inactivity (MIC 256 µg/mL). Consequently, we presumed that the three phenolic portions in position 5, 3, 2 of benzofuran skeleton are all essential and synergic for antimicrobial activity.

On the contrary, SAR studies on the derivatives of compound **22** revealed that the removal of ring B rose the activity of the derivative; in fact, compound **27** showed a MIC 8 µg/mL (compound **22**: MIC of 16 µg/mL). Conversely, the antimicrobial activity against *L. monocytogenes* decreased 4-fold for compounds **26** and **28**, obtained by selective removal of moieties A and C, respectively (MIC 64 µg/mL vs 16 µg/mL for **22**). It is important to observe that compound **27** bears three phenolic moieties with a spatial orientation comparable to that of compound **21**. Additionally, the introduction of a hydroxy group on the benzofuran skeleton of compound **23** (**26** vs. **23**) resulted in a four-fold decrease of the activity (MIC 64 µg/mL, MBC >512 µg/mL vs. MIC 16 µg/mL, MBC 64 µg/mL).

Moreover, we could underline the different activity of compounds with hydroxy groups with respect to those with methoxy groups. The substitution of phenolic hydroxyl groups with methoxy groups in any case was destructive, giving inactive compounds (compounds **29**, **30**, **31**). Interestingly, also the distance between substituents of the rings seems to play a role. In fact, compound **29** diverges from pterostilbene only in a longer spacer linking the two substituted rings (the benzofuran core). This change gives a loss of compound activity (MIC >512 µg/mL vs 64 µg/mL).

The antiproliferative activity of the synthesized molecules and the natural compounds, resveratrol and pterostilbene, was evaluated on skin normal fibroblast WS1 cells to evaluate the potential toxicity of the compounds on healthy human cells (Table 3.4). The IC_{50} (concentration of compound causing 50% cell growth inhibition) of resveratrol was > 200 µM, while the IC_{50} of all the other molecules ranged from 33 to >100 µM. Comparing the IC_{50} values with the MIC of the compounds against *L. monocytogenes* Scott A (µM concentration), we can notice that **21** has an excellent profile of selectivity. In

fact, cytotoxic results are observed at a concentration ~10-fold higher than the lowest concentration of the compound that prevents the visible growth of bacteria. Additionally, simplified analogues **23**, **25**, **27** showed cytotoxic activity at concentration two-fold higher than their MIC values.

Table 3.4 *Antimicrobial activity of synthesized compounds against L. monocytogenes Scott A[a] and cytotoxic*

Compound	***L. monocytogenes* Scott A**	***L. monocytogenes* Scott A**	**WS1**
	MIC (MBC) µg/mL [a]	**MIC** (µM)[a]	**IC_{50}** (µM)[b]
resveratrol	200 (-)[c]	876	>200
pterostilbene	64 (128)	250	57±10
21 dehydro-*δ*-viniferin	2 (16)	4.42	37.0±1.4
22 viniferifuran	16 (> 512)	35.4	33.0±1.4
23	16 (64)	50.3	98.7±1.8
24	256 (> 512)	743	97.8±3.0
25	16 (64)	44.4	96.8±4.5
26	64 (> 512)	191	98.5±2.0
27	8 (64)	23.2	45.0±1.2
28	64 (> 512)	178	85.0±4.6
29	> 512 (> 512)	1370	95.0±2.3
30	>256 (> 256)	662	>100
31	>256 (> 256)	656	>100
Chlorhexidine	8 (32)	15.8	-

[a]MIC is the minimal inhibitory concentration tested on *L. monocytogenes* Scott A; MBC (in brackets) is the minimal bactericidal concentration.
[b]IC_{50} is defined as the concentration of compound causing 50% cell growth inhibition. Twenty-four hours after seeding, cells were exposed for 48 h to the compounds and cytotoxicity was measured using MTS assay. Data represent mean values ± SD of three independent experiments.
[c]*L. monocytogenes* LMG 16779 (Ferreira and Domingues, 2016).

In conclusion, this SAR study demonstrated that the shape and geometry of the molecules play a key role on the antibacterial activity. Indeed, it can be confirmed that hydroxy groups in polyphenolic compounds can interact with the bacterial cell membrane (Chibane *et al.*, 2019) and the relative position of the -OH groups on the phenolic moieties deeply influences the antimicrobial potency (Wu *et al.*, 2016; Singh *et al.*, 2019).

Furthermore, we identified the dehydro-δ-viniferin **21** and compound **7**, the simplified derivative of viniferifuran without aromatic ring B, as the most promising scaffolds for further developments of nature-inspired antimicrobials active against foodborne pathogenic species.

3.2.4 Experimental section

3.2.4.1 General information

See chapter 3.1.2.1 for General information.

3.2.4.2 Experimental procedures

2-(4-methoxyphenyl)benzofuran (34)

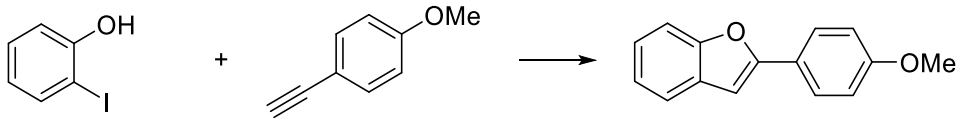

32 **33** **34**

A solution of 2-iodophenol **32** (0.45 mmol, 1 eq.), 1-ethynyl-4-methoxybenzene **33** (0.54 mmol, 1.2 eq.), CuI (0.013 mmol, 0.03 eq.) and $PdCl_2(PPh_3)_2$ (0.02 mmol, 0.05 eq.) in TEA (9.09 mmol, 20 eq.) and THF (1.2 mL) was degassed and heated to 40 °C under N_2 for 40 min. After addition of ACN (2.4 mL) the reaction mixture was heated to 100 °C for 90 min. Then, it was allowed to cool to room temperature and concentred under reduced pressure. The residue was purified by flash chromatography (FC) with CHX/EtOAc (98:2) as eluent to give the desired product. Yield: 50%, white solid. Spectral data were in accordance with literature report (Jaseer *et al.*, 2010).

M.p.: 148-150 °C. **R_f:** 0.3 (cyclohexane/AcOEt 98:2)

^{1}H NMR: (300 MHz, C*D*Cl$_3$) δ (ppm): 7.85-7.78 (m, 2H), 7.59-7.49 (m, 2H); 7.31-7.19 (m, 2H), 7.02- 6.96 (m, 2H), 6.90 (d, *J* = 0.9 Hz, 1H), 3.87 (s, 3H).

^{13}C NMR: (75 MHz, C*D*Cl$_3$) δ (ppm): 160.1, 156.17, 154.8, 129.6, 126.5 (x2C), 123.9, 123.5, 123.0, 120.7, 114.4 (x2C), 111.1, 99.8, 55.5.

3-Iodo-2-(4-methoxyphenyl)benzofuran (35)

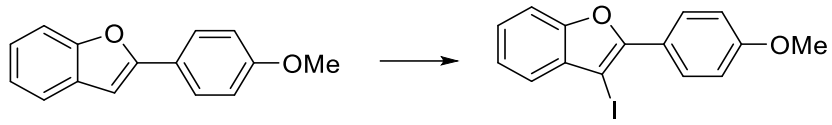

34 **35**

To the suspension of **34** (0.22 mmol, 1 eq.) in CH_3CN (6.7 mL) *N*-iodosuccinimide (0.22 mmol, 1 eq.) and *p*-toluensulfonic acid (0.22 mmol, 1 eq.) were added. The reaction mixture was stirred overnight under nitrogen atmosphere at room temperature. Then, the resulting brownish mixture was diluted with EtOAc (20 mL), washed with aq saturated $NaHCO_3$ (20 mL), 10% aq saturated $Na_2S_2O_3$ (20 mL), and brine (20 mL). The organic layer was dried over anhydrous Na_2SO_4 and concentrated under reduced pressure. The residue was purified by FC with CHX/AcOEt (99:1) as eluent to give the desired product. Yield: 74%, white solid. Spectral data were in accordance with literature report (Yao *et al.*, 2014).

M.p.: 59-61 °C **R_f:** 0.25 (cyclohexane/AcOEt 99:1)

^{1}H NMR (300 MHz, C*D*Cl$_3$) δ (ppm): 8.10 (d, *J* = 8.8 Hz, 2H), 7.45 - 7.39 (m, 2H), 7.31 - 7.28 (m, 2H), 6.99 (d, *J* = 8.0 Hz, 2H), 3.84 (s, 3H).

^{13}C NMR (75 MHz, C*D*Cl$_3$) δ (ppm): 160.5, 153.9, 153.4, 132.8, 129.2 (x2C), 125.4, 123.6, 122.8, 121.7, 114.1 (x2C), 111.2, 59.7, 55.5.

(3,5-dimethoxyphenyl)boronic acid

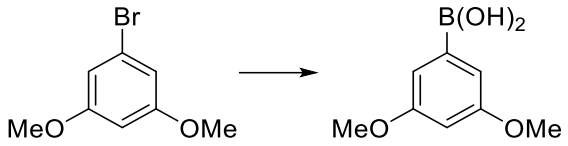

1-bromo-3,5-dimethoxybenzene

(3,5-dimethoxyphenyl) boronic acid

To the solution of 1-bromo-3,5-dimethoxybenzene (1g, 4.606 mmol, 1 eq) in dry THF (22 mL) at -78°C, *n*-BuLi 1.6 M in hexane (3.46 mL, 5.527 mmol, 1.2 eq) was added dropwise and the mixture was stirred at -78°C for 1h. Then, trimethylborate (1.54 mL, 13.818 mmol, 3 eq) was added in one portion and the reaction mixture was stirred for 30 min at - 78°C and then at room temperature for 4h. The reaction mixture was quenched with aq saturated NH_4Cl solution (100 mL) and aq 2M HCl (10 mL). The aqueous layer was extracted with DCM (3 x 80 mL). The combined organic layers were washed with brine, dried over anhydrous Na_2SO_4, filtered and evaporated. The crude was washed with hexane (4 x 15 mL) to give the product as a white solid. Analytical data were in agreement with literature (Elbert *et al.*, 2017).

M.p.: 203°C **R_f:** 0.42 (CHX/AcOEt 1:1)

^{1}H-NMR (300 MHz, DMSO-*d*$_6$) δ (ppm): 8.02 (s, 2H), 6.95 (d, 2H, *J* = 2.3 Hz), 6.51 (t, 1H, J = 2.3 Hz), 3.73 (s, 6H).

^{13}C-NMR (75 MHz, DMSO-*d*$_6$) δ (ppm): 160.8 (x2C), 112.3, 103.3, 55.9 (x2C).

3-(3,5-dimethoxyphenyl)-2-(4-methoxyphenyl)benzofuran (36)

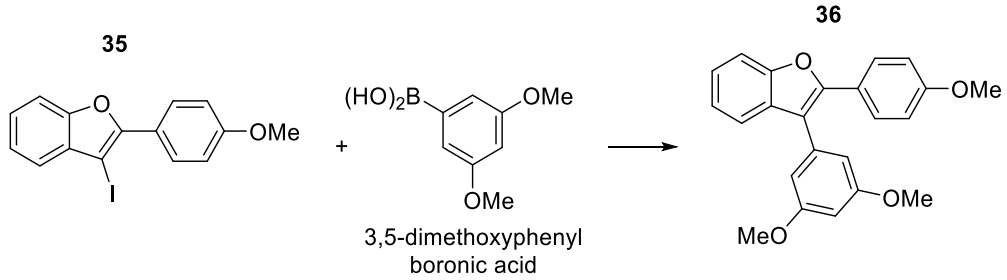

A mixture of **35** (0.04 mmol, 1 eq.), (3,5-dimethoxyphenyl)boronic acid (0.06 mmol, 1.4 eq.), K_2CO_3 (0.13 mmol, 3 eq.), $PdCl_2$(dppf)·DCM (0.0021 mmol, 0.05 eq.) in a mixture of previously degassed THF/H_2O 1:1, was heated at 70 °C for 30 min, under microwave irradiation. After cooling down, the mixture was diluted with EtOAc and washed with H_2O. The aqueous phase was extracted with EtOAc. The combined organic phases was washed with brine, dried over anhydrous Na_2SO_4 and concentrated under reduced pressure. The residue was purified by FC with CHX/EtOAc 93:7 as eluent. Yield: 83%, light brown amorphous solid.

R_f: 0.15 (cyclohexane/AcOEt 99:1)

^{1}H NMR (300 MHz, C*D*Cl_3) δ (ppm): 7.69 – 7.62 (m, 2H), 7.56 – 7.50 (m, 2H), 7.34 – 7.28 (m, 1H), 7.26 – 7.20 (m, 1H), 6.91 – 6.84 (m, 2H), 6.66 (d, *J* = 2.3 Hz, 2H), 6.52 (t, *J* = 2.3 Hz, 1H), 3.83 (s, 3H), 3.79 (s, 6H).

5-(2-(4-hydroxyphenyl)benzofuran-3-yl)benzene-1,3-diol (23)

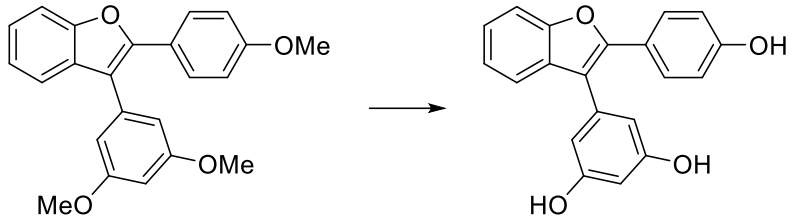

36 **23**

To a solution of **36** (0.11 mmol, 1 eq.) in dry DCM (1.3 mL), under nitrogen atmosphere at 0°C, a 1M BBr_3 solution in DCM (0.33 mmol, 2.9 eq.) was added dropwise. Then mixture was allowed to warm to room temperature. After 16 h the reaction solution was quenched at 0°C with a cold saturated solution of $NaHCO_3$ (0 °C), concentrated under reduced pressure and diluted with H_2O. The aqueous phase was extracted three times with EtOAc. The combined organic phases were dried over anhydrous Na_2SO_4, and concentrated under reduced pressure. The residue was purified by FC with DCM/MeOH (95:5) as eluent to give the desired product as a light brown amorphous solid. Yield: 61%.

R_f: 0.45 (DCM/MeOH 95:5)

^{1}H NMR (300 MHz, CD_3OD) δ (ppm): 7.56 – 7.51 (m, 2H), 7.50 – 7.41 (m, 2H), 7.31 – 7.16 (m, 2H), 6.79 – 6.73 (m, 2H), 6.40 (d, *J* = 2.2 Hz, 2H), 6.31 (t, *J* = 2.2 Hz, 1H).

^{13}C NMR (75 MHz, CD_3OD) δ (ppm): 158.7 (×2), 157.7, 153.7, 150.7, 134.7, 130.2, 128.3 (×2), 123.7, 122.4, 121.9, 119.2, 115.4, 114.8 (×2), 110.2, 107.7 (×2), 101.5.

Methyl 2-(4-methoxyphenyl)benzofuran-5-carboxylate (38)

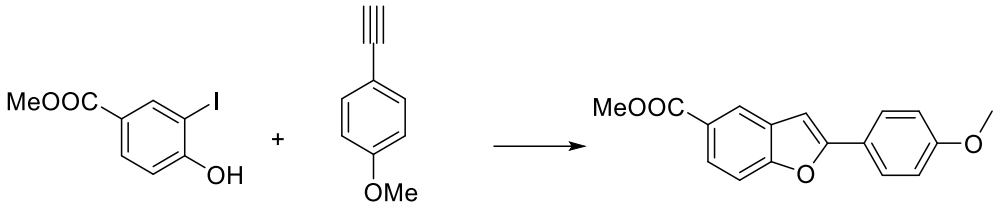

To a solution of methyl 4-hydroxy-3-iodobenzoate **37** (0.36 mmol, 1 eq.) in dry THF (0.95 mL) and dry TEA (1 mL, 7.19 mmol, 20 eq.), 1-ethynyl-4-methoxybenzene **33** (0.43 mmol, 1.2 eq.), CuI (0.01 mmol, 0.03 eq.) and $PdCl_2(PPh_3)_2$ (0.02 mmol, 0.05 eq.) were added under nitrogen atmosphere. The mixture was degassed and heated at 40 °C for 40 min. Then CH_3CN (1.9 mL) was added and the resulting mixture was heated at 100 °C for 90 min. The reaction mixture was allowed to cool to room temperature, washed twice with H_2O and concentred under reduced pressure. The residue was purified by FC with CHX/EtOAc (95:5) as eluent to give the desired product as a white sticky solid. Yield: 62%. Spectral data were in accordance with literature report (Wang *et al.*, 2015).

R_f: 0.42 (CHX/DCM 1:1)

^{1}H NMR (300 MHz, C*D*Cl$_3$) δ (ppm): 8.28 (d, *J*=1.8 Hz, 1H), 7.98 (dd, J_1 =8.6 Hz, J_2 = 1.8 Hz, 1H), 7.80 (d, *J* = 8.9 Hz, 2H), 7.51 (d, *J* = 8.6 Hz, 1H), 6.99 (d, *J* = 8.9 Hz, 2H), 6.93 (d, *J* = 0.8 Hz, 1H), 3.94 (s, 3H), 3.87 (s, 3H).

^{13}C NMR (75 MHz, C*D*Cl$_3$) δ (ppm): 167.4, 160.3, 157.5, 157.3, 129.5, 126.6 (x2C), 125.6, 125.8, 122.9, 122.7, 114.3 (x2C), 110.8, 99.8, 55.4, 52.1.

2-(4-methoxyphenyl)benzofuran-5-carbaldehyde (39)

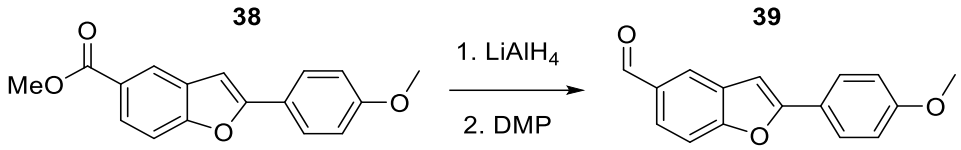

To the solution of compound **38** (0.99 mmol, 1 eq.) in dry THF (9.5 mL), under nitrogen atmosphere, at 0 °C, 1M $LiAlH_4$ in THF (2.97 mmol, 3 eq.) was added dropwise. The mixture was stirred for 10 min at 0 °C, then was quenched with aq 1M HCl at 0 °C. The aqueous phase was extracted three times with EtOAc. The combined organic phases were dried over anhydrous Na_2SO_4, filtered, and concentrated under reduced pressure. The residue (0.82 mmol, 1 eq.) was dissolved in DCM (4.7 mL) and DMP (1.07 mmol, 1.3 eq.) was added at 0 °C. The mixture was stirred at room temperature for 2 h and the solvent was evaporated under reduced pressure. The residue was purified by FC with CHX/EtOAc (8:2) as eluent. Yield: 85%, white solid. Spectral data were in agreement with literature report (Vo and Elofsson, 2016).

M.p.: 121 °C **R_f:** 0.34 (CHX/AcOEt 85:15)

^{1}H NMR (300 MHz, Acetone-*d_6*) δ (ppm): 10.09 (s, 1H), 8.20 (dd, J_1 = 2.3 Hz, J_2 = 0.5 Hz, 1H), 7.92 (d, J = 9.2 Hz, 2H), 7.89 (dd, J_1 = 9.0, J_2= 2.0 Hz, 1H), 7.73 (d, J = 8.4 Hz, 1H), 7.32 (d, J = 0.8 Hz, 1H), 7.09 (d, J = 8.9 Hz, 2H), 3.88 (s, 3H).

^{13}C NMR (75 MHz, C*D*Cl_3) δ (ppm): 191.8, 160.5, 158.1, 132.3, 130.1, 126.7 (x2C), 125.6, 123.5, 122.4, 114.4 (x2C), 111.6, 99.8, 55.4

(*E*)-5-(3,5-dimethoxystyryl)-2-(4-methoxyphenyl)benzofuran (30)

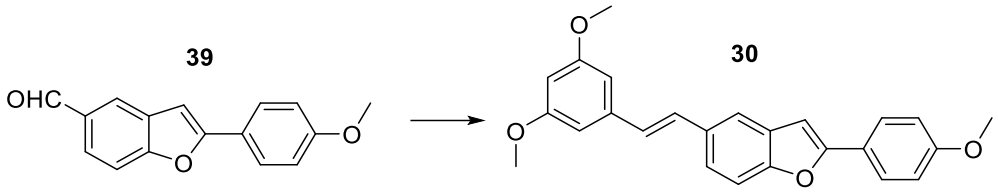

In a MW vial, compound **39** (0.55 mmol, 1 eq.) and diethyl (3,5-dimethoxybenzyl)phosphonate (0.83 mmol, 1.5 eq.) were solubilized in THF dry under nitrogen atmosphere. Then 60% NaH in mineral oil (1.66 mmol, 3 eq.) was added to the solution and the mixture was heated under microwave irradiation at 120 °C for 30 min. After cooling, the mixture was quenched by aq saturated NH_4Cl and the aqueous phase was extracted three times with EtOAc. The organic phases were washed with brine, dried over anhydrous Na_2SO_4, and concentrated under reduced pressure. The crude product was purified by FC with CHX/EtOAc (8:2) as eluent. Yield: 76%, light yellow solid.

M.p.: 169-171 °C **R_f:** 0.41 (CHX/AcOEt 85:15)

^{1}H NMR (300 MHz, C*D*Cl$_3$) δ (ppm): 7.80 (d, *J*=8.8 Hz, 2H), 7.67 (s, 1H), 7.48 (d, *J* = 8.4 Hz, 1H), 7.44 (dd, J_1 = 8.6 Hz, J_2 = 1.6 Hz, 1H), 7.19 (d, *J*= 16.2 Hz, 1H), 7.03 (d, *J* = 15.7 Hz, 1H), 6.99 (d, *J* = 8.8 Hz, 2H), 6.88 (d, *J* = 0.5 Hz, 1H), 6.70 (d, *J* = 2.2 Hz, 2H), 6.40 (t, *J* = 2.2 Hz, 1H), 3.87 (s, 3H), 3.85 (s, 6H).

^{13}C NMR (75 MHz, C*D*Cl$_3$) δ (ppm): 161.0 (x2C), 160.1, 156.8, 154.6, 139.7, 132.3, 130.0, 129.6, 127.5, 126.4 (x2C), 123.2, 122.7, 118.6, 114.3 (x2C), 111.1, 104.5 (x2C), 99.7, 99.6, 55.3 (x2C).

(*E*)-4-(5-(3,5-dimethoxystyryl)benzofuran-2-yl)phenol (29)

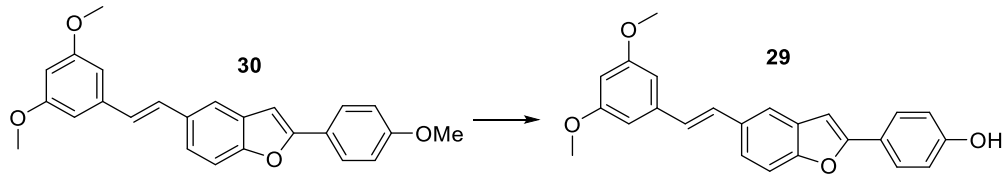

To a solution of **30** (0.12 mmol, 1 eq.) in dry DCM (1.3 mL), under nitrogen atmosphere at 0 °C, a 1M BBr_3 solution in DCM (0.34 mmol, 2.9 eq.) was added dropwise. The mixture was allowed to warm to room temperature. After 16 h the reaction was quenched with H_2O (0 °C) and concentrated under reduced pressure. The aqueous phase was extracted three times with EtOAc. The combined organic phases were dried over anhydrous Na_2SO_4, filtered and concentrated under reduced pressure. The residue was purified by FC with CHX/EtOAc (8:2) as eluent to give the desired product. Yield: 60%, pale yellow solid.

M.p.:194 – 195 °C **R_f:** 0.23 (CHX/AcOEt 8:2)

^{1}H NMR: (300 MHz, Acetone-d_6) δ (ppm): 7.80 (d, *J* = 9.0 Hz, 2H), 7.78 (s, 1H), 7.55 (dd, J_1 = 2.3 Hz, J_2 = 0.9 Hz, 1H), 7.51 (d, *J* = 2.3 Hz, 1H), 7.36 (d, *J* = 8.4 Hz, 1H), 7.17 (d, *J* = 15.0 Hz, 1H), 7.09 (d, *J* = 15.0 Hz, 1H), 6.98 (d, *J* = 9.0 Hz, 2H), 6.80 (d, *J* = 0.9 Hz, 2H), 6.41 (t, *J* = 2.3 Hz, 1H), 3.83 (s, 6H).

^{13}C NMR (75 MHz, Acetone-d_6) δ (ppm): 161.2 (x2C), 158.3, 157.1, 154.4, 139.8, 132.7, 130.2, 129.3, 127.5, 126.5 (x2C), 122.7, 121.9, 118.6, 115.8 (x2C), 110.8, 104.3 (x2C), 99.5, 99.3, 54.7 (x2C).

(*E*)-5-(2-(2-(4-hydroxyphenyl)benzofuran-5-yl)vinyl)benzene-1,3-diol (24)

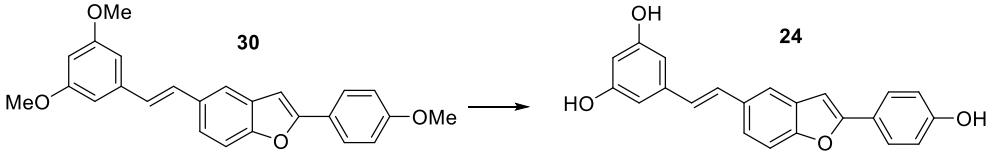

To a solution of compound **30** (0.08 mmol, 1 eq.) and TBAI (0.70 mmol, 9 eq.) in dry DCM (4.8 mL) 1M BCl_3 in DCM (0.70 mmol, 9 eq.) was added dropwise at 0 °C, under nitrogen atmosphere. The mixture was stirred at room temperature. After 6 h the reaction solution was quenched with H_2O at 0 °C and diluted with EtOAc. The organic phase was washed with aq 10% Na_2SO_3. The aqueous phase was extracted twice with EtOAc. The combined organic phases were washed with brine, dried over anhydrous Na_2SO_4, filtered and concentrated under reduced pressure. The residue was purified by FC with CHX/Acetone (6:4) as eluent. The product needed to be purified by preparative HPLC-UV. Chromatographic separation was performed using Kromasil 5 – AmyCoat (250 × 21.2 mm, λ = 220 nm) and an isocratic elution (hexane: *i*PrOH 60:40, rate flow 15 mL/min). Product **24**, t_R = 6.75 min. Yield: 35%, white sticky solid.

R_f: 0.35 (CHX/Acetone 6:4)

^{1}H NMR: (300 MHz, CD_3OD) δ (ppm): 7.80 (d, *J* = 9.0 Hz, 2H), 7.78 (s, 1H), 7.55 (dd, J_1 = 2.3 Hz, J_2 = 0.9 Hz, 1H), 7.51 (d, *J* = 2.3 Hz, 1H), 7.36 (d, *J* = 8.4 Hz, 1H), 7.17 (d, *J* = 15.0 Hz, 1H), 7.09 (d, *J* = 15.0 Hz, 1H), 6.98 (d, *J* = 9.0 Hz, 2H), 6.80 (d, *J* = 0.9 Hz, 2H), 6.41 (t, *J* = 2.3 Hz, 1H) 3.83 (s, 6H).

^{13}C NMR (75 MHz, CD_3OD) δ (ppm): 158.3 (x2C), 158.1, 157.1, 154.3, 139.7, 132.7, 130.1, 128.5, 127.4, 126.1 (x2C), 122.1, 121.9, 118.0, 115.3 (x2C), 110.4, 104.6 (x2C), 101.5, 98.7.

Methyl 4-(2,2-dimethoxyethoxy)benzoate (41)

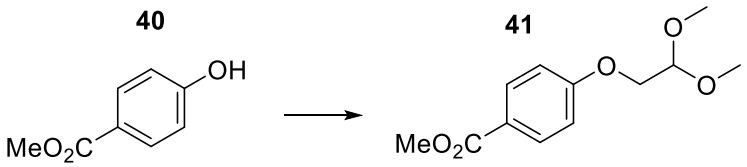

To a solution of methyl 4-hydroxybenzoate **40** (3.29 mmol, 1 eq.) in dry ACN under nitrogen atmosphere, 2-bromo-1,1-dimethoxyethane (4.98 mmol, 1.5 eq.) and Cs_2CO_3 (6.64 mmol, 2 eq.) were added. The mixture was stirred at reflux for three days. After cooling the reaction to room temperature, the solvent was evaporated under reduced pressure. The crude was diluted in EtOAc and washed with H_2O. The aqueous phase was extracted twice with EtOAc. The combined organic phases were dried over anhydrous Na_2SO_4 and concentrated under reduced pressure. The residue was purified by FC with CHX/DCM/EtOAc (10:2:1) as eluent. Yield: 61%, yellow oil.

R_f: 0.36 (CHX/AcOEt 8:2)

^{1}H NMR (300 MHz, C*D*Cl$_3$) δ (ppm): 8.0 (d, *J* = 9.2 Hz, 2H), 6.94 (d, *J* = 9.2 Hz, 2H), 4.73 (t, *J* = 5.2 Hz, 1H), 4.05 (d, *J* = 5.2 Hz, 2H), 3.88 (s, 3H), 3.46 (s, 6H).

^{13}C NMR (75 MHz, C*D*Cl$_3$) δ (ppm): 166.6, 162.1, 131.5 (x2C), 122.9, 114.1 (x2C), 101.9, 67.6, 54.2 (x2C), 51.8.

Methyl benzofuran-5-carboxylate (42)

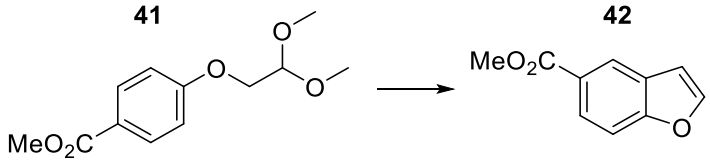

To a solution of compound **41** (1.55 mmol, 1 eq.) in toluene (22.8 mL), amberlyst-15 (10 wt%) was added. The mixture was refluxed for 6 h. After cooling, the mixture was filtered, and the solvent was evaporated under reduced pressure. The residue was purified by FC using CHX/EtOAc (8:2) as eluent. Yield: 51%, white solid. Analytical data were in accordance with literature report (Várela-Fernández *et al.*, 2009).

M.p.: 69-70°C **R_f:** 0.52 (CHX/AcOEt 9:1)

^{1}H NMR (300 MHz, C*D*Cl$_3$) δ (ppm): 8.35 (d, *J* = 1.8 Hz, 1H), 8.03 (dd, *J*= 8.7, 1.8 Hz, 1H), 7.69 (d, *J*= 2.2 Hz, 1H), 7.53 (dd, *J*= 8.7, 0.8 Hz, 1H), 6.84 (dd, J= 2.2, 0.8 Hz, 1H), 3.89 (s, 3H).

^{13}C NMR (75 MHz, C*D*Cl$_3$) δ (ppm): 167.2, 157.4, 146.2, 127.5, 126.0, 125.1, 123.7, 111.2, 107.1, 52.1.

Methyl 2,3-dibromo-2,3-dihydrobenzofuran-5-carboxylate (43)

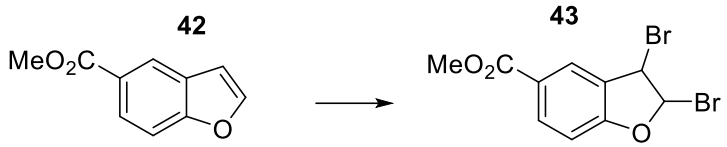

To a solution of compound **42** (0.79 mmol, 1 eq.) in dry DCM (0.6 mL) under N_2 at 0 °C, Br_2 (0.79 mmol, 1 eq.) was added dropwise and the mixture was stirred at room temperature for 75 min. The solution was quenched with aq 1M Na_2SO_3. The aqueous phase was extracted three times with EtOAc. The combined organic phases were washed with brine, dried over anhydrous Na_2SO_4, filtered, and concentrated under reduced pressure. The residue was purified by FC with CHX/EtOAc (95:5) as eluent. Yield: 82%, white sticky solid.

R_f: 0.59 (CHX/AcOEt 9:1)

^{1}H NMR (300 MHz, C*D*Cl$_3$) δ (ppm): 8.23 (d, *J* = 1.9 Hz, 1H), 8.11 (dd, J_1 = 8.6 Hz, J_2 = 1.9 Hz, 1H), 7.10 (d, *J* = 8.6 Hz, 1H), 6.93 (s, 1H), 5.75 (s, 1H), 3.92 (s, 3H).

^{13}C NMR (75 MHz, C*D*Cl$_3$) δ (ppm): 165.8, 160.3, 133.7, 127.8, 126.8, 126.6, 112.3, 90.2, 52.3, 51.6.

Methyl 3-bromobenzofuran-5-carboxylate (44)

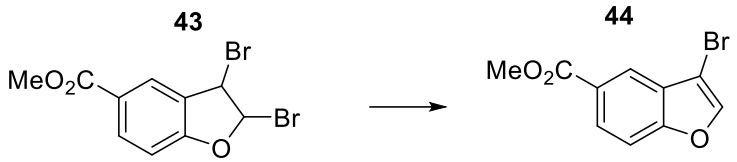

To a solution of compound **43** (0.56 mmol, 1 eq.) in dry THF (0.76 mL) at 0 °C, KOH 85% (0.56 mmol, 1 eq.) and MeOH (152 µL) were added. The mixture was stirred for 20 min, then diluted with EtOAc and washed with H_2O. The aqueous phase was extracted twice with EtOAc. The combined organic phases were washed with aq saturated $NaHCO_3$, dried over anhydrous Na_2SO_4, filtered and concentrated under reduced pressure. The residue was purified by FC with CHX/EtOAc (95:5) as eluent. Yield: 82%, white sticky solid.

R_f: 0.40 (CHX/AcOEt 95:5)

^{1}H NMR (300 MHz, C*D*Cl$_3$) δ (ppm): 8.30 (d, *J* = 1.8 Hz, 1H), 8.09 (dd, J_1 = 8.8 Hz, J_2 = 1.8 Hz, 1H), 7.72 (s, 1H), 7.53 (d, *J* = 8.8 Hz, 1H), 7.26 (s, 1H), 3.97 (s, 3H).

^{13}C NMR (75 MHz, C*D*Cl$_3$) δ (ppm): 166.7, 156.8, 143.9, 143.8, 127.1, 125.9, 122.3, 111.7, 98.4, 52.2.

Methyl 3-(3,5-dimethoxyphenyl)benzofuran-5-carboxylate (45).

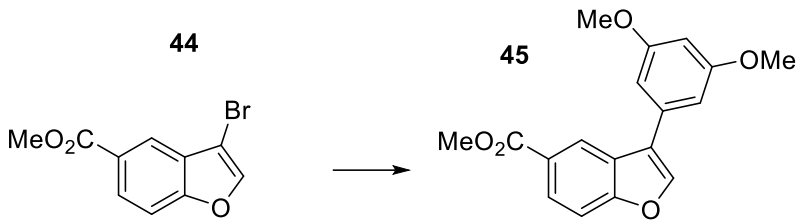

A solution of compound **44** (0.45 mmol, 1 eq.), 3,5-dimethoxyphenylboronic acid (0.50 mmol, 1.1 eq.) and Na_2CO_3 (1.0 mmol, 2.2 eq.) in a mixture DME/H_2O 5:1 was degassed for 30 min. Then, $Pd(PPh_3)_4$ (0.01 mmol, 0.03 eq.) was added and the mixture was degassed again. The reaction was heated at 80 °C overnight. After cooling, the mixture was quenched with water and the aqueous phase was extracted three times with EtOAc. The organic phases were washed with brine, dried over anhydrous Na_2SO_4 and concentrated. The crude was purified by FC with CHX/EtOAc 9:1 as eluent. Yield: 74%, white solid.

M.p.:101-103 °C. **R_f:** 0.35 (CHX/AcOEt 9:1)

^{1}H NMR (300 MHz, C*D*Cl$_3$) δ (ppm): 8.56 (d, *J* = 1.7 Hz, 1H), 8.09 (dd, J_1 = 8.7 Hz, J_2 = 1.7 Hz, 1H), 7.84 (s, 1H), 7.57 (d, *J* = 8.7 Hz, 1H), 6.78 (d, *J* = 2.3 Hz, 2H), 6.52 (t, *J* = 2.3 Hz, 1H), 3.96 (s, 3H), 3.87 (s, 6H).

^{13}C NMR (75 MHz, C*D*Cl$_3$) δ (ppm): 166.2, 160.2, 159.3 (x2C), 143.0, 141.7, 136.2, 132.3, 130.9, 129.4, 128.7, 112.1, 104.5 (x2C), 99.9, 55.8 (x2C), 51.7.

(3-(3,5-dimethoxyphenyl)benzofuran-5-yl)methanol (46')

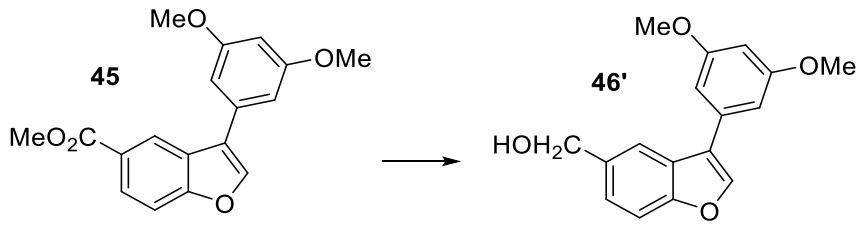

To a solution of compound **45** (0.23 mmol, 1 eq.) in dry THF, under nitrogen atmosphere at 0°C, $LiAlH_4$ 1M in THF (0.70 mmol, 3 eq.) was added dropwise. The mixture was stirred for 10 minutes at 0 °C, and then quenched with HCl 1M at 0°C. The aqueous phase was extracted three times with EtOAc. The combined organic phases were dried over anhydrous Na_2SO_4, filtered, and concentrated under reduced pressure. Purification by FC using CHX/EtOAc (6:4) as eluent afforded the desired product as a brown sticky solid. Yield: 97%.

R_f: 0.21 (CHX/AcOEt 7:3)

^{1}H NMR (300 MHz, C*D*Cl$_3$) δ (ppm): 7.83 (d, *J* = 1.1 Hz, 1H), 7.80 (s, 1H), 7.53 (d, *J* = 8.5 Hz, 1H), 7.37 (dd, J_1 = 8.5, J_2 = 1.7 Hz, 1H), 6.78 (d, *J* = 2.3 Hz, 2H), 6.50 (t, *J* = 2.3 Hz, 1H), 4.80 (s, 2H), 3.86 (s, 6H).

^{13}C NMR (75 MHz, C*D*Cl$_3$) δ (ppm): 161.2 (x2C), 155.3, 142.0, 136.0, 133.7, 126.5, 124.2, 122.3, 119.1, 111.8, 105.8 (x2C), 99.3, 65.6, 55.4 (x2C).

3-(3,5-dimethoxyphenyl)benzofuran-5-carbaldehyde (46)

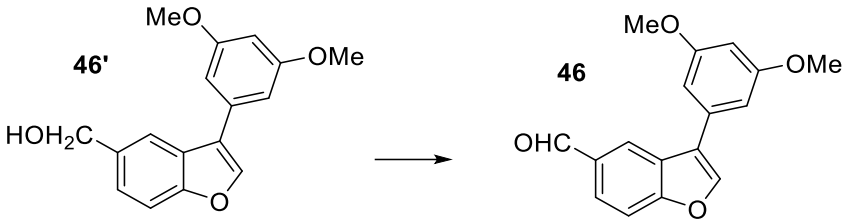

To a solution of compound **46** (0.21 mmol, 1 eq.) in dry DCM, DMP (0.27 mmol, 1.3 eq.) was added at 0 °C. The mixture was stirred at room temperature for 90 min. The solvent was evaporated under reduced pressure and the residue was purified by FC using as eluent CHX/EtOAc (8:2). Yield: 78%, yellow solid.

M.p.: 96 - 98 °C. **R_f:** 0.48 (CHX/AcOEt 8:2)

^{1}H NMR (300 MHz, C*D*Cl$_3$) δ (ppm): 10.09 (s, 1H), 8.36 (d, *J* = 1.6 Hz, 1H), 7.93 (dd, J_1 = 8.6, J_2 = 1.6 Hz, 1H), 7.88 (s, 1H), 7.66 (d, *J* = 8.6 Hz, 1H), 6.53 (t, *J* = 2.3 Hz, 1H), 3.87 (s, 6H).

^{13}C NMR (75 MHz, C*D*Cl$_3$) δ (ppm): 191.6, 161.4 (x2C), 159.0, 143.0, 132.7, 132.4, 127.1, 125.9, 124.1, 123.0, 112.6, 105.9 (x2C), 99.7, 55.5 (x2C).

(*E*)-3-(3,5-dimethoxyphenyl)-5-(3,5-dimethoxystyryl)benzofuran (47)

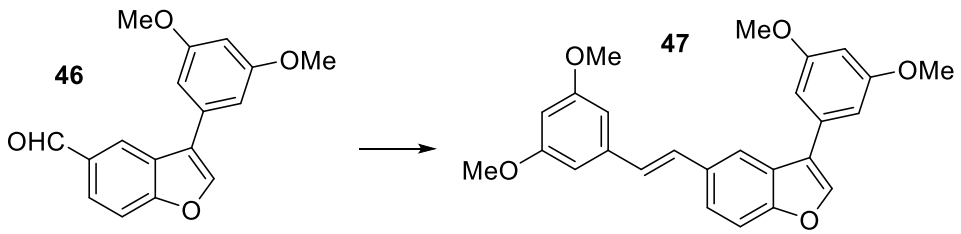

In a MW vial, compound **46** (0.15 mmol, 1 eq.) and diethyl (3,5-dimethoxybenzyl)phosphonate (0.22 mmol, 1.5 eq.) were solubilized in dry THF (2 mL) under nitrogen atmosphere, followed by the addition of 60% NaH in mineral oil (0.45 mmol, 3 eq.). The mixture was heated under microwave irradiation at 120 °C for 30 min. After cooling, the mixture was quenched with an aq saturated solution of NH_4Cl and the aqueous phase was extracted three times with EtOAc. The organic phases were washed with brine, dried over anhydrous Na_2SO_4, and concentrated under reduced pressure. Purification by FC with CHX/EtOAc (8:2) as eluent gave the title compound as a white sticky solid. Yield: 80%.

R_f: 0.43 (CHX/AcOEt 85:15)

^{1}H NMR (300 MHz, C*D*Cl$_3$) δ (ppm): 7.85 (d, *J* = 1.5 Hz, 1H), 7.77 (s, 1H), 7.53 (dd, J_1 = 8.6, J_2 = 1.5 Hz, 1H), 7.49 (d, *J* = 8.6 Hz, 1H), 6.92 (d, *J* = 16.3 Hz, 1H), 6.89 (d, *J* = 16.3 Hz, 1H), 6.65 (d, *J* = 2.2 Hz, 2H), 6.51 (d, *J* = 2.2 Hz, 2H), 6.40 (t, *J* = 2.2 Hz, 1H), 6.35 (t, *J* = 2.2 Hz, 1H), 3.87 (s, 6H), 3.82 (s, 6H).

^{13}C NMR (75 MHz, C*D*Cl$_3$) δ (ppm): 161.3 (x2C), 161.0 (x2C), 155.5, 142.1, 139.5, 132.6, 129.5, 127.9, 126.9, 123.2, 122.4, 118.8, 111.9, 110.0, 105.4 (x2C), 104.3 (x2C), 99.9, 99.3, 55.5 (x2C), 55.4 (x2C).

(*E*)-5-(2-(3-(3,5-dihydroxyphenyl)benzofuran-5-yl)vinyl)benzene-1,3-diol (25)

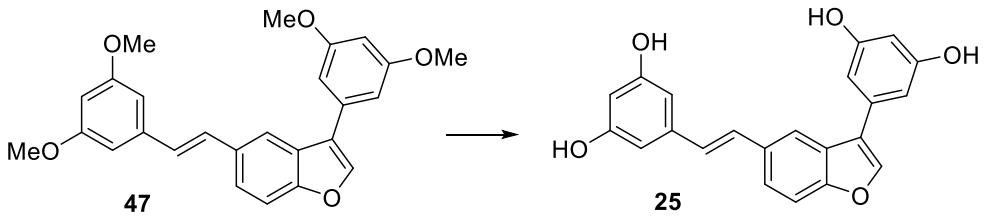

To a solution of compound **47** (0.11 mmol, 1 eq.) in dry DCM (7 mL) under nitrogen atmosphere, a 1M BBr_3 solution in DCM (1.37 mmol, 12 eq.) was added dropwise at 0 °C. The mixture was stirred at room temperature for 9 h. The reaction was quenched with H_2O at 0 °C. The aqueous phase was extracted three times with EtOAc. The combined organic phases were dried over anhydrous Na_2SO_4, and concentrated under reduced pressure. The residue was purified by FC with DCM/MeOH (95:5) to give the desired product. Yield: 14%, light brown sticky solid.

R_f: 0.48 (DCM/MeOH 9:1)

^{1}H NMR (300 MHz, CD_3OD) δ (ppm): 7.93 (d, *J* = 1.5 Hz, 1H), 7.90 (s, 1H), 7.57 (dd, J_1 = 8.6, J_2 = 1.5 Hz, 1H), 7.49 (d, *J* = 8.6 Hz, 1H), 7.19 (d, *J* = 16.3 Hz, 1H), 7.00 (d, *J* = 16.3 Hz, 1H), 6.65 (d, *J* = 2.2 Hz, 2H), 6.51 (d, *J* = 2.2 Hz, 2H), 6.31 (t, *J* = 2.2 Hz, 1H), 6.19 (t, *J* = 2.2 Hz, 1H).

^{13}C NMR (150 MHz, CD_3OD) δ (ppm): 160.1 (x2C), 159.7 (x2C), 156.9, 143.4, 140.9, 134.8, 134.2, 129.7, 129.2, 128.0, 124.2, 123.6, 119.5, 112.7, 106.9 (x2C), 106.0 (x2C), 103.0, 102.8.

2-bromo-1-(3,5-dimethoxyphenyl)ethan-1-one (49).

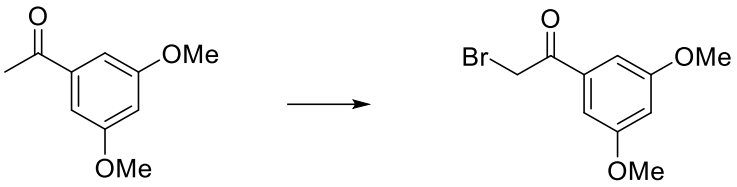

48 **49**

To a solution of 1-(3,5-dimethoxyphenyl)ethan-1-one **48** (11.09 mmol, 1 eq) in a mixture of EtOAc/$CHCl_3$ (1:1, v/v, 30 mL), $CuBr_2$ (22.19 mmol, 2 eq) was added. The mixture was stirred at reflux overnight. The green reaction mixture was cooled to room temperature and filtered on a celite pad using EtOAc to wash the filter. The solvent was evaporated under reduced pressure. The crude was purified by FC with CHX/DCM/EtOAc 10:1:0.5 as eluent. Yield: 67%; orange amorphous solid. Analitical data were in accordance with literature report (Lindgren *et al.*, 2016)

R_f: 0.32 (cyclohexane/AcOEt/DCM 10:0.5:1)

^{1}H NMR (300 MHz, C*D*Cl_3) δ (ppm): 7.11 (d, 2H, *J*=2.3 Hz), 6.69 (t, 1H, *J*=2.3 Hz), 4.42 (s, 2H), 3.84 (s, 6H).

^{13}C NMR (75 MHz, C*D*Cl_3) δ (ppm): 191.2, 161.1 (x2C), 135.9, 106.8 (x2C), 106.3, 55.8 (x2C), 31.1.

1-(3,5-dimethoxyphenyl)-2-(3-methoxyphenoxy)ethan-1-one (50)

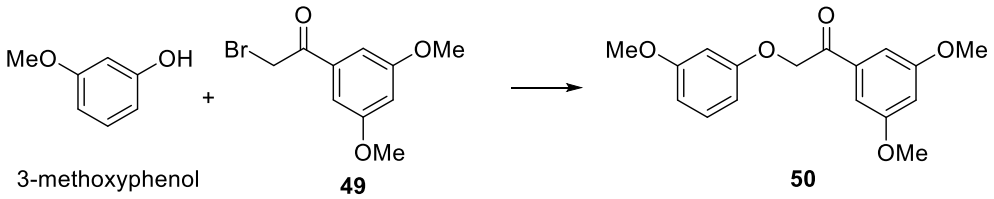

A solution of **49** (1.15 mmol), 3-methoxyphenol (1.23 mmol, 1.1 eq) and K_2CO_3 (3.47 mmol, 3 eq) in dry acetone (3.2 mL) under nitrogen atmosphere was heated at reflux. After 2h, the reaction mixture was cooled to room temperature, concentrated under reduced pressure, diluted with EtOAc and washed with H_2O. The aqueous phase was extracted twice with EtOAc. The combined organic phases were washed with H_2O, dried over anhydrous Na_2SO_4 and concentrated under reduced pressure. The residue was purified by FC with CHX/AcOEt/DCM (10:1:2) as eluent. Yield: 90%, yellow-orange sticky solid. Analytical data were in accordance with literature report (Lindgren *et al.*, 2016)

R_f: 0.32 (CHX/AcOEt/DCM 10:1:2)

^{1}H NMR (300 MHz, C*D*Cl$_3$) δ 7.22 – 7.14 (m, 1H), 7.12 (d, *J* = 2.3 Hz 2H), 6.69 (t, *J* = 2.3 Hz, 1H), 6.58 – 6.49 (m, 3H), 5.23 (s, 2H), 3.84 (s, 6H), 3.78 (s, 3H).

^{13}C NMR (75 MHz, C*D*Cl$_3$) δ (ppm): 193.3, 161.4, 161.2 (x2C), 159.7, 136.2, 123.1, 111.1, 110.6, 106.3, 105.9 (x2C), 100.9, 70.8, 55.8 (x2C), 55.7.

3-(3,5-dimethoxyphenyl)-6-methoxybenzofuran (51)

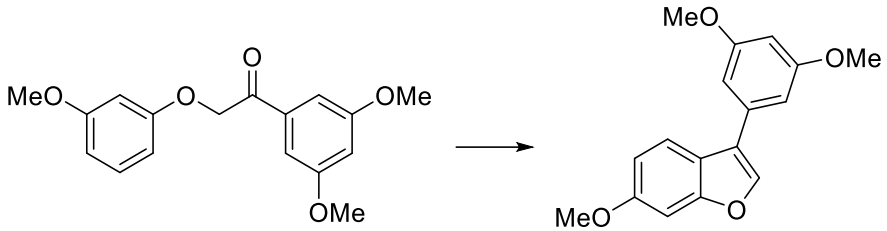

50 **51**

To a solution of compound **50** (0.33 mmol, 1 eq.) in dry DCM (3.9 mL) under nitrogen atmosphere $Bi(OTf)_3$ (0.07 mmol, 0.2 eq.) was added. The mixture was stirred at reflux overnight. After cooling, the mixture was filtered on a celite pad washing with DCM and then concentrated under reduced pressure. The crude was purified by FC (CHX/EtOAc from 9:1 to 7:3). Yield: 43%, white solid.
M.p. 87 °C. **R_f:** 0.47 (cyclohexane:AcOEt 85:15)
^{1}H NMR (300 MHz, C*D*Cl$_3$) δ (ppm): 7.72 (s, 1H), 7.70 (d, *J* = 8.6 Hz, 1H), 7.07 (d, *J* = 2.3 Hz, 1H), 6.95 (dd, J_1 = 8.6, J_2 = 2.3 Hz, 1H), 6.78 (d, *J* = 2.3 Hz, 2H), 6.49 (t, *J* = 2.3 Hz, 1H), 3.88 (s, 3H), 3.86 (s, 6H).
^{13}C NMR (75 MHz, C*D*Cl$_3$) δ (ppm): 161.2 (x2C), 158.2, 156.8, 140.6, 134.0, 122.2, 120.6, 119.7, 112.1, 105.6 (x2C), 99.4, 96.2, 55.7, 55.4 (x2C).

3-(3,5-dimethoxyphenyl)-6-methoxy-2-(4-methoxyphenyl)benzofuran (31)

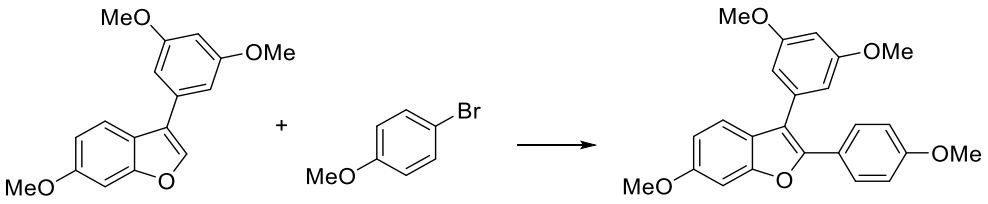

51 1-bromo-4-methoxybenzene **31**

A mixture of compound **51** (0.14 mmol, 1eq.), $Pd(OAc)_2$ (0.01 mmol, 0.1 eq.), 1-bromo-4-methoxybenzene (0.28 mmol, 2 eq.), $PCy_3 \cdot HBF_4$ (0.03 mmol, 0.2 eq.), K_2CO_3 (0.21 mmol, 1.5 eq.) and pivalic acid (0.42 mmol, 3 eq.) in DMA (0.6 mL) was degassed. Then, the reaction mixture was heated at 100 °C under stirring for 20 h. After cooling, the mixture was diluted with EtOAc, washed with H_2O and aq saturated $NaHCO_3$. The organic phase was dried over anhydrous Na_2SO_4 and concentrated under reduced pressure. FC was used to purify the crude with CHX/AcOEt/DCM (from 10:0.1:1 to 9:1:2) as eluent. Yield: 80%, orange sticky solid.

R_f: 0.31 (cyclohexane/AcOEt/DCM 10:0.5:1)

^{1}H NMR (300 MHz, C*D*Cl$_3$) δ (ppm): 7.64 – 7.57 (m, 2H), 7.38 (d, *J* = 8.6 Hz, 1H), 7.08 (d, *J* = 2.2 Hz, 1H), 6.89 – 6.83 (m, 3H), 6.64 (d, *J* = 2.3 Hz, 2H), 6.50 (t, *J* = 2.3 Hz, 1H), 3.89 (s, 3H), 3.82 (s, 3H), 3.78 (s, 6H).

^{13}C NMR (75 MHz, C*D*Cl$_3$) δ (ppm): 161.2 (x2C), 159.5, 158.1, 154.7, 149.9, 135.1, 128.2 (x2C), 123.7, 123.5, 120.0, 115.8, 113.8 (x2C), 111.7, 107.6 (x2C), 99.8, 95.7, 55.8, 55.4 (x2C), 55.3.

3-bromo-5-methoxyphenol

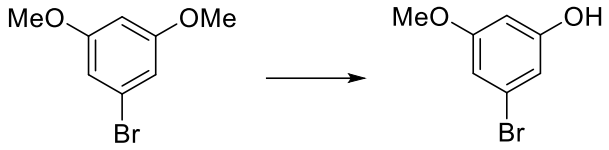

1-bromo-3,5-dimethoxybenzene 3-bromo-5-methoxyphenol

To a solution of 1-bromo-3,5-dimethoxybenzene (1 g, 4.60 mmol) in dry DCM (3.2 mL) BBr_3, solution 1M in DCM (1.52 mL, 1.52 mmol, 0.33 eq) was added at 0°C under nitrogen. The mixture was slowly warmed to room temperature. After 22 h the reaction mixture was quenched with MeOH under nitrogen atmosphere and concentrated under reduced pressure. The residue was purified by FC (cyclohexane/AcOEt 9:1) to give the desired product as a yellow sticky solid in 58% yield. Analytical data were in accordance with literature report (Lindgren *et al.*, 2016)

R_f: 0.2 (cyclohexane/AcOEt 9:1)

^{1}H NMR (300 MHz, C*D*Cl$_3$) δ (ppm): 6.63 (dd, J_1 = 2.2, J_2 = 1.5 Hz, 2H), 6.33 (t, J = 2.2 Hz, 1H), 3.77 (s, 3H).

^{13}C NMR (75 MHz, C*D*Cl$_3$) δ (ppm): 161.4, 157.1, 122.9, 111.5, 110.1, 100.9, 55.6.

2-(3-bromo-5-methoxyphenoxy)-1-(3,5-dimethoxyphenyl)ethan-1-one (52)

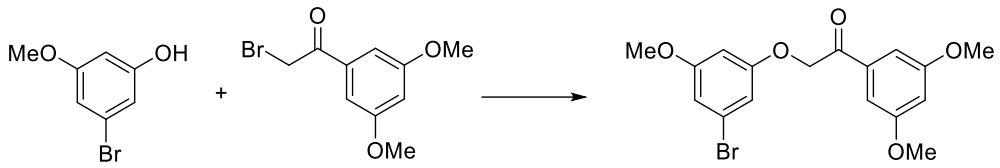

3-bromo-5-methoxyphenol **49** **52**

A mixture of compound **49** (2.46 mmol, 1 eq.), 3-bromo-5-methoxyphenol (2.46 mmol, 1 eq.) and K_2CO_3 (7.39 mmol, 3 eq) in dry acetone (7 mL) was stirred at reflux. After 2h, the mixture was cooled to room temperature, concentrated under reduced pressure, diluted with EtOAc and washed with H_2O. The aqueous phase was extracted again with EtOAc. The collected organic phases dried over anhydrous Na_2SO_4, filtered and concentrated. The crude was purified by FC (CHX/EtOAc from 9:1 to 8:2). Yellow solid, yield: 89%,

M.p.:106-108 °C. **R_f:** 0.24 (cyclohexane/AcOEt/DCM 10:1:2)

^{1}H NMR (300 MHz, C*D*Cl$_3$) δ (ppm): 7.10 (d, *J* = 2.3 Hz, 2H), 6.70 (t, *J* = 2.1 Hz, 2H), 6.67 (dd, J_1 = 2.3, J_2 = 1.6 Hz, 1H), 6.45 (t, *J* = 2.3 Hz, 1H), 5.21 (s, 2H), 3.85 (s, 6H), 3.76 (s, 3H).

^{13}C NMR (75 MHz, C*D*Cl$_3$) δ (ppm): 193.3, 161.4, 161.2 (x2C), 159.7, 136.2, 123.1, 111.1, 110.6, 106.3, 105.9 (x2C), 100.9, 70.8, 55.8 (x2C), 55.7.

4-bromo-3-(3,5-dimethoxyphenyl)-6-methoxybenzofuran (53)

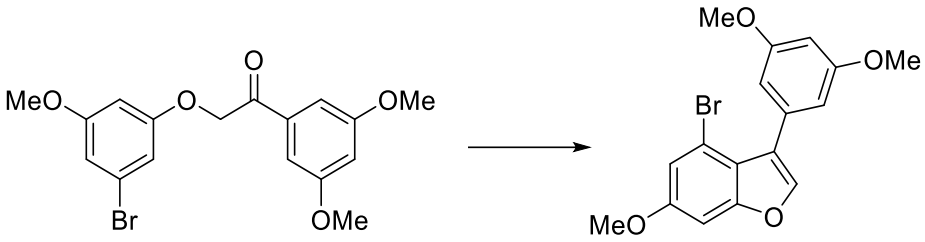

52 **53**

To a solution of compound **52** (0.33 mmol, 1 eq) in dry DCM (3.9 mL) under nitrogen atmosphere, $Bi(OTf)_3$ (0.07 mmol,0.2 eq.) was added. The mixture was stirred at reflux overnight. After cooling, the mixture was filtered on a celite pad, washing the filter with DCM. The filtrate was concentrated under reduced pressure, and the resulting residue was purified by FC (CHX/EtOAc from 9:1 to 7:3). Yield: 83%, white sticky solid. Analytical data were in agreement with literature report (Lindgren *et al.*, 2016)

R_f: 0.49 (cyclohexane/AcOEt 9:1)

^{1}H NMR (300MHz, C*D*Cl_3) δ (ppm): 7.54 (s, 1H), 7.10 (d, *J* = 2.2 Hz, 1H), 7.03 (d, *J* = 2.2 Hz, 1H), 6.66 (d, *J* = 2.3 Hz, 2H), 6.51 (t, *J*= 2.3 Hz, 1H), 3.86 (s, 3H), 3.83 (s, 6H).

^{13}C NMR (75 MHz, C*D*Cl_3) δ (ppm): 160.1 (x2C), 158.3, 156.6, 142.5, 132.8, 123.2, 119.9, 116.6, 114.0, 109.1 (x2C), 100.2, 95.9, 56.1, 55.5 (x2C).

5-(4-bromo-6-hydroxybenzofuran-3-yl)benzene-1,3-diol (54)

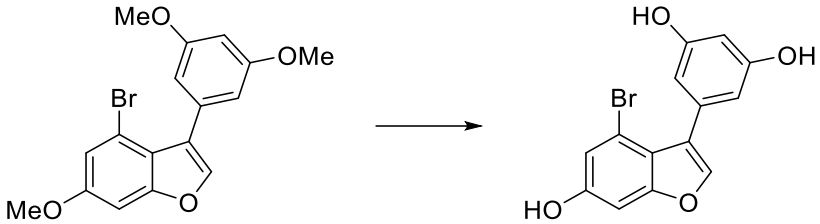

53 **54**

To a solution of **53** (0.14 mmol, 1 eq.) in dry DCM (1.45 mL), under nitrogen atmosphere, at 0 °C, a 1M BBr_3 solution in DCM (0.40 mmol, 3 eq.) was added dropwise. The reaction mixture was allowed to warm to room temperature. After 16 h, the reaction mixture was quenched with a cold saturated aq solution of $NaHCO_3$ (0°C), and the organic solvent was evaporated. The aqueous phase was extracted with EtOAc three times. The combined organic phases were dried over anhydrous Na_2SO_4, and concentrated under reduced pressure. The residue was purified by FC with DCM/MeOH (95:5) as eluent to give the desired product. Yield: 91%, light brown oil. Analytical data were in accordance with literature report (Lindgren *et al.*, 2016).

R_f: 0.49 (DCM/MeOH 9:1)

^{1}H NMR (300 MHz, CD_3OD) δ (ppm): 7.54 (s, 1H), 6.95 (d, *J* = 2.0 Hz, 1H), 6.90 (d, *J* = 2.0 Hz, 1H), 6.39 (d, *J* = 2.2 Hz, 2H), 6.29 (t, *J* = 2.2 Hz, 1H).

^{13}C NMR (75 MHz, DMSO-d_6) δ (ppm): 157.6 (x2C), 156.2, 156.0, 142.4, 132.0, 122.6, 118.0, 116.6, 112.8, 108.9 (x2C), 101.9, 97.7.

5-(6 hydroxy-2-(4-hydroxyphenyl)benzofuran-3-yl)benzene-1,3-diol (26)

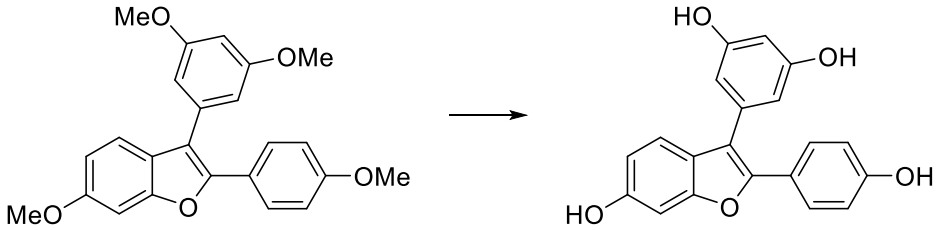

31 **26**

To a solution of **31** (0.12 mmol, 1 eq.) in dry DCM (1.2 mL), under nitrogen atmosphere, at 0°C, a 1M BBr_3 solution in DCM (0.45 mmol, 3.9 eq.) was added dropwise. The reaction mixture was allowed to warm to room temperature. After 16 h, the mixture was quenched with a cold aq saturated $NaHCO_3$ solution (0°C), and the organic solvent was evaporated. The aqueous phase was extracted three times with EtOAc. The combined organic phases were dried over anhydrous Na_2SO_4, and concentrated under reduced pressure. The residue was purified by FC using CHX/acetone (6:4) as eluent to give the desired product. Yield: 52%, light brown solid.

M.p.: 239-240°C. **R_f:** 0.2 (cyclohexane/acetone 6:4)

^{1}H NMR (300 MHz, CD_3OD) δ (ppm): 7.50 – 7.43 (m, 2H), 7.24 (d, *J* = 8.6 Hz, 1H), 6.91 (d, *J* = 2.2 Hz, 1H), 6.77 – 6.70 (m, 3H), 6.38 (d, *J* = 2.2 Hz, 2H), 6.29 (t, *J* = 2.2 Hz, 1H).

^{13}C NMR (75 MHz, CD_3OD) δ (ppm): 158.6 (x2C), 157.2, 155.3, 154.7, 149.3, 135.1, 127.8 (x2C), 122.8, 122.3, 119.4, 115.4, 114.8 (x2C), 111.5, 107.7 (x2C), 101.3, 96.9.

(E)-5-(6-hydroxy-4-(4-hydroxystyryl)benzofuran-3-yl)benzene-1,3-diol (28)

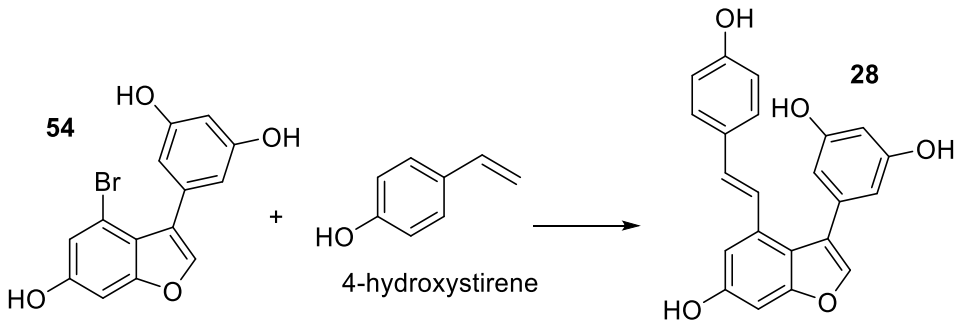

A mixture of compound **54** (0.45 mmol, 1eq.), 4-hydroxystirene (0.78 mmol, 1.5 eq.), 1,3-bis(diphenylphosphino)propane (dppp) (0.05 mmol, 0.1 eq.) and dry TEA (0.91 mmol, 2 eq.) in dry DMF (14.6 mL) was degassed. $Pd(OAc)_2$ (0.05 mmol, 0.1 eq.) was added to the mixture, and the reaction mixture was heated at 120 °C under stirring for 20 h. After cooling, DMF was evaporated, and the residue was diluted with EtOAc, washed with H_2O and brine. The organic phase was dried over anhydrous Na_2SO_4 and concentrated under reduced pressure. The crude was purified by FC using CHX/Acetone 6:4 as eluent. Yield: 80%, light brown solid.

M.p.: 234-235°C. **R_f:** 0.22 (cyclohexane/acetone 6:4)

^{1}H NMR (300 MHz, CD_3OD) δ (ppm): 7.50 (s, 1H), 7.20 (d, *J* = 16.3 Hz, 1H), 7.11 – 7.06 (m, 2H), 7.05 (d, *J* = 2.0 Hz, 1H), 6.91 (d, *J* = 16.3 Hz, 1H), 6.79 (d, *J* = 2.0 Hz, 1H), 6.70 – 6.64 (m, 2H), 6.43 (d, *J*= 2.2 Hz, 2H), 6.38 (t, *J*= 2.2 Hz, 1H).

^{13}C NMR (75 MHz, CD_3OD) δ (ppm): 158.2 (x2C), 156.9, 155.4, 140.4, 135.1, 132.2, 129.2, 128.4, 127.4 (x2C), 123.2, 122.4, 117.8, 114.9 (x2C), 110.0, 108.4 (x2C), 106.5, 101.4, 96.4.

Methyl 3-hydroxy-5-methoxybenzoate (56)

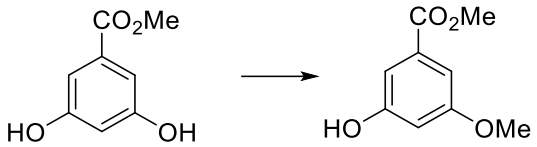

To a solution of 3,5-hydroxymethoxybenzoate **56** (5.94 mmol, 1 eq.) in dry DMF (7.5 mL) under hydrogen atmosphere, CH_3I (5.94 mmol, 1 eq.) and K_2CO_3 (8.92 mmol, 1.5 eq.) were added. The mixture was stirred at room temperature for 2 days. Then, the reaction was quenched with aq saturated NH_4Cl and the mixture was extracted three times with EtOAc. The collected organic phases were dried over anhydrous Na_2SO_4, and concentrated under reduced pressure. FC was used to purify the crude with CHX/EtOAc 7:3 as eluent. Yield: 35%, white solid. Analytical data were in accordance with literature report (Hoffmann and Pete, 2001).

M.p.: 93-94°C **R_f:** 0.43 (CHX/AcOEt 7:3)

^{1}H NMR (300 MHz, C*D*Cl$_3$) δ (ppm): 7.17 - 7.15 (m, 2H), 6.63 (t, *J*= 2.4 Hz, 1H), 5.52 (s, 1H), 3.91 (s, 3H), 3.82 (s, 3H).

^{13}C NMR (75 MHz, C*D*Cl$_3$) δ (ppm): 167.5, 160.7, 157.1, 131.6, 109.4, 107.1, 106.8, 55.5, 52.5.

Methyl 3-(2,2-dimethoxyethoxy)-5-methoxybenzoate (57)

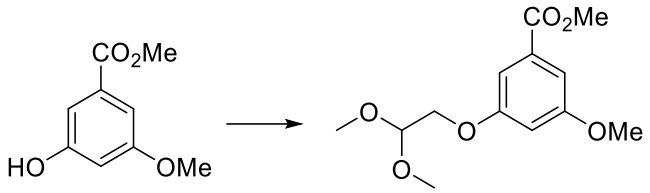

56 **57**

To a solution of compound **56** (2.74 mmol, 1 eq.) in dry ACN, under nitrogen atmosphere, 2-bromo-1,1-dimethoxyethane (4.18 mmol, 1.5 eq.) was added dropwise, followed by Cs_2CO_3 (5.54 mmol, 2 eq.). The mixture was refluxed for three days. After cooling, the solvent was evaporated under reduced pressure, and the residue was diluted with EtOAc and washed with H_2O. The aqueous phase was extracted with EtOAc and the collected organic phases were dried over anhydrous Na_2SO_4, and concentrated under reduced pressure. The residue was purified by FC with CHX/DCM/EtOAc (10:2:1) as eluent. Yield: 67%, yellow oil. Analytical data were in accordance with literature report (Liu *et al.*, 2016)

R_f: 0.36 (CHX/AcOEt 8:2)

^{1}H NMR (300 MHz, C*D*Cl$_3$) δ (ppm): 7.20 (d, *J* = 2.3 Hz, 2H), 6.69 (t, *J* = 2.3 Hz, 1H), 4.72 (t, *J* = 5.2 Hz, 1H), 4.03 (d, *J* = 5.1 Hz, 3H), 3.90 (s, 3H), 3.82 (s, 3H), 3.46 (s, 6H).

^{13}C NMR (75 MHz, C*D*Cl$_3$) δ (ppm): 166.8, 160.8, 159.7, 132.2, 107.9, 107.7, 106.4, 102.1, 68.0, 55.7, 54.3 (x2C), 52.4.

Methyl 6-methoxybenzofuran-4-carboxylate (58)

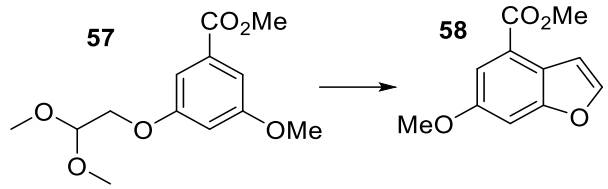

To a solution of compound **57** (0.37 mmol, 1 eq.) in chlorobenzene (3 mL) amberlyst-15 (10 wt%) was added. The mixture was heated at 120 °C for 4 h. After cooling, the mixture was filtered, and the solvent was evaporated under reduced pressure. The residue was purified by FC with CHX/EtOAc 9:1 as eluent. Yield: 63%, white solid. Analytical data were in accordance with literature report (Liu *et al.*, 2016).

M.p.: 49-50°C **R_f:** 0.42 (CHX/AcOEt 9:1)

^{1}H NMR (300 MHz, C*D*Cl$_3$) δ (ppm): 7.63 (d, *J* = 2.2 Hz, 1H), 7.60 (d, *J* = 2.2 Hz, 1H), 7.26 – 7.20 (m, 2H), 3.98 (s, 3H), 3.89 (s, 3H).

^{13}C NMR (300 MHz, C*D*Cl$_3$) δ (ppm): 166.8, 157.4, 156.4, 145.7, 122.8, 121.7, 113.4, 107.7, 101.5, 56.1, 52.2.

Methyl 2-bromo-6-methoxybenzofuran-4-carboxylate (59)

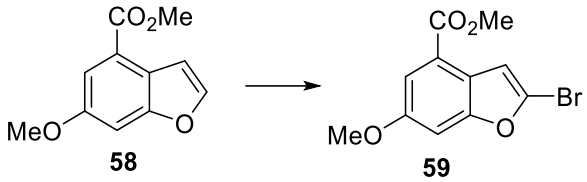

To a solution of compound **58** (0.23 mmol, 1 eq.) in 1,2 dichloroethane, *N*-bromosuccinimide (0.35 mmol, 1.5 eq) and a catalytic quantity of DMF (12 µL) were added. The mixture was stirred at 70 °C for 4h. To quench the reaction, aq saturated $Na_2S_2O_3$ was added to the mixture and the aqueous phase was extracted three times with EtOAc. The organic phases were combined, dried over anhydrous Na_2SO_4, and concentrated under reduced pressure. The crude was purified by FC with CHX/EtOAc 95:5 as eluent. Yield: 80%, white solid. Analytical data were in agreement with literature report (Liu *et al.*, 2016).

M.p.: 92-93°C **R_f:** 0.42 (CHX/AcOEt 95:5)

^{1}H NMR (300 MHz, C*D*Cl$_3$) δ (ppm): 7.57 (d, *J* = 2.3 Hz, 1H), 7.22 (d, *J* = 0.9 Hz, 1H), 7.18 (dd, J_1 = 2.3, J_1 = 0.9 Hz, 1H), 3.97 (s, 3H), 3.88 (s, 3H).

^{13}C NMR (75 MHz, C*D*Cl$_3$) δ (ppm): 166.4, 157.3, 157.0, 128..8, 122.9, 122.0, 113.5, 109.5, 101.3, 56.3, 52.4.

Methyl 6-methoxy-2-(4-methoxyphenyl)benzofuran-4-carboxylate (64)

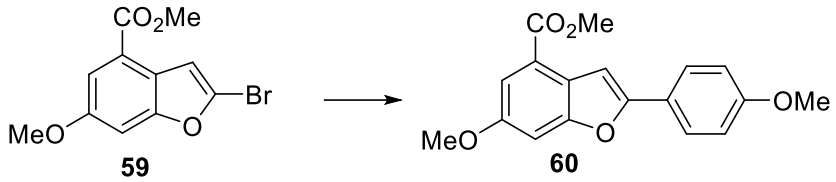

A solution of compound **59** (0.17 mmol, 1 eq.), 4-methoxyphenylboronic acid (0.35 mmol, 2 eq.), and K_2CO_3 (0.92 mmol, 5.3 eq.) was degassed for 30 min. Then, $Pd(PPh_3)_4$ (0.005 mmol, 0.03 eq.) was added and the mixture was degassed again. The reaction was heated at 70 °C overnight. After cooling, the mixture was quenched with water and the aqueous phase was extracted three times with EtOAc. The organic phases were washed with brine, dried over anhydrous Na_2SO_4, and concentrated. The crude was purified on FC with CHX/EtOAc (9:1) as eluent. Yield: 91%, white solid. Analytical data were in agreement with literature report (Liu *et al.*, 2016)

M.p.: 101-103 °C. **R_f:** 0.25 (CHX/AcOEt 9:1)

^{1}H NMR (300 MHz, C*D*Cl$_3$) δ (ppm): 7.79 (d, *J* = 9.0 Hz, 2H), 7.56 (d, *J* = 2.3 Hz, 1H), 7.39 (d, *J* = 0.9 Hz, 1H), 7.25 (dd, J_1 = 2.3 Hz, J_2 = 0.9 Hz, 1H), 6.97 (d, *J* = 9.0 Hz, 2H), 4.00 (s, 3H), 3.90 (s, 3H), 3.87 (s, 3H).

^{13}C NMR (75 MHz, C*D*Cl$_3$) δ (ppm): 166.8, 160.1, 157.0, 156.7, 156.0, 126.4 (x2C), 124.0, 123.0, 121.7, 114.3 (x2C), 112.5, 101.4, 100.6, 56.0, 55.3, 52.0.

(6-methoxy-2-(4-methoxyphenyl)benzofuran-4-yl)methanol (61')

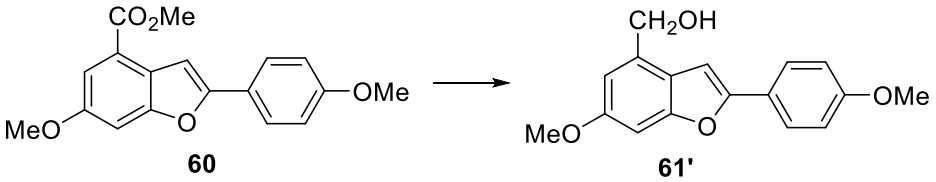

To the solution of compound **60** (0.38 mmol, 1 eq.) in dry THF, under nitrogen atmosphere, at 0 °C was added $LiAlH_4$ 1M in THF (1.06 mmol, 3 eq.) dropwise. The mixture was stirred for 10 minutes at 0 °C. Then, the reaction mixture was quenched with HCl 1M at 0 °C. The aqueous phase was extracted with EtOAc three times. The organic phases were combined, dried over anhydrous Na_2SO_4, filtered and concentrated under reduced pressure. Purification by FC with CHX/EtOAc (7:3) as eluent gave compound **61'** as a yellow solid. Yield: 89%.

M.p.: 98-99 °C. **R_f:** 0.26 (CHX/AcOEt 8:2)

^{1}H NMR (300 MHz, C*D*Cl$_3$) δ (ppm): 7.74 (d, *J* = 9.0 Hz, 2H), 6.99 – 6.93 (m, 4H), 6.86 (d, *J* = 0.9 Hz, 1H), 4.88 (s, 2H), 3.86 (s, 3H), 3.85 (s, 3H).

^{13}C NMR (75 MHz, C*D*Cl$_3$) δ (ppm): 159.7, 157.7, 155.8, 155.7, 133.5, 126.0 (x2C), 123.6, 121.3, 114.3 (x2C), 110.0, 98.1, 95.3, 63.6, 55.9, 55.4.

6-methoxy-2-(4-methoxyphenyl)benzofuran-4-carbaldehyde (61)

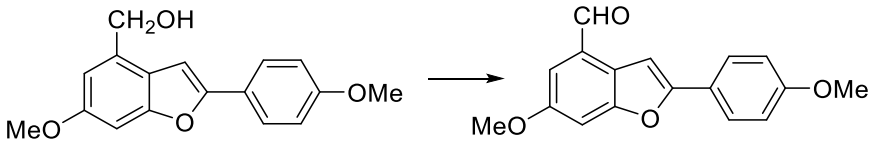

61' **61**

To the solution of compound **61'** (0.27 mmol, 1 eq.) in dry DCM, DMP (0.35 mmol, 1.3 eq.) was added at 0 °C. The mixture was stirred at room temperature for 75 min. Then, the solvent was evaporated under reduced pressure. The residue was purified by FC with CHX/EtOAc as eluent (9:1 to 7:3). Yield: 97%, yellow solid.

M.p.: 121 °C. **R_f:** 0.45 (CHX/AcOEt 8:2)

^{1}H NMR (300 MHz, C*D*Cl$_3$) δ (ppm): 10.14 (s, 1H), 7.80 (d, *J* = 9.0 Hz, 2H), 7.52 (d, *J* = 0.9 Hz, 1H), 7.30 – 7.28 (m, 2H), 6.98 (d, *J* = 9.0 Hz, 1H), 3.92 (s, 3H), 3.86 (s, 3H).

^{13}C NMR (75 MHz, C*D*Cl$_3$) δ (ppm): 191.6, 160.2, 158.3, 157.1, 156.1, 128.2, 126.4 (x2C), 122.7, 122.5, 115.3, 114.3 (x2C), 102.2, 99.3, 56.0, 55.4.

(*E*)-6-methoxy-2-(4-methoxyphenyl)-4-(4-methoxystyryl)benzofuran (62)

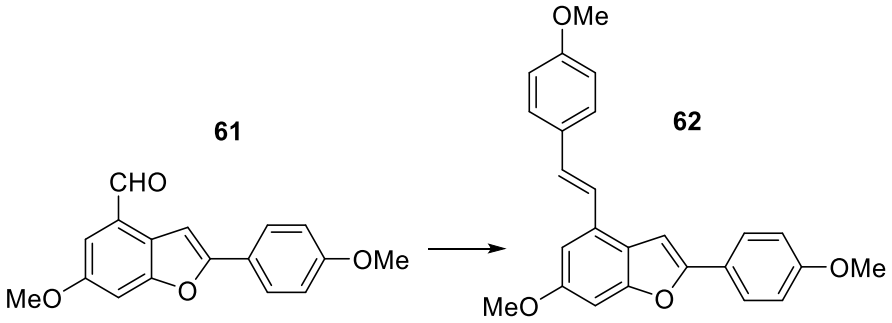

In a MW vial, compound **61** (0.23 mmol, 1 eq.) and diethyl (4-methoxybenzyl)phosphonate (0.46 mmol, 2 eq.) were solubilized in dry THF, under nitrogen atmosphere. Then, 60% NaH in mineral oil (0.69 mmol, 3 eq.) was added to the solution and the mixture was heated under microwave irradiation at 120 °C for 30 min. After cooling, the mixture was quenched by aq saturated solution of NH_4Cl and the aqueous phase was extracted with EtOAc three times. The organic phases were washed with brine, dried over anhydrous Na_2SO_4 and concentrated under reduced pressure. Purification of the crude by FC with CHX/EtOAc (8:2) as eluent gave the title compound. Yield: 54%, light yellow oil.

R_f: 0.33 (CHX/AcOEt 9:1)

^{1}H NMR (300 MHz, C*D*Cl$_3$) δ (ppm): 7.78 (d, *J* = 9.0 Hz, 2H), 7.52 (d, *J* = 9.0 Hz, 2H), 7.20 (d, *J* = 2.3 Hz, 2H), 7.08 (d, *J* = 0.9, 1H), 7.04 (d, *J* = 2.3 Hz, 1H), 6.99 – 6.92 (m, 5H), 3.90 (s, 3H), 3.86 (s, 3H), 3.85 (s, 3H).

^{13}C NMR (75 MHz, C*D*Cl$_3$) δ (ppm): 159.7, 159.6, 157.7, 156.0, 155.3, 130.6, 130.2, 129.9, 127.8, 126.0 (x2C), 124.0, 123.5, 121.6, 114.3 (x2C), 114.2, 113.7, 110.0, 107.9, 98.4, 95.2, 55.8, 55.3 (x2C).

(*E*)-2-(4-hydroxyphenyl)-4-(4-hydroxystyryl)benzofuran-6-ol (27)

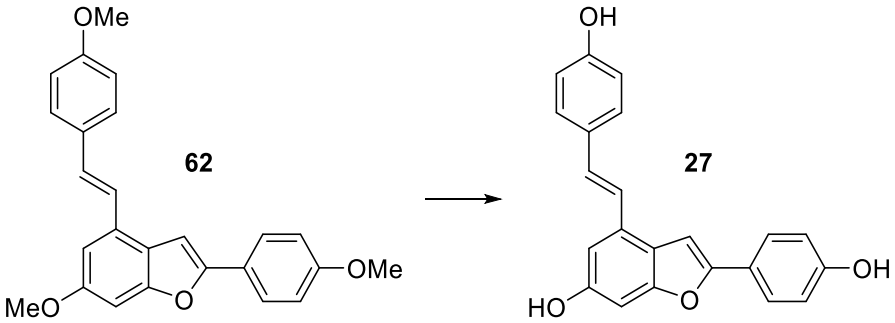

To a solution of compound **62** (0.07 mmol, 1 eq.) a 1M solution of BBr_3 in DCM (0.65 mmol, 9 eq.) was added dropwise at 0°C. The mixture was stirred at room temperature for 6 h. The reaction was quenched with H_2O at 0 °C. The aqueous phase was extracted with EtOAc three times. The combined organic phases were dried over anhydrous Na_2SO_4, and concentrated under reduced pressure. The residue was purified by FC (DCM/MeOH 95:5) to give the desired product. Yield: 24%, brown sticky solid.

R_f: 0.31 (DCM/MeOH 95:5)

^{1}H NMR (300 MHz, CD_3OD) δ (ppm): 7.70 (d, *J* = 9.0 Hz, 2H), 7.47 (d, *J* = 9.0 Hz, 2H), 7.26 – 7.12 (m, 3H), 6.93 (d, *J* = 2.3 Hz, 1H), 6.87 – 6.79 (m, 5H).

^{13}C NMR (150 MHz, CD_3OD) δ (ppm): 158.9, 158.6, 157.4, 156.5, 156.3, 132.1, 130.9, 130.5, 129.0 (x2C), 127.0 (x2C), 124.0, 123.8, 122.2, 116.6 (x2C), 116.5 (x2C), 108.2, 98.8, 97.5.

3.2.5 Bibliography

Akinwumi, B.C., Bordun, K.A.M. and Anderson, H.D., 2018. Biological activities of stilbenoids, Int. J. Mol. Sci., 19(3), 1–25. doi:10.3390/ijms19030792.

Catinella, G., Mattio, L.M., Musso, L., Arioli, S., Mora, D., Beretta, G.L., Zaffaroni, N., Pinto, A. and Dallavalle, S., 2020. Structural requirements of benzofuran derivatives dehydro-δ-and dehydro-ε-viniferin for antimicrobial activity against the foodborne pathogen listeria monocytogenes, Int. J. Mol. Sci., 21(6). doi:10.3390/ijms21062168.

Chand, K., Rajeshwari, Hiremathad, A., Singh, M., Santos, M.A. and Keri, R.S., 2017. A review on antioxidant potential of bioactive heterocycle benzofuran: Natural and synthetic derivatives, Pharmacol. Reports, 69(2), 281–295. doi:10.1016/j.pharep.2016.11.007.

Chibane, B.L., Degraeve, P., Ferhout, H., Bouajila, J. and Oulahal, N., 2019. Plant antimicrobial polyphenols as potential natural food preservatives, J. Sci. Food Agric., 99, 1457–1474. doi:10.1002/jsfa.9357.

Elbert, S.M., Wagner, P., Kanagasundaram, T., Rominger, F. and Mastalerz, M., 2017. Boroquinol Complexes with Fused Extended Aromatic Backbones: Synthesis and Optical Properties, Chem. - A Eur. J., 23(4), 935–945. doi:10.1002/chem.201604421.

Ferreira, S. and Domingues, F., 2016. The antimicrobial action of resveratrol against Listeria monocytogenes in food-based models and its antibiofilm properties, J. Sci. Food Agric., 96(13), 4531–4535. doi:10.1002/jsfa.7669.

Hoffmann, N. and Pete, J.-P., 2001. Intramolecular [2 + 2] Photocycloaddition of Bichromophoric Derivatives of, Synthesis (Stuttg)., 8, 1236–1242. doi:10.1055/s-2001-15076.

Iino, T., Tsukahara, D., Kamata, K., Sasaki, K., Ohyama, S., Hosaka, H., Hasegawa, T., Chiba, M., Nagata, Y., Eiki, J. ichi and Nishimura, T., 2009.

Discovery of potent and orally active 3-alkoxy-5-phenoxy-N-thiazolyl benzamides as novel allosteric glucokinase activators, Bioorganic Med. Chem., 17(7), 2733–2743. doi:10.1016/j.bmc.2009.02.038.

Ito, J., Takaya, Y., Oshima, Y. and Niwa, M., 1999. New oligostilbenes having a benzofuran from Vitis vinifera 'Kyohou', Tetrahedron, 55, 2529–2544. doi:10.1016/S0040-4020(99)00039-3.

Jaseer, E.A., Prasad, D.J.C. and Sekar, G., 2010. Domino synthesis of 2-arylbenzo[b]furans by copper(II)-catalyzed coupling of o-iodophenols and aryl acetylenes, Tetrahedron, 66(11), 2077–2082. doi:10.1016/j.tet.2010.01.026.

Khanam, H. and Shamsuzzaman, 2015. Bioactive Benzofuran derivatives: A review, Eur. J. Med. Chem., 97, 483–504. doi:10.1016/j.ejmech.2014.11.039.

Kim, I. and Choi, J., 2009. A versatile approach to oligostilbenoid natural products - Synthesis of permethylated analogues of viniferifuran, malibatol A, and shoreaphenol, Org. Biomol. Chem., 7(13), 2788–2795. doi:10.1039/b901911a.

Kraus, G.A. and Gupta, V., 2009. A new synthetic strategy for the synthesis of bioactive stilbene dimers. A direct synthesis of amurensin H, Tetrahedron Lett., 7180–7183. doi:10.1016/j.tetlet.2009.10.040.

de La Rosa, L.A., Alvarez-Parrilla, E. and Gonzalez-Aguilarez, G.A., 2010. *Fruit and Vegetable Phytochemicals*. 1th Editio, Fruit Veg. Phytochem. 1th Editio. Edited by J. Wiley and Sons. doi:10.1002/9781119158042.

Lindgren, A.E.G., Öberg, C.T., Hillgren, J.M. and Elofsson, M., 2016. Total synthesis of the resveratrol oligomers (±)-Ampelopsin B and (±)-σ-Viniferin, European J. Org. Chem., 2016(3), 426–429. doi:10.1002/ejoc.201501486.

Liu, J.T., Do, T.J., Simmons, C.J., Lynch, J.C., Gu, W., Ma, Z.X., Xu, W. and Tang, W., 2016. Total synthesis of diptoindonesin G and its analogues as selective modulators of estrogen receptors, Org. Biomol. Chem., 14(38), 8927–8930. doi:10.1039/c6ob01657j.

Markina, N.A., Chen, Y. and Larock, R.C., 2013. Efficient microwave-assisted one-pot three-component synthesis of 2,3-disubstituted benzofurans under Sonogashira conditions, Tetrahedron, 69(13), 2701–2713. doi:10.1016/j.tet.2013.02.003.

Mattio, L.M., Dallavalle, S., Musso, L., Filardi, R., Franzetti, L., Pellegrino, L., D'Incecco, P., Mora, D., Pinto, A. and Arioli, S., 2019. Antimicrobial activity of resveratrol-derived monomers and dimers against foodborne pathogens, Sci. Rep., 9, 19525. doi:10.1038/s41598-01955975-1.

Miao, Y.H., Hu, Y.H., Yang, J., Liu, T., Sun, J. and Wang, X.J., 2019. Natural source, bioactivity and synthesis of benzofuran derivatives, RSC Adv., 9(47), 27510–27540. doi:10.1039/c9ra04917g.

Miliovsky, M., Svinyarov, I., Mitrev, Y., Evstatieva, Y., Nikolova, D., Chochkova, M. and Bogdanov, M.G., 2013. A novel one-pot synthesis and preliminary biological activity evaluation of cis-restricted polyhydroxy stilbenes incorporating protocatechuic acid and cinnamic acid fragments, Eur. J. Med. Chem., 66, 185–192. doi:10.1016/j.ejmech.2013.05.040.

Naik, R., Harmalkar, D.S., Xu, X., Jang, K. and Lee, K., 2015. Bioactive benzofuran derivatives: Moracins A-Z in medicinal chemistry, Eur. J. Med. Chem., 90, 379–393. doi:10.1016/j.ejmech.2014.11.047.

Ofosu, F.K., Daliri, E.B., Elahi, F., Chelliah, R., Lee, B. and Oh, D., 2020. New Insights on the Use of Polyphenols as Natural Preservatives and Their Emerging Safety Concerns, Front. Sustain. food Syst., 4(525810). doi:10.3389/fsufs.2020.525810.

Pecyna, P., Wargula, J., Murias, M. and Kucinska, M., 2020. More than resveratrol: New insights into stilbene-based compounds, Biomolecules, 10(8), 1–40. doi:10.3390/biom10081111.

Richter, M.F. and Hergenrother, P.J., 2019. The challenge of converting Gram-positive-only compounds into broad-spectrum antibiotics, Ann. N. Y. Acad. Sci., 1435, 18–38. doi:10.1111/nyas.13598.

Rivière, C., Pawlus, A.D. and Mérillon, J.M., 2012. Natural stilbenoids: Distribution in the plant kingdom and chemotaxonomic interest in Vitaceae, Nat. Prod. Rep., 29(11), 1317–1333. doi:10.1039/c2np20049j.

Saitoh, M., Kunitomo, J., Kimura, E., Iwashita, H., Uno, Y., Onishi, T., Uchiyama, N., Kawamoto, T., Tanaka, T., Mol, C.D., Dougan, D.R., Textor, G.P., Snell, G.P., Takizawa, M., Itoh, F. and Kori, M., 2009. 2-{3-[4-(Alkylsulfinyl)phenyl]-1-benzofuran-5-yl}-5-methyl-1,3,4-oxadiazole derivatives as novel inhibitors of glycogen synthase kinase-3β with good brain permeability, J. Med. Chem., 52(20), 6270–6286. doi:10.1021/jm900647e.

Singh, D., Mendonsa, R., Koli, M., Subramanian, M. and Nayak, S.K., 2019. Antibacterial activity of resveratrol structural analogues: A mechanistic evaluation of the structure-activity relationship, Toxicol. Appl. Pharmacol., 367(January), 23–32. doi:10.1016/j.taap.2019.01.025.

Várela-Fernández, A., González-Rodríguez, C., Varela, J.A., Castedo, L. and Saá, C., 2009. Cycloisomerization of aromatic homo and bis-homopropargylic alcohols via catalytic ru vinylidenes: Formation of benzofurans and isochromenes, Org. Lett., 11(22), 5350–5353. doi:10.1021/ol902212h.

Vo, D.D. and Elofsson, M., 2016. Total Synthesis of Viniferifuran, Resveratrol-Piceatannol Hybrid, Anigopreissin A and Analogues – Investigation of Demethylation Strategies, Adv. Synth. Catal., 358(24), 4085–4092. doi:10.1002/adsc.201601089.

Wang, M., Liu, X., Zhou, L., Zhu, J. and Sun, X., 2015. Fluorination of 2-substituted benzo[b]furans with Selectfluor™, Org. Biomol. Chem., 13(11), 3190–3193. doi:10.1039/c4ob02691h.

Wu, Y., Bai, J., Zhong, K., Huang, Y., Qi, H., Jiang, Y. and Gao, H., 2016. Antibacterial activity and membrane-disruptive mechanism of 3-p-trans-coumaroyl-2-hydroxyquinic acid, a novel phenolic compound from pine needles of Cedrus deodara, against Staphylococcus aureus, Molecules, 21, 1084. doi:10.3390/molecules21081084.

Yao, T., Yue, D. and Larock, R.C., 2014. Synthesis of 2,3-Disubstituted Benzofurans by the Palladium-Catalyzed Coupling of 2-Iodoanisoles and Terminal Alkynes, Followed by Electrophilic Cyclization: 3-Iodo-2-phenylbenzofuran, Org. Synth., 91, 283–292. doi:10.15227/orgsyn.091.0283.

3.3 SYNTHESIS OF NITROGEN CONTAINING-STILBENOID DERIVATIVES POTENTIALLY ACTIVE AGAINST GRAM-NEGATIVE BACTERIA

ABSTRACT. Nowadays, Gram-negative bacteria are the most difficult pathogens to hit. For this reason, it is necessary and urgent to find new antibiotics suitable to prevent their proliferation. To extend the spectrum of antimicrobial activity of natural stilbenoids also against Gram-negative bacteria, we focused on synthetic strategies modify the stilbenoid skeleton of both monomer and dimer resveratrol-derived compounds by introducing molecular functionalities which could increase the activity against Gram-negative bacteria. In particular, we concentrated our efforts on the synthesis of a series of nitrogen-containing derivatives with the challenge of improving the interaction with the negatively charged moiety of the lipopolysaccharide forming the outer membrane of Gram-negative bacteria. Resveratrol and compound **27**, the best compounds emerging from the SAR study of viniferifuran against L. monocytogenes, were modified for this scope.

3.3.1 Introduction

Among the bacterial pathogens in food supply chain, Gram-negative bacteria are the main culprits of the antibacterial resistance. As reported in the main introduction, four out of the six ESKAPE pathogens belong to the family of Gram-negative bacteria (*K. pneumoniae*/*E. coli*, *A. baumannii*, *P. aeruginosa*, and *Enterobacter* species) (Domalaon et al., 2018; Richter and Hergenrother, 2019). The feature that distinguishes them from Gram-positive bacteria is the presence of an outer membrane (OM) that covers the ordinary inner membrane (IM), a thin layer of peptidoglycan chains (Richter and Hergenrother, 2019). The permeation of the OM is very hard due to its structural conformation (see Section 1.1.2). For this reason, to design antimicrobials active on Gram-negative bacteria results to be difficult to rationalize.

In the review by Richter and Hergenrother (Richter and Hergenrother, 2019) the indispensable features to convert molecules active against Gram-positive bacteria into molecules active against Gram-negative bacteria were reported. The author defined a series of rules, called “eNTRy Rules”. Primarily, compounds may hold a no-sterically hindered ionisable **Nitrogens**, for example primary amines as first choice, but also more substituted amines; as second point, molecules should have low **Three-dimensionality** (globularity ≤ 0.25) and finally, they might be relatively **Rigid** (rotatable bonds ≤ 5) and preferably to contain some nonpolar functional groups. The characteristics of three-dimensionality are given by globularity values, defined in a range from 0 (indicating two- or one-dimensional object, i.e. benzene) to 1 (referring to a perfect sphere, i.e. adamantane). About rigidity, rotatable bonds involve single bonds with a nonterminal heavy atom, excluding those ones in a ring and C-N bonds that need high energy to rotate. Additionally, the nonpolar moiety in the molecule helps to create an amphiphilic moment, a measure of a vector pointing from the hydrophobic core to the hydrophilic portion (amine). Molecules without a hydrophobic domain and consequently lacking the amphiphilic moment are difficult to accumulate.

3.3.2 Materials and Methods

Procedures for the synthesis, isolation, and characterization data for the various compounds obtained are detailed in the experimental section 3.3.4.

3.3.3 Results and Discussion

In order to achieve novel stilbenoid derivatives capable to act against Gram-negative bacteria, we decided to follow the “eNTRY rules” described above and to design a series of resveratrol and pterostilbene analogues containing a nitrogen function. The same strategy was used also for the most active benzofuran-simplified derivative **27**, obtained from the SAR studies described in section 3.2. The insertion of a basic group should increase the interaction

of the structures of stilbenoids with the negatively charged portion of the lipopolysaccharides of the OM of Gram-negative bacteria.

Primarily, we modified resveratrol and pterostilbene replacing one hydroxy group with an amine and an acetanilide, as isosteric substitution, as reported in figure 3.15.

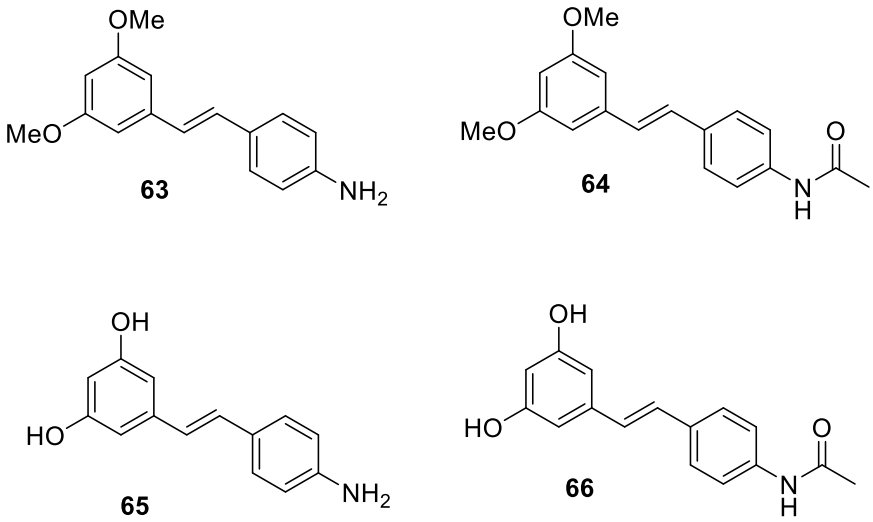

Figure 3.15 *Structures of anilines (**63** and **65**) and acetanilides (**64** and **66**) of resveratrol and pterostilbene*

Starting from pterostilbene we decided to take advantage of the Smiles rearrangement of aryloxyamides and subsequent hydrolysis to replace hydroxyl group with amide (Coutts and Southcott, 1990). Specifically, following the procedure reported by Yu *et al.* (Yu *et al.*, 2013), we successfully obtained the product by this three-step procedure (phenol alkylation, rearrangement and hydrolysis (Mizuno and Yamano, 2005)) in a one-pot reaction. The reaction was conducted in a microwave reactor combining pterostilbene with 2-bromopropionamide in DMSO as solvent at 60°C. After hydrolysis with KOH at 140°C aniline derivative **63** was obtained in 40% yield. To prepare acetanilide **64**, a standard acetylation with acetyl chloride was performed efficiently. Compounds **65** and **66,** the aniline and acetanilide analogues of resveratrol, were synthesized by usual BBr_3 demethylation of compounds **63** and **64**, respectively (Scheme 3.10).

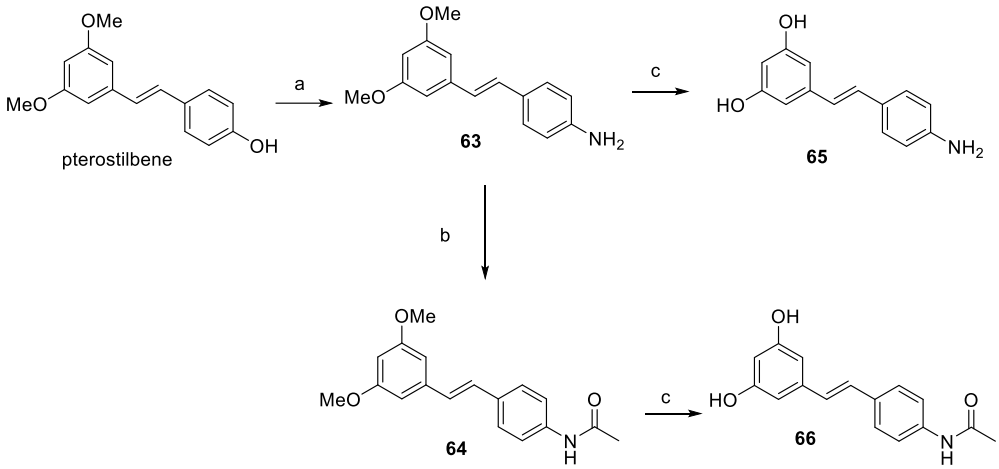

Scheme 3.3.33.10 *Reagents and conditions: a) i) 2-bromopropionamide, KOH, DMSO, 60°C, 3h, MW, ii) KOH, 140°C, 3h, 40%; b) acetylchloride, TEA, DCM, 0°C to rt, 2h, 86%; c) BBr_3 1M DCM, dry DCM, 0°C to rt, 8-18h, 45-54%*

In recent years, numerous studies have shown the interesting antibacterial activity against both Gram-negative and Gram-positive bacteria of molecules bearing guanidine as chemical function (Ghamrawi *et al.*, 2017; Hagras *et al.*, 2017; Heydarifard *et al.*, 2017; Kuppusamy *et al.*, 2018; Song *et al.*, 2019). Thus, we chose to insert a guanidine moiety starting from the aniline-containing derivatives obtained (Figure 3.16).

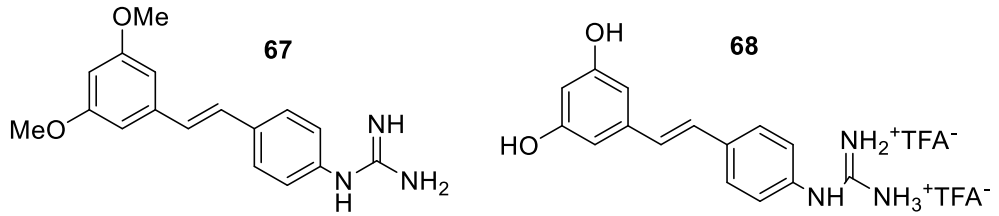

Figure 3.16 *Guanidine derivatives of pterostilbene (**67**) and resveratrol (**68**)*

For the synthesis of guanidines, various methods from amines are described in literature, e.g. the use of cyanamide, carbodiimides, thioureas, isothioureas, or *S*-methylisothioureas. All these reactions typically need toxic metals as catalysts for the reagents' activation. As a result, other procedures were developed: pyrazole and benzotriazole activated carboxamidines showed their efficacy in the guanylation process in mild conditions. Notably, these reagents demonstrated their efficacy also on anilines that usually are less

reactive for guanidinylation than aliphatic amines (Katritzky and Rogovoy, 2005). For the synthesis of compound **69**, we used the procedure reported by Dud *et al* (Đud *et al.*, 2019) employing the guanidinylation reagent *N*,*N*'-Di-*Boc*-1H-pyrazole-1-carboxamidine and we obtained the intermediate in excellent yield (93%) from **63**. Then, the derivative obtained was easily deprotected with TFA to give compound **67**. On the contrary, we were not able to isolate in a pure form compound **68** by demethylation reaction of compound **67** (Scheme 3.11).

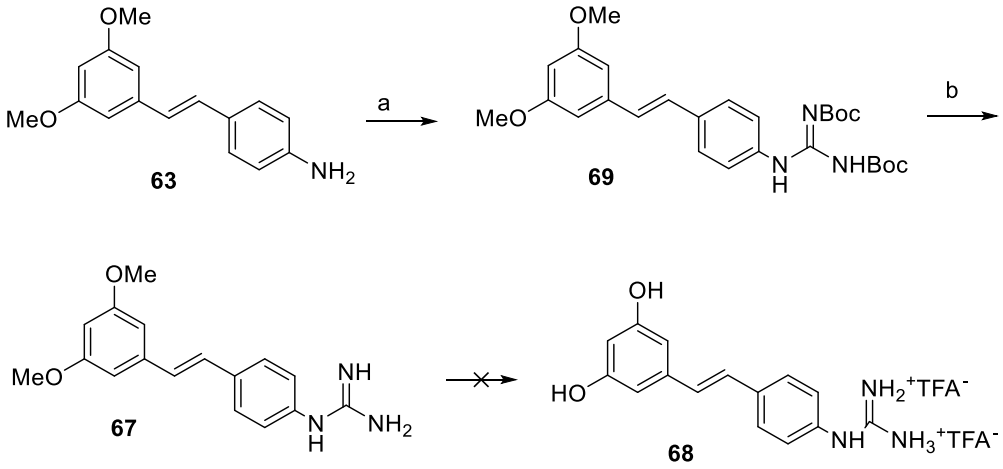

Scheme 3.11 *Reagents and conditions: a) N,N'-Di-Boc-1H-pyrazole-1-carboxamidine, $CHCl_3$, rt, overnight, 93%; b) TFA, DCM, 0°C to rt, 20h, 95%.*

Thus, we decided to follow another route, performing the guanidilnyation of **65**, and obtaining in this way compound **70**, in 42% yield. We tried again the deprotection step with TFA in DCM, but also this time we were not successful, obtaining a mixture of products which was difficult to separate, the derivatives being not stable in strong acidic conditions. Finally, we decided to attempt the reaction adding TES to TFA (Salvio *et al.*, 2016) and we were able to isolate the desired product **68** as trifluoroacetic salt of guanidium (Scheme 3.12).

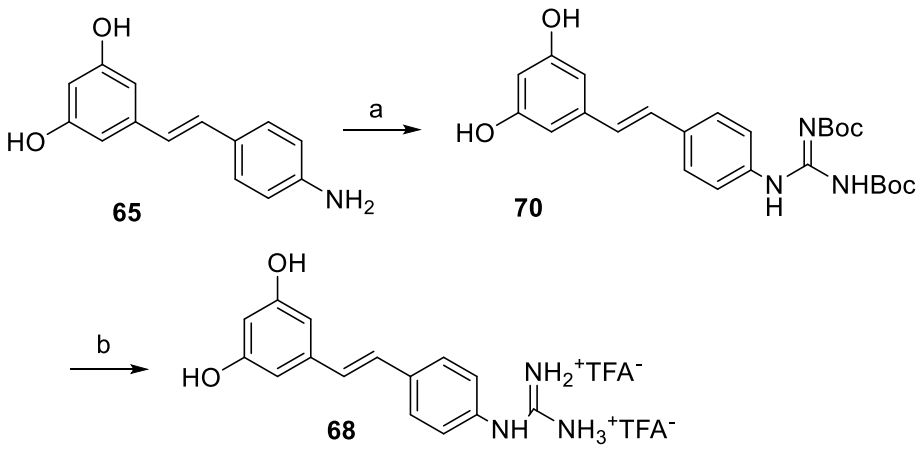

Scheme 3.12 *Reagents and conditions: a) N,N'-Di-Boc-1H-pyrazole-1-carboxamidine, $CHCl_3$, rt, 48h, 42%; b) TFA, TES, DCM, rt, overnight, 82%.*

In a second time, we planned to apply the same approaches used for monomeric derivatives to the most active benzofuran-simplified derivative **27**, achieved from the SAR studies reported in section 3.2. Hence, the corresponding aniline (**71**), acetanilide (**72**) and guanidinium (**73**) derivatives of compound **27** were designed and synthesized (Figure 3.17).

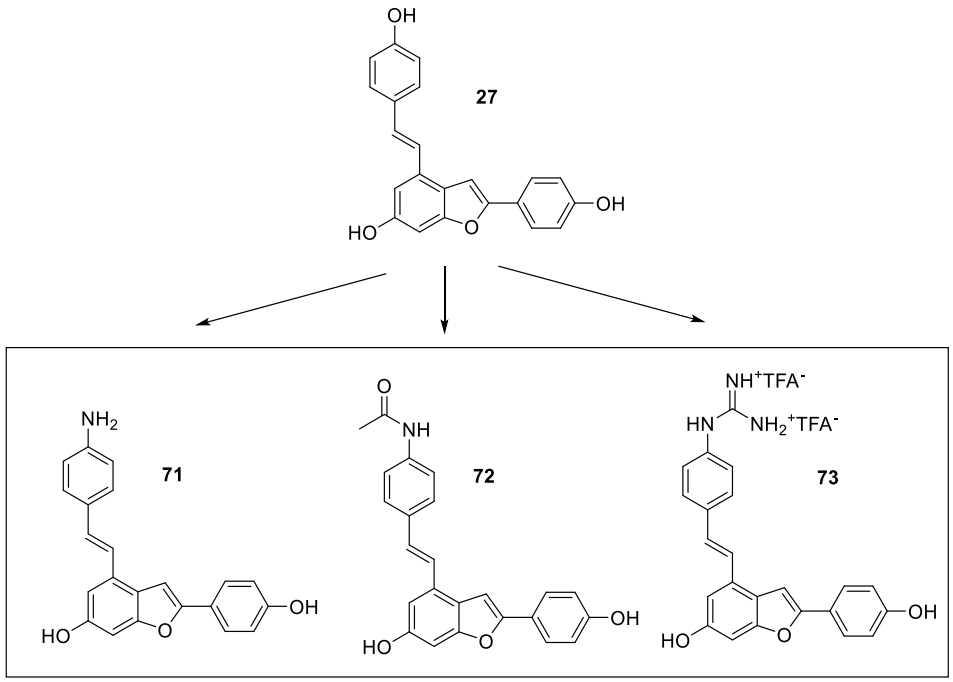

Figure 3.17 *Aniline (**71**), acetanilide (**72**) and guanidine (**73**) derivatives of compound **27**.*

Starting from the aldehyde **61** previously described (section 3.2.3), we prepared compound **74** throughout a Horner-Emmons reaction with (4-aminobenzyl)phosphonate under microwave irradiation in mediocre yield. Compound **74** was easily acetylated with acetylchloride in standard conditions to give the corresponding acetanilide **75**. The last step was the demethylation of **74** and **75** with BBr_3 to obtain compounds **71** and **72**, in 57% and 54% yield, respectively (Scheme 3.13).

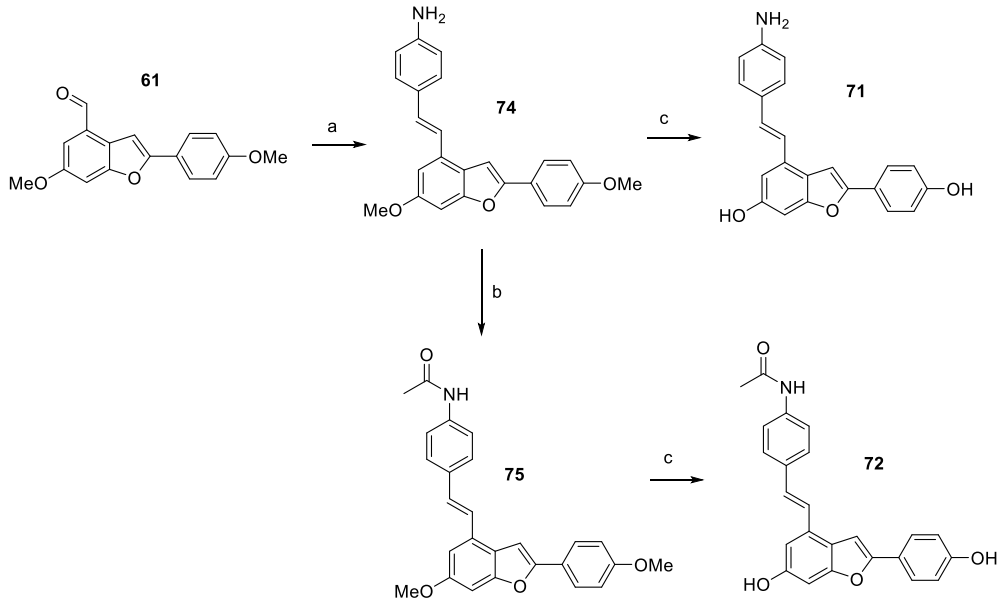

Scheme 3.13 *Reagents and conditions: a) (4-aminobenzyl)phosphonate, NaH, THF, 120°C, 30 min, MW; b) acetylchloride, TEA, DCM, 0°C to rt, 2h, 96%; c) BBr_3 1M DCM, DCM, -78°C to rt, 54-57%.*

Also in this case, we attempted to obtain the guanidinium derivative and successfully we performed the guanidylation of the methoxylated derivative **74**, but we were not able to simultaneously eliminate the methoxy and the Boc groups to give the pure derivative **73** (Scheme 3.14).

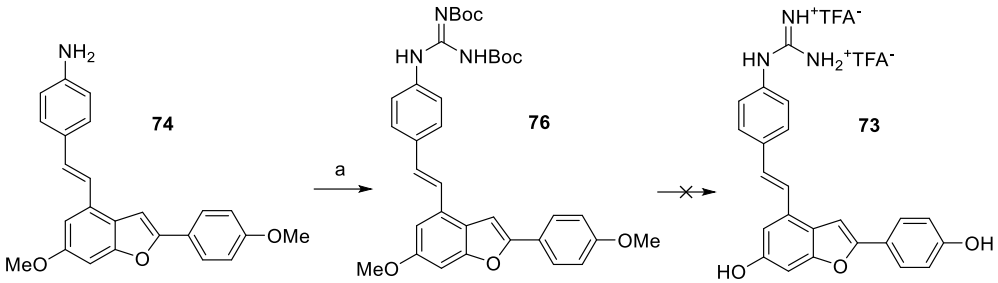

Scheme 3.14 *Reagents and conditions: a) N,N'-Di-Boc-1H-pyrazole-1-carboxamidine, $CHCl_3$, rt, 7h, 60%*

Thus, we decided to follow the previous approach successfully used on monomers. Firstly, guanydinylation of aniline **71** was performed to give compound **77** in 60% yield. Then, deprotection of **77** was carried out adding TFA at 0°C to a solution of the compound in anhydrous DCM, following standard procedures. Again, we did not isolate the pure product, even after various purification steps with different chromatographic systems. Thus, a last effort was made to apply the conditions that afforded compound **68** (Scheme 3.12), adding TES to TFA in the DCM solution (Scheme 3.15). Nonetheless, also in this case we were not able to obtain the pure product, as we observed a partial deprotection and the formation of degradation products.

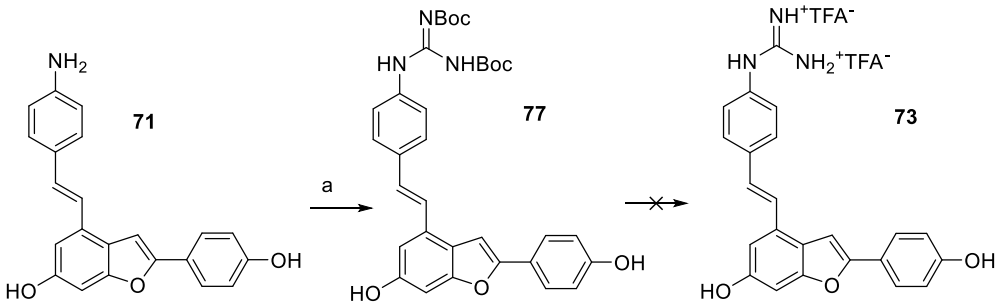

Scheme 3.15 *Reagents and conditions: a) N,N'-Di-Boc-1H-pyrazole-1-carboxamidine, $CHCl_3$, rt, 7h, 60%*

The activity of the synthesized compounds is under evaluations.

3.3.4 Experimental section

3.3.4.1 General procedures

See chapter 3.1.2 for General information.

3.3.4.2 Experimental procedures

(*E*)-4-(3,5-dimethoxystyryl)aniline (63)

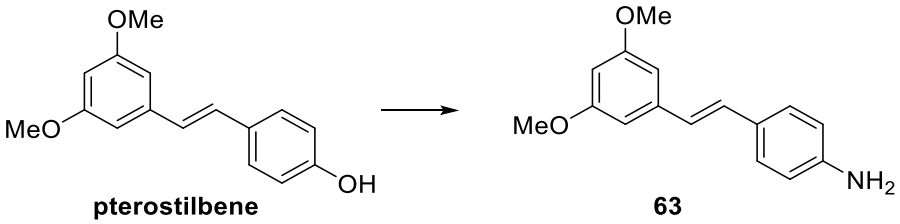

A mixture of pterostilbene (3.90 mmol, 1 eq), 2-bromopropionamide (4.29 mmol, 1.1 eq) and KOH 85% (3.90 mmol, 1 eq) in DMSO (11.5 mL) was heated at 60 °C for 3h, under microwave irradiation. Then KOH 85% (4.29 mmol, 1.1 eq) was added to the solution and the mixture was heated under microwave irradiation at 140 °C for 3h. After cooling, the mixture was quenched with brine solution. The aqueous phase was extracted three times with DCM. The combined organic phases were washed twice with brine, dried over anhydrous Na_2SO_4, filtered and concentrated under reduced pressure. The crude product was purified by FC with CHX/EtOAc (from 8:2 to 7:3) as eluent. Yield: 40%, light brown solid.

M.p.: 87 – 89°C **R_f:** 0.51 (CHX/AcOEt 6:4)

^{1}H NMR (300 MHz, C*D*Cl$_3$) δ (ppm): 7.33 (d, *J* = 8.5 Hz, 2H), 7.00 (d, *J* = 16.2 Hz, 1H), 6.85 (d, *J* = 16.2 Hz, 1H), 6.68 – 6.63 (m, 4H), 6.36 (t, *J* = 2.3 Hz, 1H), 3.83 (s, 6H).

^{13}C NMR (75 MHz, C*D*Cl$_3$) δ (ppm): 160.9 (×2C), 146.3, 140.0, 129.2, 127.8 (×3C), 125.1, 115.2 (×2C), 104.2 (×2C), 99.4, 55.3 (×2C).

(*E*)-*N*-(4-(3,5-dimethoxystyryl)phenyl)acetamide (64)

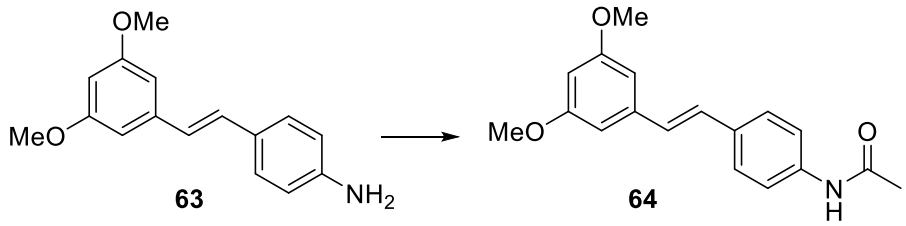

To a solution of compound **63** (0.078 mmol, 1 eq) in DCM (200 μL) TEA (0.156 mmol, 2 eq) was added and the mixture was stirred at 0 °C for 10 min. Then, acetyl chloride (0.086 mmol, 1.1 eq) was added and the reaction mixture was stirred at room temperature for 2h. The reaction was quenched with water and the solution was diluted with DCM. The organic phase was washed with aq 0.5 M HCl three times, dried over anhydrous Na_2SO_4, filtered, and evaporated. The crude was purified by FC with CHX/EtOAc as eluent (from 7:3 to 3:7) to afford the product as a white solid. Yield: 86%.

M.p.: 139 – 141°C **R_f:** 0.25 (CHX/AcOEt 1:1)

^{1}H NMR (300 MHz, C*D*Cl$_3$) δ (ppm): 7.52 – 7.43 (m, 4H), 7.33 (bs, 1H (NH)), 7.03 (d, *J* = 16.3 Hz, 1H), 6.95 (d, *J* = 16.3 Hz, 1H), 6.65 (d, *J* = 2.3 Hz, 2H), 6.38 (t, *J* = 2.3 Hz, 1H), 3.82 (s, 6H), 2.18 (s, 3H).

^{13}C NMR (75 MHz, C*D*Cl$_3$) δ (ppm): 168.2, 160.9 (×2C), 139.4, 137.4, 133.3, 128.4, 127.9, 127.2 (×2C), 119.9 (×2C), 104.5 (×2C), 99.4, 55.3 (×2C), 24.6.

(*E*)-5-(4-aminostyryl)benzene-1,3-diol (65)

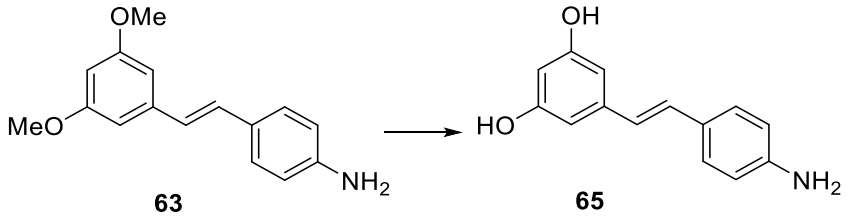

63 **65**

To a solution of **63** (200 mg, 0.783, 1 eq) in dry DCM (11.6 mL), under N_2 at 0 °C, BBr_3 1M DCM solution (3.92 mL, 3.92 mmol, 5 eq) was added dropwise. The mixture was allowed to warm to room temperature, and stirred overnight. The reaction solution was quenched with an aqueous 5% $NaHCO_3$ solution at 0 °C (pH 8-9). The aqueous phase was extracted with EtOAc four times. The combined organic layers were dried over anhydrous Na_2SO_4, filtered, and concentrated under reduced pressure. The residue was purified by FC with CHX/EtOAc (from 1:1 to 4:6) as eluent to give the desired product as a brownish solid. Yield: 45%.

M.p.: 194 – 196 °C **R_f:** 0.20 (CHX : AcOEt 6:4)

^{1}H NMR (300 MHz, CD_3OD) δ (ppm): 7.26 (d, *J* = 8.3 Hz, 2H), 6.91 (d, *J* = 16.3 Hz, 1H), 6.73 (d, *J* = 16.3 Hz, 1H), 6.68 (d, *J* = 8.5 Hz, 2H), 6.42 (d, *J* = 2.2 Hz, 2H), 6.14 (t, *J* = 2.2 Hz, 1H).

^{13}C NMR (75 MHz, CD_3OD) δ (ppm): 158.2 (×2C), 147.3, 140.2, 128.4, 127.3, 127.1 (×2C), 124.3, 115.0 (×2C), 104.2 (×2C), 101.0.

(*E*)-*N*-(4-(3,5-dihydroxystyryl)phenyl)acetamide (66)

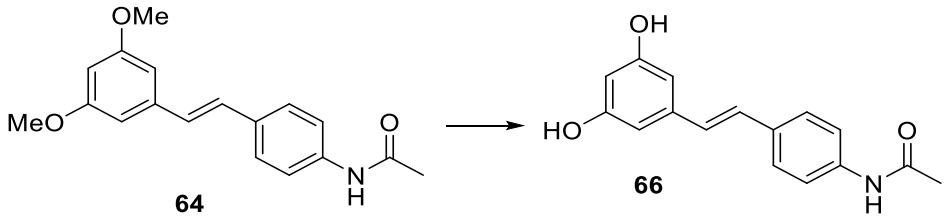

To a solution of compound **64** (0.134 mmol, 1 eq) in dry DCM (2.6 mL), BBr_3 1M DCM solution (0.807 mmol, 6 eq) was added dropwise at 0 °C. The mixture was stirred at room temperature for 9 hours. The reaction was quenched with H_2O at 0 °C. The aqueous phase was extracted three times with EtOAc. The combined organic phases were dried over anhydrous Na_2SO_4, filtered, and concentrated under reduced pressure. The residue was purified by FC with CHX/EtOAc (from 4:6 to 2:8) as eluent to give the desired product as a pale yellow solid. Yield: 54%.

M.p.: 210°C (dec) **R_f:** 0.1 (CHX/AcOEt 1:1)

^{1}H NMR (300 MHz, CD_3OD) δ (ppm): 7.53 (d, *J* = 8.8 Hz, 2H), 7.45 (d, *J* = 8.8 Hz, 2H), 6.99 (d, *J* = 16.3 Hz, 1H), 6.91 (d, *J* = 16.3 Hz, 1H), 6.47 (d, *J* = 2.3 Hz, 2H), 6.18 (t, *J*= 2.3 Hz, 1H), 2.12 (s, 3H).

^{13}C NMR (75 MHz, CD_3OD) δ (ppm): 170.1, 158.3 (×2C), 139.5, 137.8, 133.3, 127.7, 127.5, 126.5 (×2C), 119.8 (×2C), 104.6 (×2C), 101.7, 22.4.

(*E*)-1-(4-(3,5-dimethoxystyryl)phenyl) (*N*,*N*-di-*tert*-butoxycarbonyl)guanidine (69)

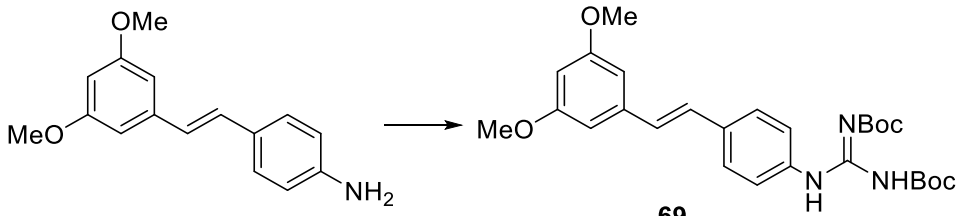

63 **69**

A solution of compound **63** (60 mg, 0.2349 mmol, 1 eq) and *N*,*N*'-Di-*Boc*-1H-pyrazole-1-carboxamidine (0.2525 mmol, 1.5 eq) in dry $CHCl_3$ (7 mL) was stirred at room temperature overnight. The solvent was evaporated under reduced pressure and the crude was purified by FC with eluent CHX/EtOAc (from 100% to 9:1). Yield: 93%, white solid.

M.p.: 133-135°C

R_f: 0.78 (CHX/AcOEt 7.3)

^{1}H NMR (300 MHz, C*D*Cl_3) δ (ppm): 11.6 (bs, 1H (NH)), 10.4 (bs, 1H (NH), 7.62 (d, *J* = 8.6 Hz, 2H), 7.46 (d, *J* = 8.6 Hz, 2H), 7.04 (d, *J* = 16.3 Hz, 1H), 6.96 (d, *J* = 16.3 Hz, 1H), 6.66 (d, *J* = 2.3 Hz, 2H), 6.39 (t, *J* = 2.3 Hz, 1H), 3.83 (s, 6H), 1.54 (s, 18H).

^{13}C NMR (75 MHz, C*D*Cl_3) δ (ppm): 163.5, 161.0 (×2C), 153.3 (×2C), 139.4, 136.4, 133.6, 128.6, 128.0, 127.0 (×2C), 122.1 (×2C), 104.5 (×2C), 99.9, 83.8, 79.7, 55.3 (×2C), 28.2 (×6C).

(E)-1-(4-(3,5-dimethoxystyryl)phenyl)guanidine (67)

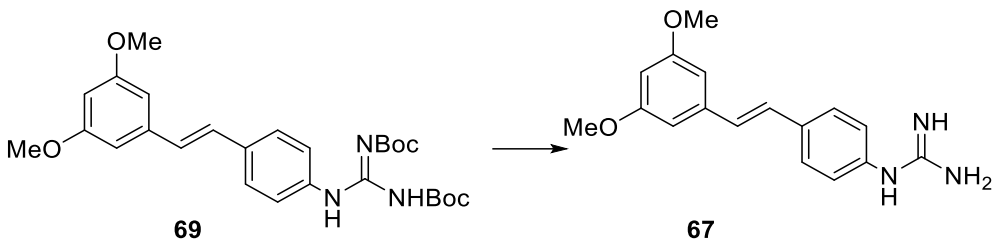

69 **67**

In a round-bottom flask, compound **69** (0.090, 1 eq) was solubilized in dry DCM (770 μL). To the solution TFA (1.809 mmol, 20 eq) was added dropwise at 0 °C. The mixture was stirred at room temperature for 20 h. The reaction was quenched with aq 5% $NaHCO_3$ and some drops of aq saturated KOH to reach pH≈11. The aqueous phase was extracted three times with EtOAc. The combined organic phases were dried over anhydrous Na_2SO_4, filtered and concentrated under reduced pressure to yield the pure product as a sticky solid (95% yield).

R_f: 0.2 (DCM/MeOH 9:1).

^{1}H NMR (300 MHz, C*D*Cl$_3$) δ (ppm): 7.44 (d, *J* = 8.6 Hz, 2H), 7.10 (d, *J* = 8.6 Hz, 2H), 6.98 (d, *J* = 16.7 Hz, 1H), 6.93 (d, *J* = 16.7 Hz, 1H), 6.61 (d, *J* = 2.3 Hz, 2H), 6.37 (t, *J* = 2.3 Hz, 1H), 3.79 (s, 6H).

^{13}C NMR (75 MHz, C*D*Cl$_3$) δ (ppm): 161.0 (×2C), 155.9, 138.8, 135.9, 135.5, 129.6, 128.0 (×2C), 127.6, 125.0 (×2C), 104.7 (×2C), 100.2, 55.3 (×2C).

(*E*)-1-(4-(3,5-dihydroxystyryl)phenyl)(*N*,*N*-di-*tert*-butoxycarbonyl)guanidine (70)

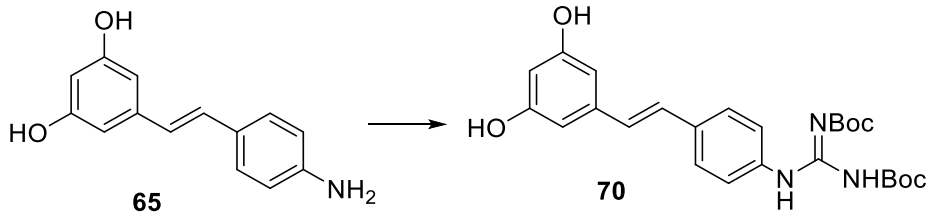

Compound **65** was dissolved (80 mg, 0.352 mmol, 1 eq) in some drops of methanol and dry $CHCl_3$ (10 mL). *N*,*N*'-Di-*Boc*-1H-pyrazole-1-carboxamidine (164 mg, 0.528 mmol, 1.5 eq), and the resulting suspension was stirred for 48 h. The solvent was evaporated and the crude was purified by FC using a gradient of a mixture of CHX/AcOEt (from 9:1 to 6:4). The compound was obtained as white solid (70 mg, 42%).

R_f: 0.44 (CHX : AcOEt 6:4)

^{1}H NMR (600 MHz, Acetone-d_6) δ (ppm): 11.73 (brs, 1H), 10.34 (brs, 1H), 8.22 (brs, 2H), 7.74 – 7.69 (m, 2H, 7.58 – 7.54 (m, 2H), 7.08 (d, *J* = 16.5 Hz, 1H), 7.05 (d, *J* = 16.5 Hz, 1H), 6.57 (d, *J* = 2.2 Hz, 2H), 6.29 (t, *J* = 2.2 Hz, 1H), 1.57 (s, 9H), 1.46 (s, 9H).

^{13}C NMR (150 MHz, Acetone-d_6) δ (ppm): 164.5, 159.7 (x2C), 154.3, 154.1, 140.5, 137.5, 134.9, 129.4, 128.5, 127.8 (x2C), 123.0 (x2C), 106.0 (x2C), 103.2, 84.6, 79.7, 28.4 (x3C), 28.2 (x3C).

(*E*)-1-(4-(3,5-dihydroxystyryl)phenyl)guanidine (68)

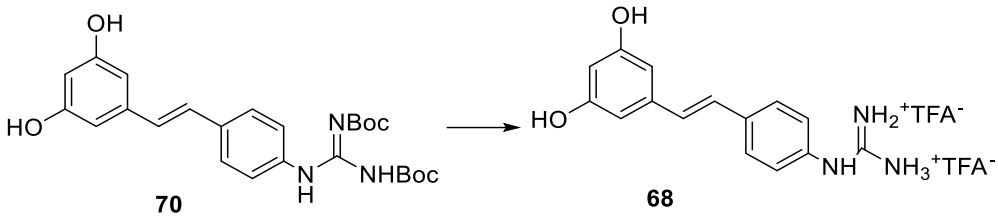

To a suspension of compound **70** (43 mg, 0.0916, 1 eq) in dry DCM (3 mL) under nitrogen atmosphere, TFA (182 µL, 2.318 mmol, 26 eq) was added dropwise, followed by the quick addition of TES (73 µL, 0.458 mmol, 5 eq). The mixture was stirred at room temperature for 24 h. A formation of a white precipitated was observed. The solvent was evaporated to give the final product as yellow brownish sticky solid in 82% yield.

R_f: 0.5 (AcOEt /MeOH 9:1)

^{1}H NMR (600 MHz, C*D$_3$OD*) δ (ppm): 7.66 – 7.58 (2H, m), 7.31 – 7.24 (2H, m), 7.07 (d, *J* = 16.7 Hz, 1H), 7.05 (d, *J* = 16.7 Hz, 1H), 6.50 (d, *J* = 1.4 Hz, 2H), 6.23 (t, *J* = 1.4 Hz, 1H).

^{13}C NMR (150 MHz, C*D$_3$OD*) δ (ppm): 159.8 (x2C), 158.1, 140.4, 138.3, 135.1, 131.2, 128.9 (x2C), 128.1, 126.6 (x2C), 106, 2 (x2C), 103.5.

(*E*)-4-(2-(6-methoxy-2-(4-methoxyphenyl)benzofuran-4-yl)vinyl)aniline (74)

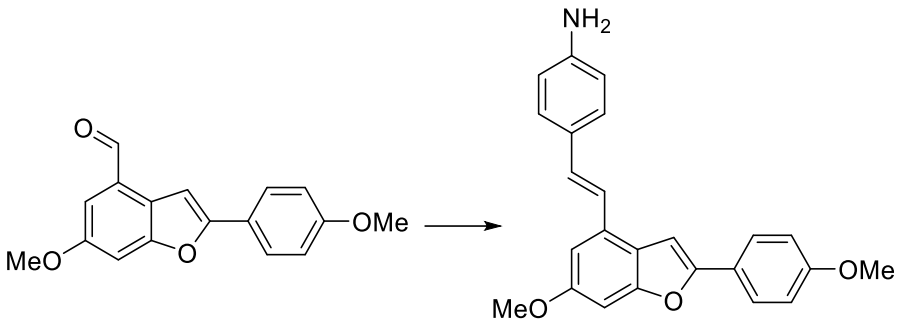

61 **74**

In a microwave vial, a suspension of compound **61** (200 mg, 0.7084 mmol, 1 eq) with diethyl (4-aminobenzyl)phosphonate (345 mg, 1.417 mmol, 2 eq) and 60 % NaH (85 mg, 2.125 mmol, 3 eq) in dry THF (6 mL) was stirred at 120 °C for 30 min under microwave irradiation. The reaction mixture was cooled, and quenched with aq NH_4Cl saturated solution. The aqueous phase was extracted three times with EtOAc. The combined organic layers were washed with brine, dried over anhydrous Na_2SO_4, filtered, and evaporated. The crude was purified by column chromatography, using CHX/AcOEt (9:1 to 7:3) as eluent to yield the product as a brown sticky solid in 23% yield.

R_f: 0.18 (CHX/AcOEt 7:3)

^{1}H NMR (300 MHz, C*D*Cl$_3$) δ (ppm): 7.82 – 7.74 (m, 2H), 7.45 – 7.36 (m, 2H), 7.19 (d, *J* = 16.4 Hz, 1H), 7.13 (d, *J* = 16.4 Hz, 1H), 7.08 (d, *J* = 0.9 Hz, 1H), 7.01 (d, *J* = 2.1 Hz, 1H), 7.00 – 6.92 (m, 3H), 6.76-6.65 (m, 2H), 3.89 (s, 3H), 3.86 (s, 3H).

^{13}C NMR (75 MHz, C*D*Cl$_3$) δ (ppm): 159.7, 157.8, 156.0, 155.2, 146.4, 131.0, 130.5, 128.0, 127.9 (×2C), 126.0 (×2C), 123.6, 122.4, 121.5, 115.2 (×2C), 114.3 (x2C), 107.7, 98.5, 94.9, 55.8, 55.4.

(E)-4-(4-aminostyryl)-2-(4-hydroxyphenyl)benzofuran-6-ol (71)

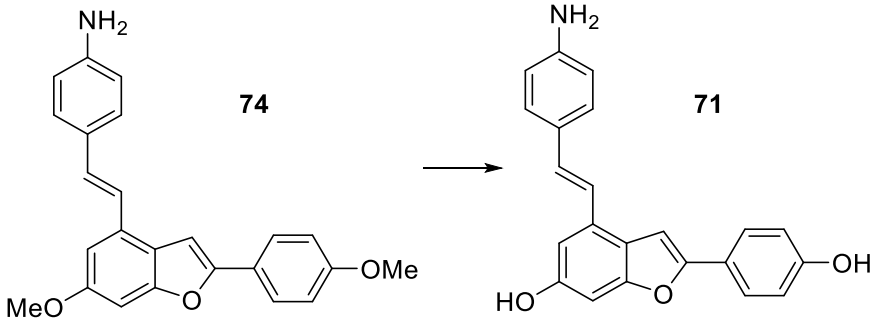

To a solution of compound **74** (61 mg, 0.164 mmol, 1 eq) in dry DCM (13 mL) under nitrogen atmosphere at -78°C, BBr_3 1M DCM solution was added dropwise and the resulting reaction mixture was slowly allowed to warm to room temperature and stirred for 7h. The mixture was quenched at 0°C with aq 5% $NaHCO_3$ (pH 7). The aqueous phase was extracted three times with EtOAc. The combined organic layers were dried over anhydrous Na_2SO_4, filtered, and evaporated. The crude was purified by column chromatography using DCM/MeOH 95:5 as eluent. The product was obtained as brown solid (57%).

M.p.: 192°C (dec) **R_f:** 0.30 (CHX/AcOEt 1:1)

^{1}H NMR (300 MHz, CD_3OD) δ (ppm): 7.74 – 7.66 (m, 2H), 7.43 – 7.34 (m, 2H, 7.18 (d, *J* = 16.4 Hz, 1H), 7.17 (d, *J* = 1.0 Hz, 1H), 7.11 (d, *J* = 16.4 Hz, 1H), 6.92 (d, *J* = 2.0 Hz, 1H), 6.89 – 6.82 (m, 2H), 6.78 (dd, J_1 = 2.0 Hz, J_2 = 1.0 Hz), 6.75 – 6.70 (m, 2H).

^{13}C NMR (75 MHz, CD_3OD) δ (ppm): 157.5, 156.0, 155.0, 154.9, 147.6, 131.1, 130.0, 127.4, 127.3 (x2C), 125.5 (x2C), 122.4, 121.3, 120.7, 115.2 (x2C), 115.0 (x2C), 107.2, 97.4, 95.9.

(E)-N-(4-(2-(6-methoxy-2-(4-methoxyphenyl)benzofuran-4-yl)vinyl)phenyl)acetamide (75)

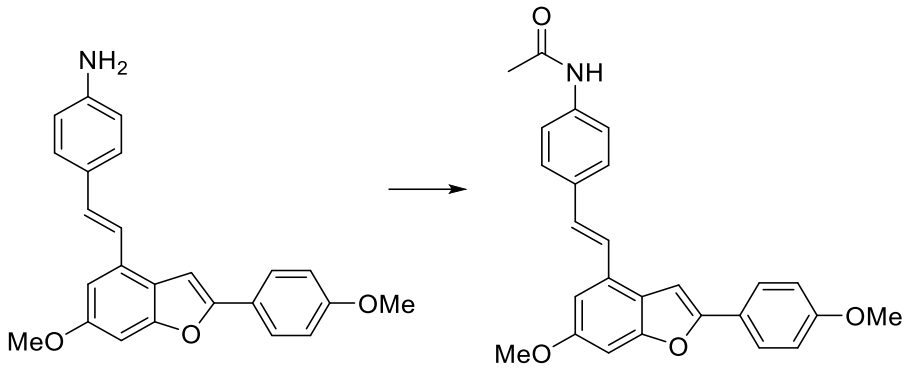

To a solution of compound **74** (30 mg, 0.081 mmol, 1 eq) in dry DCM (0.6 mL), TEA (22.5 µL, 0.162 mmol, 2 eq) and acetyl chloride (6.3 µL, 0.089 mmol, 1.1 eq) were added at 0°C and the mixture was stirred 10 min at the same temperature and 2h at room temperature. The reaction mixture was quenched with brine at 0°C. The aqueous layer was extracted three times with DCM, and the combined organic layers were dried over anhydrous Na_2SO_4, filtered, and evaporated to yield the product as a brown sticky solid in 96% yield.

R_f: 0.31 (CHX/AcOEt 1:1)

^{1}H NMR (300 MHz, DMSO-d_6) δ (ppm): 10.04 (s, 1H), 7.88 – 7.75 (m, 2H), 7.70 (s, 1H), 7.68 – 7.58 (m, 4H), 7.43 (d, *J* = 16.6 Hz, 1H), 7.35 (d, *J* = 8.6 Hz, 1H), 7.16 – 7.10 (m, 2H), 7.09 – 6.98 (m, 2H), 3.84 (3H, s), 3.81 (s, 3H), 2.05 (3H, s).

^{13}C NMR (75 MHz, DMSO-d_6) δ (ppm): 168.7, 159.3, 158.1, 155.9, 155.0, 139.5, 132.4, 130.7, 130.3, 127.6 (x2C), 126.2 (x2C), 124.6, 123.2, 121.6, 119.4 (x2C), 115.0 (x2C), 108.3, 99.9, 95.9, 56.2, 55.7, 24.5.

(*E*)-*N*-(4-(2-(6-hydroxy-2-(4-hydroxyphenyl)benzofuran-4-yl)vinyl)phenyl)acetamide (72)

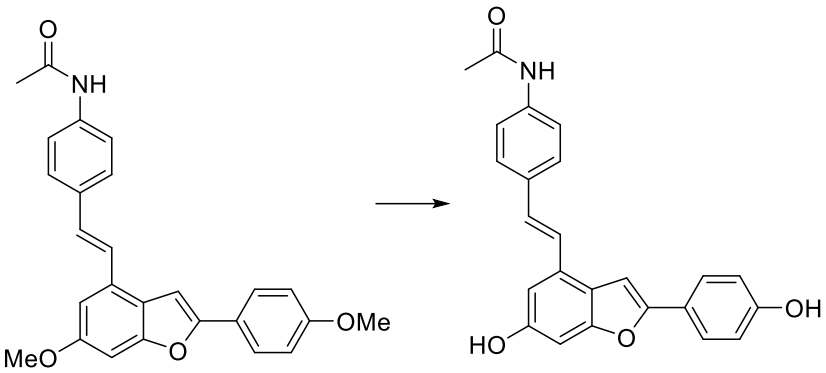

75 **72**

To a solution of compound **75** (25 mg, 0.06 mmol, 1 eq) in dry DCM (1.4 mL) at 0°C, BBr_3 1M in DCM (0.363 mL, 0.363 mmol, 6 eq) was added and the mixture was allowed to warm to room temperature and stirred overnight. The reaction mixture was quenched with water at 0°C and the aqueous layer was extracted three times with EtOAc. The combined organic layers were dried over anhydrous Na_2SO_4, filtered, and evaporated. The crude was purified on silica gel by FC using as eluent DCM/MeOH (from 9:1 to 8:2). The product was afforded as a brownish solid in 54% yield.

M.p.: 205-207°C **R_f:** 0.36

^{1}H NMR (300 MHz, MeOD) δ (ppm): 7.74 – 7.67 (m, 2H), 7.62 – 7.55 (m, 4H), 7.35 (d, *J* = 16.6 Hz, 1H), 7.21 (d, *J* = 0.9 Hz, 1H), 7.19 (d, *J* = 16.6 Hz, 1H), 6.97 (d, *J* = 2.0 Hz, 1H), 6.89 – 6.83 (m, 2H), 6.82 (dd, J_1 = 2.0 Hz, J_2 = 0.9 Hz, 1H), 2.13 (s, 3H).

^{13}C NMR (75 MHz, MeO*D*) δ (ppm): 170.2, 157.5, 156.0, 155.3, 154.9, 138.0, 133.4, 130.2, 128.9, 126.6 (x2C), 125.6 (x2C), 124.8, 122.4, 121.0, 119.8 (x2C), 115.2 (x2C), 107.8, 97.4, 96.6, 22.4.

(*E*)-1-(4-(2-(6-methoxy-2-(4-methoxyphenyl)benzofuran-4-yl)vinyl)phenyl)(*N*,*N*-di-*tert*-butoxycarbonyl)guanidine (76)

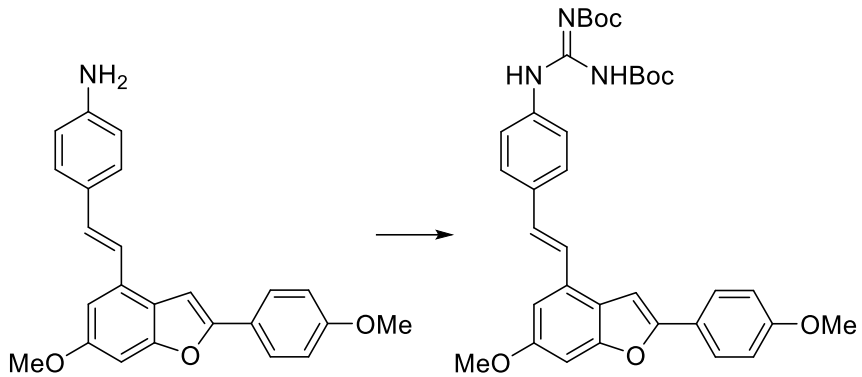

To the solution of compound **74** (73 mg, 0.1965 mmol, 1 eq) in dry $CHCl_3$ (5.8 mL), *N*,*N*'-Di-*Boc*-1H-pyrazole-1-carboxamidine was added and the mixture was stirred for 5h at room temperature. The solvent was evaporated and the crude was purified on silica gel using as eluent CHX/AcOEt (from 100% to 90%) to afford the product as brownish sticky solid in 60% yield.

R_f: 0.71 (CHX/AcOEt 7:3)

^{1}H NMR (300 MHz, C*D*Cl_3) δ (ppm): 11.65 (brs, 1H), 10.43 (s, 1H), 7.83 – 7.74 (m, 2H), 7.71 – 7.62 (m, 2H), 7.59 – 7.50 (m, 2H), 7.29 (d, *J* = 16.3 Hz, 1H), 7.18 (d, *J* = 16.3 Hz, 2H), 7.08 (d, *J* = 1.08 Hz, 1H), 7.05 (d, *J* = 2.1 Hz), 7.01 – 6.93 (m, 3H), 3.90 (s, 3H), 3.86 (s, 3H), 1.59 – 1.50 (s, 18 H).

^{13}C NMR (75 MHz, C*D*Cl_3) δ (ppm): 163.5, 159.7, 157.7 (x2C), 156.0, 155.4, 153.3, 136.4, 133.8, 130.3, 129.5, 127.1 (x2C), 126.0 (x2C), 125.4, 123.5, 122.2 (x2C), 121.7, 114.3 (x2C), 108.0, 98.4, 95.5, 83.8, 79.7, 55.8, 55.4, 28.2 (x6C).

(*E*)-1-(4-(2-(6-hydroxy-2-(4-hydroxyphenyl)benzofuran-4-yl)vinyl)phenyl))(*N*,*N*-di-*tert*-butoxycarbonyl)guanidine (77)

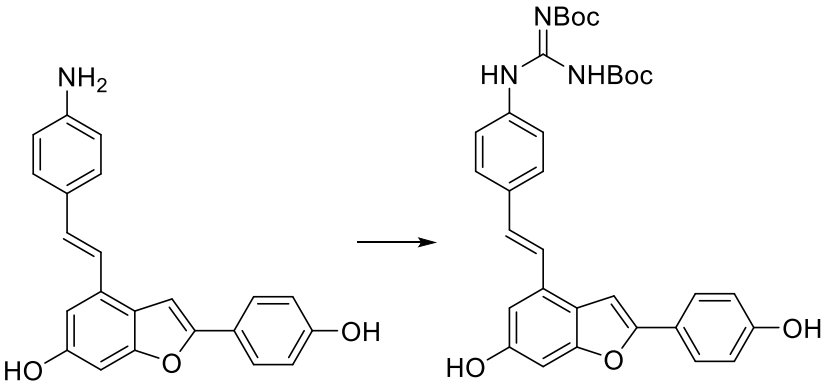

71 **77**

To the solution of compound **71** (32.4 mg, 0.094 mmol, 1 eq) in MeOH (0.1 mL) and dry $CHCl_3$ (2.4 mL), *N*,*N*'-Di-*Boc*-1H-pyrazole-1-carboxamidine was added and the mixture was stirred at room temperature for 24h. The solvent was evaporated and the crude was purified on silica gel using as eluent hexane/AcOEt 1:1, followed by a second column chromatography using DCM/MeOH (98:2) as eluent to afford the product as brown sticky solid in 39% yield.

R_f: 0.44 (DCM/MeOH 98:2)

^{1}H NMR (300 MHz, C*D*Cl_3) δ (ppm): 11.68 (brs, 1H), 10.26 (s, 1H), 7.65 – 7.61 (m, 2H), 7.41 – 7.36 (m, 2H), 7.28 – 7.22 (m, 2H), 6.97 (d, *J* = 16.3 Hz, 1H), 6.91 (d, *J* = 16.3 Hz, 1H), 6.88 (s, 1H), 6.85 – 6.81 (m, 2H), 6.79 – 6.75 (m, 2H), 1.55 (s, 9H), 1.51 (s, 9H).

^{13}C NMR (75 MHz, C*D*Cl_3) δ (ppm): 163.2, 155.9, 155.7, 155.0, 154.7, 153.9, 153.3, 135.1, 134.8, 129.9, 128.7, 126.9 (x2C), 126.0 (x2C), 125.4, 124.0, 123.5 (x2C), 121.4, 115.9 (x2C), 108.4, 98.2, 97.7, 84.0, 80.3, 28.1 (x6C).

3.3.5 Bibliography

Coutts IGC, Southcott MR., 1990. The conversion of phenols to primary and secondary aromatic amines via a Smiles rearrangement. J Chem Soc Perkin Trans 1, 767–71. https://doi.org/10.1039/p19900000767.

Domalaon R, Idowu T, Zhanel GG, Schweizer F., 2018. Antibiotic hybrids: The next generation of agents and adjuvants against gram-negative pathogens? Clin Microbiol Rev, 31, 1–45. https://doi.org/10.1128/CMR.00077-17.

Đud M, Glasovac Z and Margetić D., 2019. The utilization of ball milling in synthesis of aryl guanidines through guanidinylation and N-Boc-deprotection sequence, Tetrahedron, 75, 109–15. https://doi.org/10.1016/j.tet.2018.11.038.

Ghamrawi, S., Bouchara, J., Tarasyuk, O., Rogalsky, S., Lyoshina, L., Bulko, O. and Bardeau, J., 2017. Promising silicones modified with cationic biocides for the development of antimicrobial medical devices, Mater. Sci. Eng. C, 75, 969–979. doi:10.1016/j.msec.2017.03.013.

Hagras, M., Mohammad, H., Mandour, M.S., Hegazy, Y.A., Ghiaty, A., Seleem, M.N. and Mayhoub, A., 2017. Investigating the Antibacterial Activity of Biphenylthiazoles against Methicillin- and Vancomycin-Resistant Staphylococcus aureus (MRSA and VRSA). J Med Chem, 60, 4074–85. https://doi.org/10.1021/acs.jmedchem.7b00392.

Heydarifard S, Pan Y, Xiao H, Nazhad MM., 2017. Water-resistant cellulosic filter containing non-leaching antimicrobial starch for water purification and disinfection. Carbohydr Polym, 163, 146–52. https://doi.org/10.1016/j.carbpol.2017.01.063.

Katritzky AR, Rogovoy B V., 2005. Recent developments in guanylating agents. Arkivoc, 2005, 49–87. https://doi.org/10.3998/ark.5550190.0006.406.

Kuppusamy R, Yasir M, Yee E, Willcox M, Black DS, Kumar N., 2018. Guanidine functionalized anthranilamides as effective antibacterials with

biofilm disruption activity. Org Biomol Chem, 16, 5871–88. https://doi.org/10.1039/c8ob01699b.

Mizuno M, Yamano M., 2005. A new practical one-pot conversion of phenols to anilines. Org Lett, 7, 3629–31. https://doi.org/10.1021/ol051080k.

Richter MF, Hergenrother PJ, 2019. The challenge of converting Gram-positive-only compounds into broad-spectrum antibiotics. Ann N Y Acad Sci, 1435, 18–38. https://doi.org/10.1111/nyas.13598.

Salvio R, Volpi S, Cacciapaglia R, Sansone F, Mandolini L, Casnati A., 2016. Phosphoryl Transfer Processes Promoted by a Trifunctional Calix[4]arene Inspired by DNA Topoisomerase I. J Org Chem, 81, 9016. https://doi.org/10.1021/acs.joc.6b01643.

Song X, Yuan G, Li P, Cao S., 2019. Guanidine-Containing Polyhydroxyl Macrolides: Chemistry, Biology, and Structure-Activity Relationship. Molecules, 24, 3913. doi: 10.3390/molecules24213913

Yu J, Wang Y, Zhang P, Wu J., 2013. Direct amination of phenols under metal-free conditions. Synlett, 24, 1448–54. https://doi.org/10.1055/s-0033-1338703.

3.4 INVESTIGATION ON GRAPEFRUIT SEEDS EXTRACTS. ISOLATION OF CITRUS LIMONOIDS AND THEIR ANTIOXIDANT AND VIRUCIDAL POTENTIAL AGAINST SARS-COV-2

The results of this section are published in Magurano *et al.* (Magurano *et al.*, 2021).

ABSTRACT. In line with the circular economy strategies for obtaining high value molecules from agri-food waste, we have focused on grapefruit waste for their interesting already demonstrated antimicrobial activities. In particular, grapefruit seed extract (GSE) has shown antibacterial, antioxidant and antiviral properties. Driven by the safe profile of a natural waste endowed with biological activities, we decided to investigate the antioxidant activity and the ability to fight the virus that still haunts us today, Sars-Cov-2, of GSE. In this direction, we prepared a small collection of extracts, enriched fractions, and single molecules, which have been completely chemically characterized, evaluating their virucidal and antioxidant activities. The most abundant components were citrus limonoids and flavonoid glycosides. The class of limonoids was provided of significant virucidal, antioxidant and mitoprotective activity.

3.4.1 Introduction

In food supply chain, during handling and processing of fruits and vegetables, a big number of agri-food by-products, including leaves, bracts, peels, seeds, roots and bark, are generated (Ezejiofor, 2014). Inside these by-products it is hidden a great quantity of primary metabolites, i.e., storage and cell wall structural carbohydrates, proteins, and lipids, together with high-value natural products such as carotenoids, phenols, vitamins and phytosterols (Kamal-Eldin and Appelqvist, 1996; Kohno *et al.*, 2004; Lenucci *et al.*, 2013). Among waste of fruits, seeds represent an abundant quantitative and although they are thrown away with other part of fruit (pomace, skins and vascular tissues), seeds can be easily separated by sifting technologies. For example, the seeds

of pomace obtained after pressing the grapes represent about 8-20% of the total waste, varying on the grape cultivar and the processing method (Antonić *et al*., 2020; Dwyer *et al.*, 2014). Furthermore, seeds represent the portion of the fruit with the highest concentration of bioactive molecules, thus the agri-food industry sustains a double loss of costs due to disposal and the loss of profits for their reuse and enhancement (Durante *et al.*, 2017). A rich resource of bioactive compounds is constituted by citrus seeds. In particular, grapefruit seed extract (GSE) is widely known for its antimicrobial properties, and it is commercially available. Some studies showed the capability of GSE to inhibit Gram-negative bacteria, such as *Pseudomonas aeruginosa* and *Escherichia coli*, as well as Gram-positive bacteria, such as *Staphylococcus* spp. and *Enterococcus* spp. (Reagor *et al.*, 2002). For this reason, the extract is extensively used in the food industry to decrease bacterial growth and to extend shelf-life of food. In recent studies the antioxidant activity of GSE has been reported, with the potential to reduce reactive free radicals and oxidative stress by activating the antioxidant enzyme system (Xu *et al.*, 2007; Lipiński *et al.*, 2017). Moreover, GSE has resulted also a good virucidal product against avian influenza virus (AIV) and Newcastle disease virus (NDV) (Komura *et al.*, 2019). Nevertheless, mechanisms of action of GSE are only partly understood, and additional investigations are necessary to understand the molecules responsible of the antioxidant and antiviral proprieties. For this promising evidence, it seemed interesting to us to investigate on the antiviral activity of GSE against SARS-CoV-2.

The bioactive content of grapefruit seeds is represented essentially by phenolic compounds, specifically flavonoids (aglycone and glycosylated forms) and terpenoids. In particular, *Citrus paradisi* seeds show the highest limonoids' content and limonin and nomilin are the most abundant (Montoya *et al.*, 2019). Limonoids are a class of natural tetracyclic triterpenoids widely distributed in the *Rutaceae* and *Meliaceae* families of the Citrus genus. These secondary metabolites can be found in several parts of plant, such as fruits, peels, root bark, roots, and seeds and are biosynthesized through isoprenoids

pathway in the citrus seeds (Roy and Saraf, 2006). This class of molecules can be present in free or glycosidic form. The first one is abundant during development of tissues, while the concentration of the second form increases during the maturation of seeds. Various interesting biological activities of limonoids are reported in the literature, including antitumoral, anti-inflammatory, anti-obesity, anti-hyperglycemic, anti-oxidative, anti-neurological diseases, anti-insecticidal, antibacterial and antiviral activities (Battinelli *et al.*, 2003; Yu *et al.*, 2015; Shi *et al.*, 2020).

3.4.2 Materials and Methods

3.4.2.1 Chemical tools

Isolation and purification of the compounds were performed by flash column chromatography on silica gel 60 (230–400 mesh). Compounds on TLC plates were detected under UV light at 254 and 365 nm or were revealed by solution of anisaldehyde (2%) and H_2SO_4 (2%) in EtOH. High Resolution Electrospray Mass Spectra were acquired with Q-TOF Synapt G2 Si (WATERS), available at COSPECT Unitech Platform (Milan, Italy).

HPLC analyses were performed with a liquid Chromatograph Varian ProStar, equipped with a ternary pump with a UV-Vis detector Varian Model 345. A RP 18 (Hypersil ODS, Thermo, 5 µm 300 × 4 mm i.d.) was used. All the sample were dissolved in ACN:H_2O 3:7 and filtered with 0.45 µm nylon filters. The elutions were performed with ACN and Water milliQ, flow 1 mL/min, λ 210 and 280 nm. The condition used were the following: t 0-15 min from ACN 10% to 60%; t 15-40 min ACN 60%.

Preparative HPLC was performed with a C-18 Ascentis, Supelco (21.2 i.d. × 250 mm, 5 µm), fitted to a 1525 Extended Flow Binary HPLC pump and a Waters 2489 UV/Vis detector (both from Waters, Milan, Italy). The separation was performed in gradient condition: t 0-30 min from ACN 10% to 30%, at a flow rate of 15 mL/min, monitoring the eluate at 210 nm.

3.4.2.2 Grapefruit seeds extractions

Citrus paradisi seeds were collected in summer 2020 in Cefalù, Sicily and they were dried using a dryer (RGV Digital Dried) at 40 °C (water loss 64%) until constant weight of grapefruit seeds. Dried seeds were grinded, and the powder (20 g) was sequentially extracted in the dark for 48 h at rt with hexane (2 × 100 mL) to remove the fatty matter, yielding **GSE1**, dichloromethane (2 × 100 mL) to give extract **GSE2**, and ethanol/water 1:1 (100 mL) to give extract **GSE3**. All the extracts were filtered and evaporated under reduced pressure to provide **GSE1** (10.0 g), **GSE2** (0.8 g), and **GSE3** (5.4 g) and analyzed by HPLC (Figures 3.18, 3.19).

3.4.2.3 Isolation and purification

The hydroalcoholic extract (**GSE3**, 3.1 g) was portioned in H_2O (100 mL) and n-BuOH (3 × 30 mL) obtaining fractions **GSE3$_{H20}$** (2.4 g) and **GSE3$_{BuOH}$** (0.62 g), analyzed by HPLC. **GSE3$_{BuOH}$** was purified by silica gel column chromatography using a mixture of EtOAc:acetone:H_2O:HCOOH (8:1:0.5:0.5 and 7:2:0.5:0.5) as eluent. Two main fractions were isolated, **F1** containing a mixture of three limonoids and **F2** containing a mixture of two flavonoid glycosides. Fraction **F1** (45 mg) was subjected to silica gel column chromatography with hex:EtOAc (3:7) to yield three fractions: obacunone (**78**) (4 mg), limonin (**79**) (30 mg), nomilin (**80**) (7 mg). Fraction **F2** (35 mg) was purified by preparative HPLC to yield narirutin (**81**) (4.8 mg, rt 17.30 min) and naringin (**5**) (2.1 mg, rt 18.15 min). Structural characterization of isolated limonoids and flavonoid glycosides is provided in experimental section 3.4.4.

3.4.2.4 Investigation on extraction production

Alternative extraction protocols were investigated after the identification of the most active compounds derived from hydroalcoholic extraction: 1) ethanol extraction (**EtE**), 2) acetone/EtOAc extraction (**AAE**) and 3) triphasic extraction (**TE**). For ethanol extraction (**EtE**), grapefruit seeds powder (3 g) was stirred with EtOH (10 mL × 2) at rt in the dark for 48 h. The extracts were filtered and evaporated under reduced pressure. The acetone/EtOAc extract (**AAE**) was prepared mixing grapefruit seeds powder (3 g) with the solution of

ACT/EtOAc 1:1 (10mL × 2) at rt in the dark for 48 h. The extracts were filtered and evaporated under reduced pressure. For triphasic extraction (**TE**), grapefruit seeds powder (3 g) was stirred with a system of five solvents with different polarity (n-heptane/EtOAc/ACN/ButOH/H_2O with proportion 22:14:29:8:27). This mixture was selected, being the most efficient for the model of natural products reported by Gori et al (Gori *et al.*, 2021). The mixture was stirred for 14 h at 35 °C and decanted. The three-phasic solvent system was filtered, separated by a separatory funnel and evaporated under reduced pressure. Limonin and nomilin content in the crude extract were determined by high-performance liquid chromatography (HPLC). The retention time was 15.68 min for limonin (**79**), 16.49 min for nomilin (**80**), and 17.35 min for obacunone (**78**). A linear correlation between limonin and nomilin concentration and area of peaks was obtained for the covered concentration ranges from 0.11 to 1.75 µg/ml, sustained by the regression coefficient (R^2 = 0.9932 and 0.9310 respectively) (Figures 3.18, 3.19).

3.4.2.5 Virus propagation

Viral isolate BetaCov/Italy/CDG1/2020|EPI ISL 412973|2020-02-20 (GISAID accession ID: EPI_ISL_412973), obtained from a COVID-19 patient, was propagated by inoculation of 70-80% confluent Vero E6 cells in 75 cm^2 cell culture flasks. Cells were observed for cytopathic effect (CPE) every 24 h. Stocks of SARS-CoV-2 virus were harvested at 72 h post infection, and supernatants were collected, clarified, aliquoted, and stored at −80 °C. Infectious virus titer was determined as Plaque Forming Units (PFU/mL). Virus propagation was conducted under biosafety level (BSL) 3 facilities at ISS (Rome, IT).

3.4.2.6 Plaque Reduction Neutralization Test (PRNT)

The method used for Plaque Reduction Neutralization Test (PRNT) was previously described (Magurano *et al.*, 2021). The GSE compounds were resuspended in 30% dimethyl sulfoxide (DMSO) leading to a final concentration of 1 mg/ml that did not affect the growth of the cells in *in vitro* experiments. Then serial 2-fold dilutions of GSE extracts (from 0.5 mg/ml to

0.015 mg/ml) were incubated with 80 PFU of SARS-CoV-2 at 4 °C overnight. The mixtures were added in triplicates to confluent monolayers of Vero E6 cells, grown in 12-well plates and incubated at 37 °C in a humidified 5% CO_2 atmosphere for 60 min. Then, 4 ml/well of a medium containing 2% Gum Tragacanth + MEM2X supplemented with 2.5% of heat-inactivated FCS were added. Plates were left at 37 °C with 5% CO_2. After 3 days, the overlay was removed, and the cell monolayers were washed with PBS to completely remove the overlay medium. Cells were stained with a crystal violet 1,5% alcoholic solution. The presence of SARS-CoV-2 virus-infected cells was indicated by the formation of plaques. The half-maximal inhibitory concentration (IC_{50}) was determined as the highest dilution of substance resulting in 50% (PRNT50) reduction of plaques as compared to the virus control. PRNT is a live neutralization assay that was conducted under biosafety level BSL3 facilities at ISS.

3.4.2.7 Cell cultures

A549 (Lung epithelial) cells were cultured in T25 tissue culture flasks. RPMI Medium was used, supplemented with 10% fetal bovine serum (FBS), 100 U/mL penicillin and 100 U/mL streptomycin and 2 mM L-glutamine in a humidified atmosphere of 95% air and 5% CO_2 at 37 °C. Vero E6 (Cercopithecus aethiops derived epithelial kidney, C1008ATCC CRL-1586) cells were grown in Minimum Essential Medium (MEM + GlutaMAX, Gibco) supplemented with 10% Fetal Calf Serum (FCS), 100 U/mL penicillin, 100 U/mL streptomycin, 1 mM sodium pyruvate, and 1% non-essential amino acids.

3.4.2.8 Cell viability and cell morphology

To define dose-dependence, A549 cells were treated with 10, 100 and 300 µg/mL of extracts for 24 hours. Cells were grown at a density of $2x10^4$ cell/well on 96-well plates in a final volume of 100 µL/well. After treatments, the cell viability was measured by MTS assay (Promega Italia S.r.l., Milan, Italy). After cell treatments, the incubation was continued for 2 hours at 37 °C in 5% CO_2. The absorbance was read at 490 nm using the Microplate Reader

GloMax fluorimeter (Promega Corporation, Italy). Cell viability was expressed as arbitrary units of absorbance, with the control group set to 1. For cytotoxicity analysis, Vero E6 cells were grown at a density of $1x10^4$ cell/well in 96-well plates and were treated for 24 h with semi-log dilutions of **GSE3**, **GSE3$_{n\text{-}BuOH}$**, obacunone (**78**), limonin (**79**) and nomilin (**80**) (from 0,5 mg to 0,125 mg). Then, 5 mL of tetrazolium salt XTT (Cell Proliferation Kit II, Roche) was added to the cells and 10% of Electron-Coupling Reagent was added, according to the manufacturer's instructions. After incubating for 2 h at 37 °C, plates were read in a spectrophotometer at 450 nm. After this incubation period, the formazan dye formed was quantified using a scanning multi-well spectrophotometer. The measured absorbance directly correlates to the number of viable cells.

3.4.2.9 Analysis of Reactive Oxygen Species (ROS)

For oxidative stress generation 500 µM of tert-butyl hydroperoxide (Luperox® TBH70X, Merck Life Science S.r.l., Italy) was used for 2 hours, alone and in combination with grapefruit seeds extracts treatment. The control (Ctrl) groups received an equal volume of the medium. For the DCFH-DA, and JC-1 assays the extract was utilized at 100 µg/mL for 2 hours. The treated and control cells were analyzed by using microscopy (Axio Scope 2 microscope; Zeiss, Germany). Then, each sample was added DCFH-DA (100 µM) and placed in the dark for 10 min at room temperature. After washing with PBS, cells were analyzed using a Microplate Reader GloMax fluorimeter (Promega Corporation, Italy) at the excitation wavelength of 475 nm and emission wavelength 530 nm for fluorescence intensity detection and results were expressed as a percentage of the control group. Cells fluorescence was also visualized using the fluorescence microscope Zeiss Axio Scope 2 microscope (Carl Zeiss, Oberkochen, Germany).

3.4.2.10 Mitocondrial membrane potential analysis

The mitochondrial transmembrane potential was measured by plating and treating the cells as mentioned above. After treatment, the cells were incubated for 30 min at 37°C with 2 µM JC-1 red dye (5,5′,6,6′-tetrachloro-

1,1′,3,3′-tetraethylbenzimidazolylcarbocyanine iodide) using the MitoProbe JC-1 assay kit (Molecular Probes, USA). Fluorescence emission shift of JC-1 from red (590 nm) to green (529 nm) was evaluated by the fluorescence microscope equipped with a 488 nm excitation laser using the Microplate Reader GloMax fluorimeter (Promega Corporation, Italy).

3.4.2.11 Mitocondrial morphology analysis

Cellular mitochondria were stained using the MitoTracker Deep Red (Invitrogen, Carlsbad, CA, USA) dye (20 nM) for 15 min, washed twice with growth medium, and observed under the fluorescence microscope (488 nm excitation/ 590 nm emission). Original fluorescence images were converted to binary images. Mitochondrial shapes were obtained by visualizing the mitochondria outlines automatically drawn by the ImageJ software (Public Domain, BSD-2 license, National Institutes of Health, Bethesda, MD, USA). Morphometric mitochondria data, length and perimeter, were calculated from each mitochondrial outline (N 500).

3.4.2.12 Statistical analysis

All experiments were repeated at least three times. Each experiment was performed in triplicate. The results are presented as a mean ± standard deviation (SD). The significance of the differences in the mean values was evaluated by using one-way analysis of variance (ANOVA) followed by Bonferroni's post hoc test. Differences were considered significant when the value was $p \leq 0.05$. SD of SARS-CoV-2 reduction in infectivity was calculated at different concentrations of each compound. In this study, 95% of confidence interval (CI) was considered.

3.4.3 Results and Discussion

3.4.3.1 Extraction, isolation, and characterization

After a preliminary screening of the virucidal activity of sequential extracts **GSE1** (hexane), **GSE2** (dichloromethane), and **GSE3** (ethanol/water 1:1), in which **GSE3** showed the most interesting activity against SARS-CoV-2, we focused our efforts to individuate the molecules responsible for the activity on

the hydroalcoholic extract (**GSE3**). Firstly, the extract was partitioned between water and n-butanol. The aqueous phase comprised mainly carbohydrate and resulted inactive in biological assays, while the alcoholic phase (**GSE3$_{n\text{-}BuOH}$**) showed good activity. **GSE3$_{n\text{-}BuOH}$** was purified by column chromatography on silica gel to obtain two main fractions. Additional purifications were carried out on **F1** and **F2**. The main isolated compounds belonged to the classes of limonoids and flavonoids. Pure obtained molecules were obacunone (**78**) (0.2 mg/g DW), limonin (**79**) (1.4 mg/g DW), nomilin (**80**) (0.3 mg/g DW), narirutin (**81**) (0.6 mg/g DW) and naringin (**82**) (0.3 mg/g DW) (Figures 3.18, 3.19)

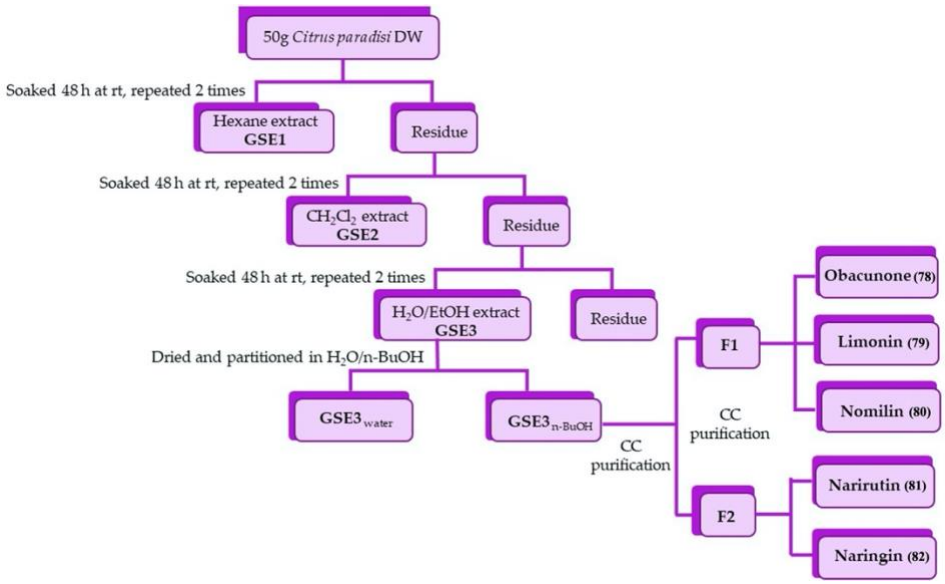

Figure 3.18 *Schematic representation of the extraction/purification process from Citrus paradisi seeds.*

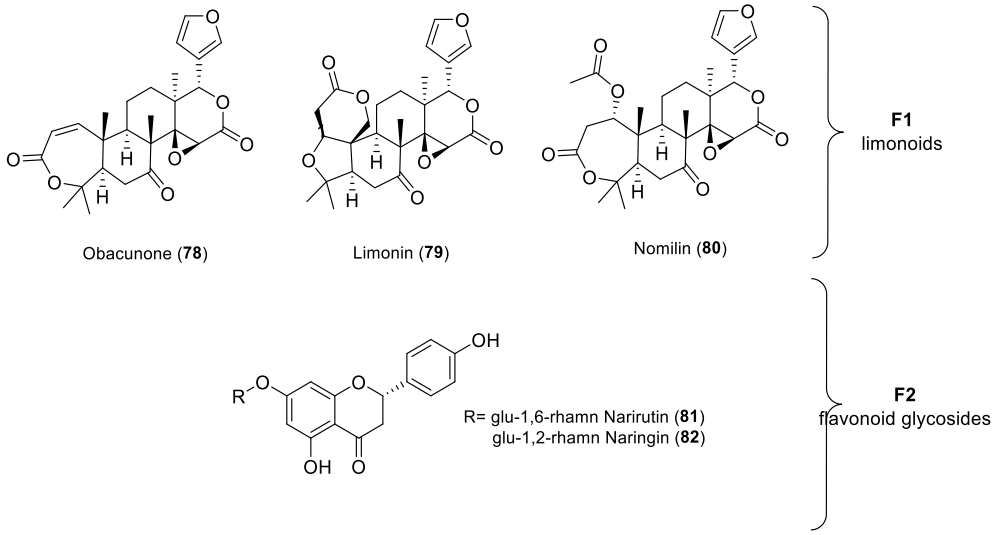

Figure 3.19 *Structures of purified limonoids and flavonoid glycosides*

To optimize the yield of the most promising compounds (**GSE3** from SE), alternative extraction methods were performed: ethanol extraction (**EtE**), acetone/EtOAc (**AAE**) and triphasic extraction (**TE**). All the conditions in detail are reported in table 3.5.

Table 3.5 *condition and yields of all the extraction.*

Entry	Solvents	Temp.	Time	Seeds/solvent (g/mL)	Yield (%)
GSE1-3	Hexane	r.t.	24h (x2)	20/100	26
	DCM				2
	Etanol/H_2O 1/1				13
EtE	EtOH	r.t.	24h (x2)	3/10	10
AAE	Ac/AcOEt	r.t.	24h (x2)	3/10	26
TE	n-Hep/EtOAc/ ACN/ButOH/H_2O (22:14:29:8:27)	35°C	7h (x2)	3/53.4	13 (Apolar phase) 5 (Intermediate phase) 8 (Polar phase)

In SE, the grapefruit seeds contained 26% of apolar compounds, like fatty materials; while the DCM (2%) and EtOH/H_2O (13%) extracts were composed of medium polar and polar compounds, like aglycons and glycosides of limonoids and flavonoids. We decided to investigate **EtE** and **AAE** to attempt

single extraction of green and sustainable solvents (Torres-Valenzuela *et al.*, 2020). As reported in table 3.6, based on the areas in HPLC chromatograms, we calculated the total quantity of main limonoids (limonin and nomilin) in percentage with respect to the dried matrix (DW). For EtE and AAE, the LM content was about 10% and 20%, respectively. In particular, the yield of EtE extraction (9.19 mg/g) was comparable to SE (DCM + EtOH/H_2O, 9.49 mg/g). On the contrary, the acetone/EtOAc extract was more abundant of limonoids than GSE (20.26 mg/g).

Although an efficient limonoid extraction by these two eco-friendly methods, the presence of big quantity of fatty acids was deleterious for the purification and isolation of pure compounds. For this reason, we decided to improve our extraction, maintaining an exhaustive quality of the extract, but considerably reducing the presence of primary metabolites. Thus, we employed the triphasic method (TE) for the extraction of grapefruit seeds with the advantage of mixing five solvents with different polarities for a single extraction step and a consequent process time and solvent consumption reduction. On the bases of the results reported in the paper of Gori et al. (Gori *et al.*, 2021), we chose the solvents for the TE. The three phases, the apolar, intermediate and polar gave yields of 13%, 5% and 8% and were constituted largely of fatty materials, secondary metabolites, and sugars, respectively, as demonstrated by NMR. Unfortunately, this method resulted not advantageous, as limonoids were distributed in all the phases and also the purification step was not improved. A possible alternative to optimize the triphasic extraction of limonoids could be the variation of mixture composition and/or ratios. Our results indicated that the best protocol for the extraction of active compounds in terms of yields of limonoids and purification energies was based on the use of environmental friendly solvents acetone and ethyl acetate.

Table 3.6 *Content of main limonoids (limonin and nomilin) in the extracts.*

Extraction method	Extract	Total LM content (mg/g DW ± SD)
SE	GSE1-Hexane	-
	GSE2-DCM	5.43 ± 1.60
	GSE3-Ethanol/H_2O 1:1	4.05 ± 1.07
		9.48
EtE	EtOH	9.19 ± 1.34
AAE	Ac/AcOEt 1:1	20.26 ± 0.90
TE	Apolar phase	4.46 ± 0.22
	Intermediate phase	12.76 ± 1.25
	Polar phase	9.59 ± 1.04
		26.81

3.4.3.2 Virucidal and antioxidant activity

In a preliminary screening of all the sequential extract (**GSE1**, **GSE2** and **GSE3**), **GSE3** and its main components showed the highest virucidal activity when used to treat the virus before its inoculum on Vero E6 monolayers. Using PRNT50 we evaluated the capacity to neutralize the authentic virus SARS-CoV-2 in vitro. To avoid the possibility that the compounds may have cytotoxic effects on the Vero E6 cells, a standard XTT viability assay was performed before the evaluation of the virucidal activity of GSE. Evaluating the inhibition rate of **$GSE3_{n\text{-}BuOH}$** and **$GSE3_{water}$** at 0.5 mg/mL, it was noted that in the alcoholic extract the inhibition was stabilized over 70% for its virucidal activity, while the second extract was completely ineffective against SARS-CoV-2 (Figure 3.20a). Moreover, the inhibitory effect of **$GSE3_{n\text{-}BuOH}$** decreased below 50% to 0.05 mg / mL, with an IC of 0.118 mg/mL (Figure 3.20b).

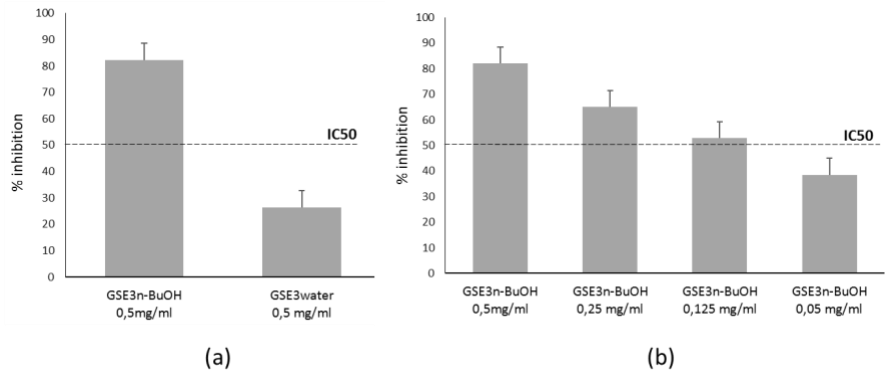

Figure 5.20 *Rate of inhibition by $GSE3_{n\text{-}BuOH}$ and $GSE3_{water}$ (a) and by $GSE3_{n\text{-}BuOH}$ dilutions (b).*

Subsequently, the single limonoids obacunone (**78**), limonin (**79**), nomilin (**80**) of the F1 fraction and the F2 fraction composed of narirutin (**81**) + naringin (**82**) were also analyzed against the virus. All the limonoid components were active against SARS-CoV-2 with IC_{50} between 15 and 31 µg/mL, as presented in Figure 3.21. Instead, the fraction F2 containing narirutin (**81**) + naringin (**82**) did not show any inhibitory effect.

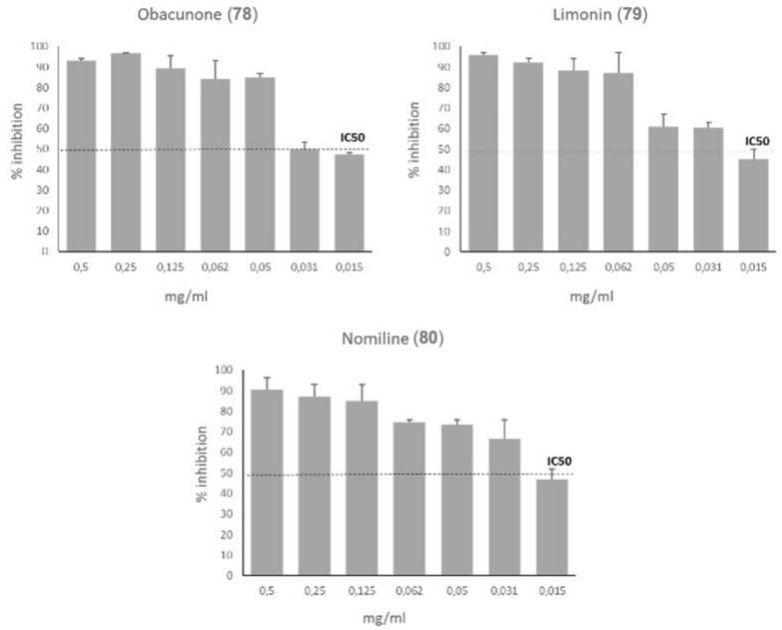

Figure 3.21 *Dose-dependent inactivation of SARS-CoV-2 by obacunone (**78**), limonin (**79**), nomiline (**80**). Half-maximal inhibitory concentration threshold, IC_{50} shown.*

The cytocompatibility of grapefruit seed extracts and isolated single molecules was assessed by MTS cell viability assay, adding different concentrations of each extract or pure molecule to lung epithelial cells - A459 for 24 hours. As shown in figure 3.22a, none of the compounds tested revealed any toxicity at concentrations of 0.01 and 0.1 mg/mL compared to the control, while a decrease in cell viability was detected at concentrations of 0.3 mg/mL. This concentration was not taken into consideration for successive biological analyzes. The morphological inspection of the cells treated with 0.1 mg/mL of extracts/pure compounds also confirmed what has already been described (Figure 3.22b). Furthermore, the protective property of grapefruit seed extracts was evaluated by treating the cells with TBH 500 µM alone or together with increasing concentrations of the extracts and pure molecules after 2 hours of incubation. In this case, only nomilin (**80**) was able to inhibit TBH-induced toxicity at 0.1 mg/mL (Figure 3.23a). The result was also confirmed by microscopic observation where a considerable recovery of altered cell morphology (Figure 3.23b)

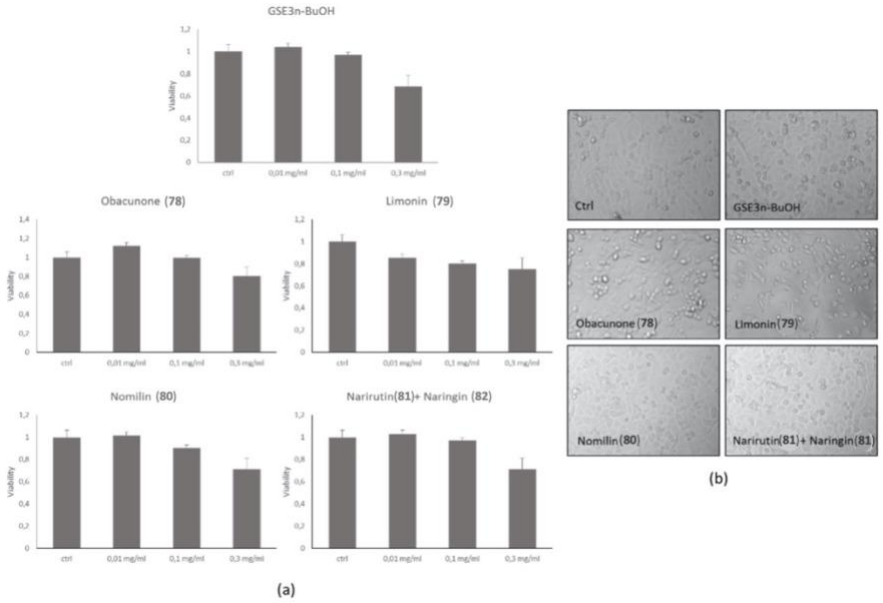

Figure 3.22 *Cytotoxicity of the grapefruit seeds on A549 cells. (a) Histograms of MTS cell viability assay. (b) Representative morphological images of untreated cells (Ctrl) and after 24 hours from the addition of 0.1mg/mL of the extracts.*

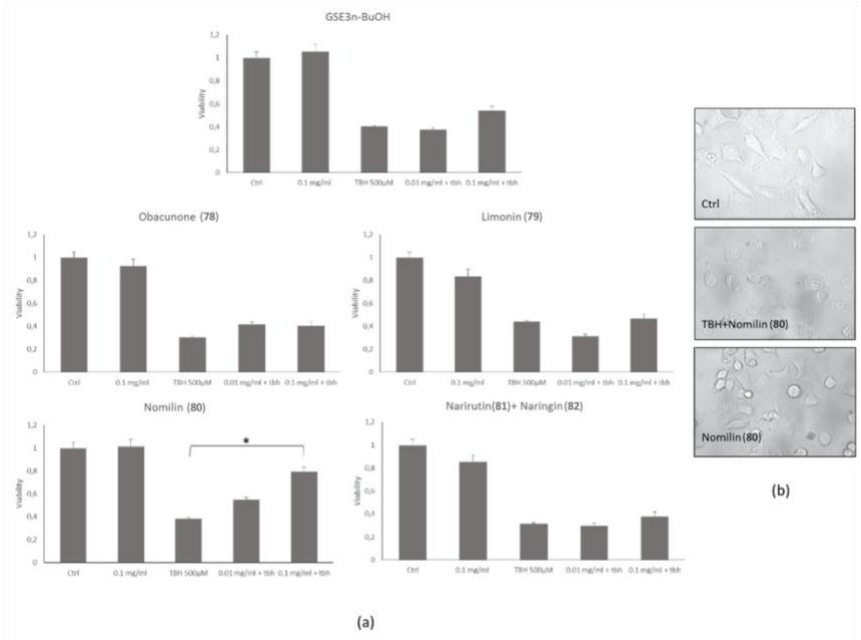

Figure 3.23 *Grapefruit seeds extracts protect A549 cells from cellular damage. (a) Histograms of viability assay on untreated cells (Ctrl) or cells treated with TBH alone or with grapefruit seeds extracts at increasing concentrations for 2 hours. (b) Representative morphological images of untreated cells (Ctrl) or cells treated with TBH or cotreated with TBH and nomilin (**80**) at 0.1 mg/ml. * p < 0.05 as compared to treated (TBH) group.*

The antioxidant activity of all GSE was evaluated using DCFH-DA assay. In general, all analyzed extracts showed a moderate decreased of TBH-induced ROS generation at 0.1mg/ml and in particular, **GSE3$_{n\text{-}BuOH}$** diminished considerably TBH-induced ROS generation at that concentration. Notably, nomilin (**80**) exhibited the best activity, decreasing significantly TBH-induced ROS generation at 0.01 and 0.1 mg/mL (Figure 3.24a). Also with the fluorescence microscope inspection, nomilin (**80**), cotreated with TBH, did not show any fluorescence, confirming the results of DFH-DA assay (Figure 3.24b). Based on these data, nomilin (**80**) dose chosen for subsequent protection experiment was 0.1 mg/mL.

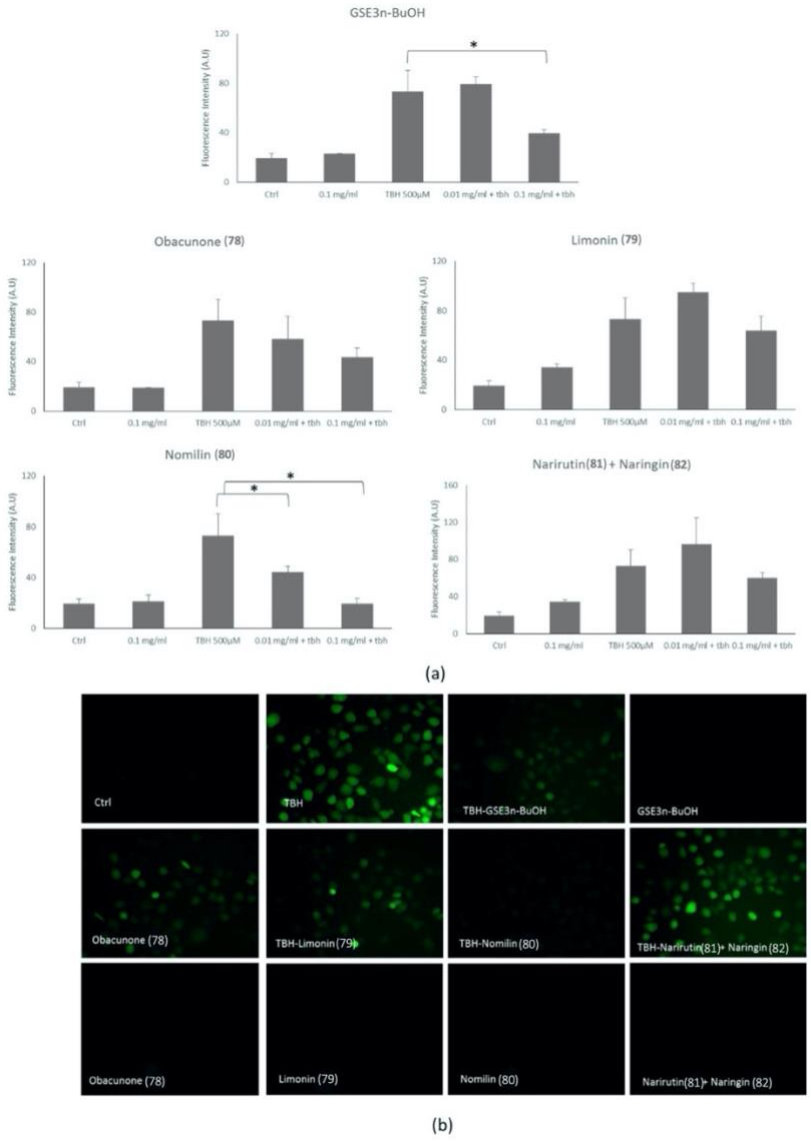

Figure 3.24 *Grapefruit seeds extracts protects cells from oxidative stress. (a) Histogram of ROS generation of untreated cells (Ctrl) or cells treated with TBH alone or in cotreatment with extracts at increasing concentrations for 2 hours. (b) Representative cells fluorescence images of untreated cells (Ctrl) or cells treated with TBH or cotreated with TBH and grapefruit seeds extracts 0.1 mg/mL and treated with the extracts at 0.1 mg/mL each. *p<0.05 as compared to treated (TBH) group.*

Successively, we evaluated the effects of nomilin (**80**) on mitochondrial membrane potential altered by TBH treatment. Usually, excessive ROS production modifies mitochondrial components leading to the mitochondrial

dysfunction. In fact, A549 cells treated with TBH at 500 µM for 2 hours appeared on the fluorescence microscope images with intense green fluorescence, indicating a high depolarization of the mitochondrial membrane. Instead, cells, cotreated with TBH and nomilin, exhibited a higher red fluorescence, like the untreated control (Ctrl) (Figure 3.25). These results indicated a mitochondria protection effect of the limonoid.

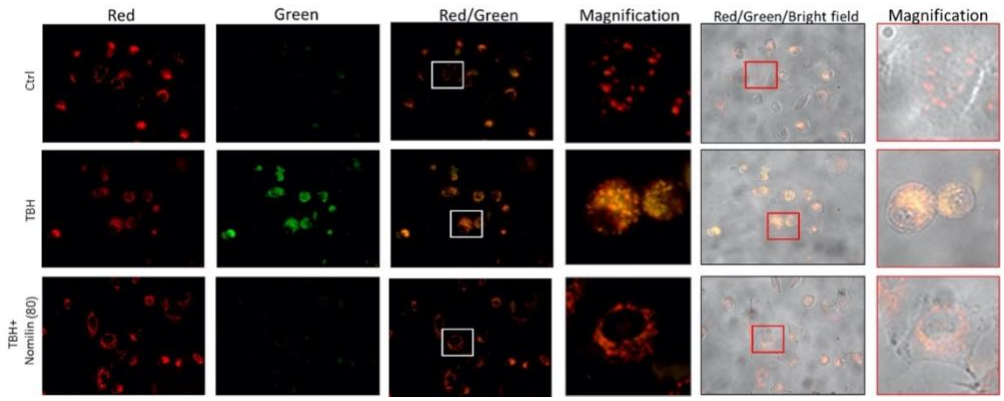

Figure 3.25 *Grapefruit seeds extracts protect against mitochondrial damage. Fluorescence microscope images of cells untreated (Ctrl) or treated with TBH alone or with the nomilin (**3**) and submitted to JC-1 assay.*

Finally, to complete the study on the influence of nomilin on mitochondrial membrane, we analyzed the mitochondria morphology. In a first step, the A549 cells were stained with MitoTracker fluorescence dye. The control was characterized by an interconnected mitochondrial network, with a tubular shape, clearly visible on microscopy fluorescence inspection. Then, Treating the cells with TBH, we were able to notice a simultaneous change in mitochondrial morphology from tubular networks to fragmented puncta (circular). At the end, treating the cells with nomilin (**80**) together the oxidizer TBH, the morphology and mitochondrial was partially restored (Figure 3.26).

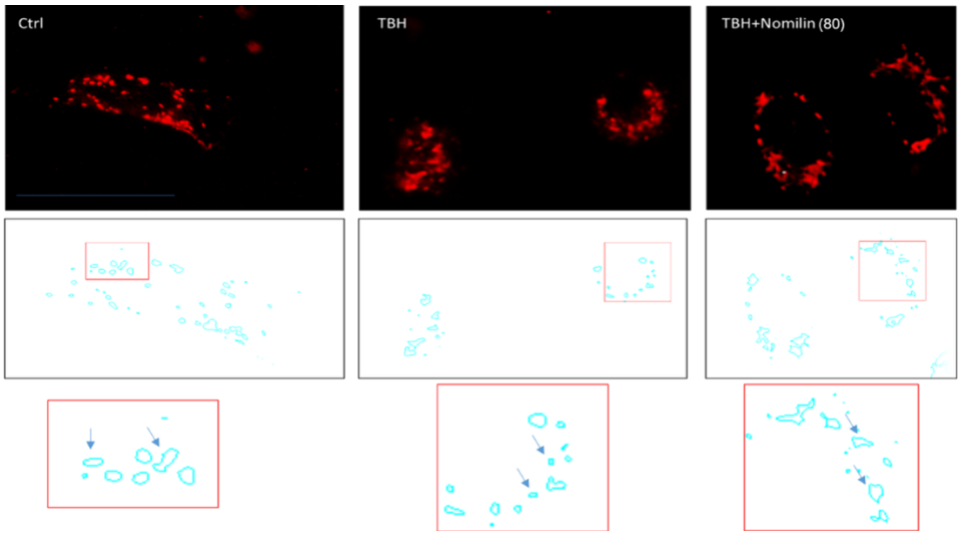

Figure 3.26 *Representative fluorescence microscopy images of mitochondria stained with the MitoTracker Deep Red in untreated cells (Ctrl) or treated with TBH alone or in combination with nomilin (**80**).*

To summarize, starting from grapefruit seeds, we isolated three compounds belonging to limonoid class. Among these, the component nomiline (**80**) and obacunone (**78**), showed a good virucidal activity against Sars-Cov-2 with IC_{50} between 15 and 30 µg/mL and without any cytotoxic effects on the Vero E6 cells. It was remarkable that the virucidal activity rises gradually following the extraction process from the GSE extract (IC_{50} >1.25 mg/mL) to the single molecules.

Moreover, we investigated the antioxidants activity of limonoids by *in vitro* experiments using the powerful oxidant TBH, the cell viability, and ROS production induced by treatment of human lung epithelial cells with TBH in the presence of limonoids. Then, for the first time, the effect of limonoids on the mitochondrial dysfunction was studied. Nomilin (**80**) was found to block the mitochondrial dysfunction driven by oxidative stress, inhibiting the oxidative-induced mitochondrial membrane damage. This capability underlined that its radical scavenging effect was also extended to mitochondrial ROS. Thus, we can conclude that nomilin (**80**) plays a protective role on the cell's central organelle.

3.4.4 Experimental section

NMR and MS characterization

The NMR experiments were performed on 600 MHz Bruker Advance instrument using deuterated chloroform (for limonoids) or methanol (flavonoid glycosides). The structures of isolated compounds were elucidated by 1D and 2D NMR experiments.

Limonin (79) (Min *et al.*, 2007)

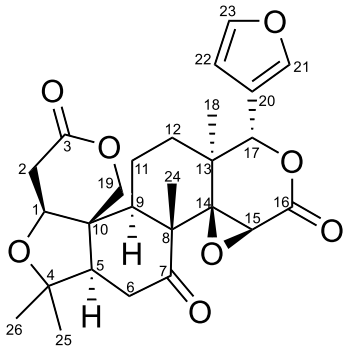

HMRS *m/z* ($C_{26}H_{30}O_8$): 493.1830 (100%, M+ Na) 494.1863 (30%, M+1+Na)

C	^{1}H-NMR	^{13}C-NMR	HMBC
1	4.03, brs	80.3	
2	2.85, t, *J*= 15.1 Hz 2.45, dd, *J*= 14.5, 3.0 Hz	36.3	C10, C5, C1
3	-	169.1	C19
4	-	79.1	
5	2.2, dd, *J*=15.6, 3.1 Hz	60.5	C25, C24, C9, C4
6	2.97, dd, *J*= 16, 3.1 Hz 2.65, dd, *J*= 14.4, 3.1 Hz	35.6	C10, C4, C1
7	-	206.1	
8	-	51.3	
9	2.54, dd, *J*= 12, 2.1 Hz	48.0	C24, C14, C4
10	-	45.9	
11	1.8, m 1.5, m	20.6	C12, C9, C13, C14
12	1.5, m 1.78, m	30.8	C13, C9
13	-	37.9	
14	-	65.6	
15	4.03, brs	53.8	C14, C9
16	-	166.6	
17	5.46, brs	77.8	C13, C14
18	1.06, s	17.6	
19	4.76, d, *J*= 13.1 Hz 4.45, d, *J*=13.1 Hz	65.3	C10, C4
20	-	119.9	C21, C22, C23, C17
21	7.40, brs	143.2	
22	6.33, brs	109.7	
23	7.41, brs	141.1	
24	1.28, s	31.0	C5, C4
25	1.16, s	18.8	
26	1.17, s	21.4	

Nomilin (80) (Hamdan *et al.*, 2011)

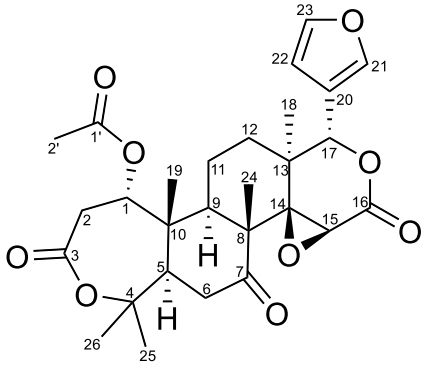

HMRS *m/z* ($C_{28}H_{34}O_9$): 537.2101 (100%, M+Na) 538.3133 (30%, M+1+Na)

C	^{1}H-NMR	^{13}C-NMR	HMBC
1	5, m	70.6	C19, C5, C3
2	3.20, d, *J*= 15.6 Hz 3.11, dd, *J*= 15.6, 7.3 Hz	35.2	C10, C1, C3
3	-	169.2	
4	-	84.3	
5	2.76, t, *J*= 15.2	50.9	C19, C9, C4, C7
6	2.57	38.7	C19, C24, C9, C4, C7
7	-	206.7	
8	-	52.8	
9	2.46, d, *J*= 10.3 Hz	44.3	C19, C 12, C15
10	-	44.1	
11	1.60, m	16.5	
12	1.77, m 1.10, m	31.9	
13	-	37.4	
14	-	65.4	
15	3.78, brs	53.3	C14, C16
16	-	166.7	
17	5.43, s	77.9	C12, C13, C14, C21, C20, C22
18	1.2, s	17.1	C9, C14, C7
19	1.3, s	17.0	C5, C1
20	-	120.0	
21	6.31, s	109.5	C20, C22
22	7.39, brs	143.2	C23, C20
23	7.39, brs	140.9	
24	1.16, s	20.8	
25	1.45, s	33.4	C4, C5
26	1.54, s	32.2	C4, C5
CH_3CO:			
1'	-	169.1	
2'	2.0, s	20.7	

Obacunone (1) (Sugimoto *et al.*, 1988)

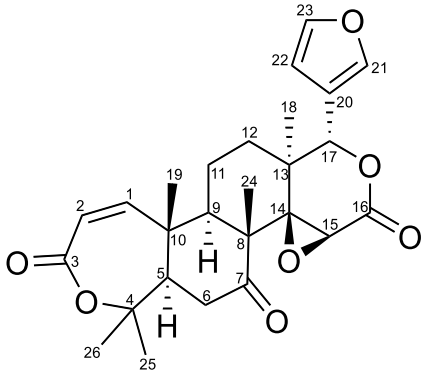

HMRS *m/z* ($C_{26}H_{30}O_7$): 477.1888 (100%, M+ Na) 478.1920 (M+1+Na)

C	^{1}H-NMR	^{13}C-NMR	HMBC
1	6.50, d, *J*= 11.8 Hz	156.7	C9, C3
2	5.96, d, J= 11.8 Hz	123.0	C10
3	-	166.9	
4	-	83.9	
5	2.59, dd, *J*= 14.0, 5.1 Hz	57.3	C25, C4
6	α- 2.29, dd, J= 14.0, 5.1 Hz β- 2.98, t, J= 14.0 Hz	39.8	C5, C4, C7
7	-	207.0	
8	-	52.9	
9	2.14, dd, *J*= 9.0, 3.6 Hz	49.2	C12, C10
10	-	53.1	
11 (α, β)	1.88, m 1.6, m	19.4	
12 (α, β)	1.88, m 1.6, m	32.7	
13	-	37.4	
14	-	65.0	
15	3.66, s	53.8	C14, C16
16	-	166.6	
17	5.46, brs	77.8	C13, C14, C22, C20, C21
18	1.12, s	16.9	C17, C14
19	1.24, s	32.0	C7, C8
20	-	120.1	
21	7.41, brs	141.0	
22	6.36, brs	109.7	C20, C23
23	7.39, t, J= 1.7 Hz	143.1	C22, C20
24 (30)	1.50, s	21.1	
25 (28)	1.45, s	16.4	
26 (29)	1.50, s	26.7	C10, C9, C5, C4

Narirutin (81) (Kim *et al.*, 2004)

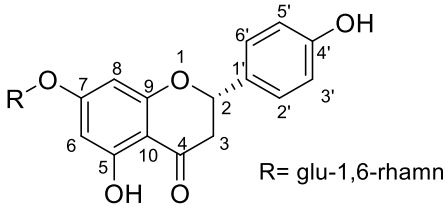

C	^{1}H-NMR	^{13}C-NMR
2	5.37, dd, J=12.80, 2.51 Hz	80.8
3	3.15, dd, J=12.80, 17.3 Hz	44.3
	2.74, dd, J=17.30, 2.85 Hz	
4		198.7
5		165.1
6	6.15, d, J=2.19 Hz	98.1
7		167.0
8	6.17, d, J= 2.19 Hz	97.2
9		159.2
10		105.1
1'		130.9
2'6'	7.31, d, J=8.40 Hz	129.3
3'5'	6.81, d, J= 8.40 Hz	116.5
4'		164.7
Glu		
1	5.09	101.3
2 - 6	3.38 – 3.86	74.8
		78.0
		71.4
		77.3
		67.5
Rha		
1	5.24	102.3
2-5	3.58 – 3.92	72.2
		72.5
		74.2
		69.9
Me	1.28	18.0

Naringin (82) (Cordenonsi *et al.*, 2017)

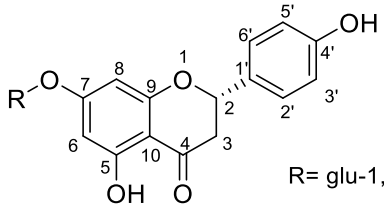

C	^{1}H-NMR	^{13}C-NMR
2	5.36,dd, J=12.68, 2.51 Hz	80.8
3	2.75, dd, J=12.80, 17.3 Hz 3.89, dd, J=17.30, 2.85 Hz	44.3
4		198.7
5		164.8
6	6.15, d, J=2.19 Hz	98.0
7		166.7
8	6.17, d, J= 2.19 Hz	96.9
9		159.3
10		105.0
1'		130.9
2'6'	7.31, d, J=8.02 Hz	129.3
3'5'	6.81, d, J= 8.02Hz	116.5
4'		165.1
Glu		
1	5.09	99.5
2 - 6	3.17 – 3.95	79.1
		78.2
		72.3
		74.1
		62.4
Rha		
1	5.24	102.7
2 - 5	3.42 – 3.66	71.4
		72.3
		79.3
		70.1
Me	1.20	18.3

HMRS *m/z* ($C_{27}H_{32}O_{14}$): 603.1697 (40%, M+Na) 604.1758 (100%, M+1+Na), 605.1809 (70%, M+2+Na)

3.4.5 Bibliography

Antonić, B., Jančíková, S., Dordević, D. and Tremlová, B., 2020. Grape Pomace Valorization: A Systematic Review and Meta-Analysis, Food, 9(11), 1627. doi: 10.3390/foods9111627.

Battinelli, L., Mengoni, F., Lichtner, M., Mazzanti, G., Saija, A., Mastroianni, C.M. and Vullo, V., 2003. Effect of Limonin and Nomilin on HIV-1 Replication on Infected Human Mononuclear Cells, Planta Med., 69(10), 910–913. doi:10.1055/s-2003-45099.

Cordenonsi, L.M., Sponchiado, R.M., Campanharo, S.C., Garcia, C. V and Raffin, R.P., 2017. Study of Flavonoids presente in Pomelo (*Citrus máxima*) by DSC , UV-VIS , IR , 1 H AND 13 C NMR AND MS, 31–37.

Durante, M., Montefusco, A., Marrese, P.P., Soccio, M., Pastore, D., Piro, G., Mita, G. and Lenucci, M.S., 2017. Seeds of pomegranate, tomato and grapes: An underestimated source of natural bioactive molecules and antioxidants from agri-food by-products, J. Food Compos. Anal., 63(July), 65–72. doi:10.1016/j.jfca.2017.07.026.

Dwyer, K., Hosseinian, F. and Rod, M., 2014. The Market Potential of Grape Waste Alternatives, J. Food Res., 3(2), 91. doi:10.5539/jfr.v3n2p91.

Ezejiofor, T., 2014. Waste to Wealth- Value Recovery from Agro-food Processing Wastes Using Biotechnology: A Review, Br. Biotechnol. J., 4(4), 418–481. doi:10.9734/BBJ/2014/7017.

Gori, A., Boucherle, B., Rey, A., Rome, M., Fuzzati, N. and Peuchmaur, M., 2021. Development of an innovative maceration technique to optimize extraction and phase partition of natural products, Fitoterapia, 148(December 2020). doi:10.1016/j.fitote.2020.104798.

Hamdan, D., El-Readi, M.Z., Tahrani, A., Herrmann, F., Kaufmann, D., Farrag, N., El-Shazly, A. and Wink, M., 2011. Chemical composition and biological activity of Citrus jambhiri Lush, Food Chem., 127(2), 394–403.

doi:10.1016/j.foodchem.2010.12.129.

Kamal-Eldin, A. and Appelqvist, L.-Å., 1996. The chemistry and antioxidant properties of tocopherols and tocotrienols, Lipids, 31(7), 671–701. doi:10.1007/BF02522884.

Kim, W.C., Lee, D.Y., Lee, C.H. and Kim, C.W., 2004. Optimization of narirutin extraction during washing step of the pectin production from citrus peels, J. Food Eng., 63(2), 191–197. doi:10.1016/j.jfoodeng.2003.07.001.

Kohno, H., Suzuki, R., Yasui, Y., Hosokawa, M., Miyashita, K. and Tanaka, T., 2004. Pomegranate seed oil rich in conjugated linolenic acid suppresses chemically induced colon carcinogenesis in rats, Cancer Sci., 95(6), 481–486. doi:10.1111/j.1349-7006.2004.tb03236.x.

Komura, M., Suzuki, M., Sangsriratanakul, N., Ito, M., Takahashi, S., Alam, M.S., Ono, M., Daio, C., Shoham, D. and Takehara, K., 2019. Inhibitory effect of grapefruit seed extract (Gse) on avian pathogens, J. Vet. Med. Sci., 81(3), 466–472. doi:10.1292/jvms.18-0754.

Lenucci, M.S., Durante, M., Anna, M., Dalessandro, G. and Piro, G., 2013. Possible Use of the Carbohydrates Present in Tomato Pomace and in Byproducts of the Supercritical Carbon Dioxide Lycopene Extraction Process as Biomass for Bioethanol Production, J. Agric. Food Chem., 61(15), 3683–3692. doi:10.1021/jf4005059.

Lipiński, K., Mazur, M., Antoszkiewicz, Z. and Purwin, C., 2017. Polyphenols in Monogastric Nutrition – A Review, Ann. Anim. Sci., 17(1), 41–58. doi:10.1515/aoas-2016-0042.

Magurano F., Sucameli M., Picone P., Micucci M., Baggieri M., Marchi A., Bucci P., Gioacchini S., Catinella G., Borgonovo G., Dallavalle S., Nuzzo D. and Pinto A., 2021. Antioxidant Activity of Citrus Limonoids and Investigation of Their Virucidal Potential against SARS-CoV-2 in Cellular Models. *Antioxidants*, 10,1794. doi: 10.3390/antiox10111794.

Magurano, F., Baggieri, M., Marchi, A., Rezza, G., Nicoletti, L., Eleonora, B., Concetta, F., Stefano, F., Maedeh, K., Paola, B., Emilio, D. and Silvia, G., 2021. SARS-CoV-2 infection: the environmental endurance of the virus can be influenced by the increase of temperature, Clin. Microbiol. Infect., 27(2), 289.e5-289.e7. doi:10.1016/j.cmi.2020.10.034.

Min, Y.D., Kwon, H.C., Yang, M.C., Lee, K.H., Choi, S.U. and Lee, K.R., 2007. Isolation of limonoids and alkaloids fromPhellodendron amurense and their multidrug resistance (MDR) reversal activity, Arch. Pharm. Res., 30(1), 58–63. doi:10.1007/bf02977779.

Montoya, C., González, L., Pulido, S., Atehortúa, L. and Robledo, S.M., 2019. Identification and quantification of limonoid aglycones content of Citrus seeds, Rev. Bras. Farmacogn., 29(6), 710–714. doi:10.1016/j.bjp.2019.07.006.

Reagor, L., Gusman, J., McCoy, L., Carino, E. and Heggers, J.P., 2002. The Effectiveness of Processed Grapefruit-Seed Extract as An Antibacterial Agent: I. An In Vitro Agar Assay, J. Altern. Complement. Med., 8(3), 325–332. doi:10.1089/10755530260128014.

Roy, A. and Saraf, S., 2006. Limonoids: Overview of significant bioactive triterpenes distributed in plants kingdom, Biol. Pharm. Bull., 29(2), 191–201. doi:10.1248/bpb.29.191.

Shi, Y.S., Zhang, Y., Li, H.T., Wu, C.H., El-Seedi, H.R., Ye, W.K., Wang, Z.W., Li, C. Bin, Zhang, X.F. and Kai, G.Y., 2020. Limonoids from Citrus: Chemistry, anti-tumor potential, and other bioactivities, J. Funct. Foods, 75(September), 104213. doi:10.1016/j.jff.2020.104213.

Sugimoto, T., Miyase, T., Kuroyanagi, M. and Ueno, A., 1988. Limonoids and quinolone alkaloids from evodia rutaecarpa bentham, Chem. Pharm. Bull., 36(11), 4453–4461. doi:10.1248/cpb.36.4453.

Torres-Valenzuela, L.S., Ballesteros-Gómez, A. and Rubio, S., 2020. Green

Solvents for the Extraction of High Added-Value Compounds from Agri-food Waste, Food Eng. Rev., 12(1), 83–100. doi:10.1007/s12393-019-09206-y.

Xu, W., Qu, W., Huang, K., Guo, F., Yang, J., Zhao, H. and Luo, Y., 2007. Antibacterial effect of Grapefruit Seed Extract on food-borne pathogens and its application in the preservation of minimally processed vegetables, Postharvest Biol. Technol., 45(1), 126–133. doi:10.1016/j.postharvbio.2006.11.019.

Yu, X., Ding, G., Zhi, X. and Xu, H., 2015. Insight into reduction of obacunone, and their ester derivatives as insecticidal agents against Mythimna separata Walker, Bioorganic Med. Chem. Lett., 25(1), 25–29. doi:10.1016/j.bmcl.2014.11.027.

4 CONCLUSIONS AND FUTURE PERSPECTIVES

This PhD thesis intended to be a multidisciplinary study focused on the synthesis/isolation of natural or nature-inspired antimicrobial agents for application at multiple levels in the food supply chain. Efficient synthetic strategies were developed to prepare novel antifungal agents against *P.oryzae* starting from the natural strobilurin pharmacophores; SAR studies on natural resveratrol-derivatives were conducted to elucidate the structural determinants necessary for the bioactivity of benzofuran-containing viniferins. Moreover, resveratrol derivative containing nitrogen groups were synthetized with the aim to overcome the Gram-negative outer membrane. At the same time, with the goal to enhance waste product recovery, we developed efficient extraction and purification methods to obtain grapefruit seeds enriched extracts and pure molecules, to test their virucidal and antioxidant activity.

In the first part, we concentrated our effort to design a new series of strobilurin-derivatives. From the evaluation of antifungal activity of all the novel compounds against wilde-type and strobilurin-resistant strains, the analogues **6b** showed a surprising activity against resistant strains of *P. oryzae.* To explain this result, we developed a 3D model of *P. oryzae* cytochrome *bc1* supramolecular assembly in complex with azoxystrobin. Future efforts will be devoted to elucidate the peculiar activity of this promising compound. Moreover, the validated new *in silico* model for *P.oryzae* will be useful for further rational design of new highly active compounds, possibly able to overcome the well-known strobilurin resistance in *P. oryzae* strains.

Moving on food supply chain, we focused on antibacterial agents. In this case, we identified the structural elements of stilbenoids dehydro-δ-viniferin and dehydro-ε-viniferin relevant to the antimicrobial potency against the foodborne pathogen *L. monocytogenes* Scott A. The selective exclusion of phenolic moieties from dehydro- δ-viniferin led to a decrease of the antibacterial activity, while a simplified analogue of dehydro-ε-viniferin was found to exert

two-fold higher potency than the natural precursor. These results shed light into the possible use of the obtained stilbenoids as both antimicrobial agents and food preservatives against foodborne pathogens and antibiotic adjuvants. Future investigation could be focused on combination studies of stilbene derivatives and antibiotics for effective combination therapies.
Starting from the “eNTRy” rules to block Gram-negative bacteria, we designed and synthesized a small collection of stilbenoids bearing a basic nitrogen function. Biological investigations on these compounds are under way.

Finally, to conclude our investigation of natural or nature-inspired compounds as potential antimicrobials in the food supply chain, we concentrated on by-product recovery. Investigating natural extracts of grapefruit seeds as a source of active molecules to fight against SARS-CoV-2 infection, we found that natural compounds belonging to the class of limonoids are endowed with very promising virucidal, antioxidant and mitoprotective activity.

5 ACKNOWLEDGEMENT

A special thanks goes to the Fondazione Fratelli Confalonieri which has supported my PhD thesis work over these three years and has allowed me to reach this important milestone.

6 SCIENTIFIC PRODUCTION

PAPERS

Catinella G., Borgonovo G., Dallavalle S., Contente M., Pinto A., 2021. From saffron residues to natural safranal: Valorization of waste through a β-glucosidase. *Food bioprod process*. Article in press. doi: 10.1016/j.fbp.2021.11.002.

Magurano F., Sucameli M., Picone P., Micucci M., Baggieri M., Marchi A., Bucci P., Gioacchini S., Catinella G., Borgonovo G., Dallavalle S., Nuzzo D. and Pinto A., 2021. Antioxidant Activity of Citrus Limonoids and Investigation of Their Virucidal Potential against SARS-CoV-2 in Cellular Models. *Antioxidants*, 10,1794. doi: 10.3390/antiox10111794.

Kunova, A., Palazzolo, L., Forlani, F., Catinella, G., Musso, L., Cortesi, P., Eberini, I., Pinto, A., Dallavalle, S., 2021. Structural investigation and molecular modeling studies of strobilurin-based fungicides active against the rice blast pathogen *Pyricularia oryzae*. *Int. J. Mol. Sci.*, 22 (7), doi: 10.3390/ijms22073731.

Mattio, L., Catinella, G., Iriti, M., Vallone, L., 2021. Inhibitory activity of stilbenes against filamentous fungi. *Ital. J. Food Saf.*, 10 (1), doi: 10.4081/ijfs.2021.8461.

Mattio, L., Catinella, G., Dallavalle, S., Pinto, A., 2020. Stilbenoids: A Natural Arsenal against Bacterial Pathogens. *Antibiotics*, 9, 336, doi:10.3390/antibiotics9060336.

Mattio, L., Catinella, G., Pinto, A., Dallavalle, S., 2020. Natural and nature-inspired stilbenoids as antiviral agents. *Eur. J. Med. Chem.*, 202, 112541, doi: 10.1016/j.ejmech.2020.112541.

Catinella, G., Mattio, L. M., Musso, L., Arioli, S., Mora, D., Beretta, G. L., Zaffaroni, N., Pinto, A., Dallavalle, S., 2020. Structural Requirements of Benzofuran Derivatives Dehydro-δ- and Dehydro-ε-Viniferin for Antimicrobial

Activity Against the Foodborne Pathogen Listeria monocytogenes. *Int. J. Mol. Sci.*, 21, 2168, doi: 10.3390/ijms21062168.

POSTER COMMUNICATIONS

14-23 September 2021 – Online – XXVII Congresso Nazionale della Società Chimica Italiana:

- "*Synthesis and Molecular Modeling Studies of Strobilurin-SDHI Based Hybrid fungicides*" – G. Catinella, C. Pinna, A. Kunova, L. Palazzolo, F. Forlani, L. Musso, P. Cortesi, I. Eberini, A. Pinto and S. Dallavalle – ORG PO023
- *"Convenient enzymatic processing for conversion of food wastes to valuable bioproducts: transformation of picrocrocin to safranal"* – G. Catinella, M.L. Contente, S. Dallavalle, G. Borgonovo, A. Pinto – FAR PO025

6-8 September 2021 – Prague, Czechia – STRATAGEM CA17104: 4th Annual Conference New diagnostic and therapeutic tools against multidrug resistant tumours – **"***Natural stilbenoids and benzofuran-containing analogues target G-quadruplex DNA and exhibit antitumor activity" – G. Catinella, C. Platella, S. Mazzini, E. Napolitano, L. M. Mattio, G. L. Beretta, N. Zaffaroni, A. Pinto, D. Montesarchio and S. Dallavalle*

ORAL COMMUNICATIONS

15th September 2021– Palermo, Italy – First Virtual Workshop on the Developments in Italian PhD Research on Food Science, Technology and Biotechnology – "*Synthesis of novel multitarget antimicrobial compounds*" – G. Catinella

1-5 July 2019 - Naples, Italy - III International Summer School on Natural Products "*Synthesis of natural Stilbenoids as Potential hypoglycaemic agents*" - G. Catinella, L. Mattio, M.Marengo, I. Eberini, C. Parravicini, S. Dallavalle, F. Bonomi, S. Iametti, A. Pinto

13-17 May 2019 **–** Spetses, Greece - Advanced school in protein structure solution, prediction and validation - "*Synthesis and alpha-amylase inhibition of some resveratrol derivatives*" - G. Catinella, L. Mattio, M. Marengo, I. Eberini, C. Parravicini, S. Dallavalle, F. Bonomi, S. Iametti, A. Pinto